Notes on the 1967

Summer Study Program

in

GEOPHYSICAL FLUID DYNAMICS

at

The WOODS HOLE OCEANOGRAPHIC INSTITUTION

Reference No. 67-54

Contents of the Volumes

Participants and Staff Members

Barcilon, Victor	Massachusetts Institute of Technology
Bisshopp, Frederic E.	Brown University
Busse, Friedrich	University of California at Los Angeles
Childress, Stephen	Courant Institute of Mathematical Sciences, N.Y.
Clark, Sydney P.	Yale University
Gilbert, Freeman	University of California at San Diego
Greenspan, Harvey P.	Massachusetts Institute of Technology
Herring, Jackson	NASA, Goddard Space Flight Center
Hide, Raymond	Massachusetts Institute of Technology
Howard, Louis N.	Massachusetts Institute of Technology
Keller, Joseph B.	Courant Institute of Mathematical Sciences, N.Y.
Kraichnan, Robert H.	Peterborough, New Hampshire
Lighthill, M. James	Imperial College, London, England
Malkus, Willem V.R.	University of California at Los Angeles
McIntyre, Michael E.	University of Cambridge, England
Onat, E. Turan	Yale University
Orszag, Steven A.	Institute of Advanced Study, Princeton
Roberts, Paul	University of Newcastle, Newcastle-upon-Tyne, England
Rossby, H. Thomas	Massachusetts Institute of Technology
Stewartson, Keith	University College, London, England
Toksöz, M. Nafi	Massachusetts Institute of Technology
Veronis, George	Yale University
Wunsch, Carl I.	Massachusetts Institute of Technology

Fellows

Blumsack, Steven L.	Applied Mathematics	Massachusetts Institute of Technology
Buzyna, George	Physics of Fluids	Yale University
Chorin, Alexandre J.	Mathematics	Courant Institute of Mathematical Sciences, N.Y.
Denis, Charles L.	Geophysics	University of Liege, Belgium
Gadgil, Sulochana	Applied Mathematics	Harvard University
Johnson, Leonard E.	Geophysics	University of California at San Diego
McIntyre, Michael E.	Fluid Dynamics	University of Cambridge, England
Somerville, Richard C.J.	Meteorology	NCAR, Boulder, Colorado
Thatcher, Wayne R.	Geophysics	California Institute of Technology at Pasadena
Thompson, Rory	Meteorology	Massachusetts Institute of Technology

Editors' Preface

This volume contains the final reports by the student participants of their research activities of the summer as well as abstracts of seminars and discussions by the staff and by invited lecturers.

As in previous years the efforts reported by the students reflect varying degrees of originality and completeness. A few of the students were guided carefully; with others there was little contact between student and staff. Some of the students either posed or were given precisely formulated problems which could be essentially completed during the summer. Others accepted problems which were not well-posed and which involved a period of groping and searching for a tractable and reasonably finite problem with a significant goal. It is noteworthy that all six of the pre-doctoral participants started on research projects which they intended to develop into Ph.D. theses after they returned to their respective universities.

Time limitations did not allow the participants to rework the manuscripts and the present records must be interpreted as only interim reports.

We who took part in the program this summer are deeply indebted to the National Science Foundation for its continued support of the program and to the Woods Hole Oceanographic Institution for its support and encouragement and for the use of its facilities.

Mary C. Thayer
George Veronis

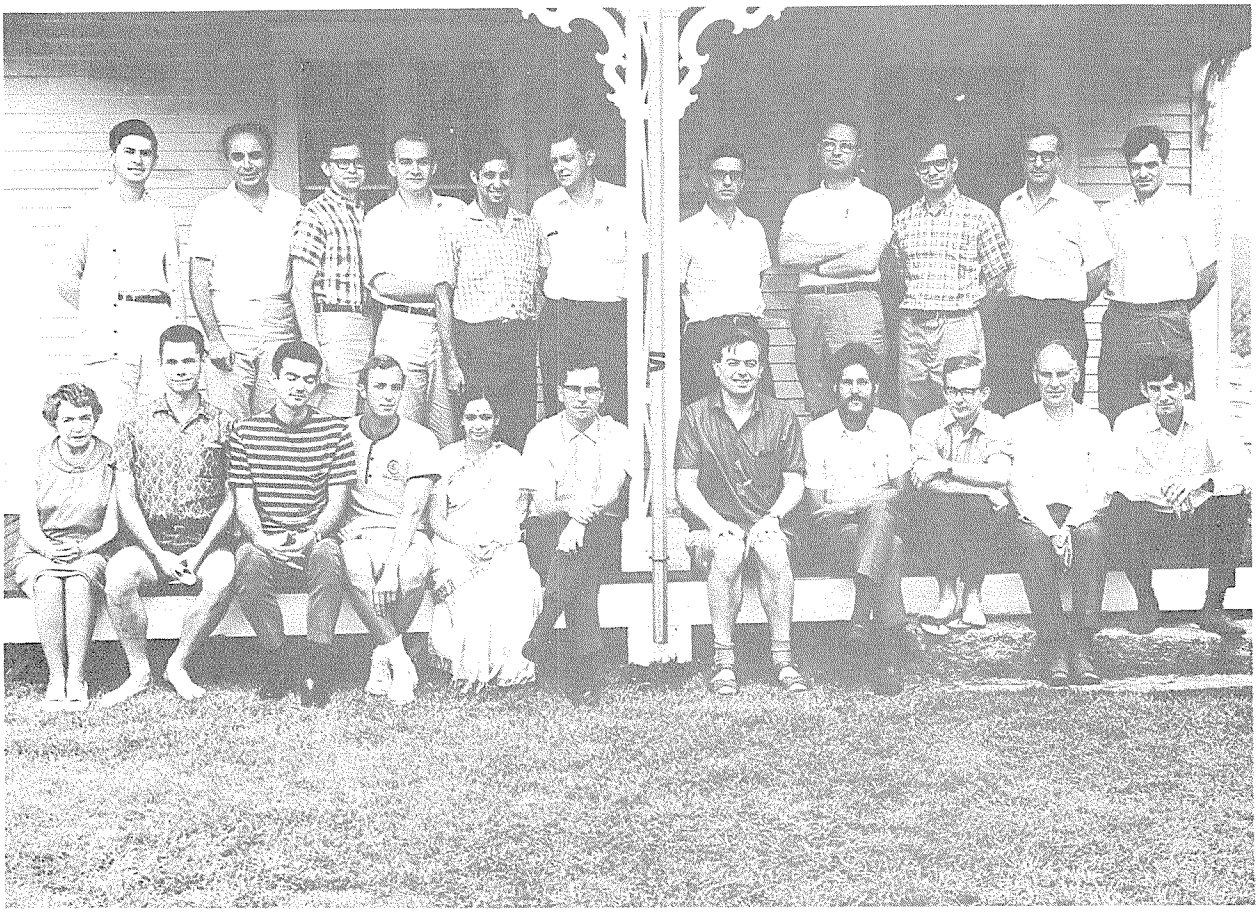

BACK ROW, LEFT TO RIGHT: Chorin, Onat, Buzyna, Denis, Blumsack, Howard, Malkus, Gilbert, Kraichnan, Veronis and Herring. FRONT ROW: Thayer, Thompson, Johnson, Thatcher, Gadgil, Busse, Roberts, Somerville, McIntyre, Hide and Childress.

CONTENTS of VOLUME II

Fellows' Lectures

CONTENTS of VOLUME II (continued)

CONTENTS of VOLUME II (continued)

Formation of Layers in a Stably Stratified Fluid

Steven L. Blumsack

Introduction

The purpose of this report is to present a possible explanation for a phenomenon that has been observed for many years now. When a container is filled with a fluid, stably stratified (with respect to the gravitational field) with some slowly diffusing substance, such as salt, and is subsequently warmed uniformly at its surfaces, the formation of layers ensues. Each layer is nearly uniform in salinity, with rather thin interfaces between the layers. A possible mechanism for forming these layers will be discussed and an appropriate length scale will be found.

The method to be used will be as follows: the effects of certain parameters will be discussed and the experimental evidence will justify their omission from the mathematical model. This simplified model will be discussed both physically and mathematically, as an initial value problem, to determine the gross features of the basic flow. Since the mathematical flow will have no vertical structure, the experiment would then have to be explained by some instability; only an infinitesimal instability theory will be attempted, consequently, only the scale of the layers will be found, not their fine structure since this would require a more exact analysis.

Description of Experiment

An exact analysis of this problem would not only entail considerable labor, but the physical mechanism that is responsible for the formation of these layers might be obscured in its complexity. Therefore, an idealized model of the experiment will be formulated, hopefully containing the essential features of the relevant mechanism.

A standard experiment will now be defined. A 1000 ml graduated cylinder, six centimeters in diameter, was filled with (dyed) salty water at room temperature; the salinity increased nearly linearly downwards. Then the container was immersed in a hot-water bath, approximately 25°C warmer than room temperature. After about a minute, one could see the aforementioned layers, about one centimeter wide, in the final stages of formation.

These layers appeared as alternating bands of dark fluid and light fluid with the general trend being lighter near the top of the container. Although it was impossible to detect the flow during the formation of the layers, one could see small protrusions of dark fluid commencing at the wall and tilted down into the interior. As the layers became visible, these protrusions had become level.

The effects of the size of the container were checked first. Its height did not seem to be important, as the layers appeared to form almost simultaneously in the middle portion of the cylinder. It was noted that, in the time required to form the layers, the heat would have penetrated less than one centimeter into the fluid, implying that the diameter of the container should not be an important parameter, at least in the early stages

of the formation of the layers.

It was noted that when the temperature difference across the glass was increased, the layers appeared to become wider and more irregular.

The discussion in the preceding paragraph suggests that an appropriate mathematical model would be a semi-infinite fluid, linearly stratified with salt, bounded on one side by an infinite plane which is heated uniformly beginning at a particular instant in time. Notice that no vertical structure is present in the model*, so that the vertical dependence will not be in the basic flow, but in those perturbations on the basic flow that grow with time. Since the perturbations need some source of energy in order to grow, the basic velocity, temperature, and salinity fields must be discussed before any stability analysis may be undertaken.

Basic Fields - Qualitative Discussion

As has been stated, at any instant in time the basic fields will be independent of the vertical coordinate, implying that there can be no horizontal flux of mass, consequently no velocity normal to the wall and no advection of either temperature or momentum.

When the wall is heated, the fluid nearest to the wall becomes warmer, thereby less dense, and would tend to rise, the motion being retarded by viscosity. As time progresses, the effects of the temperature

---

*Although the salinity does have a vertical dependence, the dynamics only involves its gradient, which is assumed constant.

move slowly inward and the temperature of the fluid closest to the wall increases, but increases continually more slowly.

If the wall was not continually heated, but instead maintained at a constant temperature, the fluid would rise until it became neutrally buoyant and then tend to remain at that level. This is not quite the story for the case at hand, but since the temperature at the side wall is increasing so slowly, it does not seem too unreasonable to suspect that most of the fluid will maintain a neutrally buoyant state. In addition, away from the wall, the fluid is being warmed very slowly, thereby introducing very slow motions.

Although the basic velocity, temperature, and salinity fields are time dependent, and spatially rather complicated, the following crude approximations of these fields will be made now and the first two justified later.

(i) Lines of constant density are horizontal.

(ii) The temperature and salinity fields are independent of time.

(iii) The fluid is infinite in extent (no wall).

In order to analyze the stability problem, the lines of constant salinity (called isohalines) will be assumed to be straight; this will force the temperature gradient to be uniform in order to satisfy (i). Hopefully, this assumption is not critical to the physics, being needed only to simplify the mathematics.

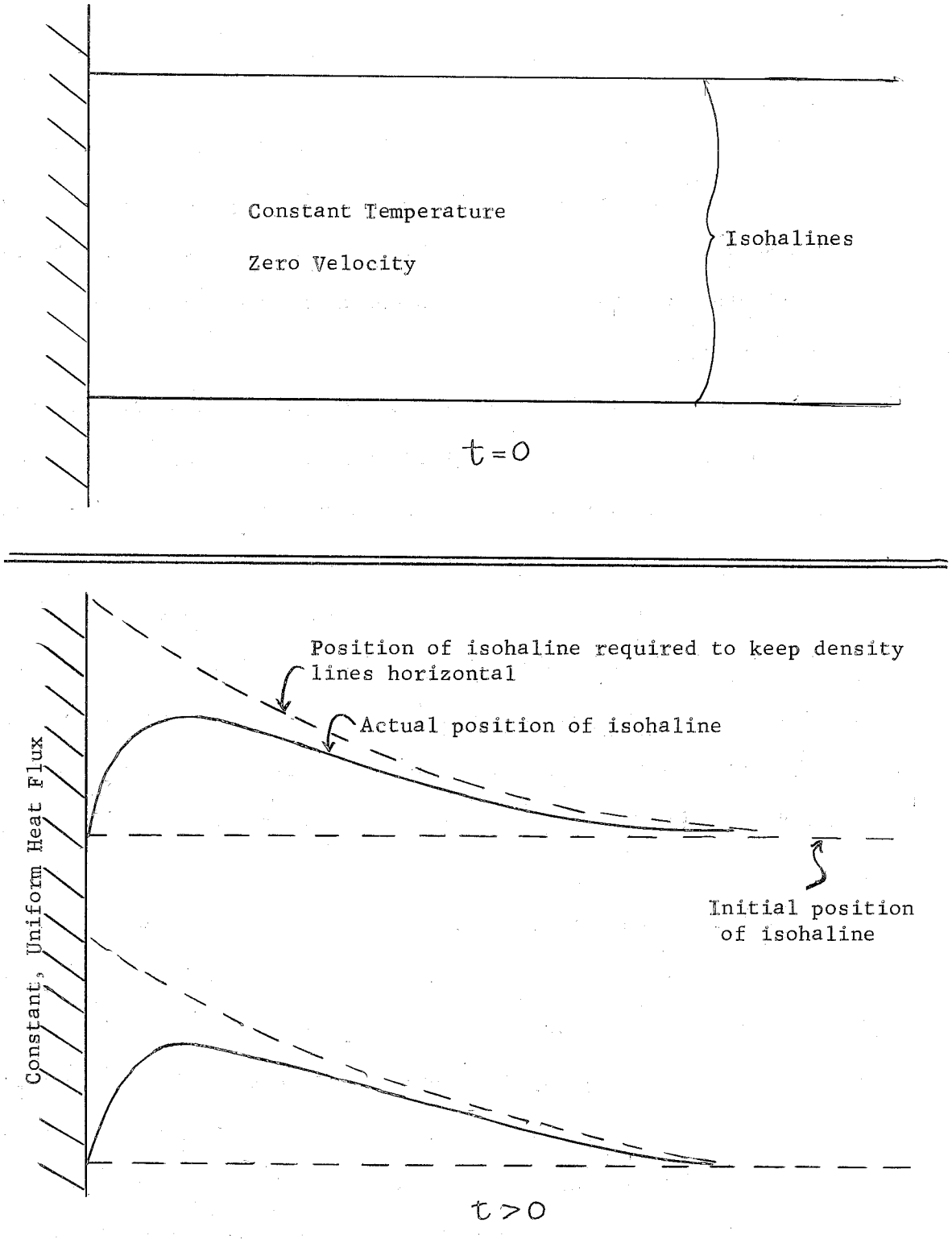

Figure 1. Time Dependence of Basic Flow

Release of Energy

An instability is dependent upon a source of energy and a mechanism for releasing this energy. For the model just described, there is no obvious source of energy since the kinetic energy of the basic field has been neglected and the lines of constant density are horizontal and stably oriented.

The density field is composed of two parts, temperature, which may be conducted away, and salinity, which tends to remain with the fluid particles; therefore, if the contribution of the density gradient due to temperature differences is negated, the remaining portion of the density surfaces will be tilted, providing some available potential energy.

More precisely, assume that the fluid is a perfect conductor of heat and is inviscid; also make the usual Boussinesq assumption on the conservation of mass equation so that the velocity field is non-divergent. The former two assumptions will be relaxed but are convenient to keep the physics in its most simple form at first.

The infinitesimal perturbation hypothesis allows one to look at the dynamics of a single plane wave since interactions between different plane waves occur only for finite amplitude disturbances. Let the wave vector of the plane wave be $\vec{k}=(\ell',m')$; the incompressibility condition says that only transverse waves exist, so that the velocity is perpendicular to the wave-vector, i.e., parallel to lines of constant phase. The dashed lines in Figures 2a and 2b are the nodes (where the perturbation velocity vanishes), and the tilted solid lines are isohalines.

In Figure 2a, both sets of lines are tilted in the same sense, but

the isohalines are steeper. If the particles in the uppermost and lowermost strips are moved to the right and down, then the salinity at points A and C will be increased, thus tending to move the strips

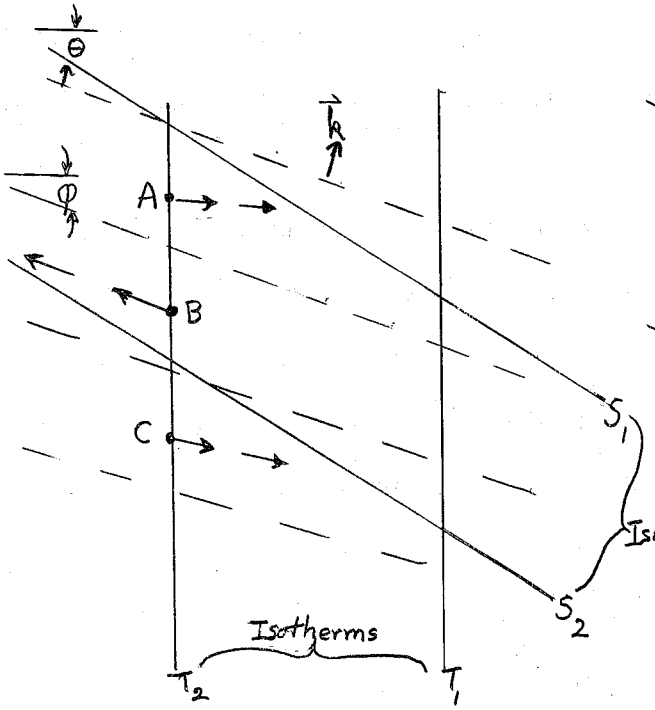

Figure 2a. Unstable Mode

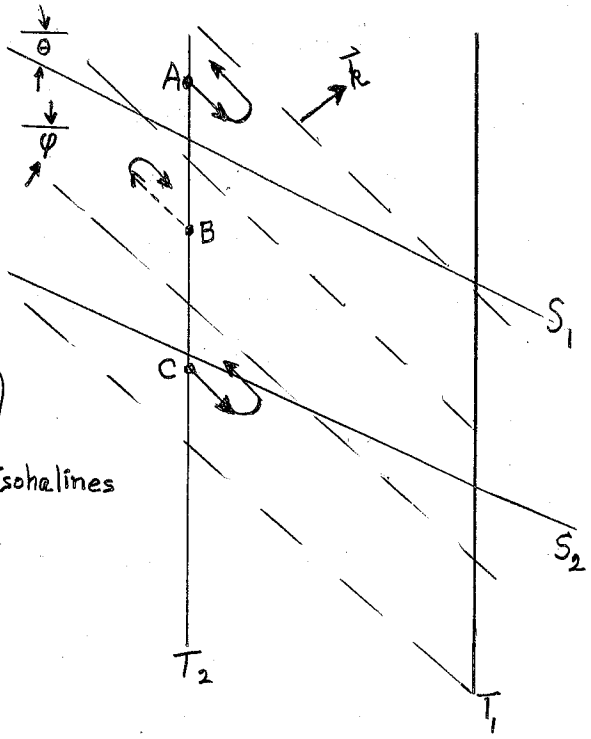

Figure 2b. Stable Mode

of fluid even more down the slope. Note that the new fluid at A and C was originally warmer, which would counteract this motion if it were not for the (assumed) large conductivity of the heat which negates this retardation. The fluid in the middle strip is moved upwards, bringing fresher and colder water to point B. Again the buoyancy due to temperature is conducted away, forcing the fresher (lighter) fluid to rise even more. Consequently, it would seem that for wave-vectors of the form described by Figure 2a, the basic field

is unstable.

On the other hand, Figure 2b demonstrates a neutrally stable mode (in the absence of viscosity). Now, when the particle originally at A is moved down and to the right, fresher (lighter) water appears at location A, resulting in a buoyancy force that would oppose the original motion, much like a simple spring.

If viscosity is included but conductivity remains infinite, those modes that were unstable in its absence remain unstable, since the viscous stress can only slow down the motion, not reverse it; the previously neutrally stable modes become damped, thereby stable.

For this case of infinite conductivity, one may make an analogy with the more familiar problem of Bénard convection. Define a Rayleigh number in the usual way, but in a slightly different form

$$R_a \equiv \frac{-\vec{g} \cdot \vec{\nabla}\left(\frac{\rho}{\rho_{REF}}\right) L^4}{\nu K}$$

Since the temperature effects are instantaneously obliterated by the infinite conductivity of temperature, this expression becomes

$$R_a = \frac{-\vec{g} \cdot (\vec{\nabla} S) L^4}{\nu K_s} = \frac{\left(-\frac{\partial \bar{S}}{\partial z} \cos\theta\right) L^4 (g \sin\varphi) \sin(\theta - \varphi)}{\nu K_s}$$

where θ is the angle of tilt (relative to the horizontal) of the isohalines

φ is the angle of tilt of the lines of constant phase

L is the characteristic length scale of the plane wave

ν is the kinematic viscosity

$\frac{\partial \bar{S}}{\partial z}$ is the original salinity gradient

K_s is the diffusivity of salinity.

The Rayleigh number is a measure of the instability of the basic fields and is maximized when $\varphi = \frac{1}{2}\theta$ and $L = \infty$. This means that the fluid wants to move down lines that are tilted half as much as the isohalines and on very large length scales (to minimize viscous dissipation).

When the conductivity of temperature is finite, very large-scale motions require a long time to create the unstable buoyancy that drives the instability, and very small-scale motions are retarded by viscosity. Physically, it seems reasonable that the maximum instability should occur for some intermediate size.

It is interesting to note the effect of allowing the conductivity of heat to be finite on the value of φ that leads to maximum instability. Finite conductivity reduces the effective density gradient along the strips; if one wants to get back some of this gradient, the value of φ must be reduced somewhat. From this argument it appears that the optimal tilt of the strips will satisfy the following relation,

$$0 < \left|\varphi_{opt}\right| \leq \left|\frac{\theta}{2}\right| .$$

Infinitesimal Instability Theory

The physics described above will now be put into mathematical form. Consider an unbounded (infinite) fluid having constant horizontal gradients of temperature and salinity, $\frac{\partial T_0}{\partial x}$ and $\frac{\partial S_0}{\partial x}$, respectively, a constant (negative) vertical gradient of salinity, $\frac{\partial S_0}{\partial z}$, subject to the condition that the lines of constant density are horizontal with heavier fluid always below lighter fluid. Utilizing the Boussinesq approximation, writing the density as

$$\rho = \rho_{REF} + \rho_{REF}\left[S - \alpha_T T\right] \tag{1}$$

and subtracting the basic hydrostatic pressure from the total pressure, the relevant equations for the perturbation quantities $\vec{u}, P, T,$ and S are

$$\frac{\partial \vec{u}}{\partial t} + (\vec{u}\cdot\vec{\nabla})\vec{u} = -\vec{\nabla}p + g(\alpha_T T - S)\hat{e}_z + \nu\nabla^2\vec{u} \tag{2a}$$

$$\vec{\nabla}\cdot\vec{u} = 0 \tag{2b}$$

$$\frac{\partial S}{\partial t} + \vec{u}\cdot\vec{\nabla}S_o + \vec{u}\cdot\vec{\nabla}S = K_S\nabla^2 S \tag{2c}$$

$$\frac{\partial T}{\partial t} + \vec{u}\cdot\vec{\nabla}T_o + \vec{u}\cdot\vec{\nabla}T = K_T\nabla^2 T \tag{2d}$$

Now make the assumption that disturbances are infinitesimal allowing the equations (2a) - (2d) to be linearized. Since density lines are horizontal,

$$\frac{\partial \rho_o}{\partial x} = 0 = \frac{\partial S_o}{\partial x} - \alpha_T\frac{\partial T_o}{\partial x} \tag{3}$$

Next, set $K_S = 0$, since salt diffuses much slower than heat and introduce a stream function to satisfy the continuity equation, $u = \psi_z$, $\omega = -\psi_x$.

$$\left(\frac{\partial}{\partial t} - \nu\nabla^2\right)\nabla^2\psi - g\frac{\partial S}{\partial x} + g\frac{\partial}{\partial x}(\alpha_T T) = 0 \tag{4a}$$

$$\left(\frac{\partial}{\partial t} - K_T\nabla^2\right)(\alpha_T T) + \left(\frac{\partial S_o}{\partial x}\right)\psi_z = 0 \tag{4b}$$

$$\left(\frac{\partial}{\partial t}\right)S - \left(\frac{\partial S_o}{\partial z}\right)\psi_x + \left(\frac{\partial S_o}{\partial x}\right)\psi_z = 0 \tag{4c}$$

Since all equations are homogeneous and linear, with constant coefficients, assume wave-like solutions,

$$(\psi, S, T) = (\hat{\psi}, \hat{S}, \hat{T})e^{p't + i a' \cos\varphi (z - x\tan\varphi)} \tag{5}$$

Thus, $\frac{2\pi}{a'}$ is the spacing between lines of constant phase and φ is the

tilt of these lines relative to the horizontal. Also, define

$$\beta \equiv -\left(\frac{\partial S_o}{\partial z}\right) > 0 \quad \text{and} \quad \tan\theta \equiv \left(\frac{dz}{dx}\right)_{S_o} = \frac{1}{\beta}\frac{\partial S_o}{\partial x} \tag{6}$$

The eigenvalue p' then satisfies a certain cubic equation, namely

$$0 = p'^3 + p'^2\left(K_T + \nu\right)a'^2 + p'\left\{\nu K_T a'^4 + g\beta \sin^2\varphi\right\} - g\beta K_T a'^2 \sin^2\varphi\left(\frac{\tan\theta}{\tan\varphi} - 1\right). \tag{7}$$

The fastest growing mode may now be determined by finding, for a particular a' and φ' the root of (7) with largest real part, $p'_{max}(a', \varphi)$. Then, maximize p'_{max} with respect to both a' and φ, noting that, in general, the maximum will occur at some non-zero and finite value of a' when K_T and ν are non-zero and finite.

Note that there is a growing mode whenever $\frac{\tan\theta}{\tan\varphi} > 1$, which is exactly the condition that was derived by the simple physical picture just described. The number of independent parameters in (7) may be reduced by introducing a length scale $\mathcal{L}$, and a time scale $\mathcal{T}$.

$$\mathcal{L} \equiv \left(\frac{\nu K_T}{g\beta}\right)^{1/4}; \quad a \equiv \mathcal{L} a' \tag{8a}$$

$$\mathcal{T} \equiv \left(\frac{\mathcal{L}^2}{\nu}\right) = \left(\frac{K_T}{g\beta\nu}\right)^{1/2}; \quad p = \mathcal{T} p' \tag{8b}$$

Finally let σ be the Prandtl number $\left(\sigma \equiv \frac{\nu}{K_T}\right)$.

$$p^3 + p^2 a^2\left(1 + \frac{1}{\sigma}\right) + p \cdot \frac{1}{\sigma}\left(a^4 + \sin^2\varphi\right) - \frac{\sin^2\varphi}{\sigma^2}\left(\frac{\tan\theta}{\tan\varphi} - 1\right) = 0. \tag{9}$$

The fastest growing mode and its growth rate were found for three values of the angle θ, each case having a Prandtl number $\sigma = 7$. The results are shown in the table below.

1. $\tan\theta$	2. θ (degrees)	3. φ_{opt} (degrees)	4. p_{max}	5. (sec^{-1})	6. a_{opt}	7. $(-a \sin\varphi_{opt})$	8. $(a\cos\varphi_{opt})$	9. Δ (cm)
- 1	-45	-15.2	.032	.088	.526	.138	.510	.77
- 5	-78.7	-32.2	.125	.333	.794	.422	.668	.58
-10	-84.3	-37.5	.198	.530	.897	.546	.712	.55

Column 8 has the wave-number in the x-direction for the most rapid growing mode which unfortunately increases for increasing $|\theta|$. This means that as the heat flux across the walls of the container is increased, the spacing of the layers decreases, contrary to observation.

The values of $\mathcal{L}$ and $\mathcal{T}$ defined in equations (8a) and (8b) respectively, depend very weakly on β. Taking $\beta = .001$, the length and time scales are $\mathcal{L} = \frac{1}{16}$ cm and $\mathcal{T} = \frac{3}{8}$ sec. The thicknesses of the layers, Δ, are defined to be vertical wavelengths corresponding to the most rapidly growing mode and are tabulated in column 9. The observed thickness when a $16^{\circ}C$ temperature difference across the wall of the cylinder was maintained, is about 1.2 cm. The magnitude of the growth rate (tabulated in column 5) indicates that the disturbances require only a fraction of a minute to reach finite amplitude.

The instability theory that has been described does indicate the method of release of energy and should yield a fairly good approximation to the size of the layers that are observed. In the absence of diffusion of salinity, the energy releasing mechanism begins at once. These modes, however, grow very slowly since the tilt of the salinity lines remains small for small values of time. At later times, more rapidly-growing modes are

allowed to release energy. It is not clear which mode one would see, thus making an application of the crude model rather difficult since there does seem to be a way of choosing the "effective value" of θ. It is fortunate that Δ, the layer thickness, is rather insensitive to the tilt of the isohalines, as may be seen in Figure 3.

Asymptotic Form of the Basic Fields

In an attempt to justify some of the assumptions made in the preceeding analysis, the form of the basic fields for large values of time will be found. Recall that the fluid is semi-infinite in extent and is heated at the wall located at $x = 0$. The horizontal velocity of this basic flow is zero, thus eliminating most of the advection terms

$$\frac{\partial \vec{u}_0}{\partial t} = -\vec{\nabla} p_0 + \nu \frac{\partial^2 \vec{u}_0}{\partial x^2} - g(S_0 - \alpha_T T_0)\hat{e}_z \tag{10a}$$

$$\frac{\partial T_0}{\partial t} = K_T \frac{\partial^2 T_0}{\partial x^2} \tag{10b}$$

$$\frac{\partial S_0}{\partial t} - \beta \omega_0 = 0 \tag{10c}$$

$$\vec{\nabla} \cdot \vec{u}_0 = 0 \tag{10d}$$

subject to the initial conditions

$$T_0(x,0) = S_0(x,0) = \omega_0(x,0) = 0 \tag{10e}$$

and the boundary conditions

$$\text{as } x = 0, \quad \frac{\partial T_0}{\partial x} = H, \quad \omega_0 = 0 \text{ (for all } t) \tag{10f}$$

$$\text{as } x \to \infty, \quad T_0, \omega_0, S_0, p_0 \to 0 \text{ (for finite } t). \tag{10g}$$

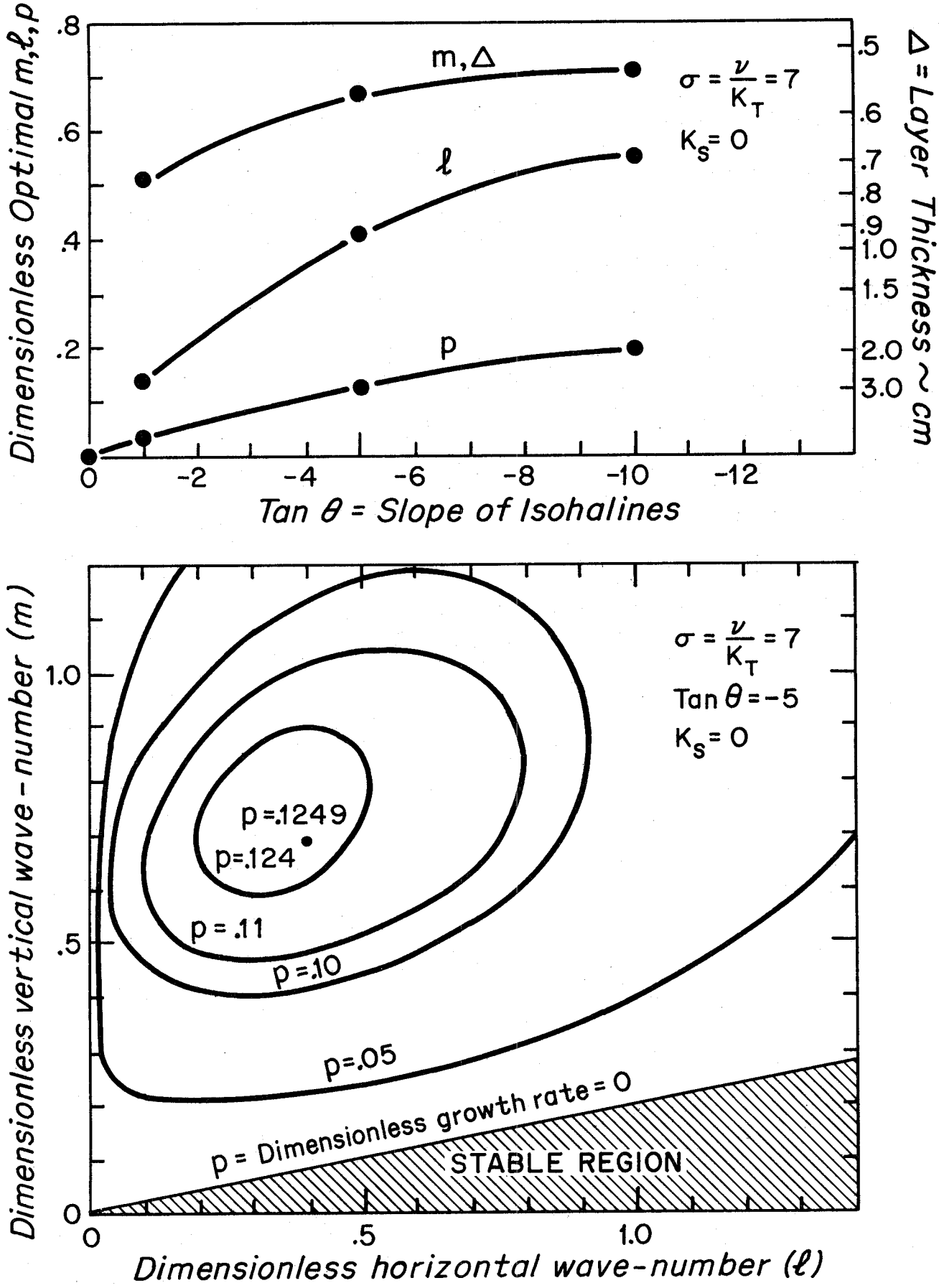

Fig. 3 Optimal Modes of Instability

The x-component of (10a), plus the last boundary condition in (10g) imply that the presure vanishes for all z and all finite t . In addition, (10b) may be solved for the temperature, independent of the other fields

$$\frac{\partial T_o}{\partial x}(x,t) = H\,\mathrm{erfc}\left(\frac{x}{2\sqrt{K_T t}}\right) \tag{11a}$$

$$T_o(x,t) = Hx\,\mathrm{erfc}\left(\frac{x}{2\sqrt{K_T t}}\right) - \frac{2H}{\sqrt{\pi}}\left(K_T t\right)^{1/2} e^{-\frac{x^2}{4K_T t}} \tag{11b}$$

Now the vertical momentum equation and the salinity equation may be combined into a relatively simple equation for S_o ,

$$\frac{\partial^2 S_o}{\partial t^2} + g\beta S_o - \nu \frac{\partial^3 S_o}{\partial x^2 \partial t} = g\alpha_T \beta T_o(x,t) \tag{12a}$$

with

$$S_o(x,0) = \frac{\partial}{\partial t} S_o(x,0) = 0 \tag{12b}$$

$$S_o(0,t) = S_o(\infty,t) = 0 \tag{12c}$$

The problem described by equations (12a) through (12c) is an initial value problem driven by a forcing term possessing a Laplace transform of a rather simple form. So, taking Laplace transforms wherever relevant

$$\frac{\partial^2 \hat{S}_o(x,p)}{\partial x^2} - \left(\frac{p^2 + g\beta}{p\nu}\right)\hat{S}_o(x,p) = \frac{g\beta\alpha_T H}{p\nu}\sqrt{K_T}\,p^{-3/2} e^{-\frac{x\sqrt{p}}{\sqrt{K_T}}} \tag{13a}$$

subject to

$$\hat{S}_o(0,p) = \hat{S}_o(\infty,p) = 0. \tag{13b}$$

The solution of (13a) - (13b) is quite simple

$$\hat{S}_o(x,p) = \alpha_T H\sqrt{K_T}\left\{\frac{p^{-3/2}}{1 + \frac{(1-\sigma)p^2}{g\beta}}\right\}\left\{e^{-\frac{x}{\nu}\sqrt{\frac{p^2+g\beta}{p}}} - e^{-\frac{x\sqrt{p}}{\sqrt{K_T}}}\right\} \tag{14}$$

One of the assumptions made at the outset of the stability analysis was that lines of constant density are horizontal. In order to check this, note that

$$\alpha_T \hat{T}_0(x,p) = -\alpha_T H \sqrt{K_T}\, p^{-3/2} e^{-\frac{x\sqrt{p}}{\sqrt{K_T}}} .$$

Then, subtracting (15) from (14), we obtain the Laplace transform of the density

$$\hat{S}_0(x,p) - \alpha_T \hat{T}_0(x,p) = \frac{H\alpha_T\sqrt{K_T}}{p^{3/2}} \left\{ \frac{\exp\left[-\frac{x}{\sqrt{\nu}}\sqrt{p+\frac{g\beta}{p}}\right]}{1+\frac{(1-\sigma)p^2}{g\beta}} + \frac{(1-\sigma)p^2}{g\beta} \frac{\exp\left[-x\sqrt{\frac{p}{K_T}}\right]}{1+\frac{(1-\sigma)p^2}{g\beta}} \right\} .$$

Taking the asymptotic form of the inversion integrals as $t \to \infty$, all terms tend to zero provided $\frac{x^2 g\beta t}{\nu} \gtrsim 1$.

Thus, the region of viscous importance has the width $\sqrt{\frac{\nu}{g\beta t}}$. Outside this region, for large values of $(g\beta)^{1/2} t$, the basic fields have their lines of constant density horizontal and vertical velocities that decrease with time, being nearly proportional to $t^{-1/2}$.

Summary

In this report, an experimental observation is discussed and a rather crude mathematical model indicates how this experiment sets up an unstable configuration of temperature and salinity, allowing energy to be released on a certain length scale. Not only has this length scale been determined, but the model also suggests other experiments that might be more suited to the assumptions made in the analysis.

Acknowledgments

The author is indebted to the following persons for their invaluable

assistance: Robert Frazel and George Buzyna for their photographic and laboratory assistance; Dr. L. N. Howard, for his assistance in using the computer for obtaining numerical results; Dr. M. McIntyre for his physical insight, and espicially to Dr. G. Veronis, for his general guidance during the entire term on the project.

REFERENCES

Turner, J. S. and Henry Stommel 1964 Proc.Nat.Acad.Sci., 52(1): 49-53

Mason, Max and C. E. Mendenhall 1923 Proc.Nat.Acad.Sci., 9: 199-207

Stern, Melvin 1960 Tellus, 12: 172-175

Hide, R. 1964 "Salt Convection due to Radial Cooling" (Scientific Note HRF/SN4 - unpublished manuscript)

Source-Sink Flow Experiments in a Rotating Fluid

George Buzyna

Introduction

The present problem concerns itself with the question of how fluid is transported from a source to a sink in a rotating system. There has been some interest in source-sink flows recently and a number of papers have appeared on this subject (e.g. Barcilon 1967, Faller 1960, Hide 1967). Source-sink flows can be classified according to where the fluid is introduced through the boundary, whether the region is simply or multiply connected, and whether there is a depth variation. In the present experiment, the fluid is introduced and withdrawn through the top boundary, and the source and sink are taken to be flush with that boundary. Experi-

ments with a depth variation are also considered.

Theoretical consideration

We shall consider the flow in a simplified model and use the results as a guide in the analysis of more complex flows. Consider two plates unbounded in the horizontal plane and separated by some characteristic distance. The system consisting of these plates and the fluid between them rotates about the vertical z-axis with angular velocity Ω . The source and sink are located at equal distances from the origin (this is not essential for the analysis), see Figure 1.

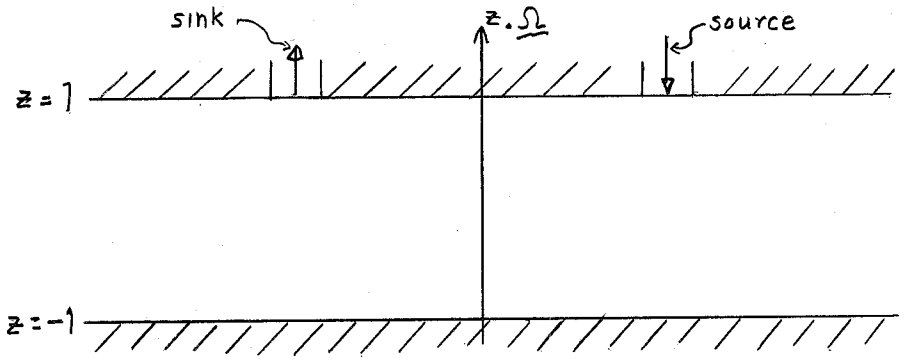

Fig. 1

The equations of motion for an incompressible rotating fluid are given in dimensionless form by

$$\underset{\sim}{v}_t + \epsilon(\underset{\sim}{v}\cdot\nabla)\underset{\sim}{v} + 2\hat{\underset{\sim}{k}}\times\underset{\sim}{v} = -\nabla p + E\nabla^2\underset{\sim}{v} \qquad (1)$$

and

$$\nabla\cdot\underset{\sim}{v} = 0 \ , \qquad (2)$$

where the subscript denotes differentiation, $\underset{\sim}{v}$ and p denote the dimensionless velocity and pressure, and ϵ and E are the Rossby and Ekman

numbers defined below,

$$\epsilon = \frac{V}{\Omega L} \quad , \quad E = \frac{\nu}{\Omega L^2} \, . \tag{3}$$

The symbols V and ν denote a characteristic velocity and the kinematic viscosity of the fluid, and L denotes some characteristic length. We shall restrict our attention in this simplified analysis to steady $(\partial/\partial t \equiv 0)$ and linearized flow ($\epsilon << 1$ or $\epsilon < E^{1/2}$, where $E << 1$). The governing equations become

$$2\hat{k} \times \underset{\sim}{v} = -\nabla p + E\nabla^2 \underset{\sim}{v} \, , \tag{4}$$

$$\nabla \cdot \underset{\sim}{v} = 0 \, , \tag{5}$$

and the boundary conditions for the above problem are given by

$$\underset{\sim}{v} = 0 \quad \text{on} \quad z = -1 \tag{6}$$

$$\underset{\sim}{v} = F(r,\theta)\hat{\underset{\sim}{n}} \quad \text{on} \quad z = 1, \; r = R \; \text{and} \; \theta = \theta_1 \; \text{and} \; \theta_2 \, , \tag{7}$$

subject to the condition that no net mass flux enters the system, i.e.

$$\int_0^{2\pi} d\theta \int_0^{\infty} F(r,\theta)\, dr = 0 \, , \tag{8}$$

where θ denotes the azimuthal angle $(\tan\theta = y/x)$, $r = (x^2 + y^2)^{1/2}$, F the injection velocity, and $\hat{\underset{\sim}{n}}$ the outer normal to the surface.

The solution to this particular problem will not be obtained here, but rather a physical argument based on this system will be given. The flow will be discussed in terms of two distinct regions, the interior flow and the flow in the Ekman boundary layers near the horizontal boundaries. The velocity and pressure variables are written as the sum of two contributions from the interior and the boundary layer, i.e.

$$\underset{\sim}{V} = \underset{\sim}{v} + \tilde{\underset{\sim}{v}} \, , \tag{9}$$

where the tilde denotes the boundary layer variable, and the boundary layer variables vanish in the interior. The governing equations are now ordered in the power of the Ekman number as represented by

$$\underset{\sim}{V} = \sum_{n=0}^{\infty} E^{n/2} \underset{\sim}{v}_n + \sum_{n=0}^{\infty} E^{n/2} \underset{\sim}{\tilde{v}}_n \tag{10}$$

and a similar relation for the pressure. In the interior the horizontal variables and all derivatives are assumed to be of order one. To zero order in E the interior flow is given by the set of equations

$$-2v_0 = -p_{0x}\,, \tag{11}$$

$$2u_0 = -p_{0y}\,, \tag{12}$$

$$0 = -p_{0z}\,, \tag{13}$$

and

$$u_{0x} + v_{0y} + w_{0z} = 0\,. \tag{14}$$

The interior flow is geostrophic given by equations (10) and (11). The equations (10) through (13) reduce to the condition that the flow is non-divergent in the horizontal plane,

$$u_{0x} + v_{0y} = 0 \tag{15}$$

and the Taylor-Proudman condition,

$$u_{0z} = v_{0z} = w_{0z} = 0\,. \tag{16}$$

The same conclusions also hold to first order in E, i.e. the subscript "0" may be replaced by the subscript "1".

In the boundary layer we expect rapid variation of the properties in the vertical direction, in particular we take $\partial/\partial z = O(E^{-1/2})$. Thus, in

the boundary layer the z coordinate is stretched in the manner

$$\zeta = (1 \pm z) E^{-1/2} , \tag{17}$$

and we obtain

$$\partial/\partial z = E^{-1/2} \partial/\partial \zeta , \tag{18}$$

where $\partial/\partial\zeta = O(1)$.

The lowest order equations in the boundary layer at $z = -1$ become

$$p_{0\zeta} = 0 \quad \text{and} \quad \tilde{w}_{0\zeta} = 0 . \tag{19}$$

Since the boundary variables must vanish in the interior, the only possible solutions to equation (19) are

$$\tilde{p}_0 = 0 \quad \text{and} \quad \tilde{w}_0 = 0 . \tag{20}$$

To the next order we have

$$-2\tilde{v}_0 = \tilde{u}_{0\zeta\zeta} , \tag{21}$$

$$2\tilde{u}_0 = \tilde{v}_{0\zeta\zeta} , \tag{22}$$

$$0 = \tilde{p}_{1\zeta} , \tag{23}$$

and

$$\tilde{w}_{1\zeta} = -\tilde{u}_{0x} - \tilde{v}_{0y} . \tag{24}$$

The Ekman boundary layer solution is obtained from equations (19) and (20) and is given by

$$\tilde{u}_0 = (\tilde{u}_0^\circ \cos\zeta + \tilde{v}_0^\circ \sin\zeta) e^{-\zeta} \tag{25}$$

and

$$\tilde{v}_0 = (\tilde{v}_0^\circ \cos\zeta - \tilde{u}_0^\circ \sin\zeta) e^{-\zeta} , \tag{26}$$

where the superscript "o" denotes a value at the boundary. From the integration of equation (24) we obtain

$$\tilde{w}_1 = -\frac{1}{\sqrt{2}}\left\{\left(\tilde{u}^o_{ox}+\tilde{v}^o_{oy}\right)\sin\left(\zeta-\frac{\pi}{4}\right)-\left(\tilde{v}^o_{ox}-\tilde{u}^o_{oy}\right)\sin\left(\zeta-\frac{\pi}{4}\right)\right\}e^{-\zeta} \qquad (27)$$

Identical results are obtained for the boundary layer at $z=1$ with the exception of the vertical velocity which has an opposite sign, i.e.

$$\tilde{w}_1\Big|_{z=1} = -\tilde{w}_1\Big|_{z=-1} . \qquad (28)$$

The source-sink flow may be visualized to take place in the following manner. The flow is induced through the boundary. A high-pressure area is established in the vicinity of the source, with the high-pressure area extending to the bottom boundary. At the same time a geostrophic flow is established in the interior around the source. Similarly, at the sink a low-pressure area and a corresponding geostrophic flow is developed. This flow may be visualized by the following diagram, Figure 2, as viewed along the vertical axis.

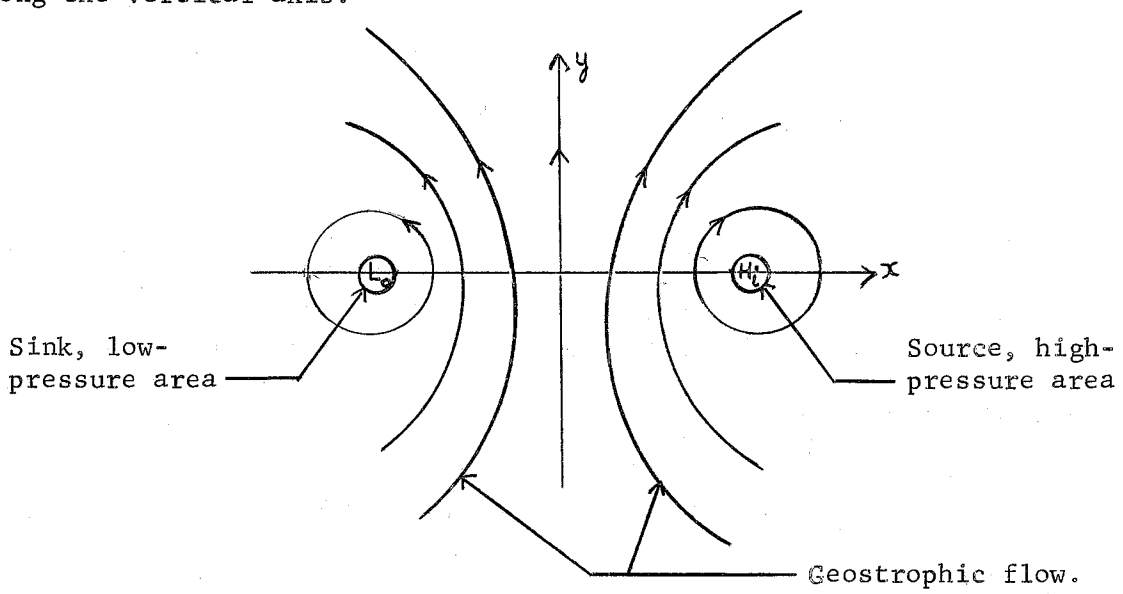

Figure 2.

Thus, the flux of fluid, Q , introduced at the source can not cross over to the sink via the interior. The only place left for the transport of fluid to take place is through the top and bottom boundary layers. Hence, the fluid leaves the source, or high-pressure region, through the boundary layers and enters the sink, or low-pressure region. The transport of fluid through the boundary layer takes place everywhere at a 45° angle to the geostrophic interior flow. This can be seen by taking a simple geostrophic flow in the interior and considering the boundary condition away from the source or sink. Consider a uniform geostrophic flow of velocity v_0 in the y direction. The total velocity at the boundaries is zero, i.e.

$$\underset{\sim}{V}_0^{\circ} = \underset{\sim}{v}_0^{\circ} + \underset{\sim}{\tilde{v}}_0^{\circ} = 0 \qquad \underset{\sim}{v}_0^{\circ} = -\underset{\sim}{\tilde{v}}_0^{\circ} \tag{29}$$

and

$$\underset{\sim}{V}_1^{\circ} = \underset{\sim}{v}_1^{\circ} + \underset{\sim}{\tilde{v}}_1^{\circ} = 0 \qquad \underset{\sim}{v}_1^{\circ} = -\underset{\sim}{\tilde{v}}_1^{\circ} \, . \tag{30}$$

But the interior is geostrophic, and we have $u_{0z} = v_{0z} = 0$, equation (16). Thus, $\tilde{v}_0^{\circ} = v_0$, $\tilde{u}_0^{\circ} = u_0 = 0$ and we obtain $\tilde{v}_0^{\circ} = -v_0$ and $\tilde{u}_0^{\circ} = 0$. The boundary layer velocities have the form (equations (25) and (26),

$$\tilde{u}_0 = -v_0 \sin\zeta \, e^{-\zeta} \, , \tag{31}$$

$$\tilde{v}_0 = -v_0 \cos\zeta \, e^{-\zeta} \, , \tag{32}$$

and the total velocities are:

$$U_0 = -v_0 \sin\zeta \, e^{-\zeta} \, , \tag{33}$$

$$V_0 = v_0 - v_0 \cos\zeta \, e^{-\zeta} \, . \tag{34}$$

The fluxes through the boundary layer in the x and y directions are

$$(\text{Flux})_x = \int_0^\delta U_0 \, d\zeta = -\frac{v_0}{2}, \tag{35}$$

$$(\text{Flux})_y = \int_0^\delta V_0 \, d\zeta = \frac{v_0}{2}, \tag{36}$$

where δ is the thickness of the boundary layer, for boundary layer variables $\delta \to \infty$. Thus the net flux through the boundary is at a 45° angle to the direction of the interior geostrophic flow. If we apply the above locally to the flow configuration represented in Figure 2, we obtain a flow similar to the configuration presented below in Figure 3.

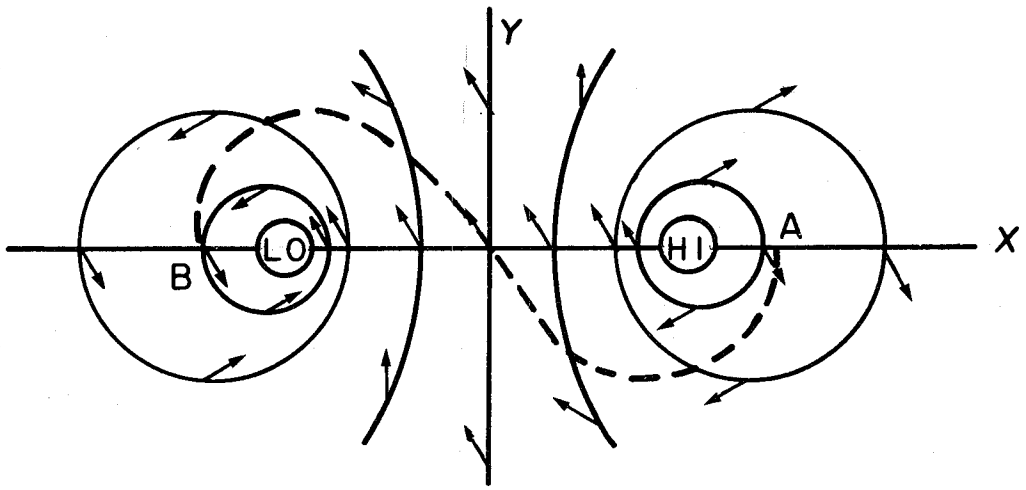

Fig. 3

In this figure, the short arrows represent the direction of the net flux through the top and bottom boundary layers. The dashed line denotes a representative path a fluid element might take from a point A near the source to a point B near the sink in the boundary layers.

During the transport of fluid from the source to the sink there is no suction of fluid from the boundary layers into the interior in the regions away from the source and sink. This can be seen by considering the boundary conditions at the wall, i.e. equations (29) and (30), $w_0^\circ = -\tilde{w}_0^\circ$ and $w_1^\circ = -\tilde{w}_1^\circ$. However, it is recalled that $\tilde{w}_0 = 0$ or $\tilde{w}_0^\circ = 0$, equation (20), and we have $w_0^\circ = w_0 = 0$. We recall further that $w_{1z} = 0$, and thus $w_1^\circ = w_1$; or $w_1 = -\tilde{w}_1^\circ\big|_{z=-1}$ and also $w_1 = -w_1^\circ\big|_{z=1}$. We thus conclude that

$$\tilde{w}_1^\circ\Big|_{z=-1} = \tilde{w}_1^\circ\Big|_{z=1} . \tag{37}$$

But from equations (27) and (28) we have

$$\tilde{w}_1^\circ = \frac{1}{2}\left\{\left(\tilde{u}_{0x}^\circ + \tilde{v}_{0y}^\circ\right) + \left(\tilde{v}_{0x}^\circ - \tilde{u}_{0y}^\circ\right)\right\} \tag{38}$$

and

$$\tilde{w}_1^\circ = -\frac{1}{2}\left\{\left(\tilde{u}_{0x}^\circ + \tilde{v}_{0y}^\circ\right) + \left(\tilde{v}_{0x}^\circ - \tilde{u}_{0y}^\circ\right)\right\} , \tag{39}$$

which leads to the conclusion that if equation (37) is to be satisfied, we must have $\tilde{w}_1^\circ = 0$ and $w_1 = 0$, or that there is no vertical velocity in the interior to the first order in E.

In order that the above flow may be realized in a laboratory it is necessary to consider the conditions under which these results were deduced. We required that $\epsilon \ll 1$, or more specifically that $\epsilon < E^{1/2}$. This inequality may be written in its equivalent form

$$\frac{V}{\Omega L} < \sqrt{\frac{\nu}{\Omega L^2}} \tag{40}$$

where V is some characteristic velocity in the interior and is of order one. Note that the only permitted vertical velocity is $w_1 = w$ and it is

of order $E^{1/2}$. Hence, to the same order we have

$$\nabla \simeq E^{-1/2} w . \tag{41}$$

If we substitute this equation into equation (40), we obtain the important relation

$$w < \frac{\nu}{L} . \tag{42}$$

To insure a flow such as discussed above we take w to be the order of the velocity of the fluid injected at the source and withdrawn at the sink. This relation will insure that we do not exceed the flux of fluid of order $E^{1/2}$ permitted through the boundary.

Experimental apparatus and technique

The experiments were conducted in plexiglass tanks of 29 cm inside diameter placed on a horizontal rotating table with the vertical axis coincident with the rotation axis. The one-meter rotating table of the Woods Hole Oceanographic Institution Theoretical Oceanography laboratory was used. The rigid tank had an inside height of 16.8 cm. Tanks with a free surface were covered during the experiment to avoid wind stresses. A range of angular speeds Ω between 1 and 4.5 rad/sec was used.

Water at room temperature served as the working fluid. The "source" water was introduced from a reservoir mounted approximately one meter above the tank, and the flow rate was controlled by means of different sizes and lengths of capillary tube. The flow rate was monitored during the experiment by a flow meter to be sure that the capillary tube did not become clogged during the course of the experiment. The flow rate was maintained relatively "constant" by the level of the reservoir water. For the

flow rates used in the present set of experiments the rate of drop of the free surface of the reservoir caused an insignificant drop in the flow rate. The "sink" water left the tank through a tube which was opened to the atmosphere in a beaker. In experiments with a free surface, the water was removed via a siphon. The flow rate through the sink would match the flow rate through the source automatically after an equilibrium level of the water was reached. In earlier experiments, a closed circuit pump was used to introduce and withdraw the water. However, the pump proved undesirable since the heating of the fluid could not be avoided.

In the earlier experiments the source and sink consisted of tubes extending 1 to 3 cm into the body of the fluid. At the end of the source a plug of larger area was attached to reduce the velocity of the entering source water. In the final experiments with the rigid surfaces both the sink and source consisted of holes of 1.3 cm in diameter and on the inside of the tank a piece of fine filter paper was taped over the holes to allow the water to reach the rotation of the tank before being introduced into the tank. The filter paper and tape were thinner than the Ekman boundary layer.

The flow was observed with the aid of "neutrally buoyant" dyes, potassium permanganate and fluorescein and by means of the pH indicator technique in a solution of thymol blue titrated to the end-point. When details of a slow flow are desired, the pH indicator technique is by far the best. However, for a qualitative observation of the flow field, fluorescein proved the most advantageous. Small quantities of dye present

in the water which could be barely visible could be more easily detected with a flashlight in a darkened room.

Experimental Observations

Before we proceed with a description of the experimental observations we recall that according to the considerations mentioned above, we desire that the fluid entering and leaving the rotating system satisfy the relation

$$w < \frac{\nu}{L}.$$

This requirement, however, seriously complicates the experiment. Note that for a characteristic length of the order of 10 cm we must have the injection velocity less than 0.001 cm/sec. For a source or sink with a diameter of 1.3 cm a flow rate of the order of 0.001 cm/sec is required. In order to observe such slow flows it is necessary to keep motion due to thermal effects less than the induced desired motions. For this reason the experiments with such slow injection velocities proved unsuccessful. Although the experiment would appear to start out properly, the motion would soon be obscured by the motions due to the thermal effects caused by fluctuations in the room temperature, particularly since several hours are required to observe a significant amount of the introduced dye.

The experiments which are to be described were conducted at higher flow rates, typically 0.1 to 0.3 cc/sec. The resulting flows, however, still preserved the essential features discussed above. The experiments conducted with rigid surfaces will be described first. The source and sink were located on the same diameter and on the circumference of a circle with

a radius of one-half the radius of the tank. As the dyed water was introduced into the rotating system, a column of dyed fluid was established directly below the source. At the same time dyed fluid was observed to move through the boundary layer towards the source. Transport of fluid took place through both boundary layers, and roughly in an s-shaped pattern. In this respect, the flow behaved as expected from the theoretical considerations discussed above. The details of the flow, however, were more complicated. The column which was established became larger than the source with time and did not always remain lodged beneath the source. In fact, the higher the flow rate (0.3 cc/cm) the larger the diameter of the source column. Furthermore, a certain amount of recirculation and mixing could be observed near the source. Due to this recirculation and mixing, it is difficult to determine whether the extension of the source tube into the fluid has an effect on the flow. Also, at the higher flow rates (0.3 cc/sec) instabilities in the boundary layer flow were observed. These instabilities introduce dyed fluid into the interior flow. This problem was noticeably reduced at lower flow rates (0.1 cc/sec). After the dyed fluid reached the area of the sink, the fluid rose off the bottom and extended towards the sink opening in the top boundary as a tightly-wound spiral rather than a simple column. As the spiral extended towards the top boundary, its base became slowly broadened. A simplified schematic diagram of the above observed flow is shown in Figure 4. Columns are shown beneath the source and sink, the spiral near the sink is greatly exaggerated. The general interior flow and its direction was inferred from independent observations using the pH

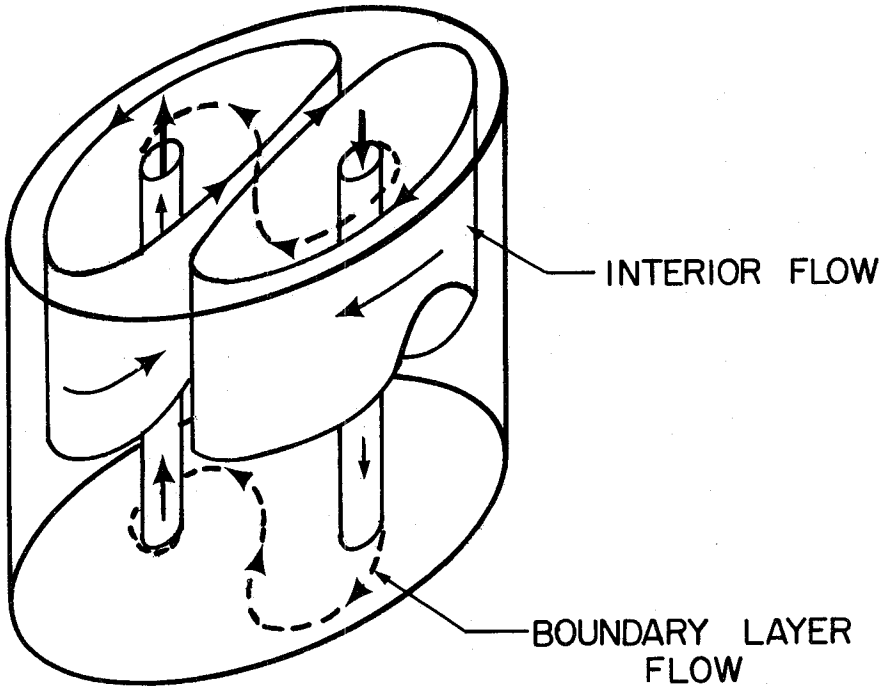

Fig. 4

indicator technique. A line of dye was marked in the interior and its subsequent motion observed. A representative path of the dye in the boundary layer is denoted by the dashed line.

In addition to the rigid top and bottom experiments, a number of experiments with a free surface were also performed. The source and sink were again located opposite each other on the same circle of radius one-half the tank radius. The depth of fluid was varied from a few centimeters (large variation of the depth) to approximately 20 centimeters (small variation of the depth) at the same angular velocity. When the depth variation was small the flow resembled the situation with rigid

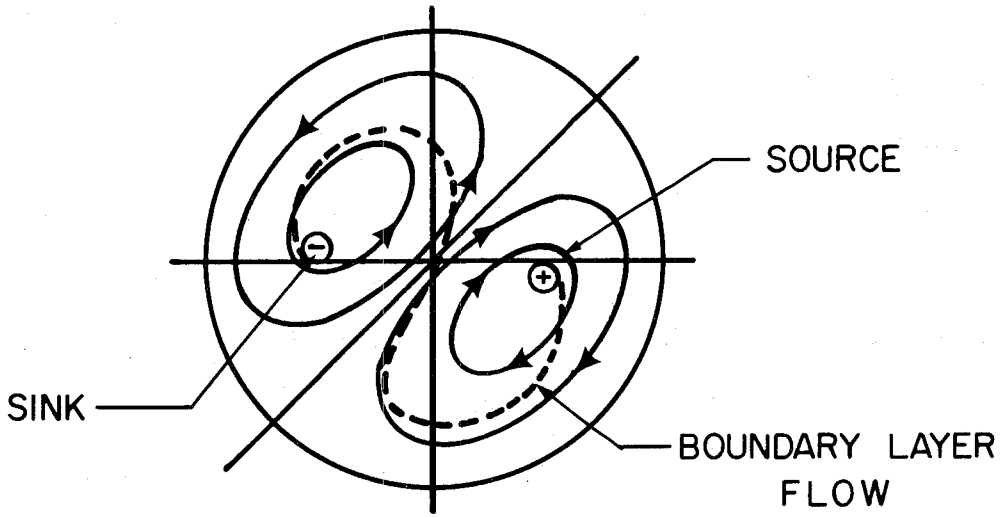

Fig. 5

surfaces. The major difference was that the source and sink were no longer located approximately in the center of the interior flow but significantly off the center and the columns of fluid beneath the source and sink also appeared at the edge of the actual source or sink. A top view of the flow field is shown in Figure 5. The path of the dye in the bottom boundary layer is shown dashed. The interior flows were observed by dropping fluorescein dye (yellow-green) in the interior near the sink and potassium permanganate (red-violet) dye in the interior near the source. The dye formed sheets which followed the general interior flow. The differently colored fluids of the interior flow did not mix, while the potassium permanganate dye introduced in the boundary layer near the source was clearly transported by the boundary layer underneath the fluorescein-colored interior into the region of the sink. When the varia-

tion of the depth of the fluid was large (e.g. the depth at the edge of the tank approximately one and one-half times the depth at the center) a considerably more complicated interior flow was observed and could not be recorded or analyzed easily. Experiments with depth variation with both a free surface and rigid surface and with the source and sink located at different radii were also attempted. These flows, however, were considerably more sensitive to the flow rate (i.e. injection velocity of the fluid through the boundary) than the experiments described above. Experiments with high flow rates (0.1 - 0.3 cc/sec) were difficult to interpret and with slow flow rates ($\sim$ 0.001 cc/sec) the thermal effects obscured and distorted the expected flows.

In the experiments performed above it appears that the velocity with which the fluid is injected through the source into the interior and from the interior through the sink is of primary importance. This point needs to be examined more closely in the future, and in particular the role of equation (42) with respect to the experiments, as well as the appropriate characteristic length in that relation. It appears that if the injection velocity, or the flow rate, is too high, the flow through the boundary layer must be modified. Furthermore, effects such as recirculation and instabilities in the boundary layer also appear.

Acknowledgments

I should like to express my gratitude to Prof. George Veronis for the suggestion of this problem and for his encouragement and guidance. Discussions with and suggestions by Prof. Harvey Greenspan are also

gratefully acknowledged. Discussions with Prof. Willem Malkus and Dr. Alan Faller were also helpful. I am also grateful to Prof. Raymond Hide for providing a tank with a rigid top. Finally, I should like to thank Mr. Robert Frezel for his help and suggestions in the laboratory.

References

Barcilon, V. 1967 J.Fluid Mech. 27: 551

Faller, A. J. 1960 Tellus 12: 159

Hide, R. 1967 (to appear)

On a Numerical Approach to the Dynamo Problem

Alexandre J. Chorin

Introduction

It would be of interest to develop a finite difference procedure for investigating the kinematic dynamo problem (5). The great advantage of finite difference methods lies in their universality, i.e. in the fact that once a numerical program has been developed, it is possible to study a variety of generating velocity fields with only minor changes in the program.

Ideally, one would want to study a dynamo mechanism in a spherical domain surrounded by an insulator extending to infinity; this is the situation of interest in geophysics. Although this can be done in principle, we have not come up with reasonable suggestions as to how this can be done in practice, with today's computers. We therefore restrict ourselves to

the periodic dynamo problem, i.e. a dynamo in a conducting fluid of infinite extent, where the velocity and magnetic induction fields are constrained to be periodic in all three space dimensions. Such dynamos have been studied by other means by G. O. Roberts (4) and S. Childress (1). The dynamo equations are

$$\partial_t \vec{B} = \mathrm{curl}\,(\vec{u} \times \vec{B}) + \eta \Delta \vec{B} \qquad \Delta \equiv \Sigma \partial_j^2 \qquad (1)'$$

$$\mathrm{div}\,\vec{B} = 0 \qquad (2)$$

where $\vec{u}'$ is the generating velocity field, $\vec{B}$ the magnetic induction, η the magnetic diffusivity, x_j are the space variables, and t the time. $\partial_j \equiv \frac{\partial}{\partial x_j}$. The equations are to be solved in a domain $D: 0 \le x_i \le a_i$ $i = 1,2,3$; the a_i are predetermined constants. The boundary conditions are

$$\vec{B}(x_i + a_i) = \vec{B}(x_i).$$

Put

$$t' = \frac{\eta}{d^2} t \qquad u' = \frac{1}{R_e} u \qquad R_e = \frac{ud}{\eta}$$

where u is a reference velocity, d a reference length, and R_e the magnetic Reynolds number. $(1)'$ becomes

$$\partial_t \vec{B} = \mathrm{curl}\,(\vec{u} \times \vec{B}) + \Delta \vec{B} \qquad (1)$$

$\vec{u}$ is a given function of a parameter λ, and the problem is to find a value λ_c of λ such that the corresponding $\vec{B}$ does not decay. λ may be identical to R_e. It is proposed to solve equations (1) - (2) in time for several values of λ, and then search for λ_c. We shall now discuss how this is to be done.

Integration of the equations

A difference scheme which, in our opinion, offers reasonable chances of success is one with which the author already has some experience. It is essentially due to Samarskii (6). We assume

$$div\ \vec{u} = 0$$

equation (1) can be written in the form

$$\partial_t \vec{B} = \Delta B_i + B_j \partial_j u_i - u_j \partial_j B$$

We write

$$B^n_{i(p,q,r)} \equiv B_i(p\Delta x_1, q\Delta x_2, r\Delta x_3, n\Delta t)$$

and we define $B^{n+1/3}, B^{n+2/3}$, and compute B^{n+1} from B^n through the equations

$$\left.\begin{aligned}
B^{n+1/3}_{1(p,q,r)} &= B^n_{1(p,q,r)} + \alpha_1\left(B^{n+1/3}_{1(p+1,q,r)} + B^{n+1/3}_{1(p-1,q,r)} - 2B^{n+1/3}_{1(p,q,r)}\right) - \\
&\quad - u_1\beta_1\left(B^{n+1/3}_{1(p+1,q,r)} - B^{n+1/3}_{1(p-1,q,r)}\right) + \Delta t(\partial_1 u_1) B^n_{1(p,q,r)} \\
B^{n+2/3}_{1(p,q,r)} &= B^{n+1/3}_{1(p,q,r)} + \alpha_2\left(B^{n+2/3}_{1(p,q+1,r)} + B^{n+2/3}_{1(p,q-1,r)} - 2B^{n+2/3}_{1(p,q,r)}\right) - \\
&\quad - u_2\beta_2\left(B^{n+1/3}_{1(p+1,q,r)} - B^{n+1/3}_{1(p-1,q,r)}\right) + \Delta t(\partial_2 u_2) B^{n+1/3}_{1(p,q,r)} \\
B^{n+1}_{1(p,q,r)} &= B^{n+2/3}_{1(p,q,r)} + \alpha_2\left(B^{n+1}_{1(p,q,r+1)} + B^{n+1}_{1(p,q,r-1)} - 2B^{n+1}_{1(p,q,r)}\right) - \\
&\quad - u_3\beta_3\left(B^{n+1}_{1(p,q,r+1)} - B^{n+1}_{1(p,q,r-1)}\right) + \Delta t(\partial_3 u_3) B^{n+2/3}_{1(p,q,r)}
\end{aligned}\right\} \quad (3)$$

$$\alpha_i \equiv \frac{\Delta t}{\Delta x_i^2} \qquad \beta_i \equiv \frac{\Delta t}{2\Delta x_i}$$

and similar expressions for B_2, B_3.

Or, symbolically

$$\left.\begin{aligned}(I-\Delta t Q_1)B_1^{n+1/3} &= B_1^n(1+O(\Delta t))\\ (I-\Delta t Q_2)B_1^{n+2/3} &= B_1^{n+2/3}(1+O(\Delta t))\\ (I-\Delta t Q_3)B_1^{n+1} &= B_1^{n+2/3}(1+O(\Delta t))\end{aligned}\right\} \qquad (4)$$

where $(I-\Delta t Q_1)$ can be written in the form

$$I+\alpha_1 R+\beta_1 J$$

$$R \equiv \begin{pmatrix} 2 & -1 & 0 & 0 & \cdots & -1 \\ -1 & 2 & -1 & 0 & \cdots & 0 \\ 0 & -1 & 2 & -1 & \cdots & 0 \\ & & & \vdots & & \\ -1 & 0 & 0 & \cdots & -1 & 2 \end{pmatrix}$$

$$J \equiv \begin{pmatrix} 0 & u_{1(1)} & 0 & \cdots & 0 & -u_{1(1)} \\ -u_{1(2)} & 0 & u_{1(2)} & 0 & \cdots & 0 \\ & & \vdots & & & \\ u_{1(m)} & \cdots & & & -u_{1(m)} & 0 \end{pmatrix}$$

with again, similar expressions for $I-\Delta t Q_i$, $i=2,3$. We assume

$$\Delta t = O(\Delta X^2) \qquad \Delta X = \min_i (\Delta X_i).$$

In practice, it is determined by the values of $\vec{u}(x)$, through the requirement that $\Delta t^2 Q_i Q_i$ be negligible compared to $\Delta t\, Q_i$. It is expected

that values of Δt larger than those allowed by an explicit scheme will be used with impunity. The scheme (3) is comparatively simple from a computing point view, and requires no intermediate storage.

Theorem 1. If $\left[\max_i \max_D |u_i|\right]\cdot\Delta X<1$, $(I-\Delta t Q_i)$ are invertible.

Indeed, if that condition is satisfied, $(I-\Delta t Q_i)$ are strictly diagonally dominant (see (7), page 23), and therefore non-singular and invertible.

It can further be shown that for reasonable values of Δt, $I-\Delta t Q_i$ are well conditioned, and can be inverted on a computer by a simple algorithm, based on a Jordan-Gauss factorisation (see (2)).

We can write then

$$B_1^{n+1} = \left[\prod_{\ell=1}^{3}\left(I-\Delta t Q_\ell\right)^{-1}\right]\left(1+O(\Delta t)\right)B_1^n \qquad (5)$$

etc. We shall henceforth assume that the inequality of Theorem 1 is satisfied.

Stability of the scheme

We have proved stability for the scheme (3) only for a constant $\vec{u}$. Experience and common sense indicate that the scheme will be stable also with variable $\vec{u}$; a definite gap in the argument remains however.

Assume $\vec{u}=\vec{C}$, $\vec{C}$ a constant vector. The stability proof for (3) in the L_2 norm is straightforward. We put (see (3))

$$B_i^n = B_i^* r^n \exp j(\ell k_\ell x_\ell) \qquad j=\sqrt{-1}$$

where $(k_1,k_2,k_3)=\vec{k}$ is a wave vector, r an amplification factor, and B_i^* a constant. We find

$$r = \prod_{\ell=1}^{3} \left[\frac{1}{1 + \alpha_\ell 2(\cos\theta_\ell - 1) + i 2\beta_\ell \sin\theta_\ell} \right] \qquad \theta_\ell \equiv k_\ell \Delta x_\ell$$

hence $|r| \leq 1$. Stability follows.

Let us rewrite this proof in the space of the operators $(I - \Delta t Q_i)$ rather than that of their Fourier transforms. Because of the form of (5), it is enough to show that the powers of each of the operators $(I - \Delta t Q_i)^{-1}$ are uniformly bounded. Let us consider the powers of $(I - \Delta t Q_1)^{-1}$. Consider the L_2 norm $\|A\|$ of a matrix A. We have

$$\|A\| = \sqrt{\sigma(AA^T)}$$

when $\sigma(AA^T)$ is the spectral radius of AA^T, and A^T is the transpose of A. We will now show that $\|(I - \Delta t Q_1)^{-1}\| \leq 1$ for $\vec{u} = \vec{c}$.

We have

(i) The eigenvalues of $I + \alpha_1 \mathcal{R}$ are real because $I + \alpha_1 \mathcal{R}$ is symmetric;

(ii) The eigenvalues of $I + \alpha_1 \mathcal{R}$ are bounded below by $+1$; indeed, for $\lambda < 1$, the matrix

$$(I + \alpha_1 \mathcal{R} - \lambda I)$$

is strictly diagonally dominant, hence non-singular.

(iii) $J^T = -J$

(iv) $J\mathcal{R} = 2J$

(v) $\mathcal{R} J^T = 2J^T = -J\mathcal{R}$

(vi) All the eigenvalues of $(I - \Delta t Q_1)(I - \Delta t Q_1^T)$ are ≥ 1 in absolute value. Indeed,

$$(I - \Delta t Q_1)(I - \Delta t Q_1^T) = (I - \alpha\mathcal{R})^2 + \beta_1^2 J J^T \text{ by (v)}$$

Let λ be an eigenvalue of $(I - \Delta t Q_1)(I - \Delta t Q_1^T)$.

$$|\lambda|^2 \geq \min_{u\neq 0}\left[\frac{(u,[(I-\alpha R)^2+\beta_1^2 JJ^T]u)}{(u,u)}\right] = \min_{u\neq 0}\left[\frac{(u,[(1-\alpha R)^2 u)}{(u,u)} + \beta_1^2\frac{(u,JJ^T u)}{(u,u)}\right]$$

$$\geq 1 + \beta_1^2\frac{(J^T u, J^T u)}{(u,u)} \quad \text{by (ii)}$$

$$\geq 1 .$$

It follows that

$$\sigma\left((I-\Delta t Q_1)^{-1}\left((I-\Delta t Q_1)^{-1}\right)^T\right) \leq 1$$

We have proved again that (3) is stable in the L_2 norm.

We would like to tighten one of these arguments so as to obtain stability in the maximum norm. Unlike what is usually done, we shall use the second argument. The proof will emphasize once again the close relation between stability theory and convergence theory for iteration schemes. Let $\overset{m}{u}$ be an arbitrary vector in E^m

$$\overset{m}{u} = (u_1, \ldots \quad u_m)$$

we define the maximum norm of u, $\|u\|_{max}$, by

$$\|\overset{m}{u}\|_{max} = \max_{1\leq j\leq m} |u_j|$$

Let $(I-\Delta t Q_1)_m^{-1}$ be the matrix representing $(I-\Delta t Q_1)^{-1}$ in E^m.

We have to show that, for n large enough

$$\|(I-\Delta t Q_1)_m^{-n}\overset{m}{u}\|_{max} \leq C\|u\|_{max}$$

for all $\overset{m}{u}$, where C is independent of both m and n.

For future use, we introduce the vector

$$\Psi = \frac{1}{\sqrt{m}}(1, 1, \ldots \quad 1)$$

we have

(i) $\mathcal{R}\psi = 0, \quad J\psi = 0, \quad J^T\psi = 0$

(ii) $(I + \alpha_1 \mathcal{R})^{-1}\psi = (I + \alpha_1 \mathcal{R} + \beta_1 J)^{-1}\psi = \psi$

That these relations must hold follows from the consistency of difference scheme.

Theorem 2. $\lambda = 1$ is a simple eigenvalue of $(I+\alpha_1\mathcal{R}+\beta_1 J)^{-1}$, and there are no other eigenvalues of modulus ≥ 1 .

Proof:

We have shown that the eigenvalues of $(I+\alpha_1\mathcal{R}+\beta_1 J)^{-1}$ are bounded in modulus by 1 , (since $\sigma(A) \leq \|A\|$, for all norms $\|\ \|$), and that the eigenvalue $\lambda = 1$ is achieved, for the eigenvector ψ .

$I+\alpha_1\mathcal{R}$ is a positive definite, symmetric, real matrix for all m , and has non-positive off-diagonal terms. Its inverse is therefore positive in the sense of Perron-Frobenius ((7), page 85). The largest eigenvalue of $(I+\alpha_1\mathcal{R})^{-1}$ is 1 , and by a standard theorem ((7), page 30), it is a simple eigenvalue. There are of course no other eigenvalues of modulus 1. Now assume that 1 is not a simple eigenvalue of $(I+\alpha_1\mathcal{R}+\beta_1 J)^{-1}$, or that there is another eigenvalue of modulus 1 . Then there exists a vector $u_1 \neq \psi$ such that

$$\|(I+\alpha_1\mathcal{R}+\beta_1 J)^{-1}u_1\|_h \geq \|u_1\|_h \qquad (\|u\|_h \equiv \sqrt{(\bar{u},u)})$$

put $$u_2 = (I+\alpha_1\mathcal{R}+\beta_1 J)^{-1}u_1$$

we have $$u_2 \neq \psi$$

and

$$\|u_2\|_h^2 \geq \|(I+\alpha_1 R+\beta_1 J)u_2\|_h^2 = ((I+\alpha_1 R+\beta_1 J^T)\bar{u}_2, (I+\alpha_1 R+\beta_1 J)u_2) =$$

$$= \|(I+\alpha_1 R)u_2\|_h^2 + \|\beta_1 J u_2\|_h^2 \geq \|(I+\alpha_1 R)u_2\|_h^2$$

however, since $u_2 \neq \psi$ and 1 is the only eigenvalue of modulus 1 of $(I+\alpha_1 R)^{-1}$, we have

$$\|(I+\alpha_1 R)u_2\|_h^2 > \|u_2\|_h^2$$

which leads to a contradiction, q.e.d.

This proof has some independent interest; it provides a convergence proof for iteration schemes for a class of non-symmetric matrixes which actually occur in practice.

Theorem 3. Let λ_2 be the second largest eigenvalue of $(I+\alpha_1 R)^{-1}$, and $\tilde{\lambda}_2$ the eigenvalue of second smallest modulus of $(I+\alpha_1 R+\beta_1 J)^{-1}$, then

$$|\tilde{\lambda}_2| \leq \lambda_2 .$$

Proof:

Let u be an eigenvector associated with $\tilde{\lambda}_2$. Let $\bar{\Phi}$ be the subspace of vector φ such that $(\bar{\varphi}, \psi) = 0$. Write

$$u = a\varphi + b\psi \qquad \varphi \in \bar{\Phi}$$

We have

$$(I+\alpha_1 R+\beta_1 J)^{-1}(a\varphi+b\psi) = \tilde{\lambda}_2 (a\varphi+b\psi)$$

or

$$(a\varphi+b\psi) = \tilde{\lambda}_2 (I+\alpha_1 R+\beta_1 J)(a\varphi+b\psi)$$

$$= \tilde{\lambda}_2 (I+\alpha_1 R+\beta_1 J) a\varphi \; \tilde{\lambda}^2 b\psi$$

since $J\psi = R\psi = 0$.

If $\varphi \in \bar{\Phi}$, so does $(I+\alpha_1 R+\beta_1 J)\varphi$, since

$$(\bar{\psi}, (I+\alpha_1 R+\beta_1 J)\varphi) = ((I+\alpha_1 R+\beta_1 J^T)\bar{\psi}, \varphi) = (\bar{\psi}, \varphi) = 0$$

Hence

$$\tilde{\lambda}_2 b = b$$

and $b=0$ since, from theorem 2, $|\tilde{\lambda}_2| < 1$. Therefore $u \in \Phi$. The theorem follows by the arguments previously used, applied to $(I+\alpha_1 R+\beta_1 J)^{-1}$ operating in Φ .

Corollary: All the eigenvalues of $(I+\alpha_1 R+\beta_1 J)^{-n}$ except $\lambda = 1$ are bounded by $e^{-Cn\Delta t}$, where C does not depend on m . This follows from theorem 3, and the fact that such estimates can be obtained for the eigenvalues of $(I+\alpha_1 R)^{-1}$, using the complete set of eigenvectors

$$1, \cos \alpha_j x_1, \sin \alpha_j x_1 .$$

Theorem 4. The scheme (3), with $\vec{u} = \vec{c}$, is stable in the maximum norm.

Proof: By theorem 3, for every m , there is an n_0 such that for each $\overset{m}{u} \in E^m$ and $n \geq n_0$

$$\| (I - \Delta t\, Q_1)^{-n} \overset{m}{u} \|_{max} \leq \| (\psi, \overset{m}{u})\psi \|_{max} + \| \overset{m}{u} \|_{max}$$

Each component of $(\psi, \overset{m}{u})$ is

$$\frac{1}{\sqrt{m}} \left(\sum_{i=1}^{m} \overset{m}{u}_i \frac{1}{\sqrt{m}} \right) \leq \frac{1}{m} \sum_{i=1}^{m} |\overset{m}{u}_i| \leq \| \overset{m}{u} \|_{max}$$

Hence

$$\| (I - \Delta t\, Q_1)^{-n} \overset{m}{u} \|_{max} \leq 2 \| \overset{m}{u} \|_{max}$$

q.e.d.

Let $D_1 u = \dfrac{u^n_{i+1,j,k} - u^n_{i-1,j,k}}{2\Delta x_1}$ and similar definitions for $D_2 u, D_3 u$.

Theorem 5. $D_i B_j$ remain bounded, when B_j are computed by (3), and $\vec{u} = \vec{C}$.

Proof: D_i and $(I - \Delta t Q_\ell)$ commute, hence $D_i B_j$ satisfy the same equations as B_j and remain bounded by theorem 4.

The error in $div \vec{B} = 0$.

From the differential equations (1), (2), we see that if $div \vec{B} = 0$ at time $t = 0$, then $div \vec{B} = 0$ for all time. The analogous statement does not hold for our difference scheme, since the finite difference analogue to $div\, curl \equiv 0$ does not hold. It is conceivable therefore that the error in the equation of continuity will grow like e^{ct} $c > 0$, the scheme being accurate to $O(\Delta t)$. This would be catastrophic, especially if the λ -search turns out to be lengthy. We shall now show that if simple precautions are taken, this growth of error does not occur.

We assume that it has been shown that scheme (3) is stable for variable $\vec{u}$.

Let

$$\varphi \equiv \sum_\ell D_\ell B_\ell$$

when the D_ℓ are, as before, centered difference approximations to ∂_ℓ. The equation

$$div \vec{B} = 0$$

is then approximated by

$$\varphi = 0 .$$

We want to show that φ remains not only bounded, but small, as a consequence of equations (3). φ may be expanded in a Fourier series, and we note that it is possible to insure that this expansion contain no

constant term, by correcting φ at the periodic boundaries. We assume that this is done.

We note then that φ^n satisfies an equation of the form

$$\varphi^{n+1} = L\varphi^n + O(\Delta t^2)$$
$$L\varphi \equiv \left[\prod_{\ell=1}^{3}(I+\alpha_\ell \mathcal{R}_\ell)^{-1}\right]\varphi$$

This is so because $\mathcal{R}_\ell$ and $\mathcal{D}_k$ commute, and the remaining terms are approximations of second order in Δx_i to differential expressions which vanish. Now because of linearity we can write

$$\varphi^{n+1} = \sum_{k=0}^{n+1} O(\Delta t^2)\, T\big((n+1-k)\Delta t\big)$$

where $T(j)$ is the solution of $\varphi^{j+1} = L\varphi^j$ at time $j\Delta t$ which had taken the value $O(1)$ at time $t=0$. We already noted that if the constant component in $T(j)$ is excluded,

$$|T(j)| \le e^{-cj\Delta t}$$

hence

$$\varphi^{n+1} \le \sum_{k=0}^{n+1} O(\Delta t^2)\, e^{-c(n+1-k)\Delta t}$$
$$\le O(\Delta t^2)\,\frac{1-e^{-c(n+1)\Delta t}}{1-e^{-c\Delta t}} = O(\Delta t)$$

and φ does not increase exponentially.

The λ search. The task of finding λ_c, the value of λ for which a dynamo exists, still remains. Let us write equation (3) symbolically as

$$D_t \vec{\mathcal{B}} = L(\lambda)\vec{\mathcal{B}} \qquad (6)$$

One possibility is to integrate (6) in time for various values of λ and then decide by inspection when the dynamo is maintained. This is however

a wasteful procedure.

For cases where there is reason to believe that a steady dynamo exists, we can construct the auxiliary system

$$D_\tau \vec{B} = L(\lambda)\vec{B}$$

$$D_\tau \lambda = -\alpha D_\tau \|\vec{B}\|$$

where τ is an artificial time, $\|\vec{B}\|$ is a measure of $\vec{B}$ (e.g. $\int B^2 dV, \int \left(\frac{\partial B}{\partial t}\right)^2 dV$), α is a constant, and it is assumed that dynamo action increases with increasing λ (if it doesn't, we redefine λ). It is hoped that the solutions of (7) converge to the steady dynamo and λ_c. We plan to investigate the system (7) by applying the underlying procedure to the search for the eigenvalues of

$$\Delta f + k^2 f = 0 \qquad \Delta \equiv \sum_\ell \partial_\ell^2$$

using the auxiliary system

$$D_\tau f = \Delta f - k^2 f$$

$$D_\tau (k^2) = -\alpha D_\tau \|f\| .$$

It is hoped that an appropriate definition of $\|f\|$ and a good value of α will emerge from such an investigation.

References

(1) Childress, S. 1967b. Report AFOSR-67-0124, Courant Institute

(2) Faddeeva, V. N. 1959 Computational methods of linear algebra. Dover.

(3) Richtmyer, R. 1957 Finite difference methods for initial value problems. Interscience.

(4) Roberts, G. O. Lecture 7 or 8. Dynamo waves (to appear in book)

(5) Roberts, P. H. 1967 Lecture notes, Geophysical Fluid Dynamics program.

(6) Samarskii, A. A. 1963 U.S.S.R. Computational Mathematics and Mathematical Physics, 5: 894

(7) Varga, R. 1962 Matrix iterative analysis. Prentice Hall.

On a Generalization of Maxwell Material

Carlo Denis

Summary.

In this paper we shall try to generalize somewhat the concept of a Maxwell body, in such a manner as to include non-isotropic behavior and finite strain, and give this simple model a physically more realistic picture than that of a spring and a dashpot connected in series. We shall show that in the general case orientation plays in fact a major role, and give a possible differential representation of such a material.

1. Introduction. Description of the gross deformation.

Let us consider a macroscopic body which we deform during time. We shall assume that this body, which we shall call a "macrostructure", is initially unstrained and under no stress (except for a hydrostatic pressure), as well as in thermal equilibrium. We also assume that the deformation which we are able to control (and which we shall call, for later use, a "gross"- or a "macro"-deformation) is very slow compared to molecular processes, so that we may speak of an isothermal deformation. We assume further that this macro-deformation can be described in terms

of continuum mechanics, and we use the Lagrange representation.

Let $\Sigma_0(\hat{X}_1, \hat{X}_2, \hat{X}_3)$ be a fixed Cartesian frame, and consider any given mass point whose position vector at time $\tau = 0$ is $\overrightarrow{OP_0}$, of components (X_1, X_2, X_3) in the frame Σ_0. We shall specify this mass point throughout the deformation of the macrostructure by

$$\vec{X} = X_i \hat{X}_i \quad , \tag{1}$$

using the summation convention of repeated indices.

At any later time τ the same mass point (always labelled $\vec{X}$) will occupy in the frame Σ_0 the geometrical position P, the position vector $\overrightarrow{OP}$ having in Σ_0 components (x_1, x_2, x_3). All information about the deformation and the successive configurations of the macrostructure is of course contained in the vector transformation relations

$$\vec{x} = \vec{x}(\vec{X}, \tau) \, , \tag{2}$$

which are supposed to be given for every mass point $\vec{X}$ in the continuum, such that

$$\vec{x}(\vec{X}, 0) = \vec{X} \, . \tag{3}$$

Consider now two mass points $\vec{X}$ and $\vec{X} + d\vec{X}$ which initially are very close to each other and which move, during the time interval $[0, \tau]$, respectively to the geometrical positions $\vec{x}$ and $\vec{x} + d\vec{x}$. (Fig. 1).

By expanding $\vec{x}(\vec{X} + d\vec{X}, \tau) = \vec{x}(\vec{X}, \tau) + d\vec{x}$ into a simple Taylor series, we get

$$x_i(\vec{X} + d\vec{X}, \tau) = x_i(\vec{X}, \tau) + \frac{1}{1!} dX_j \left(\frac{\partial x_i}{\partial X_j}\right)_{\vec{X}, \tau} + \frac{1}{2!} dX_j dX_k \left(\frac{\partial^2 x_i}{\partial X_j \partial X_k}\right)_{\vec{X}, \tau} + \cdots$$

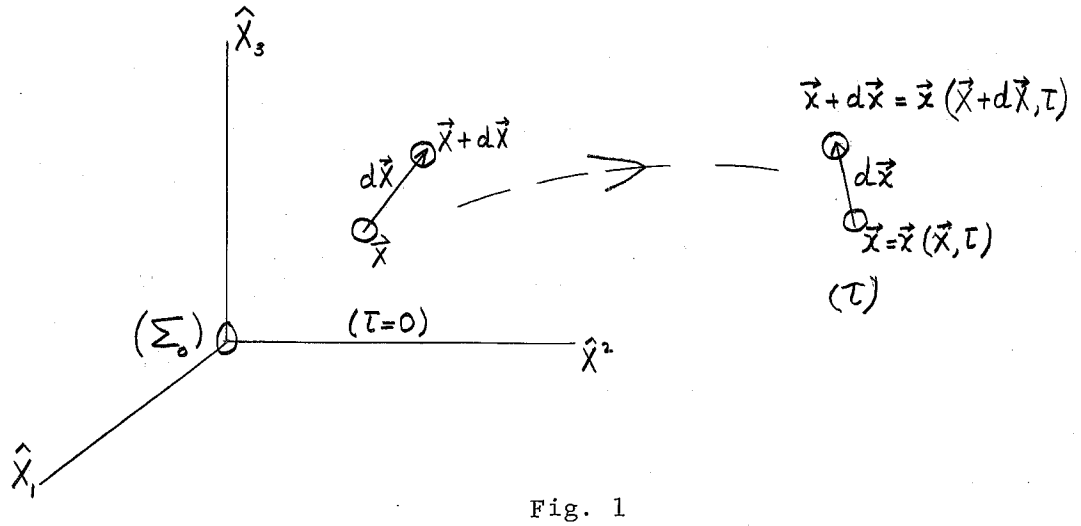

Fig. 1

i.e.

$$dx_i = x_i(\vec{X}+d\vec{X},\tau) - x_i(\vec{X},\tau) = D_{ij}\,dX_j + \tfrac{1}{2} D_{ijk}\,dX_j\,dX_k + \cdots \qquad (4)$$

where

$$D_{ij} \equiv \left(\frac{\partial x_i}{\partial X_j}\right)_{\vec{X},\tau} \quad , \text{ etc.} \qquad (5)$$

is the (i,j)-component of the Jacobian matrix of the transformation, which we shall look at in this context as the tensor of deformation gradients $\underset{\sim}{D}$. In general, this tensor is composed of 9 <u>independent</u> quantities.

In the undeformed initial state, the metric is of course

$$(\tau=0): \qquad dX^2 = dX_i\,dX_i = g_{ij}(0)\,dX_i\,dX_j ,$$

i.e.

$$g_{ij}(0) = \delta_{ij} \cdot \qquad (6)$$

At time τ , the macrostructure is generally in a deformed state, and we define a tangential metric by

$$(\tau=\tau) \qquad dx^2 = dx_i\, dx_i$$

$$= D_{ij}\, dX_j\, D_{ik}\, dX_k$$

$$= D_{ij}\, D_{ik}\, dX_j\, dX_k$$

$$= g_{jk}\, dX_j\, dX_k \,,$$

i.e.

$$g_{jk}(\tau) = D_{ij}\, D_{ik} \,; \tag{7}$$

Eqn. (7) defines the (j,k)-component of a symmetric tensor

$$\underset{\sim}{g} = \underset{\sim}{D}^T \underset{\sim}{D} \tag{7'}$$

called the metric tensor or Green's strain tensor.

This metric assumes that we limit the description of the deformation to first order terms: parallel features remain parallel all the time, and we assume that curvature effects are negligible. Under these circumstances the deformation is completely defined by the tensor of deformation gradients $\underset{\sim}{D}$:

$$d\vec{x} = \underset{\sim}{D} \cdot d\vec{X} \tag{4'}$$

The determinant of $\underset{\sim}{D}$ measures the ratio of the deformed volume to the initial one:

$$\det \underset{\sim}{D} = \frac{v}{v_0} \,. \tag{8}$$

Clearly

$$\det \underset{\sim}{D}(0) = 1 \,; \tag{9}$$

we assume that

$$\det \underset{\sim}{D}(\tau) > 0 \,, \qquad \forall \tau \,. \tag{10}$$

The strain tensor $\underset{\sim}{g}$ however, which is a symmetric tensor, contains at most 6 independent quantities, and thus contains less information than $\underset{\sim}{D}$.

From a fundamental theorem in algebra we know that $\underset{\sim}{D}$ can be written

$$\underset{\sim}{D} = \underset{\sim}{R}\,\underset{\sim}{g}^{1/2} \quad , \tag{11}$$

where $\underset{\sim}{g}^{1/2}$ is symmetric like $\underset{\sim}{g}$, and $\underset{\sim}{R}$ is a matrix describing an adequate orthogonal transformation.

Moreover, taking the time-derivative of $\underset{\sim}{D}$, we get

$$\dot{D}_{ij} = \frac{\partial v_i}{\partial x_p}\,\frac{\partial x_p}{\partial X_j} = \frac{\partial v_i}{\partial x_p}\,D_{pj} \quad ,$$

or

$$\dot{D}_{ij}\,D^{-1}_{jp} = \frac{\partial v_i}{\partial x_p} \quad . \tag{12}$$

We define

$$\dot{\underset{\sim}{D}}\,\underset{\sim}{D}^{-1} = \underset{\sim}{V} + \underset{\sim}{\Omega} \quad , \tag{13}$$

where

$$\begin{cases} V_{ip} = V_{pi} = \frac{1}{2}\left(\frac{\partial v_i}{\partial x_p} + \frac{\partial v_p}{\partial x_i}\right) \quad , \\ \Omega_{ip} = -\Omega_{pi} = \frac{1}{2}\left(\frac{\partial v_i}{\partial x_p} - \frac{\partial v_p}{\partial x_i}\right) \quad , \end{cases} \tag{14}$$

$\underset{\sim}{V}$: rate of strain tensor (symmetric),

$\underset{\sim}{\Omega}$: rate of rotation tensor (antisymmetric).

2. Concept of a Maxwell body and certain aspects of viscoelastic behavior.

Let us consider the following simple model of an elastic element (spring) and a viscous element (dashpot) connected in series. (Fig. 2). Under a uniaxial tension the rate of strain of such a system will be

$$\dot{\epsilon} = \dot{\epsilon}_s + \dot{\epsilon}_D \quad . \tag{1}$$

The most simple behavior which such a system could possibly show is given by

$$\dot{\epsilon}_s = \frac{\dot{\sigma}}{E} \qquad \text{(linear elasticity),} \tag{2}$$

$$\dot{\epsilon}_D = \frac{\sigma}{\eta} \qquad \text{(Newtonian viscosity);} \tag{3}$$

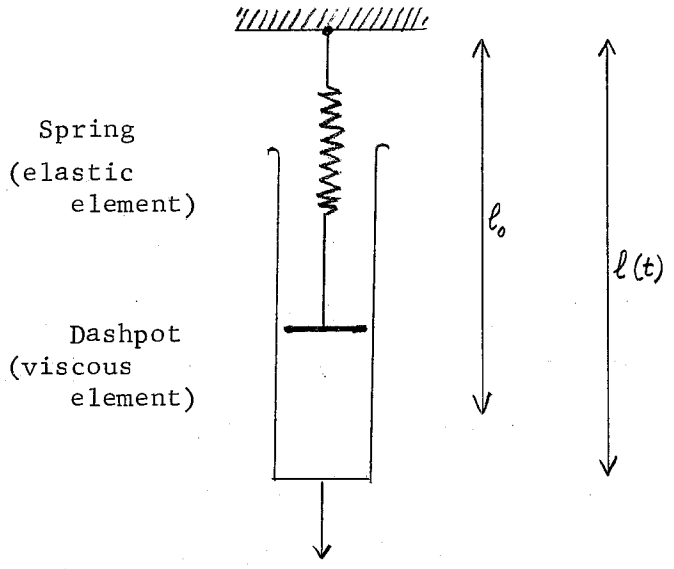

Fig. 2.

Eqn. (1) becomes then

$$\dot{\epsilon} = \frac{\dot{\sigma}}{E} + \frac{\sigma}{\eta} \quad , \tag{4}$$

or

$$\dot{\sigma} + \frac{\sigma}{T} = E\dot{\epsilon} \quad , \tag{4'}$$

where

$$T = \frac{\eta}{E} \tag{5}$$

is a relaxation time.

Note that the differential equation (4) [resp. (4')] is equivalent to the system of equations (1), (2) and (3). The latter system, however, gives a description of the system in terms of its internal components, which we may call state variables. Eqn. (4) was first considered by J. C. Maxwell (1867). Therefore a material whose (ideal) behavior obeys the differential equation (4) is called a Maxwell body.

First of all, it is easy to see that the general solution of (4'), with initial conditions

$$\sigma(0) = 0 \quad , \quad \epsilon(0) = 0 \tag{6}$$

is

$$\sigma(t) = E \int_0^t \exp\left[(\tau - t)/T\right] \dot{\epsilon}(\tau)\, d\tau \; ; \tag{7}$$

the function $E \exp\left[(\tau-t)/T\right]$ is a special case of a more general memory function $G(t-\tau)$, called in this special context relaxation function.

In this way of looking at things, we consider the rate of strain $\dot{\epsilon}$ as the stimulus (quantity which we are able to control), and the resulting stress σ as the response to this stimulus. But it is also quite possible to control the stress σ (which then acts as the stimulus) and look at the strain ϵ as the response. In the latter case, the general solution of (4), under the initial conditions (6), becomes:

$$\epsilon(t) = \frac{1}{E}\sigma(t) + \frac{1}{\eta}\int_0^t \sigma(\tau)\, d\tau \; . \tag{8}$$

Eqn. (4') [resp. (7)] tells us that if we apply suddenly a unit strain at time $\tau = 0$, and then keep this strain constant, the stress will take an initial value

$$\sigma(0+) = E \quad , \tag{9}$$

and then relax exponentially with time (see Fig. 3a). On the other hand, Eqn. (4) [resp. (8)] implies that if we apply at time $\tau = 0$ suddenly a unit stress and then keep that stress constant, the strain will increase linearly with time, starting from the initial value

$$\epsilon(0+) = \frac{1}{E} \; . \tag{10}$$

However, if at time $\tau = t$ we decrease suddenly the stress to zero, the strain will experience a jump down by an amount $1/E$, and then remain con-

stant (no elastic afterworking; the material has experienced plastic flow during $[0,t]$). Fig. 3b illustrates this typical behavior of a simple Maxwell body. Finally, if we apply from $\tau = 0$ onwards a constant unit rate of strain, Eqn. (7) gives

$$\sigma(t) = \eta\,(1 - \exp[-t/T]). \tag{11}$$

This behavior is illustrated in Fig. 3c.

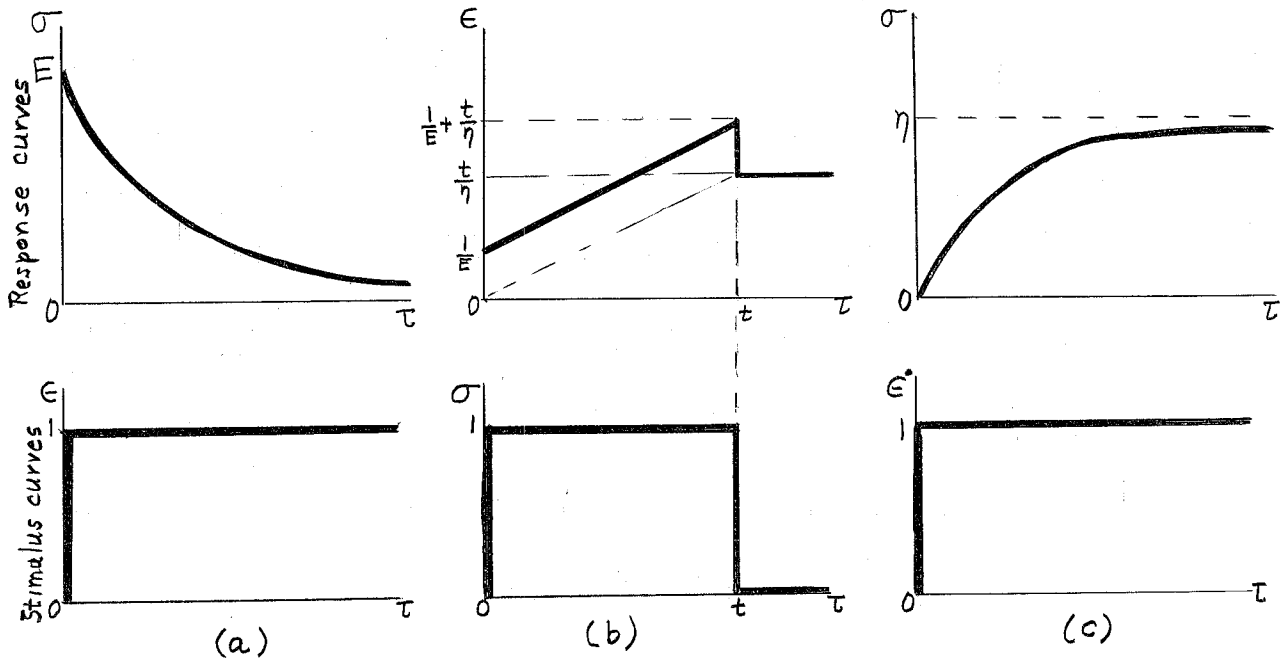

Fig. 3. Typical behavior of a simple Maxwell body.

A Maxwell material has two limiting cases which are of special interest.

Let us first assume that the time interval $[0,t]$ we are dealing with is very short compared to the relaxation time T. Under these circumstances

$$\exp[(\tau - t)/T] \simeq 1 \quad , \quad \forall \tau \in [0,t] \tag{12}$$

and Eqn. (7) yields

$$\sigma(t) \simeq E\,\epsilon(t) \tag{13}$$

Clearly, this is equivalent to the assumption that

$$\left|\frac{\sigma}{T}\right| \ll \left|\frac{d\sigma}{dt}\right| \tag{14}$$

[see Eqn. (4')]. Eqn. (13) means that under rapidly changing stimuli a Maxwell body behaves essentially as a perfectly elastic solid.

The second limiting case of interest is obtained when we consider the time interval $[0,t]$ during which the stimulus acts, to be very large compared to the relaxation time T. With the restriction that the rate of strain $\dot{\epsilon}(\tau)$ be a sufficiently smooth function of time, the main contribution in the integral (7) comes then from the exponential, and we may write approximately

$$\sigma(t) \simeq E\,\dot{\epsilon}(t)\int_0^t \exp[(\tau-t)/T]\,d\tau = ET\dot{\epsilon}(t)\left(1-\exp[-t/T]\right) \simeq \eta\dot{\epsilon}(t) \tag{15}$$

Interpreting

$$\eta = ET \tag{16}$$

as some effective dynamic viscosity of the material, Eqn. (15) corresponds to a viscous flow of Newton type.

3. Limitations of the former concept of a Maxwell body. Introduction of the notions of a "generalized lattice" and "virtual deformations".

The model of ideal material behavior we described in section 2 has rather severe limitations, due to the fact that only one-dimensional conditions are considered. As soon as we have to deal with higher-dimensional problems, we must worry about finite changes in orientation during deformation (measured with respect to a frame Σ_0 fixed once and for all), unless there is complete isotropy.

However, in crystals as well as in rocks such a complete isotropy (not altered by the application of stress) is not likely to occur, and therefore the former model can hardly give us a correct answer to the question how stresses are distributed during and after a given strain history. So it seems to us that for slow mantle convection it is not obvious that the mantle material, whatever it is, can be treated as a Newtonian fluid. We shall come back to this question later. Let us note however that, as far as the passage of seismic waves through the Earth's interior is concerned, we do not expect large deformations to be produced, so that under the assumption of (local) isotropy, unelastic processes may be taken into account by generalizing formula (2.4') in terms of the deviatoric (or distortional) stress and strain tensors (see Bullen, 1963, pp. 31-38)

$$\begin{cases} S_{ij} = \sigma_{ij} - \frac{1}{3}\sigma_{kk}\delta_{ij} \ , \\ e_{ij} = \epsilon_{ij} - \frac{1}{3}\epsilon_{kk}\delta_{ij} \ , \end{cases} \tag{1}$$

i.e.

$$\dot{S}_{ij} + \frac{1}{\tau} S_{ij} = E\,\dot{e}_{ij} \ , \tag{2}$$

and

$$3K\,\sigma_{kk} = \epsilon_{kk} \ . \tag{3}$$

In order to get a three-dimensional representation of Maxwell-type behavior under finite strain conditions, we must introduce a more sophisticated physical picture of a Maxwell material than the previous one.

Probably the most simple idea comes from our knowledge about the physical constitution of mono-crystals. Indeed, single crystals result from quite an ordered packing of atoms or groups of atoms, which defines some regular pattern called <u>lattice</u>. The crystallographical lattice is

a purely geometrical structure; to give it physical properties, we assume that the atoms or groups of atoms occupy mean positions corresponding to given lattice sites. As thermal motions tend to destroy this ordering, the atoms must be held together in their ordered mean positions by "lattice forces" which generally correspond to strong short-range interactions between neighboring atoms. However, the effect of thermodynamics is to introduce some disordering into such perfect crystals, giving rise to different kinds of defects, which may migrate "thermally" through the entire crystal or may be driven through it by externally applied stresses. Such isolated defects cause local deformations and weakening of the lattice known as faulting. However, as long as the density of these defects does not become too large, the lattice as a whole will not be affected and its response to rapid changes in stress or strain will be elastic.

For our consideration the most interesting type of faulting corresponds to dislocations; these are line defects which may be driven through the crystal under applied external stresses. The motion of a dislocation is associated with a slip of atoms from one lattice row to another one, and results finally in the slip of a lattice plane with respect to the next one. It is evident that without dislocations, such a slip would hardly be possible. Now, many such movements on atomic scale may finally cause a macroscopic deformation; during these processes individual atomic neighbors are displaced with respect to each other. However, if we assume chemical homogeneity on some given scale, and exclude the possibility of phase changes, the neighboring conditions remain essentially unchanged and therefore the lattice undergoes only very slight deformations. We neglect all

arising unharmonicities, i.e. we consider the deformations as "infinitesimal". These deformations are essentially of a geometrical nature and we shall refer to them as "lattice deformations", "microdeformations", or better (for a reason seen later) "virtual deformations". They are of course reversible in nature, and are only introduced to store instantaneously a great amount of energy, the relaxation of which through slip processes ("real" deformations) is not instantaneous, but involves a certain time delay characterized by some mean time interval called relaxation time.

As far as single crystals are concerned, this picture is quite adequate. For polycrystals however, or minerals made up of different crystallites, and finally for rocks made up of various minerals, the structural lattice viewed as a regular geometrical pattern loses its meaning. However, under rapidly varying stimuli (of not too high amplitudes) all these materials undergo elastic deformations, and so it seems obvious that for these materials we may still define a "generalized lattice" whose "virtual deformations" can store instantaneously an amount of energy high compared to that required to drive a dislocation or any other fault (grain boundaries, a.s.o.). This concept of lattice has even the advantage that we do not need any more to worry about the discontinuous nature of matter, and thus we may apply to the virtual lattice deformations the results of section 1. In particular, we define the orientation of the lattice with respect to the fixed frame Σ_o at time t by an orthogonal matrix $\underset{\sim}{Q}(t)$ such that

$$\underset{\sim}{Q}\,\underset{\sim}{Q}^T = \underset{\sim}{I} \tag{4}$$

is the identity matrix, and we require that for all the best specimens considered, we have

$$\underset{\sim}{Q}(0) = \underset{\sim}{I} \ . \tag{5}$$

The internal deformations of the lattice will be taken into account by the virtual (symmetric) strain tensor

$$\underset{\sim}{g}^*(t) = \underset{\sim}{D}^{*T}\underset{\sim}{D}^* \ ; \tag{6}$$

we require furthermore that initially the lattice be unstrained, i.e.

$$\underset{\sim}{g}^*(0) = \underset{\sim}{I} \ . \tag{7}$$

For convenience, we shall introduce another symmetric strain tensor

$$\underset{\sim}{q}(t) = \tfrac{1}{2}\left(\underset{\sim}{g}^* - \underset{\sim}{I}\right) \ , \quad \underset{\sim}{q}^T = \underset{\sim}{q} \tag{8}$$

which takes equally well into account instantaneous virtual deformations of the lattice. The 6 independent quantities defining $\underset{\sim}{q}$ at any time are said to be "state variables" of the material. For a mathematically rigorous introduction of the concept of state variables of a viscoelastic material, see Onat [(1966 a/b)]. With this notation, Eqn. (7) becomes

$$\underset{\sim}{q}(0) = 0 \ . \tag{9}$$

We now possess all the elements required to generalize the concept of a Maxwell body. We shall consider here the rate of deformation of the macrostructure ($\underset{\sim}{V}$ and $\underset{\sim}{\Omega}$) as a controllable stimulus, and try to find out the corresponding stress $\underset{\sim}{\sigma}$ at any moment.

A direct generalization of (2.2) taking correctly into account the tensorial character of the stress tensor (as revealed during an orthogonal transformation) is of course

$$\boxed{\underset{\sim}{\sigma} = \underset{\sim}{Q}\,\underset{\sim}{f}(\underset{\sim}{q})\,\underset{\sim}{Q}^T} \ , \tag{10}$$

where $\underset{\sim}{f}$ is some symmetric tensor function of the virtual lattice strains $\underset{\sim}{q}$. (Note: All these quantities are of course functions of time.) Eqn. (10) is a basic equation which is characteristic of the type of material considered. We shall first leave it in this quite general form, without special assumptions concerning $\underset{\sim}{f}$. Together with some equations of evolution (growth equations) for $\underset{\sim}{q}$ and $\underset{\sim}{Q}$, Eqn. (10) gives a mathematical representation of the behavior of a certain class of materials. Our major problem will be to make some plausible guesses concerning the equations of evolution of a Maxwell-type material. In order to do this, we shall use explicitly the picture of a generalized lattice.

In Fig. 4 we consider two different (but very simple) deformations, both of a given macrostructure and of the underlying lattice. We start in both cases with an unstressed and unstrained test specimen of a given geometrical shape (f.i. a cube), and suppose that the underlying lattices are identically oriented with respect to the fixed frame Σ_o . In Fig. 4a, we deform the cube into a parallelipiped by applying a simple shear and rotating the macrostructure concomitantly back, so that the orientation of the macrostructure remains essentially unchanged during the deformation. Our lattice picture tells us that during this deformation the lattice experiences at each point a shearing stress which tends to strain it very slightly, but is not rotated (except over "infinitesimal" angles) with respect to the fixed frame Σ_o , provided the rate of shear strain is sufficiently slow. In Fig. 4b, we still apply a shearing stress to the macrostructure to get the same amount of (finite) strain, but in

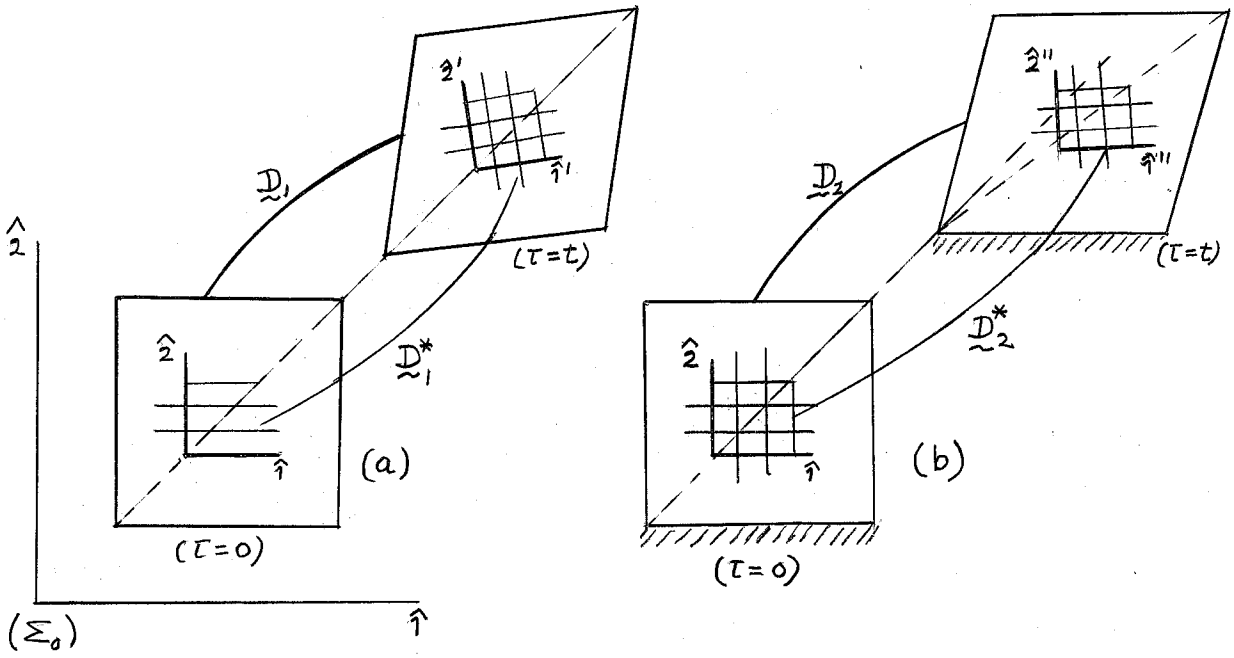

Fig. 4

this case we do not rotate back during the deformation. (This may be realized in the laboratory by fixing one base of the cube to the fixed frame Σ_o, or any other fixed frame.) Then the macrostructure as a whole is of course rotated with respect to the frame Σ_o, and so is generally the underlying lattice in the picture we gave before of a Maxwell body.

This latter point is essential in our discussion. Indeed, for a viscous fluid, we do not expect such a change in orientation of the microstructure to occur, for there is not such a thing as a restoring lattice force which is able to hold atoms together in some mean positions. For more complicated situations than the previous ones, the lattice at a given time may be oriented quite differently with respect to the fixed frame, but the main features of the preceding discussion must hold. (Orientation of the lattice results both from rotation of the macro-

structure as a whole and from relaxation processes.)

Most generally, we may assume that the rate of strain at time t of a rotating lattice is related to the actual state of strain of the lattice (slightly perturbed lattice parameters) and to the rate of strain of the macrostructure "as seen by the rotating lattice" (i.e. measured in a frame Σ_t^L attached to the rotating lattice, but supposed to be kept fixed at time t). Because of the tensorial character of $\underset{\sim}{V}$, the latter quantity is simply $\underset{\sim}{Q}^T \underset{\sim}{V} \underset{\sim}{Q}$.

Assuming further that both effects are not coupled and thus can be separated, taking into account relaxation processes by a term independent of the rate of macrodeformation, we write simply

$$\boxed{\underset{\sim}{\dot{q}} = \underset{\sim}{a}(\underset{\sim}{q}) + \underset{\approx}{\mathcal{B}}(\underset{\sim}{q}) \cdot (\underset{\sim}{Q}^T \underset{\sim}{V} \underset{\sim}{Q})} \quad . \tag{11}$$

Eqn. (11) is a second basic equation for the considered material; it is called "growth equation of $\underset{\sim}{q}$" , and corresponds to one of the most simple guesses one can make for viscoelastic behavior. Its relation to the picture given above is however rather obvious.

Finally, the rate of rotation of the lattice as measured at each moment in the rotated lattice frame Σ_t^L is $\underset{\sim}{Q}^T \underset{\sim}{\dot{Q}}$. We assume, on the basis of the underlying lattice picture, that it is related to the rate of rotation as measured at each moment in Σ_t^L , by the basic equation

$$\boxed{\underset{\sim}{Q}^T \underset{\sim}{\dot{Q}} = \underset{\sim}{c}(\underset{\sim}{q}) + \underset{\approx}{\mathcal{D}}(\underset{\sim}{q}) \cdot (\underset{\sim}{Q}^T \underset{\sim}{V} \underset{\sim}{Q}) + \underset{\sim}{Q}^T \underset{\sim}{\Omega} \underset{\sim}{Q}} \quad , \tag{12}$$

where $\underset{\sim}{Q}^T \underset{\sim}{V} \underset{\sim}{Q}$ and $\underset{\sim}{Q}^T \underset{\sim}{\Omega} \underset{\sim}{Q}$ are respectively the rate of actual strain and the rate of actual rotation of the macrostructure as measured in the

frame Σ_t^L. The term $\underset{\sim}{\ell}(\underset{\sim}{q})$ takes into account possible relaxation processes.

Note that the three basic equations (10), (11), (12) have been obtained by Onat (1966b) in a much more axiomatic way, without trying to give a physical interpretation of the state varuables $\underset{\sim}{q}$ and the orientations $\underset{\sim}{Q}$. However, the assumptions made in Onat's paper are quite plausible as regards our concept of a Maxwell body, though they are certainly less restrictive and thus include more general material behavior.

4. Discussion of the basic equations.

As we pointed out at the end of section 3, the basic equations (3.10), (3.11) and (3.12) may well define a more general material behavior than a Maxwell one. We impose therefore, in agreement with our lattice picture and the topics discussed in section 2, that the generalized Maxwell material should exhibit two limiting properties under extreme conditions:

(1) for very rapidly varying stimuli the material should behave as an elastic solid;

(2) for very slowly varying stimuli the material should exhibit some kind of viscous flow.

Condition (1) can be expressed mathematically by neglecting $\underset{\sim}{a}(\underset{\sim}{q})$ before $\underset{\approx}{\mathcal{D}}(\underset{\sim}{q})\cdot(\underset{\sim}{Q}^T\underset{\sim}{V}\underset{\sim}{Q})$ and $\underset{\sim}{\ell}(\underset{\sim}{q})$ before the terms involving $\underset{\sim}{V}$ and $\underset{\approx}{\Omega}$. Moreover, we must write

$$\underset{\sim}{q}^* = \underset{\sim}{q}\,, \tag{1}$$

$$\underset{\sim}{Q} = \underset{\sim}{R}\,, \tag{2}$$

so that

$$\underset{\sim}{q} = \tfrac{1}{2}\left(\underset{\sim}{g} - \underset{\sim}{I}\right) , \tag{3}$$

$$\dot{\underset{\sim}{q}} = \tfrac{1}{2}\,\dot{\underset{\sim}{g}} = \underset{\sim}{D}^{T}\underset{\sim}{V}\,\underset{\sim}{D} , \tag{4}$$

where

$$\underset{\sim}{D} = \underset{\sim}{R}\,\underset{\sim}{g}^{1/2} = \underset{\sim}{Q}\,\underset{\sim}{g}^{1/2} . \tag{5}$$

The basic equation (3.11) becomes then, in component form

$$\left(\mathcal{B}_{r s \alpha\beta}(\underset{\sim}{q}) - g^{1/2}_{\alpha r}\, g^{1/2}_{\beta s}\right) Q_{\mu\alpha}\, V_{\mu\nu}\, Q_{\nu\beta} = 0 . \tag{6}$$

Owing to symmetry properties, Eqn. (6) is equivalent to a system of 6 homogeneous equations in the 6 completely independent parameters $(\underset{\sim}{Q}^{T}\underset{\sim}{V}\underset{\sim}{Q})_{\alpha\beta}$. Therefore, all coefficients must vanish separately, i.e.

$$\mathcal{B}_{r s \alpha\beta}(\underset{\sim}{q}) = g^{1/2}_{\alpha r}\, g^{1/2}_{\beta s} . \tag{7}$$

If we limit ourselves to linear elasticity, we have

$$\underset{\sim}{g}^{1/2} \simeq \underset{\sim}{I} , \tag{8}$$

and Eqn. (7) yields

$$\mathcal{B}_{r s \alpha\beta} \simeq \delta_{\alpha r}\, \delta_{\beta s} . \tag{9}$$

Similarly, we must investigate what Eqn. (3.12) becomes under the condition of very rapidly varying stimuli, i.e. when conditions (1) and (2) hold and when $\underset{\sim}{\mathcal{C}}(\underset{\sim}{q})$ may be neglected. We write successively

$$\underset{\sim}{Q} = \underset{\sim}{D}\,\underset{\sim}{g}^{-1/2} \tag{10}$$

$$\dot{\underset{\sim}{Q}} = \dot{\underset{\sim}{D}}\,\underset{\sim}{g}^{-1/2} + \underset{\sim}{D}\,\dot{\underset{\sim}{g}}^{-1/2} ; \tag{11}$$

using (5) and (1.13) we obtain

$$\underset{\sim}{Q}^{T}\dot{\underset{\sim}{Q}} = \underset{\sim}{Q}^{T}\underset{\sim}{V}\underset{\sim}{Q} - \underset{\sim}{g}^{-1}\underset{\sim}{\underset{\sim}{I}}\cdot\left(\underset{\sim}{g}^{1/2\,T}\underset{\sim}{Q}^{T}\underset{\sim}{V}\underset{\sim}{Q}\,\underset{\sim}{g}^{1/2}\right) + \underset{\sim}{Q}^{T}\underset{\sim}{\Omega}\underset{\sim}{Q} . \tag{12}$$

A comparison of the latter equation with (3.12), where $\underset{\sim}{\mathcal{C}}(\underset{\sim}{q}) \approx 0$, yields

$$\underset{\sim}{\underset{\sim}{\mathcal{D}}}(\underset{\sim}{q})\cdot(\underset{\sim}{Q}^{T}\underset{\sim}{V}\underset{\sim}{Q}) = \underset{\sim}{Q}^{T}\underset{\sim}{V}\underset{\sim}{Q} - \underset{\sim}{g}^{-1}\underset{\sim}{\underset{\sim}{I}}\cdot\left(\underset{\sim}{g}^{1/2\,T}\underset{\sim}{Q}^{T}\underset{\sim}{V}\underset{\sim}{Q}\,\underset{\sim}{g}^{1/2}\right) , \tag{13}$$

or, in component form

$$\mathcal{D}_{ij\alpha\beta} Q_{\mu\alpha} V_{\mu\nu} Q_{\nu\beta} = \delta_{i\alpha} Q_{\mu\alpha} V_{\mu\nu} Q_{\nu\beta} \delta_{\beta j} - g^{-1}_{i\omega} \delta_{\omega j \varsigma\eta} g^{1/2}_{\alpha\varsigma} Q_{\mu\alpha} V_{\mu\nu} Q_{\nu\beta} g^{1/2}_{\beta\eta} \tag{14}$$

This gives

$$\left(\mathcal{D}_{ij\alpha\beta} - \delta_{i\alpha}\delta_{\beta j} - g^{-1}_{i\omega}\delta_{\omega j\varsigma\eta} g^{1/2}_{\alpha\varsigma} g^{1/2}_{\beta\eta}\right) Q_{\mu\alpha} V_{\mu\nu} Q_{\nu\beta} = 0 \tag{15}$$

The symmetry-antisymmetry requirements for $\underset{\approx}{\mathcal{D}}$:

$$\mathcal{D}_{ij\alpha\beta} = \mathcal{D}_{ij\beta\alpha} = -\mathcal{D}_{ji\alpha\beta} \ , \tag{16}$$

together with the fact that the six quantities $(\underset{\sim}{Q}^T \underset{\sim}{V} \underset{\sim}{Q})_{\alpha\beta}$ vary independently, yield

$$\underset{\approx}{\mathcal{D}}(\underset{\sim}{q}) \equiv 0 \ . \tag{17}$$

We assume that for a Maxwell body the fourth-rank tensor functions $\underset{\approx}{\mathcal{B}}$ and $\underset{\approx}{\mathcal{D}}$ possess always the forms (9) and (17). This point is merely a generalization of the one-dimensional case, and is also contained in the assumption that the deformations of the lattice be small. The basic viscoelastic equations then become

$$\boxed{\begin{aligned} \underset{\sim}{\sigma} &= \underset{\sim}{Q}\, \underset{\sim}{f}(\underset{\sim}{q})\, \underset{\sim}{Q}^T && (18)\\ \dot{\underset{\sim}{q}} &= \underset{\sim}{a}(\underset{\sim}{q}) + \underset{\sim}{Q}^T \underset{\sim}{V}\, \underset{\sim}{Q} && (19)\\ \underset{\sim}{Q}^T \dot{\underset{\sim}{Q}} &= \underset{\sim}{b}(\underset{\sim}{q}) + \underset{\sim}{Q}^T \underset{\sim}{\Omega}\, \underset{\sim}{Q} && (20) \end{aligned}}$$

Condition (2), requiring passage to viscosity for very slow rates of macrodeformation, contains less useful information. As in the unidimensional case discussed in section 2, we may assume that all components of $\dot{\underset{\sim}{q}}$ are very small quantities as compared to the still very small components of $\underset{\sim}{V}$ and $\underset{\sim}{\Omega}$. Eqn. (19) may then be written

$$\underset{\sim}{a}(\underset{\sim}{q}) + \underset{\sim}{Q}^T \underset{\sim}{V}\, \underset{\sim}{Q} \simeq 0 \ . \tag{21}$$

We assume the matrix $\underset{\sim}{a}$ invertible, so that we may solve for $\underset{\sim}{q}$:

$$\underset{\sim}{q} \simeq -\underset{\sim}{a}^{-1}(\underset{\sim}{Q}^T \underset{\sim}{V} \underset{\sim}{Q}) \,. \tag{22}$$

Eqn. (18) becomes then

$$\underset{\sim}{\sigma} = \underset{\sim}{Q}\,\underset{\sim}{F}(\underset{\sim}{Q}^T \underset{\sim}{V} \underset{\sim}{Q})\underset{\sim}{Q}^T \,, \tag{23}$$

where $\underset{\sim}{F}(\underset{\sim}{Q}^T \underset{\sim}{V} \underset{\sim}{Q})$ stands for $\underset{\sim}{f}[-\underset{\sim}{a}^{-1}(\underset{\sim}{Q}^T \underset{\sim}{V} \underset{\sim}{Q})]$.

Eqn. (23) corresponds to some sort of viscous flow (stress related to the rate of strain), but this flow is in general highly nonlinear, and thus non-Newtonian. Moreover, unless $\underset{\sim}{b}(\underset{\sim}{q}) = 0$, the previous results limit somewhat the flow pattern, for Eqn. (20) can be written as

$$\underset{\sim}{Q}^T \dot{\underset{\sim}{Q}} = \underset{\sim}{\mathcal{E}}(\underset{\sim}{Q}^T \underset{\sim}{V} \underset{\sim}{Q}) + \underset{\sim}{Q}^T \underset{\sim}{\Omega} \underset{\sim}{Q} \,, \tag{24}$$

where $\underset{\sim}{\mathcal{E}}(\underset{\sim}{Q}^T \underset{\sim}{V} \underset{\sim}{Q})$ stands for $\underset{\sim}{b}[-\underset{\sim}{a}^{-1}(\underset{\sim}{Q}^T \underset{\sim}{V} \underset{\sim}{Q})]$.

Another case of interest is pure relaxation, i.e. when

$$\underset{\sim}{V} = 0 \,, \quad \underset{\sim}{\Omega} = 0 \quad \text{(independently or together)}.$$

In this case, Eqn. (19) becomes simply

$$\dot{\underset{\sim}{q}} = \underset{\sim}{a}(\underset{\sim}{q}) \,, \tag{25}$$

and Eqn. (20) is

$$\underset{\sim}{Q}^T \dot{\underset{\sim}{Q}} = \underset{\sim}{b}(\underset{\sim}{q}) \,. \tag{26}$$

The latter equation implies that $\underset{\sim}{b}(\underset{\sim}{q})$ cannot be a constant or contain a constant term, unless it is zero. The simplest case we may think of is then $\underset{\sim}{b}(\underset{\sim}{q}) = 0$, or

$$\underset{\sim}{Q}^T \dot{\underset{\sim}{Q}} = 0 \,; \tag{27}$$

integrating Eqn. (27) yields that $\underset{\sim}{Q}$ is a constant tensor at any moment during relaxation; stated otherwise, this means that the orientation of the lattice does not relax at all.

Considering now the time-derivative of Eqn. (18), it is easy to show that

$$\underset{\sim}{\sigma}^{\circ} = \underset{\sim}{Q}\left\{[\underset{\sim}{\ell}(\underset{\sim}{q}), \underset{\sim}{f}(\underset{\sim}{q})] + [\underset{\sim}{Q}^T\underset{\sim}{\Omega}\underset{\sim}{Q}, \underset{\sim}{f}(\underset{\sim}{q})] + \underset{\approx}{\Psi}(\underset{\sim}{q})\cdot\underset{\sim}{Q}(\underset{\sim}{q}) + \underset{\approx}{\Psi}(\underset{\sim}{q})\cdot(\underset{\sim}{Q}^T\underset{\sim}{V}\underset{\sim}{Q})\right\}\underset{\sim}{Q}^T \quad , \tag{28}$$

where $$\underset{\approx}{\Psi}(\underset{\sim}{q}) \equiv \frac{\partial \underset{\sim}{f}(\underset{\sim}{q})}{\partial \underset{\sim}{q}} \quad ,$$

and $$[\underset{\sim}{A}, \underset{\sim}{B}] \equiv \underset{\sim}{A}\underset{\sim}{B} - \underset{\sim}{B}\underset{\sim}{A} \ : \text{ commutator of } \underset{\sim}{A} \text{ and } \underset{\sim}{B} .$$

Eqn. (28) is a generalization of Eqn. (2.4)

5. Isotropic case.

Given a stimulus $\underset{\sim}{D}^{\circ}\underset{\sim}{D}^{-1}$ and the corresponding response $\underset{\sim}{\sigma}$, we say that there is isotropy if for any stimulus $\underset{\sim}{R}\underset{\sim}{D}^{\circ}\underset{\sim}{D}^{-1}\underset{\sim}{R}^T$, where $\underset{\sim}{R}$ is a constant orthogonal transformation, the response is $\underset{\sim}{R}\underset{\sim}{\sigma}\underset{\sim}{R}^T$.

By analogy with the cases of isotropic elasticity or isotropic viscosity, we write the basic equations (4.18), (4.19) and (4.20) in the following form:

$$\underset{\sim}{\sigma} = \lambda \operatorname{tr} \underset{\sim}{q}\,\underset{\sim}{I} + 2\mu\,\underset{\sim}{Q}\underset{\sim}{q}\underset{\sim}{Q}^T \quad , \tag{1}$$

$$\underset{\sim}{q}^{\circ} = L \operatorname{tr} \underset{\sim}{q}\,\underset{\sim}{I} + 2M\underset{\sim}{q} + \underset{\sim}{Q}^T\underset{\sim}{V}\underset{\sim}{Q} \quad , \tag{2}$$

$$\underset{\sim}{Q}^T\underset{\sim}{Q}^{\circ} = \underset{\sim}{Q}^T\underset{\sim}{\Omega}\underset{\sim}{Q} \quad , \tag{3}$$

assuming moreover that $\underset{\sim}{\ell}(\underset{\sim}{q}) = 0$ in the isotropic case. This need not be true, but we introduce this statement as a simplifying assumption. Indeed, it is easy to check that the system of equations (1), (2), (3) describes the behavior of an isotropic material in agreement with the above definition of isotropy.

Let $\mathcal{V}$ be the volume of the macrostructure at any moment t ; then

(for the gross deformation)

$$\frac{v^{\cdot}}{v} = \mathrm{tr}\, \underset{\sim}{V} . \tag{4}$$

On the other hand, taking the trace of $\underset{\sim}{q}^{\cdot}$ in Eqn. (2), we obtain

$$\mathrm{tr}\, \underset{\sim}{V} = \frac{v^{\cdot}}{v} = \mathrm{tr}\, \underset{\sim}{q}^{\cdot} - (3L + 2M)\,\mathrm{tr}\, \underset{\sim}{q} . \tag{5}$$

Eqn. (5) implies that the assumption

$$3L + 2M = 0 \tag{6}$$

is equivalent to the assumption that the rate of volume change of the macrostructure is entirely due to an (elastic) rate of strain of the lattice. Thus, the assumption (6) seems quite plausible in most cases, at least as long as we keep a lattice picture for a Maxwell material. Under this restriction, Eqns. (2) and (5) become respectively

$$\underset{\sim}{q}^{\cdot} = -\frac{2}{3} M\, \mathrm{tr}\, \underset{\sim}{q}\, \underset{\sim}{\underset{\sim}{I}} + 2M \underset{\sim}{q} + \underset{\sim}{\underset{\sim}{Q}}^{T} \underset{\sim}{\underset{\sim}{V}}\, \underset{\sim}{\underset{\sim}{Q}} , \tag{7}$$

and

$$\mathrm{tr}\, \underset{\sim}{V} = \frac{v^{\cdot}}{v} = \mathrm{tr}\, \underset{\sim}{q}^{\cdot} . \tag{8}$$

It is worthwhile studying the behavior of an isotropic Maxwell material described by Eqns. (1), (7) and (3) in some simple cases.

For instance, if the gross deformation is a uniform dilatation (or compression), i.e. $\underset{\sim}{V} = a(\tau)\, \underset{\sim}{\underset{\sim}{I}}$, $\underset{\sim}{\underset{\sim}{\Omega}}$ arbitrary, the lattice undergoes the same deformation. The associated stresses are bulk stresses, which may be written as

$$\underset{\sim}{\sigma} = (\lambda + \tfrac{2}{3}\mu) \int_0^t a(\tau)\, d\tau\, \underset{\sim}{\underset{\sim}{I}} , \tag{9}$$

where $\lambda + \frac{2}{3}\mu = K$ is the bulk modulus.

If the macrodeformation is shear, the lattice also is simply sheared, and the only stresses which do not vanish are shearing stresses.

Finally, let us suppose that $\underset{\sim}{V}$ is sufficiently "smooth" and small enough, so that we may neglect $\dot{\underset{\sim}{q}}$ before quantities involving $\underset{\sim}{q}$ (see section 2). Under these circumstances, Eqn. (8) becomes

$$\mathrm{tr}\,\underset{\sim}{V} = \mathrm{tr}\,\dot{\underset{\sim}{q}} \simeq 0 \,, \tag{10}$$

so that approximately

$$\mathrm{tr}\,\underset{\sim}{q}(t) = \int_0^t \mathrm{tr}\,\underset{\sim}{V}(\tau)\,d\tau \simeq 0 \,. \tag{11}$$

Eqn. (1) becomes then

$$\underset{\sim}{\sigma}(t) = \left(\lambda + \tfrac{2}{3}\mu\right)\int_0^\tau \mathrm{tr}\,\underset{\sim}{V}(\tau)\,d\tau\,\underset{\approx}{I} - \frac{\mu}{M}\,\underset{\sim}{V}(t) \,, \tag{12}$$

or approximately

$$\underset{\sim}{\sigma}(t) \simeq -\frac{\mu}{M}\,\underset{\sim}{V}(t) \,. \tag{13}$$

As M must be intrinsically negative in order to get relaxation, we have

$$\underset{\sim}{\sigma} \simeq \frac{\mu}{|M|}\,\underset{\sim}{V} \,. \tag{13'}$$

Eqn. (13') corresponds simply to an incompressible viscous shear flow of effective Newtonian viscosity

$$\eta = \frac{\mu}{|M|} \,. \tag{14}$$

6. Conclusion.

This paper gives one example of how we could possibly treat viscoelastic behavior of materials. In fact, the method suggested here is full of possibilities, as more complicated behavior is easily included into this theory. For instance, plastic flow with elastic afterworking can be treated essentially along the same lines. Moreover, even in the very simple case of a Maxwell material, the orientation of the stress-carrying microstructure plays an essential role, which is not easily taken into account by

other representations. It clarifies a good deal the meaning of some state variables, which until now had been introduced axiomatically, without discussing their physical nature. Thermodynamic effects may easily be included as well, although this has not been done in the present paper. (See Onat, 1966b).

Finally, a remark concerning the Earth's mantle convection problem should be made. Indeed, although the previous treatment of some viscoelastic materials does by no means give any information about the real behavior of the material the Earth's mantle consists of, it seems however to indicate that viscous flow of Newtonian type demands rather drastic conditions, one of which may be that isotropy exists throughout and is not altered by the convective processes and the applied stresses. As for processes which do not involve extreme time intervals, some of the previous results may well prove very useful.

Acknowledgment.

I wish to express here my sincerest gratitude to Dr. E. Turan Onat for suggesting this problem, as well as for his kind and patient guidance throughout the whole project.

References

Batchelor, G. K. and R. M. Davies, editors 1956 "Surveys in Mechanics", Cambridge University Press.

Bullen, K. E. 1963 "An Introduction to the Theory of Seismology" (Third Edition), Cambridge University Press.

Flügge, S., editor 1958 Handbuch der Physik, Bd. 6, "Elastizität und Plastizität", Springer Verlag.

Fung, Y. C. 1965 "Foundations of Solid Mechanics", Prentice-Hall.

Gilbert, J. F. 1967 "Lecture Notes", This G.F.D. program.

Hounrink, R. 1958 "Elasticity, Plasticity and Structure of Matter", Dover.

Kittel, C. 1956 "Introduction to Solid State Physics", (Second Edition). John Wiley & Sons.

Kolsky, H. 1963 "Stress Waves in Solids", Dover.

Maxwell, J. C. 1867 "On the Dynamical Theory of Gases". Phil.Trans. Roy.Soc.London, 157: 49.

Onat, E. T. 19662 Proc. Vth U.S.Nat.Congress of Appl.Mech., 421-434.

Onat, E. T. 1966b IUTAM - Symposium on Irreversible Aspects of Continuum Mechanics, Vienna, June 1966 (to appear).

Prager, W. 1961 "Introduction to Mechanics of Continua", Ginn & Co.

A Two-layer Model of Ocean Circulation with Upwelling from the Lower Layer

Sulochana Gadgil

Introduction

Heat is supplied to the ocean mainly through the surface, where the water is in contact with the atmosphere. The surface temperature decreases from equator to pole. In a study of the convective motions arising due to the latitudinal variation of the surface temperature, where the temperature at great depths is taken to be uniform, Robinson and Welander have shown that upwelling from deep waters is necessary for the existance of a thermal boundary layer. That such a distribution of surface temperature would give rise to a highly asymmetric circulation in which there would be slow upwelling

in most of the region with sinking in a relatively narrow region has been suggested by Stommel's pipe models and Rossby's experiments. This is the rationale for investigating the circulation in a two-layered model, with upwelling from the lower layer in most of the region. Observations indicate that at a given longitude, the depth of the thermocline increases northward up to a certain latitude and then decreases sharply, almost to zero, in a very narrow region. One could associate the latter region with the one in which the upper layer loses warm water by eddies etc. Thus in this model the whole process is parameterised into a flux in or out of the upper layer.

1. Two-layered model

The x, y and z axes point eastward, northward and upward. If one assumes that there are no horizontal pressure gradients in the lower layer, the hydrostatic relation can be used to express the pressure gradients in the upper layer in terms of its depth. Integrating the equations from the bottom of the lower layer to the surface of the ocean and assuming that

$$\int_{\text{interface}}^{\text{surface}} u'u'_{x'}\,dz = (h'u'^2)_{x'} \quad \text{etc.}$$

the equations of momentum and continuity for the upper layer become, on neglecting friction

$$(h'u'^2)_{x'} + (h'u'v')_{y'} - f'v' = -g'h'_{x'} \tag{1.1}$$

$$(h'u'v')_{x'} + (h'v'^2)_{y'} + f'u' = -g'h'_{y'} \tag{1.2}$$

$$(h'u')_{x'} + (h'v')_{y'} = q' \tag{1.3}$$

where $u'v' \rightarrow$ velocities in x and y

$h' \rightarrow$ depth of the upper layer

$g' = g\frac{\Delta\rho}{\rho} \rightarrow$ reduced gravity

$q' =$ flux of water into or out of the upper layer

$f' =$ coriolis parameter

(1.1) and (1.2) can be simplified by using (1.3) and then dividing by h to give

$$u'u'_{x'} + u'v'_{y'} + \frac{q'u'}{h'} - f'v' = -g'h'_{x'} \qquad (1.4)$$

$$u'v'_{x'} + v'v'_{y'} + \frac{q'v'}{h'} + f'u' = -g'h'_{y'} \qquad (1.5)$$

These equations are now non-dimensionalised as follows:

$u' = Uu \quad v' = Uv \quad x' = Lx \quad y' = Ly \quad h' = (\Delta h)h \quad q' = Qq$

$f' = f_0 f \quad$ where $f = 1 + \beta y \quad \beta = \frac{L}{R}\cot\theta \quad \theta =$ latitude

On substitution of these, into equations (1.4), (1.5) and (1.3) and dividing throughout by $f_0 U$, those equations become

$$\epsilon(uu_x + vu_y) + \epsilon\delta\frac{qu}{h} - (1+\beta Y)v = -\alpha h_x \qquad (1.6)$$

$$\epsilon(uv_x + vv_y) + \epsilon\delta\frac{qv}{h} + (1+\beta Y)u = -\alpha h_y \qquad (1.7)$$

$$(hu)_x + (hv)_y = \delta q \qquad (1.8)$$

where $\epsilon = \frac{U}{f_0 L}$ and $\frac{QL}{\Delta h U} = \delta \qquad \frac{g'\Delta h}{f_0 L U} = \alpha$

For

$U \sim 1$ cm/sec, $\quad L \sim 7\times10^7$ cms, $\quad f_0 = .7\times10^{-4}$

$\frac{\Delta\rho}{\rho} = 2\times10^{-3}$; $\quad g' = 2 \quad \epsilon = 2\times10^{-4} \quad \beta = 10^{-1}$

Geostrophy implies $\alpha = 1$ which gives $\Delta h \sim 25$ metres $\quad \delta$ can be at most of order 1 as can be seen from equation (1.8).

The ocean basin is taken to be rectangular with boundaries parallel to the x and y axes. Since friction is neglected, the boundary conditions are that of no normal flow. One expects geostrophic balance to hold over most of the region. The basin is, therefore, divided into an interior region in which there is geostrophy, and boundary layers.

2. Interior

In the interior u, v, h, q are expanded in powers of β i.e.

$$u = u_0 + \beta u_1 + \ldots$$
$$v = v_0 + \beta v_1 + \ldots$$
$$h = h_0 + \beta h_1 + \ldots$$
$$q = q_0 + \beta q_1 + \ldots$$

Noting that $\beta^4 = \epsilon$, the zeroth and first order equations in β are

Zeroth order

$$v_0 = h_{0x} \tag{2.1}$$

$$u_0 = -h_{0y} \tag{2.2}$$

$$(h_0 u_0)_x + (h_0 v_0)_y = q_0 \tag{2.3}$$

(2.1) and (2.2) imply that $q_0 = 0$ i.e. $\delta \leq \beta$

First order

$$y v_0 + v_1 = h_{1x} \tag{2.4}$$

$$y u_0 + u_1 = -h_{1y} \tag{2.5}$$

$$(h_1 u_0)_x + (h_0 u_1)_x + (h_1 v_0)_y + (h_0 v_1)_y = q_1 \tag{2.6}$$

Cross differentiation of (2.4) and (2.5) gives the vorticity equation

$$u_{1x} + v_{1y} + v_0 + y(u_{0x} + v_{0y}) = 0$$

But (2.1) and (2.2) imply

$$u_{0x} + v_{0y} = 0 \tag{2.7}$$

The vorticity equation becomes

$$u_{1x} + v_{1y} + v_0 = 0 \tag{2.8}$$

Using (2.7), (2.6) is simplified to

$$h_0 (u_{1x} + v_{1y}) + u_1 h_{0x} + v_1 h_{0y} + u_0 h_{1x} + v_0 h_{1y} = q_1$$

Using (2.1) and (2.2), this becomes

$$h_0 (u_{1x} + v_{1y}) + h_{0x} (u_1 + h_{1y}) + h_{0y} (v_1 h_{1x}) = q_1$$

We have, from (2.4), (2.5) and (2.1), (2.2)

$$u_1 + h_{1y} = -y u_0 = y h_{0y}$$
$$v_1 - h_{1x} = -y v_0 = -y h_{0x}$$

Therefore,

$$q_1 = h_0 (u_{1x} + v_{1y}) \tag{2.9}$$

(2.8) and (2.9) imply

$$q_1 + h_0 h_{0x} = 0 \tag{2.10}$$

At this stage two assumptions are made. If one associates the region in which h_y is small and positive with weak upwelling and where h_y is large and negative with loss of upper layer water by eddies, etc., then q can be taken as a function of h_y. take the simplest case q is taken proportional to h_y. Thus we take

$q = c' h_y$ in the interior

$q = c h_y$ in the boundary layer near the northern boundary of the basin. c and c' are constants.

The variation of height in the interior is assumed to be small compared to the height. This means the height h can be written as

$$h_0 = H + h'(x,y) \tag{2.11}$$

where H is a constant and $h' \ll H$. With this assumption, equation (2.10) can be simplified by linearisation to give

$$q_1 + H h'_x = 0$$

With $q = c' h_y$, and $q = \beta q_1$

$$c' h'_y + \beta H h'_x = 0 \qquad (2.12)$$

This equation has a solution of the form,

$$h' = \phi(\beta H y - c' x)$$

where ϕ is an arbitrary function.

$$h_0 = H + \phi(\beta H y - c' x)$$

Consider

$$\phi(\beta H y - c' x) = K(\beta H y - c' x)$$

where K is a constant and $K \ll 1$.

$$h_0 = H + K(\beta H y - c' x)$$

$$u_0 = -K \beta H \qquad v_0 = -K c'$$

Equation (2.3) and $q_0 = 0$, imply that a stream function ψ_0 can be defined.

$$\psi_{0x} = h_0 v_0 \qquad \psi_{0y} = -h_0 u_0$$

$$\psi_{0x} = -K c' h_0 \qquad \psi_{0y} = +K \beta H h_0$$

$$\psi_0 = -K c'\left(Hx + K\beta H yx - K\frac{c' x^2}{2}\right) + K\beta H\left(Hy + K\beta\frac{Hy^2}{2} - Kc'xy\right)$$

$$\psi_0 = (K\beta H)^2 \frac{y^2}{2} + 2K\beta H xy + \frac{(Kc')^2}{2} x^2 + K\beta H^2 y - Kc'Hx \qquad (2.13)$$

The zonal flow in the interior is towards the west and the meridional flow is southwards, thus one expects an inertial boundary current on the western boundary, which transports the water northwards.

3. Boundary layers

Equations (1.6) and (1.7) give the vorticity equation when cross-differentiating. The vorticity equation is

$$\epsilon\left[u(v_x-u_y)_x+v(v_x-u_y)_y+(v_x-u_y)(u_x+v_y)\right]+f(u_x+v_y)+\beta v+\epsilon\delta\left[\left(\frac{qv}{h}\right)_x-\left(\frac{qu}{h}\right)_y\right]=0 \quad (3.1)$$

Using (1.8), we have

$$h(u_x+v_y)=q\delta-(uh_x+vh_y) \quad (3.2)$$

Using (3.2), (3.1) becomes

$$\epsilon\left[u(v_x-u_y)_x-\frac{(v_x-u_y)uh_x}{h}+v(v_x-u_y)_y-\frac{(v_x-u_y)vh_y}{h}\right]+$$
$$+\frac{\delta f q}{h}+\beta v-\frac{f(uh_x+vh_y)}{h}+\delta\epsilon\left[(v_x-u_y)\frac{q}{h}+\left(\frac{qv}{h}\right)_x-\left(\frac{qu}{h}\right)_y\right]=0$$

This can be simplified to

$$hu\left[\frac{\epsilon(v_x-u_y)+f}{h}\right]_x+hv\left[\frac{\epsilon(v_x-u_y)+f}{h}\right]_y+\frac{q\delta}{h}\left[f+\epsilon(v_x-u_y)\right]+\delta\epsilon\left[\left(\frac{qv}{h}\right)_x-\left(\frac{qu}{h}\right)_y\right]=0 \quad (3.3)$$

Using $q=ch_y$, (3.3) becomes

$$hu\left[\frac{\epsilon(v_x-u_y)+f}{h}\right]_x+hv\left[\frac{\epsilon(v_x-u_y)+f}{h}\right]_y+\frac{\delta ch_y}{h}\left[f+\epsilon(v_x-u_y)\right]+c\delta\epsilon\left[\left(\frac{h_yv}{h}\right)_x-\left(\frac{h_yu}{h}\right)_y\right]=0 \quad (3.4)$$

The system as a whole has to satisfy the following constraints:

(i) $\iint q\,dx\,dy=0$

(ii) $\iint \nabla\times\left(\frac{q\underline{v}}{h}\right)dx\,dy=0$

The first means there is no gain or loss of water and the second means the second is the integrated vorticity constraint.

Western Boundary Layer

In this boundary layer one expects the effects due to upwelling to be an order of magnitude smaller than the inertial effects. Thus the first

approximation would be to neglect the former in comparison with the latter. This is the same sort of assumption as that in the inertial theories of Charney and Morgan in which the effect of wind-stress over the boundary layer is neglected, even though the flow into the boundary layer is due to the cumulative effect of wind-stress over the entire basin, i.e. $\delta = 0$ in this region.

Thus the equations of continuity and vorticity become

$$(hu)_x + (hv)_y = 0 \tag{3.5}$$

$$hu\left[\frac{\epsilon(v_x - u_y) + f}{h}\right]_x + hv\left[\frac{\epsilon(v_x - u_y) f}{h}\right]_y = 0 \tag{3.6}$$

Defining

$$hu = -\psi_y \qquad hv = \psi_x$$

(3.6) becomes

$$\psi_x\left[\frac{\epsilon}{h}\left[\left(\frac{\psi_x}{h}\right)_x + \left(\frac{\psi_y}{h}\right)_y\right] + \frac{f}{h}\right]_y - \psi_y\left[\frac{\epsilon}{h}\left[\left(\frac{\psi_x}{h}\right)_x + \left(\frac{\psi_y}{h}\right)_y\right] + \frac{f}{h}\right] = 0 \tag{3.7}$$

In this boundary layer, the x-scale is much smaller than the y-scale, and, therefore, x-derivatives much larger than the y-derivatives. The x-scale is stretched to take this into account,

$$\xi = \epsilon^{-1/2} x \tag{3.8}$$

Giving

$$\psi_x = \psi_\xi \epsilon^{-1/2} \; ; \quad \psi_{xx} = \psi_{\xi\xi} \epsilon^{-1}$$

(3.7) becomes

$$\epsilon^{-1/2}\psi_\xi\left[\frac{1}{h}\left(\frac{\psi_\xi}{h}\right)_\xi + \frac{\epsilon}{h}\left(\frac{\psi_y}{h}\right)_y + \frac{f}{h}\right]_y - \epsilon^{1/2}\psi_y\left[\frac{1}{h}\left(\frac{\psi_\xi}{h}\right)_\xi + \frac{\epsilon}{h}\left(\frac{\psi_y}{h}\right)_y + \frac{f}{h}\right]_\xi = 0$$

To order ϵ, this is

$$\psi_\xi\left[\frac{1}{h}\left(\frac{\psi_\xi}{h}\right)_\xi + \frac{f}{h}\right]_y - \psi_y\left[\frac{1}{h}\left(\frac{\psi_\xi}{h}\right)_\xi + \frac{f}{h}\right]_\xi = 0 \tag{3.9}$$

(3.5) becomes

$$(hu)_\xi \epsilon^{-1/2} + (hv)_y = 0$$

If both terms in the above equation are to be equally important, we must have

$$v \sim \epsilon^{-1/2} u \; ; \; h_x \sim \epsilon^{-1/2} \tag{3.10}$$

If we take

$$u \sim 1, \quad v \sim \epsilon^{-1/2}, \quad y \sim 1, \quad \xi \sim \epsilon^{-1/2}$$

equations (1.6) and (1.7) become on taking $\delta = 0, \alpha = 1$

$$\epsilon^{1/2}(uu_x + vu_y) - \epsilon^{-1/2} fv = -\epsilon^{-1/2} h_\xi \tag{3.11}$$

$$uv_x + vv_y + fu = -h_y \tag{3.12}$$

Thus one can take the down-stream component to be geostrophic, to order ϵ . Equation (3.9) has an immediate first integral

$$\frac{1}{h}\left(\frac{\psi_\xi}{h}\right)_\xi + \frac{f}{h} = F(\psi) \tag{3.13}$$

To find $F(\psi)$, we can utilise the fact that in the interior, the potential vorticity is given by

$$\frac{f}{h_0} = F(\psi_0) \tag{3.14}$$

At the outer boundary, ψ_0 is a given function of y according to (2.13) to be

$$\psi_0(0,y) = \frac{(K\beta H)^2 y^2}{2} + K\beta H^2 y$$

h_0 is also a given function of y at $x = 0$, and therefore also of ψ_0. Thus f/h_0 as a function of ψ_0 determines the function F .

We have, in the interior,

$$u_0 = -h_{0y} \qquad v_0 = h_{0x}$$

$$\therefore \quad \psi_{0y} = h_0 h_{0y} \qquad \psi_{0x} = h_0 h_{0x}$$

and

$$\psi_0 = \tfrac{1}{2} h_0^2 + \text{constant}$$

Thus $F(\psi_0)$ will be a function of h_0, say $F_1(h_0)$. Let $\bar{h}$ denote the value of h_0 at $x=0$.

i.e. $\bar{h} = H + K\beta H y$

Then

$$y = \bar{h} - H/K\beta H \tag{3.15}$$

$$f = 1+\beta y = K\beta H + \beta(\bar{h}-H)/K\beta H = (K-1)H + \bar{h}/KH$$

which gives $F(\psi_0)$ to be

$$F_1(\bar{h}) = \frac{(K-1)H+\bar{h}}{KH\bar{h}} \tag{3.16}$$

Using (3.11) we have, geostrophically,

$$v = \frac{h_\xi}{f} = \frac{\psi_\xi}{h} \tag{3.17}$$

The equation (3.13) becomes, on using (3.16) and (3.17)

$$\frac{h_{\xi\xi}+f}{h} = \frac{(K-1)H+h}{KHh}$$

$$h_{\xi\xi} - \frac{h}{KH} = \frac{(K-1)H}{KH} - f = -\frac{\bar{h}}{KH}$$

$$\therefore h = Ae^{-\xi/\sqrt{KH}} + \bar{h} \tag{3.18}$$

If $h=h_c$ at $x=0$, then we have

$$h = (h_c - \bar{h})e^{-\xi/\sqrt{KH}} + \bar{h} \tag{3.19}$$

$h_c(y)$ can be determined by matching the transports. Since friction has been neglected in this theory, the velocity cannot obey the no-slip condition. The meridional velocity has a maximum at the boundary. The transport in this boundary layer increases as the stream flows northwards. At the northern boundary the stream has to leave the western boundary and will start going along the northern wall.

Northern boundary layer

In this region, we expect the upper layer to loose warm water by means of eddies. The effect of downwelling, therefore, will be at

least as important as the inertial effect. The y-scale will be small compared with the x-scale and so a stretched coordinate η is introduced

$$\eta = \epsilon^{-1/2} y \tag{3.20}$$

For all the terms to be of equal importance in the equation of continuity, we must have

$$u \sim \epsilon^{-1/2} v \tag{3.21}$$

If $v \sim 1$, (3.20) and (3.21) when substituted into (1.6), (1.7) and (3.4) give,

$$(uu_x + vu_\eta) + \epsilon^{-1/2}\delta \frac{q_\eta u}{h} - fv = -h_x \tag{3.22}$$

$$\epsilon^{1/2}(uv_x + vv_\eta) + \epsilon\delta \frac{q_\eta v}{h} + \epsilon^{-1/2} f u = -\epsilon^{-1/2} h_\eta$$

i.e. $$\epsilon(uv_x + vv_\eta) + \epsilon^{3/2}\delta \frac{q_\eta v}{h} + fu = -h_\eta \tag{3.23}$$

$$\epsilon^{-1/2}(hu)\left[\frac{\epsilon v_x - u_\eta + f}{h}\right]_x + \epsilon^{-1/2}(hv)\left[\frac{\epsilon v_x - u_\eta + f}{h}\right]_\eta +$$

$$+ \delta\left[\frac{\epsilon^{-1/2} c h_\eta}{h}(f + \epsilon v_x - u_\eta) + c\epsilon^{1/2}\left(\frac{h_\eta v}{h}\right)_x - c\epsilon^{-1/2}\left(\frac{h_\eta u}{h}\right)_\eta\right] = 0 \tag{3.24}$$

To order ϵ, equation (3.24), is

$$hu\left(\frac{f - u_\eta}{h}\right)_x + hv\left(\frac{f-u_\eta}{h}\right)_\eta + \delta \frac{c h_\eta}{h}(f - u_\eta) - \delta c\left(\frac{h_\eta u}{h}\right)_\eta = 0 \tag{3.25}$$

$$f = 1 + \beta y = 1 + \beta\epsilon^{1/2}\eta \qquad f_\eta = \epsilon^{1/2}\beta$$

The variation of f with latitude is neglected in this boundary layer. Equation (3.25) then reduces to

$$hu\left(\frac{-u_\eta}{h}\right)_x + hv\left(\frac{-u_\eta}{h}\right)_\eta + f(u_x + v_\eta) + \delta c\left(\frac{-u_\eta}{h}\right)h_\eta - \delta c\left(\frac{u h_\eta}{h}\right)_\eta = 0 \tag{3.26}$$

Equation (3.23) implies geostrophy in u, namely

$$u = -h_\eta \tag{3.27}$$

The equation of continuity is

$$(hu)_x + (hv)_\eta = \delta c\, h_\eta$$

One can, therefore, define a streamlike function ϕ,

$$\phi_x = h(v - c\delta) \qquad \phi_\eta = -hu \tag{3.28}$$

Equations (3.27) and (3.28) imply,

$$\phi_\eta = hh_\eta \; ; \quad \phi = \frac{h^2}{2} + g(x) \tag{3.29}$$

where g is an arbitrary function.

The meridional velocity v is then given by

$$h(v - c\delta) = hh_x + g'(x) \tag{3.30}$$

If the thermocline actually reaches the surface at the northern boundary, $g'(x)$ must be identically zero. Then

$$u = -h_\eta \qquad v = h_x + \delta c \tag{3.31}$$

In this special case, equation (3.26) reduces to

$$h_x h_{\eta\eta\eta} - h_\eta h_{\eta\eta x} + \delta c\, h_{\eta\eta\eta} + \delta c \left(\frac{h_\eta^2}{h}\right)_\eta = 0 \tag{3.32}$$

If h_η is assumed to be a function of h and x alone this equation is simplified. We have

$$h_\eta = F(h, x)$$

$$h_{\eta\eta} = F_h h_\eta = F_h F$$

$$h_{\eta x} = F_h h_x + F_x$$

$$h_\eta h_{x\eta} - h_x h_{\eta\eta} = h_\eta F_h h_x + h_\eta F_x - h_x F_h h_\eta = h_\eta F_x$$

Using above, equation (3.32) can be simplified to

$$-\left[(FF_x)\right]_h F + \delta c \left(FF_h\right)_h F + \delta c \left(\frac{F^2}{h}\right)_h F = 0$$

Since F is not zero in the boundary layer, we have

$$-(F^2)_{xh} + \delta c (F^2)_{hh} + 2\delta c \left(\frac{F^2}{h}\right)_h = 0$$

If $F^2(x,h) \equiv G(x,h)$

$$-G_{xh} + c\delta G_{hh} + 2c\delta\left(\frac{G}{h}\right)_h = 0 \tag{3.33}$$

This equation has an immediate first integral.

$$-G_x + \delta c G_h + 2\delta c \frac{G}{h} = \alpha(x) \tag{3.34}$$

where $\alpha(x)$ is a function that is to be determined by the boundary conditions. The boundary condition in this case is

$$h = 0 \quad \text{at} \quad y = 1.$$

By equations (1.4) and (1.5), this implies that

$$q = 0$$

or

$$u = 0 \quad \text{and} \quad v = 0$$

Since in this model q is proportional to u, we must have

$$q = 0 \quad \text{at} \quad h = 0 \quad \text{i.e.} \quad y = 1$$

This means

$$G = 0 \quad \text{at} \quad h = 0, \quad y = 1.$$

$$\therefore \quad \alpha(x) = \delta c G_h\Big|_{h=0} + \lim_{h\to 0} \frac{2c\delta G}{h}$$

Equation (3.34) can be solved by a change of coordinates

$$\xi' = x \qquad \eta' = h + x c\delta \tag{3.35}$$

We have

$$G_x = G_{\xi'} + c\delta G_{\eta'}; \quad G_h = G_{\eta'}$$

Equation (3.34) becomes

$$G_{\xi'} - \frac{2\delta c G}{\eta' - c\delta\xi'} = -\alpha(\xi') \tag{3.36}$$

This equation has a solution

$$(\eta'-c\delta\xi')^2 G = -\int \alpha(\xi')(\eta'-c\delta\xi')^2 d\xi' + \gamma(\eta') \tag{3.37}$$

If G has to vanish at $h=0$, then we must have

$$\gamma(xc) = 0$$

and

$$G = \frac{-1}{h^2}\int \alpha(\xi')(\eta-\delta c\,\xi')^2 d\xi' + \frac{\gamma(h+xc)}{h^2} \tag{3.38}$$

In the special case where $\alpha(x)$ is a constant and $G_x = 0$, above reduces to

$$G = \frac{\alpha h}{3c\delta} \tag{3.39}$$

which gives

$$h_y = -\sqrt{\frac{\alpha h}{3c\delta}}$$

$$2\sqrt{h} = +\sqrt{\frac{\alpha}{3c\delta}}\,(1-y)$$

$$h = \frac{\alpha}{12c\delta}(1-y)^2 \tag{3.40}$$

This solution is one in which there is no x-structure. The stream would therefore go along the northern boundary and turn around to become an eastern boundary current when it reaches the eastern boundary. In this case one expects to get a Fofonoff-type solution.

The problem would be somewhat different, if the thermocline does not actually reach the surface at the northern boundary. In this case $g(x)$ in equation (3.29) does not vanish. We have, instead

$$\phi = \frac{h^2}{2} + g(x) \tag{3.28}$$

$$u = -h_\eta \qquad v = h_x + \delta c + \frac{g'(x)}{h} \tag{3.41}$$

$$u_x + v_\eta = -\frac{g'(x)h_\eta}{h^2} \tag{3.42}$$

Equation (3.26) becomes, on setting f on $y=1$ to be f^*,

$$-hh_\eta\left(-\frac{u_\eta}{h}\right)_x+hh_x\left(-\frac{u_\eta}{h}\right)_\eta+h\delta c\left(-\frac{u_\eta}{h}\right)_\eta+g'\left(-\frac{u_\eta}{h}\right)_\eta-\frac{f^*g'h_\eta}{h^2}+\delta c\left(-\frac{u_\eta}{h}\right)h_y-\delta c\left(\frac{uh_\eta}{h}\right)_\eta=0$$

Using (3.41), above equation can be simplified to,

$$h_xh_{\eta\eta\eta}-h_\eta h_{\eta\eta x}+\delta c\left[h_{\eta\eta\eta}+\left(\frac{h_\eta^2}{h}\right)_\eta\right]+g'\left[\left(\frac{h_{\eta\eta}}{h}\right)_\eta-\frac{f^*h_\eta}{h^2}\right]$$

The function g has to be chosen so as to satisfy the condition of no normal flow at the northern boundary. Thus we have

$$hh_x+\delta ch\Big|_{y=1}=g'(x)$$

Again on taking

$$h_\eta^2=G(h,x)$$

we get

$$-G_{hx}+\delta c\,G_{hh}+2\delta c\left(\frac{G}{h}\right)_h+g'(x)\left[\left(\frac{G_h^2}{2h}\right)_h-\frac{f^*}{h^2}\right]=0 \qquad (3.43)$$

This is the most general equation. The solution of this equation has to satisfy the initial conditions at the west coast, matching of the thermocline depth at the junction of the interior and the northern boundary layer and satisfying the condition of no normal flow at the northern boundary. The parameter δ measures the dissipation of vorticity by downwelling. If this is very large, the stream could lose all its water before reaching the east coast. If δ is large, perturbation method may prove to be useful in solving (3.43). That would be the next thing to do in this problem.

So far we have considered the case in which upwelling gives rise to uniform zonal and meridional velocities in the interior. However, this driving mechanism is not expected to be the dominant one everywhere in the ocean. In fact, this mechanism is most likely to be important in the region

where the boundary current separates from the coast, and might perhaps cause the separation. An extremely interesting case, would be one in which the velocities are considerable near the northwestern corner and very small elsewhere.

Acknowledgements

I would like to thank Prof. George Veronis for suggesting this fascinating problem and for the many fruitful discussions which brought it to its present stage. I am also grateful to Prof. Louis Howard for his comments.

The Precessing Cylinder

Leonard E. Johnson

1. Introduction:

The problem of fluid flow in precessing cavities has attracted special attention because of its relevance to geophysical and astrophysical phenomena and also because of the unusual properties of the flow itself. In this paper, we will investigate the flow of a viscous, incompressible fluid in a precessing cylinder as seen in the coordinate system rotating with the precession frequency.

The method of solution used will essentially be an application of Greenspan's (1964) general theory of contained rotating fluid motions. The basic procedure is as follows: expand the appropriate quantities in the equations of motion in powers of E, the Ekman number; obtain the

eigenmodes of the homogeneous inviscid problem; correct these eigenmodes for viscosity; use the viscosity-corrected modes to expand the forcing function due to precession in the solution of the non-homogeneous problem.

2. Mathematical Formulation:

We consider an incompressible, viscous fluid which completely fills a cylindrical container with axis of symmetry L_B. The cylinder rotates with a constant angular velocity $\vec{\omega}$ about the axis L_B which, in turn, precesses with a constant angular velocity $\vec{\Omega}$ about an axis L_S fixed in space $(\Omega/\omega \ll 1)$. L_B intersects L_S at a point O, and is inclined to L_S at an angle φ. (See Fig. 1)

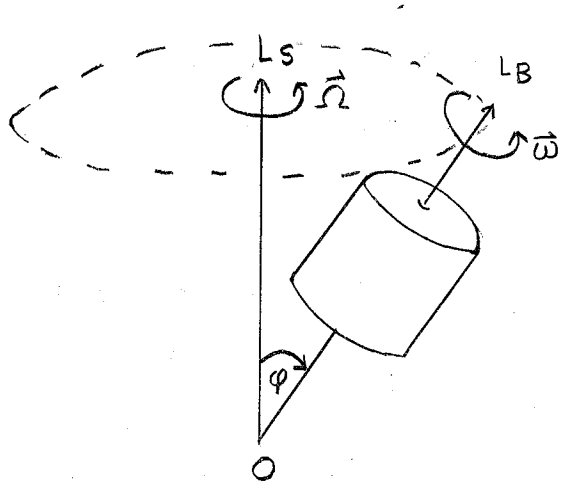

Fig. 1

We shall formulate the problem in a reference frame rotating with $\vec{\Omega}$ relative to which L_B and L_S are stationary (this frame will be referred to as the precessing frame). The precessing frame has the advantage that in this frame the forcing term due to the precessional motion appears steady.

The velocity of the fluid in the container relative to this frame is

$$\vec{v} = \vec{u} + \vec{\omega} \times \vec{r} \tag{2.1}$$

where $\vec{u}$ is the velocity of the fluid relative to the container. The equations of motion relative to the precessing frame are:

$$\frac{\partial \vec{v}}{\partial t} + (\vec{v}\cdot\nabla)\vec{v} + 2\vec{\Omega}\times\vec{v} + \vec{\Omega}\times(\vec{\Omega}\times\vec{r}) = -\nabla\left[\frac{p}{\rho} + \Phi\right] + \nu\nabla^2\vec{v} \tag{2.2}$$

$$\nabla\cdot\vec{v} = 0 \tag{2.3}$$

where p = pressure

Φ = potential of conservative external forces

ν = kinematic viscosity

ρ = density

We can write (2.2) in terms of $\vec{u}$, obtaining after some manipulation

$$\frac{\partial \vec{u}}{\partial t} + (2\vec{\omega} + 2\vec{\Omega})\times\vec{u} - (\vec{u} + (\vec{\omega}\times\vec{r}))\times \operatorname{curl}\vec{u} = -\nabla P^{+} + \nu\nabla^2\vec{u} - 2(\vec{\Omega}\cdot\vec{r})\vec{\omega} \tag{2.4}$$

where

$$P^{+} = \frac{p}{\rho} + \Phi + \tfrac{1}{2}\Omega^2 r^2 + \tfrac{1}{2}u^2 + (\vec{\omega}\times\vec{r})\cdot\vec{u} - \tfrac{1}{2}(\vec{\omega}\times\vec{r}) - (\vec{\Omega}\cdot\vec{\omega})r^2 \tag{2.5}$$

and

$$\nabla\cdot\vec{u} = 0 \tag{2.6}$$

If we neglect squares and products of $\vec{\Omega}$ and $\vec{u}$ we have

$$\frac{\partial \vec{u}}{\partial t} + 2\vec{\omega}\times\vec{u} - (\vec{\omega}\times\vec{r})\times\operatorname{curl}\vec{u} = -\nabla P^{+} + \nu\nabla^2\vec{u} - 2(\vec{\Omega}\cdot\vec{r})\vec{\omega} \tag{2.7}$$

$$\nabla\cdot\vec{u} = 0 \tag{2.8}$$

with

$$P^{+} = \frac{p}{\rho} + \Phi + (\vec{\omega}\times\vec{r})\cdot\vec{u} - \tfrac{1}{2}(\vec{\omega}\times\vec{r})^2 - (\vec{\Omega}\cdot\vec{\omega})r^2 \tag{2.9}$$

and boundary conditions

$$\vec{u} = 0 \text{ on the container surface} \tag{2.10}$$

Now, we consider a cylindrical polar coordinate system in which the

z-axis lies along the L_B or $\vec{\omega}$ axis, r measures the distance of a point $P(\vec{r})$ from L_B and θ measures the angle between the planes defined by $P(\vec{r})$ and L_B and L_B and L_S. In this system $\vec{\omega} = \omega \hat{k}$.

Let L, ωL, ω^{-1} characterize the container height, fluid velocity, and time respectively. These quantities can be used to make (2.7) and (2.8) dimensionless. We let $\vec{\omega} = \omega \hat{k}$, $\vec{u} = \omega L \vec{u}^*$, $t = \omega^{-1} t^*$, $P = \omega^2 L^2 P^*$, $r = L r^*$, $\vec{\Omega} = \omega \vec{\Omega}^*$ where q^*, t^*, P^* are dimensionless. Then we have, (dropping the *)

$$\frac{\partial \vec{u}}{\partial t} + 2\hat{k} \times \vec{u} + \operatorname{curl} \vec{u} \times (\hat{k} \times \vec{r}) = -\nabla P^t + E \nabla^2 \vec{u} - 2(\vec{\Omega} \cdot \vec{r})\hat{k} \tag{2.11}$$

$$\nabla \cdot \vec{u} = 0 \tag{2.12}$$

where $E = \frac{\nu}{L^2 \omega}$ is the Ekman number.

In the cylindrical polar coordinate system described above we have for (2.11) and (2.12)

$$\frac{\partial u_r}{\partial t} - 2u_\theta + \frac{\partial u_r}{\partial \theta} + \frac{\partial P}{\partial r} = E \nabla^2 u_r \tag{2.13}$$

$$\frac{\partial u_\theta}{\partial t} + 2u_r + \frac{\partial u_\theta}{\partial \theta} + \frac{1}{r}\frac{\partial P}{\partial \theta} = E \nabla^2 u_\theta \tag{2.14}$$

$$\frac{\partial u_z}{\partial t} + \frac{\partial u_z}{\partial \theta} + \frac{\partial P}{\partial z} = E \nabla^2 u_z - 2\Omega r \sin\varphi \cos\theta \tag{2.15}$$

$$\frac{1}{r}\frac{\partial}{\partial r}(r u_r) + \frac{1}{r}\frac{\partial u_\theta}{\partial \theta} + \frac{\partial u_z}{\partial z} = 0 \tag{2.16}$$

where $P = P^t - r u_\theta - \Omega z^2 \cos\varphi$.

It is known that, for E small, direct viscous effects take place in a thin layer of thickness $O(E^{1/2})$ near the top $(z = L)$ and bottom $(z = 0)$ of the cylinder. In this viscous layer we introduce a stretched boundary layer coordinate η given by

$$z = E^{1/2}\eta \tag{2.17}$$

Then, $\hat{n}\cdot\nabla = -E^{-1/2}\frac{\partial}{\partial\eta}$ where $\frac{\partial}{\partial\eta}$ is an $O(1)$ quantity in the boundary layer, and $\hat{n}$ is the unit outwardly pointing normal at the boundary.

Now, we seek a solution to (2.11) and (2.12) in the form of a superposition of all the normal modes of the inviscid homogeneous problem, (i.e. equation (2.11) with $E = 0$ and the forcing term $-2(\Omega\cdot\vec{r})\hat{k} = 0$) each of which has been corrected for the effects of viscosity.

Before plunging ahead with this method of solution, we might ask ourselves at this point whether or not we can find (guess) a constant vorticity solution to the steady inviscid precession problem i.e. (2.11) with $E = 0$ but $-2(\Omega\cdot\vec{r})\hat{k} \neq 0$. We would require this solution to satisfy the condition of no normal flow on the boundaries and then would adjust the solution with a boundary layer to fit the no-slip condition. Such a solution was found by Roberts and Stewartson (1964) for flow in a precessing spheroid. To this end, we postulate a solution to the equations

$$\left.\begin{aligned} 2\vec{\omega}\times\vec{u} + \operatorname{curl}\vec{u}\times(\vec{\omega}\times\vec{r}) &= -\nabla P - 2(\vec{\Omega}\cdot\vec{r})\vec{\omega} \\ \nabla\cdot\vec{u} &= 0 \end{aligned}\right\} \tag{2.18}$$

with $\vec{u}\cdot\hat{n} = 0$ on the boundary (2.19)

of the form

$$\vec{u} = \vec{\omega}'\times\vec{r} + \nabla A \tag{2.20}$$

where $\vec{\omega}'$ is some constant vector. Now,

$$\left.\begin{aligned} \operatorname{curl}\vec{u} &= 2\vec{\omega}' \\ \nabla\cdot\vec{u} &= \nabla^2 A = 0 \end{aligned}\right\} \tag{2.21}$$

If we substitute (2.20) into (2.18) and make use of (2.21) we get,

after some manipulation,

$$\vec{\omega}' \times \nabla(\vec{\omega}\cdot\vec{r}) + \vec{\omega} \times \nabla(\vec{\omega}'\cdot\vec{r}) + \nabla(\vec{\omega}\cdot\nabla A) = -\vec{\omega} \times \nabla(\vec{\Omega}\cdot\vec{r}) \tag{2.22}$$

Now, consider (2.18) in a cartesian coordinate system rotating with $\vec{\Omega}$ where the z-axis is along $\vec{\omega}$ and the x-axis is in the plane of $\vec{\Omega}$ and $\vec{\omega}$. Then we have

$$\left.\begin{aligned} \vec{\omega}' &= (\omega_x', \omega_y', \omega_z') \\ \vec{\omega} &= (0, 0, \omega) \\ \vec{r} &= (x, y, z) \\ \vec{\Omega} &= (\Omega \sin\varphi, 0, \Omega\cos\varphi) \end{aligned}\right\} \tag{2.23}$$

So we have for (2.18)

$$\vec{\omega}\cdot\nabla A = (\vec{\Omega}\times\vec{\omega})\cdot\vec{r}$$

or

$$\frac{\partial A}{\partial z} = \Omega y \sin\varphi \,. \tag{2.24}$$

Thus,

$$A = \Omega y z \sin\varphi + B(x,y) \tag{2.25}$$

If we look at (2.25) in the cylindrical polar system described earlier we have

$$A = \Omega r z \sin\theta \sin\varphi + B(r,\theta)$$

$$\nabla A = \left(\Omega z \sin\theta\sin\varphi + \frac{\partial B}{\partial r},\ \Omega z\cos\theta\sin\varphi + \frac{\partial B}{\partial\theta},\ \Omega r\sin\theta\sin\varphi\right) \tag{2.26}$$

and the expression for $\vec{u}$ becomes

$$\left.\begin{aligned} u_r &= z(-\omega_x'\sin\theta + \omega_y'\cos\theta) + \Omega z\sin\theta\sin\varphi + \frac{\partial B}{\partial r}(r,\theta) \\ u_\theta &= \omega_z' r - z(\omega_x'\cos\theta + \omega_y'\sin\theta) + \Omega z\cos\theta\sin\varphi + \frac{\partial B}{\partial\theta} \\ u_z &= -r(-\omega_x'\sin\theta + \omega_y'\cos\theta) + \Omega r\sin\theta\sin\varphi \end{aligned}\right\} \tag{2.27}$$

We must have $\vec{u}\cdot\hat{n} = 0$ on all boundaries of the container. In par-

ticular, we must have $u_z = 0$ on $z = 0, L$ for any r . From (2.27) we see that u_z does not depend on z . Thus if we take $\omega_y' = 0$ and $\omega_x' = -\Omega \sin\varphi$ we can make u_z vanish on $z = 0, L$ for any r <u>but</u> we will then <u>not</u> be able, with this value of ω_x' and ω_y' , to make $u_r = 0$ on $r = r_0$ (the radius of the cylinder) for any z . Similarly, we see that if we make $u_r = 0$ on $r = r_0$ for any z by a suitable choice of ω_x' , ω_y' we will <u>not</u> be able to satisfy the boundary condition on u_z . Thus, we conclude that we cannot find a constant vorticity solution about an arbitrary axis for the precessing cylinder.

The reason that one can find a constant vorticity solution in the case of a spheroid is that by a suitable choice of $\vec{u}$, one can make the quadratic expression $\hat{n} \cdot \vec{u}$ the equation for the surface of the spheroid and thus automatically satisfy the condition $\hat{n} \cdot \vec{u} = 0$ on the surface. In the case of the cylinder, this is not possible as one does not have a simple quadratic expression for the entire surface.

Now, we return to the normal mode expansion method and write (following the notation of Greenspan)

$$\vec{u} = \sum_\alpha \vec{U}_\alpha(r) e^{s_\alpha t} + E^{1/2}\left\{\sum_\alpha \vec{u}_{\alpha 1}(\vec{r}) e^{s_\alpha t}\right\} + \sum_\alpha \tilde{\vec{u}}_\alpha(\vec{r}) e^{s_\alpha t} + E^{1/2}\left\{\sum_\alpha \tilde{\vec{u}}_{\alpha 1}(\vec{r}) e^{s_\alpha t}\right\} + \cdots \quad (2.28)$$

$$P = \sum_\alpha P_\alpha(\vec{r}) e^{s_\alpha t} + E^{1/2}\left\{\sum_\alpha p_{\alpha 1}(\vec{r}) e^{s_\alpha t}\right\} + \sum_\alpha \tilde{p}_\alpha(\vec{r}) e^{s_\alpha t} + E^{1/2}\left\{\sum_\alpha \tilde{p}_{\alpha 1}(\vec{r}) e^{s_\alpha t}\right\} + \cdots \quad (2.29)$$

$$s_\alpha = i\sigma + E^{1/2} s_{\alpha 1} \quad (2.30)$$

where: the tilde symbol denotes a boundary layer function (a function of

η which goes to zero exponentially as $\eta \to \infty$), σ denotes an inviscid eigenfrequency, and $s_{\alpha 1}$ denotes the $O(E^{1/2})$ viscous correction to the inviscid eigenfrequency. Note that we have not included any geostrophic modes in our expansion. This omission will be justified later.

Substitution of the expansions (2.28), (2.29), (2.30) into (2.13), (2.14), (2.15), (2.16) leads to a series of problems for the inviscid and boundary-layer flows and their mutual interaction. The sequence of problems for a typical normal mode represented as:

$$\vec{u} = \vec{U}_\alpha e^{s_\alpha t} + E^{1/2}\vec{u}_{\alpha 1} e^{s_\alpha t} + \vec{\tilde{u}}_\alpha e^{s_\alpha t} + E^{1/2}\vec{\tilde{u}}_{\alpha 1} e^{s_\alpha t} + \dots$$

$$p = P_\alpha e^{s_\alpha t} + E^{1/2} p_{\alpha 1} e^{s_\alpha t} + \tilde{p}_\alpha e^{s_\alpha t} + E^{1/2}\tilde{p}_{\alpha 1} e^{s_\alpha t} + \dots$$

$$s_\alpha = i\sigma + E^{1/2} s_{\alpha 1} + \dots$$

is the following (super scripts r, θ, z denote components):

$E^{-1/2}$

$$\frac{\partial \tilde{p}_\alpha}{\partial \eta} = 0 \quad ; \quad \frac{\partial \tilde{u}_\alpha^z}{\partial \eta} = 0 \tag{2.31}$$

E^{0}

$$\left.\begin{aligned} &i\sigma U_\alpha^r - 2U_\alpha^\theta + \frac{\partial U_\alpha^r}{\partial \theta} + \frac{\partial P_\alpha}{\partial r} = 0 \\ &i\sigma U_\alpha^\theta + 2U_\alpha^r + \frac{\partial U_\alpha^\theta}{\partial \theta} + \frac{1}{r}\frac{\partial P_\alpha}{\partial \theta} = 0 \\ &i\sigma U_\alpha^z + \frac{\partial U_\alpha^z}{\partial \theta} + \frac{\partial P_\alpha}{\partial z} = -2\Omega r \sin\varphi \cos\theta \\ &\text{with} \quad \nabla\cdot\vec{U}_\alpha = 0, \quad \vec{U}_\alpha \cdot \hat{m} = 0 \quad \text{on the boundary} \end{aligned}\right\} \tag{2.32}$$

$$
\left.
\begin{aligned}
&i\sigma \tilde{u}_\alpha^r - 2\tilde{u}_\alpha^\theta + \frac{\partial \tilde{u}_\alpha^r}{\partial \theta} + \frac{\partial \tilde{p}_\alpha}{\partial r} = \frac{\partial^2 \tilde{u}_\alpha^r}{\partial \eta^2} \\
&i\sigma \tilde{u}_\alpha^\theta + 2\tilde{u}_\alpha^r + \frac{\partial \tilde{u}_\alpha^\theta}{\partial \theta} + \frac{1}{r}\frac{\partial \tilde{p}_\alpha}{\partial \theta} = \frac{\partial^2 \tilde{u}_\alpha^\theta}{\partial \eta^2} \\
&i\sigma \tilde{u}_\alpha^z + \frac{\partial \tilde{u}_\alpha^z}{\partial \theta} + \frac{\partial \tilde{p}_{\alpha 1}}{\partial \eta} = \frac{\partial^2 \tilde{u}_\alpha^z}{\partial \eta^2} \\
&\frac{1}{r}\frac{\partial}{\partial r}(r\tilde{u}_\alpha^r) + \frac{1}{r}\frac{\partial \tilde{u}_\alpha^\theta}{\partial \theta} + \frac{\partial \tilde{u}_{\alpha 1}^z}{\partial \eta} = 0 \\
&\text{with } \vec{\tilde{u}}_\alpha = -\vec{U}_\alpha \text{ on } \eta = 0
\end{aligned}
\right\} \qquad (2.33)
$$

$E^{1/2}$

$$
\left.
\begin{aligned}
&s_{\alpha 1} U_\alpha^r + i\sigma u_{\alpha 1}^r - 2u_{\alpha 1}^\theta + \frac{\partial u_{\alpha 1}^r}{\partial \theta} + \frac{\partial p_{\alpha 1}}{\partial r} = 0 \\
&s_{\alpha 1} U_\alpha^\theta + i\sigma u_{\alpha 1}^\theta + 2u_{\alpha 1}^\theta + \frac{\partial u_{\alpha 1}^\theta}{\partial \theta} + \frac{1}{r}\frac{\partial p_{\alpha 1}}{\partial \theta} = 0 \\
&s_{\alpha 1} U_\alpha^z + i\sigma u_{\alpha 1}^z + \frac{\partial u_{\alpha 1}^z}{\partial \theta} + \frac{\partial p_{\alpha 1}}{\partial z} = 0 \\
&\text{with } \nabla \cdot \vec{u}_{\alpha 1} = 0, \quad (\vec{u}_{\alpha 1} + \vec{\tilde{u}}_{\alpha 1}) \cdot \hat{n} = 0 \text{ on the boundary}
\end{aligned}
\right\} \qquad (2.34)
$$

3. The Homogeneous Inviscid Problem:

First, we consider the homogeneous inviscid problem i.e. (2.32) with the forcing term in the z-equation equal to zero. From an inspection of (2.32) we try solutions of the form (neglecting the subscript α for the present):

$$
\left.
\begin{aligned}
U^r &= u(r)\cos kz\, e^{im\theta + i\sigma t} \\
U^\theta &= v(r)\cos kz\, e^{im\theta + i\sigma t} \\
U^z &= w(r)\sin kz\, e^{im\theta + i\sigma t} \\
P &= p(r)\cos kz\, e^{im\theta + i\sigma t}
\end{aligned}
\right\} \qquad (3.0)
$$

with $k = \frac{j\pi}{L}$, $j = 0, 1, 2, \ldots$ and $u(r) = 0$ on $r = r_0$.

Substituting these assumed product solutions into equations (2.32) we have:

$$i(\sigma+m)u - 2v + \frac{dp}{dr} = 0 \tag{3.1}$$

$$i(\sigma+m)v + 2u + \frac{imp}{r} = 0 \tag{3.2}$$

$$i(\sigma+m)w - kp = 0 \tag{3.3}$$

$$\frac{1}{r}\frac{d}{dr}(ru) + \frac{imv}{r} + kw = 0 \tag{3.4}$$

By manipulation of (3.1), (3.2), (3.3) we can solve for $\frac{d}{dr}(ru)$ and v in terms of w and by substitution into (3.4) we get the following equation for w

$$r^2\frac{d^2w}{dr^2} + r\frac{dw}{dr} + (\lambda^2 r^2 - m^2)w = 0 \tag{3.5}$$

with

$$\lambda^2 = k^2\frac{[4-(\sigma+m)^2]}{(\sigma-m)^2} \tag{3.6}$$

which we recognize as a Bessel equation. The boundary condition that $u(r)=0$ on $r=r_0$ becomes, in terms of w

$$\left.\frac{dw}{dr}\right|_{r=r_0} + \frac{2m}{r_0(\sigma+m)}w = 0 \tag{3.7}$$

The solution to (3.5) where m is an integer is

$$w(r) = J_m(\lambda r) \tag{3.8}$$

where $J_m(\lambda r)$ is the Bessel function of order m. The boundary condition (3.7) is then

$$\left.\frac{d}{dr}\left(J_m(\lambda r_0)\right)\right|_{r=r_0} + \frac{2m}{r_0(\sigma+m)}J_m(\lambda r_0) = 0. \tag{3.9}$$

Making use of the identity $J_n'(x) = \frac{nJ_n(x)}{x} - J_{n+1}(x)$ we have from (3.9) and (3.6) that

$$m J_m(\lambda r_0)\left[1+\left(\left(\frac{\lambda}{k}\right)^2+1\right)^{1/2}\right] = (\lambda r_0) J_{m+1}(\lambda r_0) \tag{3.10}$$

Equation (3.10) is a transcendental equation for λ which can be solved by plotting the left and right-hand sides and inspecting where they intersect. Having thus solved for the λ_n's of which there are an infinite but discrete number (n indexes the λ's), we can obtain the various values of σ (the eigenfrequency) from (3.6). We see that σ depends on m, k, n and should thus be written $\sigma_{m,k,n}$, however, we will delete the subscripts in what follows except where needed.

Having obtained $w(r)$ and the eigenfrequencies $\sigma_{m,k,n}$, we can write down $u(r)$, $p(r)$ and $v(r)$ which we have in terms of w from the elimination procedure involved in arriving at (3.5); they are

$$u(r) = \frac{(\sigma+m)[2+(\sigma+m)]}{k[4-(\sigma+m)^2]}\frac{m J_m(\lambda_n r)}{r} - \frac{\lambda_n(\sigma+m)^2}{k[4-(\sigma+m)^2]} J_{m+1}(\lambda_n r) \tag{3.11}$$

$$v(r) = \frac{i(\sigma+m)[2+(\sigma+m)]}{k[4-(\sigma+m)^2]}\frac{m J_m(\lambda_n r)}{r} - \frac{i 2\lambda_n(\sigma+m)}{k[4-(\sigma+m)^2]} J_{m+1}(\lambda_n r) \tag{3.12}$$

$$p(r) = \frac{i}{k}(\sigma+m) J_m(\lambda_n r) \tag{3.13}$$

Now, we will depart slightly from our outlined procedure by investigating the steady non-homogeneous inviscid problem instead of first correcting the inviscid normal modes for viscosity and then looking at the non-homogeneous problem. This will allow us to see explicitly the role viscosity must play in order for there to be a physically acceptable solution.

4. The Non-homogeneous Inviscid Problem:

The steady non-homogeneous problem is given by (2.32) with the

$\frac{\partial}{\partial t}$ terms omitted i.e.

$$-2U^{\theta} + \frac{\partial U^{r}}{\partial \theta} + \frac{\partial P}{\partial r} = 0 \tag{4.1}$$

$$2U^{r} + \frac{\partial U^{\theta}}{\partial \theta} + \frac{1}{r}\frac{\partial P}{\partial \theta} = 0 \tag{4.2}$$

$$\frac{\partial U^{z}}{\partial \theta} + \frac{\partial P}{\partial z} = -2\Omega r \sin\varphi \cos\theta = f \tag{4.3}$$

$$\frac{1}{r}\frac{\partial}{\partial r}(rU^{r}) + \frac{1}{r}\frac{\partial U^{\theta}}{\partial \theta} + \frac{\partial U^{z}}{\partial z} = 0 \tag{4.4}$$

Before solving this problem, we return to the question of the geostrophic modes which were omitted in the expansions (2.28) and (2.29). Theoretically, the geostrophic modes must be included to give a complete set of eigenfunctions of the homogeneous inviscid problem in which to expand the forcing term in the non-homogeneous problem.

Geostrophic modes are characterized by two-dimensional motion which, in our case, means no variation in the z-direction, i.e. $k = 0$. Since U^{z} in (2.32) is zero at $z = 0, L$ we must have $U^{z} = 0$ throughout the cylinder. Thus, for equations (3.1) to (3.4) we have

$$i(\sigma + m)u(r) - 2v(r) + \frac{dp(r)}{dr} = 0 \tag{4.5}$$

$$i(\sigma + m)v(r) + 2u(r) + \frac{imp(r)}{r} = 0 \tag{4.6}$$

$$\frac{d}{dr}(ru(r)) + imv(r) = 0 \tag{4.7}$$

Provided $\sigma \neq -m$ these equations give

$$\frac{d}{dr}\left(r\frac{d}{dr}(ru(r)\right) - m^{2}u(r) = 0 \tag{4.8}$$

which is Laplace's equation in the (r, θ) plane.

Now, $u(r)$ must be zero on the boundary i.e. at $r = r_{0}$ and since a

function which satisfies Laplace's equation in a region must take its maximum value on the boundary of that region we conclude that under the assumption $\sigma \neq -m$, $u(r)=0$ in $r=0$ to $r=r_0$. Thus, we must have $\sigma=-m$ or, in dimensional form, $\sigma=-m\omega$ which gives the frequency of the geostrophic modes as seen in the precessing frame. Note that we can pick for $u(r)$ any arbitrary function of r which is regular at $r=0$ and vanishes at $r=r_0$, and that the total velocity $\vec{U}=U^r\hat{r}+U^\theta\hat{\theta}$ can be chosen as any arbitrary function of the two variables r and θ which satisfies continuity and the $\vec{U}\cdot\hat{n}=0$ boundary condition. Being able to choose $\vec{U}$ as an arbitrary function of two variables is a consequence of the fact that we have a cylinder with flat plates on the ends and since geostrophic motion is motion on contours of constant depth we see that any contour in the r,θ plane will do. In the case of the sphere or spheroid, however, not just any contour is a contour of constant depth and so, in a sense, we have a "bigger infinity" of geostrophic modes in the cylinder than in the sphere or spheroid.

Why, then, do we omit this infinity of eigenmodes needed to form a complete set of functions for the solution of the non-homogeneous problem? The answer is that none of them are excited by the forcing term $-2\Omega r\sin\varphi\cos\theta$. Note that the forcing term appears only in the z-equation in the statement of the steady non-homogeneous problem i.e. only in (4.3). Thus, it will be expanded in a sine series of $\sin kz$. The first non-zero term appearing in this expansion will be $k=1$, but geostrophic modes have $k=0$ and are thus not excited by the forcing term. This can be seen physically from the following: we write the forcing term

in its dimensional vector form as $-2(\vec{\Omega}\cdot\vec{r})\vec{\omega}$; the curl of this force is $2\vec{\omega}\times\vec{\Omega}$ which is perpendicular to the plane defined by $\vec{\omega}$ and $\vec{\Omega}$. Now, to drive geostrophic motion in our cylinder, the force must have a curl which lies along the $\vec{\omega}$ axis. But, as we have seen, it is perpendicular to this axis and thus will not drive any geostrophic motions.

We return to (4.1) to (4.4) and write $\vec{U}$, P, and f as expansions in the eigenfunctions of the homogeneous inviscid problem:

$$\left.\begin{aligned} U^r &= \sum_{m,k,n} B_{m,k,n}\, u_{m,k,n}(r)\cos kz\, e^{im\theta} \\ U^\theta &= \sum_{m,k,n} C_{m,k,n}\, v_{m,k,n}(r)\cos kz\, e^{im\theta} \\ U^z &= \sum_{m,k,n} A_{m,k,n}\, w_{m,k,n}(r)\sin kz\, e^{im\theta} \\ P &= \sum_{m,k,n} D_{m,k,n}\, p_{m,k,n}(r)\cos kz\, e^{im\theta} \\ f &= \sum_{m,k,n} F_{m,k,n}\, w_{m,k,n}(r)\sin kz\, e^{im\theta} \end{aligned}\right\} \qquad (4.9)$$

where $w_{m,k,n}(r) = J_m(\lambda_n r)$ and $u_{m,k,n}$, $v_{m,k,n}$ and $p_{m,k,n}$ are given by (3.11), (3.12) and (3.13) respectively. We substitute (4.9) into (4.1) to (4.4) and consider a particular m,k,n . After some algebra, we arrive at one equation relating the $A_{m,k,n}$ to the $F_{m,k,n}$ which is (dropping the m,k,n for the present)

$$L(Aw) + \gamma^2 r(Aw) + \frac{i}{m} L(Fw) = 0 \qquad (4.10)$$

where

$$\gamma^2 = \frac{k^2(4-m^2)}{m^2} \qquad (4.11)$$

and

$$L \equiv \frac{d}{dr}\left(r\frac{d}{dr}\right) - \frac{m^2}{r}$$

We recall from the homogeneous problem that

$$Lw = -\lambda_n^2 r w \tag{4.12}$$

Thus, making use of (4.12) we have from (4.10)

$$A_{m,k,n} = \frac{i}{m} \frac{\lambda_n^2}{(\gamma^2 - \lambda_n^2)} F_{m,k,n} \tag{4.13}$$

The $B_{m,k,n}$, $C_{m,k,n}$, $D_{m,k,n}$ are known in terms of the $A_{m,k,n}$ from the elimination procedure used in arriving at (4.10). The $F_{m,k,n}$ are known constants gotten from integrating the forcing function and using the orthogonality properties of the Bessel Functions and the sines and cosines. Explicitly we have (for $m=\pm 1$) for reasons discussed below)

$$F_{\pm 1,k,n} = \mp \frac{\theta \Omega r_0^2 \lambda_n J_2(\lambda_n r_0)}{k L \left(\lambda_n^2 r_0^2 + \frac{4}{(\sigma \pm 1)^2} - 1\right) \left(J_1(\lambda_n r_0)\right)^2} \tag{4.14}$$

where $k = \frac{j\pi}{L}$ and j an odd integer.

From (4.13) it is apparent that there will be resonance when $\gamma^2 = \lambda_n$. From (3.6) and (4.11) we see that $\lambda_n^2 = \gamma^2$ when $\sigma = 0$. Now, we must see if this value of λ_n can satisfy (3.10). Note that since $f \propto \cos\theta$ we need only consider the cases $m = \pm 1$ at resonance. For $m = +1$ (3.10) becomes

$$\frac{(1+\sqrt{3})}{a\sqrt{3}} = \frac{J_2(a\sqrt{3})}{J_1(a\sqrt{3})} \tag{4.15}$$

where $a = k r_0$. Thus, at the values of a (call them a_ϵ; $\epsilon = 1, 2, \cdots$) for which (4.15) is satisfied, we will have resonance. There are an infinite number of discrete roots to (4.15) and as a_ϵ gets large, the roots approach the zeroes of J_2. We have

$$\frac{a_\epsilon}{r_0} = k = \frac{j\pi}{L} \quad \text{or} \quad \frac{r_0}{L} = \frac{a_\epsilon}{j\pi} \tag{4.16}$$

and so for discrete values of $\frac{r_0}{L}$ we will have a resonance. The first two roots of (4.15) are $a_1 = 1.54$ and $a_2 = 3.26$, so for $j = 1$, $a_\epsilon = a_1$ we have

$$\frac{2r_0}{L} = \frac{D}{L} = \frac{2a_1}{\pi} = 0.98 \tag{4.17}$$

where D is the diameter of the cylinder. Thus, the first mode resonance $(a_\epsilon = a_1, j = 1)$ occurs for that cylinder which is "most sphere-like" i.e. that cylinder with $D/L \simeq 1$.

For $m = -1$ (3.10) becomes

$$\frac{(1+\sqrt{3})}{a\sqrt{3}} = \frac{J_0(a\sqrt{3})}{J_1(a\sqrt{3})} \tag{4.18}$$

and the same comments apply as for the $m = +1$ case except that now, for a_ϵ large the roots approach the zeros of J_0 and the first root is $a_1 = 2.88$. Thus, for $m = -1$, the first mode resonance is for

$$\frac{2r_0}{L} = \frac{D}{L} = \frac{2a_1}{\pi} = 1.84 \tag{4.19}$$

Now, for a_ϵ large, the roots of the Bessel Functions are evenly spaced and can be approximated by an integer multiple of pi, say $s\pi$ where s is an integer. For a_ϵ large we have

$$\frac{r_0}{L} = \frac{a_\epsilon}{j\pi} \simeq \frac{s}{j} \tag{4.20}$$

where $\frac{s}{j}$ is a rational number. Thus, for high enough mode numbers (high enough j and a_ϵ) we can come arbitrarily close to any r_0/L. This means that for high enough mode numbers we can find a resonant cylinder arbitrarily close to any given cylinder. However, at these high mode numbers viscosity will damp out the resonance and we also see from (4.14) that the coefficients $F_{\pm 1, k, m}$ are proportional to $\frac{1}{k^3}$ (since $\lambda_n^2 \propto k^2$) and so will be small for high k (i.e. high j).

Nevertheless, at the resonance point, in the absence of viscosity, the $F_{+1,k,m}$ do not vanish and so the $A_{m,k,m}$ in (4.13) go to infinity. It is at this point that we must call upon viscosity and the boundary layers to get rid of this infinity and give us a physically acceptable solution.

5. Viscous Corrections

We now turn our attention to equations (2.33) for the boundary layer flow. Using the fact that $\frac{\partial}{\partial\theta} = im$ and $\tilde{p}_\alpha = \tilde{u}^z_\alpha = 0$ we have

$$\left.\begin{aligned} i(\sigma+m)\tilde{u}^r_\alpha - 2\tilde{u}^\theta_\alpha &= \frac{\partial^2\tilde{u}^r_\alpha}{\partial\eta^2} \\ i(\sigma+m)\tilde{u}^\theta_\alpha + 2\tilde{u}^r_\alpha &= \frac{\partial^2\tilde{u}^\theta_\alpha}{\partial\eta^2} \end{aligned}\right\} \tag{5.1}$$

$$\frac{\partial\tilde{p}_{\alpha 1}}{\partial\eta} = 0$$

$$\frac{1}{r}\frac{\partial}{\partial r}\left(r\tilde{u}^r_\alpha\right) + \frac{1}{r}\frac{\partial\tilde{u}^\theta_\alpha}{\partial\theta} + \frac{\partial\tilde{u}^z_{\alpha 1}}{\partial\eta} = 0 \tag{5.2}$$

with $\vec{\tilde{u}}_\alpha = -\vec{U}_\alpha$ on $\eta = 0$. (5.3)

The physical content of (5.1) and (5.2) is the following: we reduce the interior flow to zero on the boundary of the container ($\eta = 0$) by means of the boundary layer (5.1), and in so doing, we induce a small $O(E^{1/2})$ flux $\tilde{u}^z_{\alpha 1}$ given by (5.2) which, in turn, forces a small $O(E^{1/2})$ interior circulation $\vec{u}_{\alpha 1}$ given by (2.34).

Now, in (5.1) we let $\Phi = \tilde{u}^r_\alpha + i\tilde{u}^\theta_\alpha$ and we can then write

$$\frac{\partial^2\Phi}{\partial\eta^2} = i(2+\sigma+m)\Phi \tag{5.4}$$

The solution which goes to zero as $\eta\to\infty$ and which satisfies (5.3) is:

$$\tilde{\Phi} = \tilde{u}^r_\alpha + i\,\tilde{u}^\theta_\alpha = -\left(U^r_\alpha + i\,U^\theta_\alpha\right) e^{-(1+i)\left(1+\frac{\sigma+m}{2}\right)^{1/2}\eta} \tag{5.5}$$

Next, we calculate the normal flux $\tilde{u}^z_{\alpha 1}$ from (5.2); we have

$$\frac{\partial \tilde{u}^z_{\alpha 1}}{\partial \eta} = \left\{ \frac{1}{r}\frac{\partial}{\partial r}\left(r U^r_\alpha\right) + \frac{1}{r}\frac{\partial U^\theta_\alpha}{\partial \theta} \right\} e^{-(1+i)\left(1+\frac{\sigma+m}{2}\right)^{1/2}\eta} \tag{5.6}$$

with the boundary condition

$$\left(\vec{u}_{\alpha 1} + \vec{\tilde{u}}_{\alpha 1}\right)\cdot \hat{n} = 0 \quad \text{on the boundary} \tag{5.7}$$

If we integrate (5.6) from zero to infinity, use (5.7), and recall that all boundary layer quantities go to zero as $\eta \to \infty$ we have

$$-\tilde{u}^z_{\alpha 1}\Big|_{\eta=0} = \frac{H}{2\beta}(1-i) = u^z_{\alpha 1}\Big|_{\eta=0} \tag{5.8}$$

where

$$H \equiv \frac{1}{r}\frac{\partial}{\partial r}\left(r U^r_\alpha\right) + \frac{1}{r}\frac{\partial U^\theta_\alpha}{\partial \theta}$$

$$\beta \equiv \left(1 + \frac{\sigma+m}{2}\right)^{1/2}.$$

Now that we have the normal flux $\tilde{u}^z_{\alpha 1}$ we consider equations (2.34) for $\vec{u}_{\alpha 1}$, the $O(E^{1/2})$ interior circulation forced by the flux $\tilde{u}^z_{\alpha 1}$ from the boundary layer. We don't really want to solve (2.34) for $\vec{u}_{\alpha 1}$, we only want $s_{\alpha 1}$, the $O(E^{1/2})$ viscous correction to the inviscid eigenfrequency σ. We can obtain $s_{\alpha 1}$ from (2.34) by making use of the appropriate orthogonality relationship between the normal modes of the inviscid homogeneous problem.

Let $(\vec{U}_1, \sigma_1), (\vec{U}_2, \sigma_2)$ be any two eigenfunction-eigenvalue pairs $(\sigma_1 \neq \sigma_2)$ satisfying (2.32) with the forcing term equal to zero i.e. the homogeneous-inviscid equations. In vector form we have

$$i\sigma \vec{U}_\alpha + 2(\hat{k} \times \vec{U}_\alpha) + \operatorname{curl} \vec{U}_\alpha \times (\hat{k} \times \vec{r}) = -\nabla P_\alpha \tag{5.9}$$

From (5.9) we can form the following expressions

$$i\sigma_1 \vec{U}_2^* \cdot \vec{U}_1 + 2\vec{U}_2^* \cdot (\hat{k} \times \vec{U}_1) + \vec{U}_2^* \cdot \text{curl}\, \vec{U}_1 \times (\hat{k} \times \vec{r}) = -\vec{U}_2^* \cdot \nabla P_1 \tag{5.10}$$

$$-i\sigma_2 \vec{U}_1 \cdot \vec{U}_2^* + 2\vec{U}_1 \cdot (\hat{k} \times \vec{U}_2^*) + \vec{U}_1 \cdot \text{curl}\, \vec{U}_2^* \times (\hat{k} \times \vec{r}) = -\vec{U}_1 \cdot \nabla P_2^* \tag{5.11}$$

where $\vec{U}_{(\cdot)}^*$ denotes complex conjugate. By adding (5.10) and (5.11) and integrating over the volume of the cylinder V, it can be shown, after some manipulation, that the orthogonality relationship satisfied by the inviscid modes is

$$\int_V \vec{U}_2^* \cdot \vec{U}_1 \, dV = 0 \tag{5.12}$$

Now, consider (2.34) in vector form

$$i\sigma \vec{u}_{\alpha 1} + 2\hat{k} \times \vec{u}_{\alpha 1} + \text{curl}\, \vec{u}_{\alpha 1} \times (\hat{k} \times \vec{r}) = -\nabla p_{\alpha 1} - s_{\alpha 1} \vec{U}_\alpha \tag{5.11}$$

with $$(\vec{u}_{\alpha 1} + \vec{\bar{u}}_{\alpha 1}) \cdot \hat{n} = 0 \quad \text{on the boundary} \tag{5.12}$$

and $$\nabla \cdot \vec{u}_{\alpha 1} = 0 \tag{5.13}$$

We know $\vec{u}_{\alpha 1} \cdot \hat{n}$ on the boundary, it is just the normal flux given by (5.8). Thus, $\vec{u}_{\alpha 1} \cdot \hat{n}$ is a known function on the boundary which we will call G_α. We now multiply (5.11) by $\vec{U}_\alpha^*$, take the complex conjugate of (5.9) and multiply by $\vec{u}_{\alpha 1}$, add the two resulting equations and integrate over the volume of the cylinder, using the relationships developed in establishing the orthogonality relation, to get

$$\int_V \vec{U}_\alpha^* \cdot \nabla p_{\alpha 1} \, dV + \int_V \vec{u}_{\alpha 1} \cdot \nabla P_\alpha^* \, dV + s_{\alpha 1} \int_V \vec{U}_\alpha^* \cdot \vec{U}_\alpha \, dV = 0 \tag{5.14}$$

But

$$\int_V \vec{U}_\alpha^* \cdot \nabla p_{\alpha 1} \, dV = \int_S p_{\alpha 1} \hat{n} \cdot \vec{U}_\alpha^* \, dS = 0$$

$$\int_V \vec{u}_{\alpha 1} \cdot \nabla P_\alpha^* \, dV = \int_S P_\alpha^* \hat{n} \cdot \vec{u}_{\alpha 1} \, dS = \int_S P_\alpha^* G_\alpha \, dS$$

so we have for (5.14)

$$s_{\alpha 1} = - \frac{\int_S P_\alpha^* G_\alpha \, dS}{\int \vec{U}_\alpha^* \cdot \vec{U}_\alpha \, dV} \tag{5.15}$$

where dS is the element of surface area of the cylinder. Everything is known in (5.15), so it is just a matter of evaluating the integrals to arrive at $s_{\alpha 1}$. The integrals are straightforward but messy, so we will just give $s_{\alpha 1}$ for the first mode resonance i.e. for $m=1$ $\sigma_{m,k,n} = 0$, $k = \frac{\pi}{L}$, $a_\alpha = a_1 = 1.54$. In this case (in dimensional form)

$$s_{\alpha 1} = -\omega(1+i)(.057) \tag{5.16}$$

and we note that $Re(s_{\alpha 1}) < 0$ as it must be.

Recall that

$$s_{\alpha 1} = i\sigma_{m,k,n} + E^{1/2} s_{\alpha 1} = i(\sigma_{m,k,n} - iE^{1/2} s_{\alpha 1}) \tag{5.17}$$

or

$$s_{\alpha 1} = i\sigma^{\nu}_{m,k,n} \tag{5.18}$$

where $\sigma^{\nu}_{m,k,n}$ is the inviscid eigenfrequency corrected to $O(E^{1/2})$ for viscosity.

Now we wish to investigate how the resonance values of $\frac{r_0}{L}$ have been affected by the correction to the eigenfrequencies (5.18). To do this, we note that the factor in (4.13) responsible for resonance is (for $m=1$)

$$\frac{\lambda_n^2}{(3k^2 - \lambda_n^2)} \tag{5.19}$$

where we now write (dropping the subscripts m,k,n on $\sigma^{\nu}_{m,k,n}$)

$$\lambda_n^2 = \frac{k^2[4 - (\sigma^{\nu}+1)^2]}{(\sigma^{\nu}+1)^2} \tag{5.20}$$

We want to find the value of $\frac{r_0}{L}$ which makes the denominator of (5.19) a

minimum. This will be the new resonance value, to $O(E^{1/2})$, of $\frac{r_0}{L}$. We write $\sigma^v(R) = \sigma^I(R) + E^{1/2} S_{\alpha 1}(R)$ where $R = r_0/L$ and σ^I is the inviscid eigenfrequency. Now, we expand $\sigma^I(R)$ about R_0, the resonance value of r_0/L in the inviscid case. Noting that $\sigma^I(R_0) = 0$ we have

$$\sigma^v(R) = \frac{d\sigma^I}{dR}(R - R_0) + E^{1/2} S_{\alpha 1}(R) \tag{5.21}$$

In the range of $(R - R_0)$ we are interested in, we define a quantity δ as $(R - R_0) = \delta E^{1/2}$. Substituting (5.21) and (5.20) into the denominator of (5.19), call it D, and keeping terms to $O(E^{1/2})$ we have (in dimensional form) for the first mode resonance $(m=1,\ k = \frac{\pi}{L},\ a_\epsilon = a_1 = 1.54)$

$$D = 8 \frac{\pi^2}{L^2} \omega E^{1/2} \left\{ \delta \frac{d\sigma^I}{dR} - \omega(1+i)(.057) \right\} \tag{5.22}$$

We can find the minimum of $|D|$ by equating real parts in the curly brackets. Thus, the new resonance value of $\frac{r_0}{L}$, call it R_p, will occur where

$$\delta \frac{d\sigma^I}{dR} = \omega(0.057) \tag{5.23}$$

or at

$$R_p = \frac{(.057) E^{1/2}}{\frac{d}{dR}\left(\frac{\sigma^I}{\omega}\right)} + R_0 \tag{5.24}$$

The width of the new resonance peak, where the amplitude is one-half its maximum value, can be obtained by equating the square of the real part to the square of the imaginary part in the curly brackets in (5.22). Let the values of R where the amplitude is one-half its maximum value (the "half power" points) be denoted by R_+ and R_-. Then the width of the peak is

$$R_+ - R_- = 2(R_p - R_0) \tag{5.25}$$

From the solution of the inviscid homogeneous problem, we can

calculate $\frac{d\sigma^I}{dR}$ near $R = R_0$. Such a calculation gives

$$\frac{d}{dR}\left(\frac{\sigma^I}{\omega}\right) \simeq -50 \tag{5.26}$$

Thus, from (5.24) we see that to $O(E^{1/4})$ viscosity has not appreciably changed the resonance value of $\frac{r_0}{L}$ for the first mode resonance. In fact, for a 4 in. diameter cylinder (see experimental results below) $L = 1.04$ for the first mode resonance, and if we take ω as 78 r.p.m. and water as the fluid we have $E \sim 10^{-5}$ and $R_p \simeq R_0 - 10^{-6}$. From (5.25) we see that the width of the first mode resonance at the "half power" points is very small.

6. Experimental Results

A very crude and hasty attempt was made, during the last few days of the summer program, to observe the predicted resonances. A 4 in. inside diameter piece of plastic tubing was fitted with end plates, the top one having a threaded hole in it. A threaded metal rod extended through the hole in the top plate and was attached to a plastic disk slightly smaller than 4 inches in diameter which could be screwed up and down to vary the height of the cylinder from about 3 in. to 8 in. The rim of the disk was fitted with an "O" ring to prevent any interaction between the cavities above and below the disk.

The cylinder was rotated at 78 r.p.m. on a record turntable which in turn was tilted about 10 degrees and placed on a large turntable which rotated at about 5 r.p.m. Aluminum powder was put in the water and was observed with a strobotac which was attached to the large turntable.

The "experiment" consisted of observing the behavior of the flow

in the cylinder as the inside disk was raised and lowered. A resonance was predicted at a diameter to height ratio of 0.98 for the first mode resonance, which should be the strongest. A pronounced, reproducible resonance was observed experimentally at a diameter to height ratio of about 1.05. The observed resonance was characterized by having a very turbulent-looking flow pattern with strong shear layers and vortices throughout the fluid in contrast to the relatively quiet laminar-looking flow pattern as the disk was moved above or below the resonance point.

The viscous correction to the predicted value of 0.98 is too small to account for the discrepancy between the observed value of 1.05 and the predicted value. However, there are many other factors that must be taken into account before anything quantitative can be said about the agreement of prediction and observation. For example, the theory assumes $\frac{\Omega}{\omega} << 1$, which was not really the case. In fact, $\vec{\Omega}$ has a component along the $\vec{\omega}$ axis which will change the effective value of $\vec{\omega}$, adding to or subtracting from it depending on whether or not the two turntables are rotating in the same or in opposite directions.

Another obvious effect to consider is the side wall boundary layers which have been completely neglected in this treatment. Also, things like end plates not being parallel and non-uniform rotation can also have important effects.

Lack of time prevented a careful experiment including a search for the resonances of other modes. However, despite all the crudeness and all the factors not taken account of it is quite remarkable to the author that it was possible to put something together in a day or two,

put it on a turntable, and get results as close to predicted values as were obtained in this case.

Acknowledgements

The author would like to thank all the staff members for a stimulating summer and especially Dr. Howard for his interest in the problem and his guidance in much of the analysis.

References

1. Greenspan, H. P. 1964 J.Fluid Mech., 22: 449

2. Roberts, P. H. and K. Stewartson 1965 Proc.Camb.Phil.Soc. 61: 279

3. Stewartson, K. and P. H. Roberts 1963 J.Fluid Mech., 17: 1

On Stationary Topography-induced Rossby-wave Patterns in a Barotropic Zonal Current

Michael McIntyre

1. Introduction

The present remarks concern the modification, by a bottom-topographical feature or other stationary perturbing effect, of a uniform zonal frictionless barotropic current in a beta-plane. Simple examples illustrate the fact that there are several qualitatively distinct ways in which the zonal current can be affected by the topography.

Porter and Rattray (1964) have given some interesting finite-amplitude analytic solutions representing stationary Rossby waves, which comprise one of the possible types of steady-flow pattern, under the hypothesis that

the topography is independent of latitude. A typical such solution, for instance, describes the effect of an infinitely long north-south downward step upon a uniform eastward current (see Figure 1). The current is first

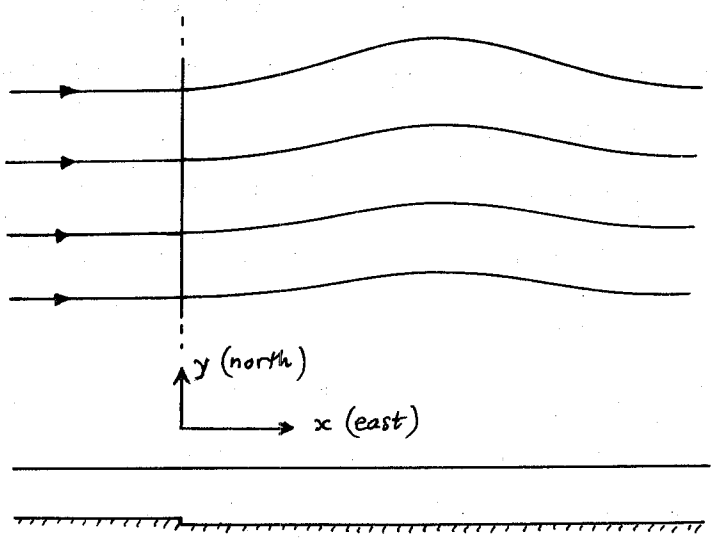

Fig. 1

deflected northward after entering the deeper region, because of the cyclonic relative vorticity associated with the stretching of a fluid column as it crosses the step. Then the beta-effect, which is associated with the variation of the Coriolis parameter with latitude, acts to provide a restoring force counteracting the initial northward deflection and so on. The end result is a stationary Rossby-wave pattern downstream of the step.

What happens if the current flows westward over such a step is not so clear from Porter and Rattray's analysis, and the desire to clarify this situation was the original motivation for the present enquiry.

If the current is westward, the beta-effect reinforces any initial

deflection, and Porter and Rattray's solution for the westward current exhibits an exponential growth of the deflection with distance downstream of the step. It is difficult however to believe that a physically real instability should exist in what looks like an energetically neutral situation, in the sense that the mean zonal current itself contains no "available" energy source (as it would if it possessed horizontal shear, for example). Indeed, Porter and Rattray themselves cast doubt on the physical relevance of their westward-flow solution, invoking "the finite meridional extent of natural bottom features" as a reason for not necessarily expecting a large deflection in practice.

However, as will be shown, the solution involving infinite deflection may be rejected as being physically irrelevant on much simpler grounds. The solution is based on the assumption that the flow is undisturbed upstream of the step. In §2 we show on the basis of a linearized initial-value approach that such an assumption is inappropriate. What the current really does is to start deflecting before it reaches the step, so as to cross the step at precisely that angle that will allow it to straighten out eventually on the other side and continue to flow due west (Figure 2).

Thus we have a simple, but perhaps pertinent, illustration of the well-known but occasionally overlooked fact that care is needed in deciding what assumptions can be made concerning the flow upstream of a local perturbing effect, in any fluid-dynamical situation of this general kind. For zonal flow in a beta-plane the assumption of no disturbance upstream happens to be justified in the case with which Porter and Rattray were primarily concerned, that of eastward flow across latitude-independent topography. As has been

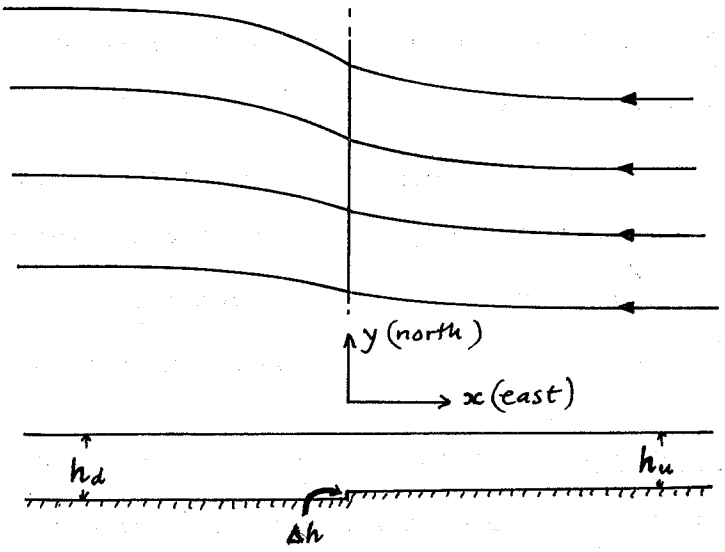

Fig. 2

noted, it is incorrect for westward flow.

The point is further underlined by the discussion of §3, where we use linear theory to explore in the simplest possible way the effect of laterally constraining the motion. The assumption of no disturbance upstream is then never correct, and moreover (in the case of a "slow" eastward current) the disturbance penetrates <u>far</u> upstream, as well as far downstream.

In §4 the results are rationalized in terms of group velocity.

The relationship and the difference between the present results and the recent work of Lighthill (1967) should be noted. Lighthill uses a general method to calculate, among other things, Rossby-wave patterns at large distances from a travelling forcing effect of general form but of limited spatial extent. Here (ignoring the trivial change in frame of reference) the forcing

effect is latitudinally extensive, but of very simple form so that solutions for the whole pattern are easy to write down. Both problems serve to illustrate the fundamental role played by the group velocity.

Porter and Rattray's finite-amplitude solutions suggest that there should exist an analogous steady finite-amplitude solution for the physically relevant type of westward-flow solution depicted in Figure 2. This is found to be the case, and the solution is given in § 5.

The beta-plane model. The discussion will be based on the well-known potential-vorticity equation for a shallow inviscid homogeneous layer of depth $h = h(x,y)$ on a rotating earth, in the beta-plane approximation (see Veronis 1963, Longuet-Higgins 1964). The local Cartesian coordinates x,y correspond to the directions east and north, and u, v are the eastward and northward velocity components. The vertical component of vorticity relative to the earth is $\zeta = \partial v/\partial x - \partial u/\partial y$, and the Coriolis parameter, or local vertical component of the absolute vorticity due to the earth's rotation, is denoted by f. Note that f increases with latitude. The potential vorticity equation is

$$\frac{D}{Dt}\left(\frac{\zeta+f}{h}\right) = 0 \tag{1.1}$$

where

$$\frac{D}{Dt} \equiv \frac{\partial}{\partial t} + u\frac{\partial}{\partial x} + v\frac{\partial}{\partial y}.$$

The horizontal component of absolute vorticity is assumed negligible in the dynamics. Hydrostatic equilibrium has been assumed, and so u, v and ζ are functions of x and y only. Columns of fluid move coherently, and change their vertical component of absolute vorticity purely as a result of vortex-

tube stretching.

The variation of f with latitude will be modeled in the usual way by regarding f as constant in (1.1) except when it is operated on by $\partial/\partial y$, when we set

$$\frac{\partial f}{\partial y} = \beta \quad = \text{constant}. \tag{1.2}$$

This variation of f is the reason why north-south motions involve changes in ζ, apart from any further changes due to topography - the so-called beta-effect.

The depth $h(x,y)$ is presumed specified independently of the fluid motions. For a free upper surface this is permissible provided gravity is strong enough, so that free-surface displacements are negligible. The formal requirement is $gh/f^2L^2 \gg 1$ where L is a characteristic horizontal length scale. Although, typically, this relation is not well satisfied for the oceans, except for rather short wavelengths, the changes introduced by allowing for free-surface displacements are probably not important qualitatively. See Lighthill (1967), Longuet-Higgins (1965).

The beta-plane is supposed horizontally unbounded; we shall ignore the fact that this is not a strictly self-consistent point of view. Throughout, the topography will be represented by a single step as in Figure 2. Such a step is perhaps best thought of as representing a smoothly sloping region whose upslope length scale is much smaller than the wavelengths of interest in the fluid motion. More elaborate and realistic-looking topography could be considered, but this limiting case, in the context of the simple beta-plane model with negligible free-surface displacements, will serve adequately to illustrate the fundamental points under discussion.

2. The latitude-independent problem for a westward current.

In this section it is verified that the type of flow shown in Figure 2 is the one that is ultimately set up if at time zero the current is supposed unperturbed. Although linearized theory is used, one would expect to see a definite indication of a growing downstream disturbance if the instability of the westward current were a real one, and no such indication is found.

In order to be able to use linear theory we must suppose that $\Delta h/h \ll 1$, where Δh is the height of the step. The basic (constant) zonal current V is westward, i.e. $V<0$. The total fluid velocity is written as $\{V+u(x), v(x)\}$ where $u, v \ll V$. The linearized form of (1.1) in $x<0$ or $x>0$ (h = constant) is

$$\left(\frac{\partial}{\partial t}+V\frac{\partial}{\partial x}\right)\frac{\partial v}{\partial x}+\beta v=0. \qquad (2.1)$$

Note that the perturbation x-velocity u does not enter into the linearized dynamics, and so may be ignored in the analysis. By continuity, u is a constant on each side of the step.

If the upstream region ($x>0$ here) is denoted by suffix u, and the downstream region ($x<0$) by suffix d, we may write the jump conditions on v as

$$\left.\begin{aligned} v_d &= v_u \\ \frac{\partial v_d}{\partial x} &= \frac{\partial v_u}{\partial x}+\Delta \end{aligned}\right\} \text{ at } x=0 \qquad (2.2)$$

where

$$\Delta \equiv \int \Delta\, h/h = \text{constant}, \qquad (2.3)$$

Δ being positive if a fluid column is stretched on passing over the step, as in Figure 2. Because of the linearization, it is immaterial whether h in (2.3) is considered to be (for instance) the upstream or the downstream depth. The conditions (2.2) are the result of supposing that the potential-vorticity equation (1.1) continues to describe the flow as h tends to a step function via a sequence of differentiable functions. (The remarks at the

end of $\S 1$ should be borne in mind.) The first of (2.2) states that the vorticity of a fluid column remains finite as it crosses the step, and the second, that the vorticity change is just that due to stretching.

The initial condition is that for all x ,

$$v = 0 \quad \text{when} \quad t = 0. \tag{2.4}$$

Then if $\hat{v}$ is the Laplace transform of v , defined as

$$\hat{v}(x,p) = \int_0^\infty e^{-pt} v(x,t)\,dt,$$

it follows from (2.1) and (2.4) that $\hat{v}$ satisfies

$$U \frac{\partial^2 \hat{v}}{\partial x^2} + p \frac{\partial \hat{v}}{\partial x} + \beta \hat{v} = 0. \tag{2.5}$$

Thus $\hat{v}$ is a linear combination of $exp(m_+ x)$ and $exp(m_- x)$, where

$$m_\pm = -\frac{1}{2U}\left\{p \pm (p^2 - 4\beta U)^{1/2}\right\}. \tag{2.6}$$

$(p^2 - 4\beta U)^{1/2}$ will be defined as positive when $p^2 - 4\beta U$ is real and positive.

As well as the jump conditions (2.2), boundary conditions as $x \to \pm\infty$ are needed to complete the determination of $\hat{v}$. The boundary conditions that naturally suggest themselves are that $v(x,t) \to 0$ as $x \to \pm\infty$ for each t . But these do not directly imply $\hat{v} \to 0$ (or even bounded) as $x \to \pm\infty$ for constant p , and a more convenient way of imposing the boundary conditions is to assume that, uniformly for large $|x|$, the disturbance velocity $v(x,t)$ does not grow faster than exponentially with time. That is, there are positive constants X, R, S such that for $|x| > X$ and for all t ,

$$|v(x,t)| < Re^{St}. \tag{2.7}$$

This is only a slight assumption; far from the step, where it applies, it still includes the possibility of an exponentially-growing solution for v with arbitrarily large growth-rate. The condition (2.7) implies that $\hat{v}(p,t)$ is bounded as $x \to \pm\infty$ for p real and greater than S . This is enough to ensure that m_+ is appropriate in $x < 0$ and m_- in $x > 0$, as can be seen by inspection of (2.6), remembering that $U < 0$. With this con-

vention, and noting that the conditions (2.2) transform to $\hat{v}_d = \hat{v}_u$ and $\partial \hat{v}_d / \partial x = \partial \hat{v}_u / \partial x + \Delta / p$, we have

$$\hat{v}_{d,u} = \frac{-V\Delta \exp(m_\pm x)}{p(p^2 - 4V\beta)^{1/2}} . \tag{2.8}$$

The formal solution for $2\pi i\, v(x,t)$ is given by the integral with respect to p of e^{pt} times (2.8), taken along the Bromwich contour $\mathcal{B}$ shown in Figure 3. The singularities of $\hat{v}$ are a simple pole at the origin $p=0$, and branch points at $p = \pm p_b \equiv \pm 2i(-V\beta)^{1/2}$. Taking the branch cuts as shown in Figure 3, we may thus write v as the residue of $\hat{v}$ at $p=0$ plus an integral along the contour C, which runs around both branch points:

$$v_{d,u} = \frac{\Delta}{2m_0} e^{\pm m_0 x} + \frac{1}{2\pi i} \int_C \frac{-V\Delta \exp\left\{pt - \frac{px}{2V} \mp \frac{x}{2V}(p^2 - p_b^2)^{1/2}\right\} dp}{p(p^2 - p_b^2)^{1/2}} \tag{2.9}$$

where m_0 is m_+ (or $-m_-$) evaluated at $p=0$, i.e.

$$m_0 = \left(\frac{\beta}{-V}\right)^{1/2} \tag{2.10}$$

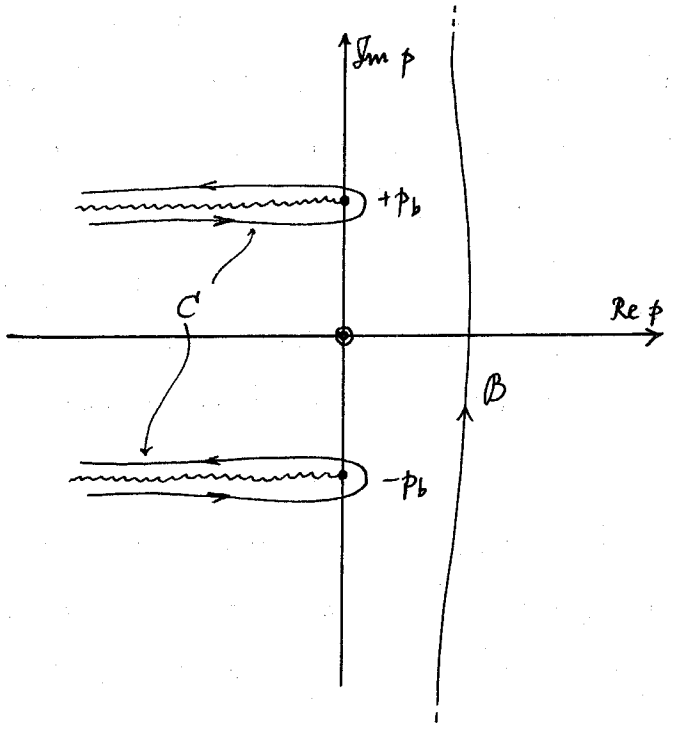

Fig. 3

The integrand behaves like $(p - p_b)^{-1/2}$ near $p = p_b$, and similarly for the

neighborhood of $p=-p_b$. For large t the dominant contributions to the integral along C come from the neighborhoods of $p=\pm p_b$, showing that for each x, as $t\to\infty$, the integral goes to zero like $t^{-1/2}$ (times a factor oscillating with frequency $2(-U\beta)^{1/2}$).

This is what we wanted to show since, therefore, the first term in (2.9) represents an ultimate steady state which is that shown schematically in Figure 2.

The second term of (2.9) may be written in a more interesting form by changing to a variable k, where

$$p=-Uik+\frac{i\beta}{k}. \tag{2.11}$$

The resulting contour integral with respect to k can be taken along the real axis, and using symmetry (2.9) can finally be written

$$v_{d,u}=\frac{\Delta}{2m_0}e^{\pm m_0 x}-\frac{\Delta}{\pi}\int_0^\infty \frac{\cos k\{x-c(k)t\}\,dk}{k^2+m_0^2}, \tag{2.12}$$

where

$$c(k)=U-\frac{\beta}{k^2}. \tag{2.13}$$

This shows that, not surprisingly, the transient part of v can be represented as a superposition of Rossby waves, the phase speed relative to the fluid of a Rossby wave of wavenumber k being $-\beta/k^2$. The behavior at large t may be recovered from (2.12) by the use of the method of stationary phase.

The problem could of course have been solved in the form (2.12) in the first place. The use of the Laplace transform together with the condition (2.7) seems, however, a more natural way of pointing up the fact that the possibility of an exponentially-growing disturbance has not been "assumed out" in treating the initial-value problem.

A similar analysis for the case $U>0$ shows that the pattern of Figure 1 is set up. In this steady state the current is completely undisturbed until it reaches the step.

3. A latitude-dependent problem.

As a simple way of looking at the effect of latitudinal constraints on the motion, we shall investigate a linearized model with boundaries at $y=0, L$ say, on which v must vanish. The various ways in which the zonal current may be modified downstream and upstream by the presence of a step at $x=0$ are quite interesting and instructive. In this section we sketch an initial-value analysis similar to that of § 2, which establishes the forms of the solutions. Then in § 4 the results are interpreted in terms of group velocity.

The total fluid velocity will now be written in terms of a perturbation stream function $\psi(x,y)$ as

$$\{U+\bar{u}-\partial\psi/\partial y,\ \partial\psi/\partial x\}, \tag{3.1}$$

where $\bar{u}$ takes (for instance) the constant value $-U\Delta h/h$ downstream and is zero upstream. As before, $\Delta h/h$ is counted positive if the fluid is moving from a shallower to a deeper region. The linearized potential vorticity equation in either region is then

$$\left(\frac{\partial}{\partial t}+U\frac{\partial}{\partial x}\right)\nabla^2\psi+\beta\frac{\partial\psi}{\partial x}=0. \tag{3.2}$$

The linearized matching conditions at the step can be written, using suffices d and u to denote the downstream and upstream sides irrespective of the sign of U,

$$\left.\begin{aligned}\psi_d &= \psi_u\\ \frac{\partial\psi_d}{\partial x} &= \frac{\partial\psi_u}{\partial x}\\ \nabla^2\psi_d &= \nabla^2\psi_u+\Delta\end{aligned}\right\}\quad \text{at } x=0 \tag{3.3}$$

where as before

$$\Delta\equiv f\Delta h/h.$$

It is convenient to represent Δ in the form

$$\Delta=\frac{4\Delta}{\pi}\left\{\sin\frac{\pi y}{L}+\frac{1}{3}\sin\frac{3\pi y}{L}+\frac{1}{5}\sin\frac{5\pi y}{L}+\cdots\right\} \tag{3.4}$$

and, correspondingly, to write ψ as

$$\psi=\frac{4}{\pi}\left\{\psi^{(1)}\sin\frac{\pi y}{L}+\frac{1}{3}\psi^{(3)}\sin\frac{3\pi y}{L}+\cdots\right\} \tag{3.5}$$

Then the problem for $\psi^{(n)}(x,t)$ has the same form as (3.2), (3.3) provided ∇^2 is interpreted as $\partial^2/\partial x^2 - n^2\pi^2/L^2$, it being sufficient to treat each such Fourier component separately. We shall now drop the superscript (n) and write ℓ for $n\pi/L$.

The Laplace-transformed problem for each component, with undisturbed flow $(\psi = 0)$ as initial condition, is thus

$$(p + U\frac{\partial}{\partial x})(\frac{\partial^2\hat{\psi}}{\partial x^2} - \ell^2\hat{\psi}) + \beta\frac{\partial\hat{\psi}}{\partial x} = 0 \tag{3.6}$$

with

$$\left.\begin{aligned} \hat{\psi}_d = \hat{\psi}_u\,, \quad & \frac{\partial\psi_d}{\partial x} = \frac{\partial\psi_u}{\partial x}\,, \\ \frac{\partial^2\hat{\psi}_d}{\partial x^2} - \ell^2\hat{\psi}_d = \frac{\partial^2\hat{\psi}_u}{\partial x^2} & - \ell^2\hat{\psi}_u + \frac{\Delta}{p} \end{aligned}\right\} \text{at } x = 0. \tag{3.7}$$

Note that the ℓ^2 terms cancel in the third of (3.7). The condition analogous to (2.7), serving as a boundary condition on $\hat{\psi}$ for large $|x|$ is also imposed. It may then be verified that

$$\left.\begin{aligned} \hat{\psi}_d &= \frac{\Delta\, e^{+p(m_2 x)}}{p(m_1 - m_2)(m_2 - m_3)} - \frac{\Delta\, e^{+p(m_3 x)}}{p(m_2 - m_3)(m_3 - m_1)} \\ \hat{\psi}_u &= \frac{\Delta\, e^{+p(m_1 x)}}{p(m_3 - m_1)(m_1 - m_2)}\,, \end{aligned}\right\} \tag{3.8}$$

where the $m_i(p)$ are the roots of

$$Um^3 + pm^2 + (\beta - U\ell^2)m - p\ell^2 = 0 \tag{3.9}$$

such that for p real and strictly positive, $\mathrm{Re}(m_1)$ has the same sign as U, and $\mathrm{Re}(m_2), \mathrm{Re}(m_3)$ both have the opposite sign to U. (It may be verified that for all real positive p this (definition) is always appropriate. By the symmetry of (3.8), m_2 and m_3 are interchangeable.) Thus labeled, the roots $m_i(p)$ can be identified in any part of the (cut) p-plane by continuation from some point on the positive real axis.

In general, $\hat{\psi}_d$ and $\hat{\psi}_u$ each have a simple pole at p = 0, and branch points at some or all of the points where two (or three) of the m_i coalesce,

given by

$$\pm \frac{p}{i} = \frac{Ul}{2\sqrt{2}}\left[\gamma^2 - 20\gamma - 8 \pm (\gamma+8)\left\{\gamma(\gamma+8)\right\}^{\frac{1}{2}}\right]^{\frac{1}{2}}, \qquad (3.10)$$

where $\gamma \equiv \beta/Ul^2$. If all four such points p_b, say, are distinct, then in the neighborhood of those p_b for which $\hat{\psi}$ has a branch point, $\hat{\psi}$ behaves like $(p-p_b)^{-1/2}$. In general, it will be found that a steady flow is ultimately set up, whose nature is determined by the values of the roots m_j at $p=0$.

It is convenient to distinguish several cases, characterized (for the Fourier component under consideration) by different ranges of U as measured in units of β/l^2:

(1) $-\beta/8l^2 < U < 0$, "slow westward". There are four branch points each behaving like $(p-p_b)^{-1/2}$ with p_b pure imaginary. (The same p-plane diagram will always apply to both $\hat{\psi}_d$ and $\hat{\psi}_u$.) Thus for given x the transients die out as $t^{-1/2}$, and involve oscillations at two frequencies which are given by (3.10), in which $\gamma < -8$ for the present case. At $p=0$ we have $m_1 = -\{l^2+\beta/(-U)\}^{1/2}$ and, say, $m_2 = +\{l^2+\beta/(-U)\}^{1/2}$ and $m_3 = 0$.

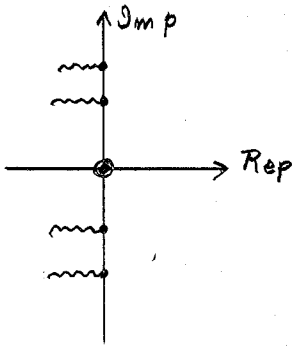

Fig. 4

The steady solution that is set up is, therefore, writing $+\{l^2+\beta/(-U)\}^{1/2} \equiv m_0$,

$$\left.\begin{aligned} \psi_d &= \frac{\Delta}{m_0^2}\left\{\frac{1}{2}e^{m_0 x} - 1\right\} \\ \psi_u &= -\frac{\Delta}{2m_0^2}e^{-m_0 x}. \end{aligned}\right\} \qquad (3.11)$$

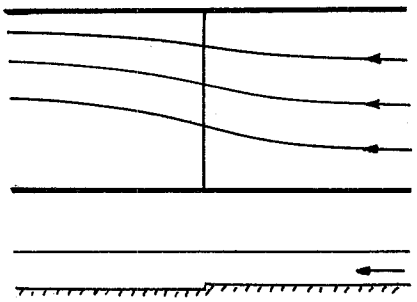

Fig. 5

When $\ell = \pi/L$, that is, when the first term in the Fourier series (3.5) is being considered so that (3.11) gives $\psi^{(1)}$, this term corresponds to the flow pattern shown in Figure 5. This is similar to the pattern in Figure 2, with the additional feature that the flow has been modified for downstream. The far upstream flow is undisturbed.

(2) $U = -\beta/8\ell^2$, "critical westward". In this and in the next case, a steady state is again reached and is again given by (3.11). The only difference in this case is that the two pairs of branch points of Figure 4 have merged, giving two branch points each behaving like $(p - p_b)^{-2/3}$, where $p_b = \mp 3\sqrt{3}\, i\, \ell U$. Thus for each x the transients die out more slowly, as $t^{-1/3}$, and oscillate at just one frequency, namely $3\sqrt{3}\,\ell U$.

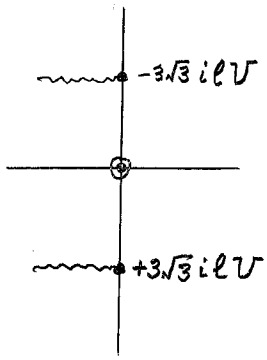

Fig. 6

(3) $U<-\beta/8\ell^2$, "fast westward". The branch points have separated and moved off the imaginary axis, but although four branch points occur in the roots $m_i(p)$, it can be shown that only two of them ($\bullet$) are branch points of $\hat{\psi}$. The transients therefore decay exponentially with time.

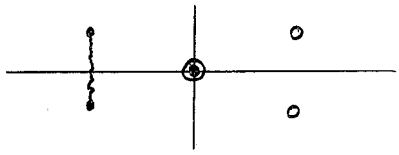

Fig. 7

(4) $U>\beta/\ell^2$, "fast eastward". As in the fast westward case the transients decay exponentially. The steady solution is now different, since at $p=0$ we have $m_1=+\{\ell^2-\beta/U\}^{1/2}$ and, say, $m_2=-\{\ell^2-\beta/U\}^{1/2}$ and $m_3=0$. Thus if we write $+\{\ell^2-\beta/U\}^{1/2}\equiv m_0$ as before, the steady solution is given by

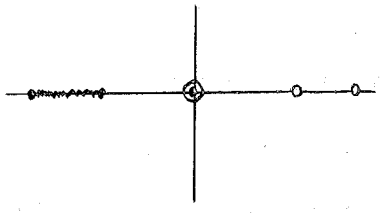

Fig. 8

$$\left.\begin{aligned}\psi_d &= \frac{\Delta}{m_0^2}\left\{\tfrac{1}{2}e^{-m_0 x}-1\right\}\\ \psi_u &= -\frac{\Delta}{2m_0^2}e^{m_0 x}\end{aligned}\right\} \qquad (3.12)$$

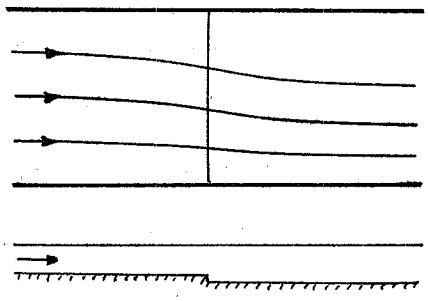

Fig. 9
(Fast eastward)

For $\ell = \pi/L$, this corresponds to the pattern shown in Figure 9. Again it is the far downstream flow that is modified.

(5) $U = \beta/\ell^2$, "critical eastward". As U decreases toward β/ℓ^2 the inner two branch points in Figure 8 move toward the pole at the origin.

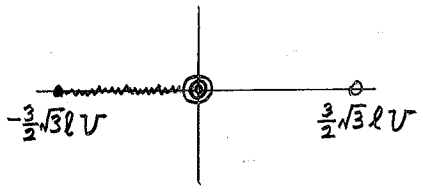

Fig. 10

In the critical case $\hat{\psi}$ behaves like $p^{-5/3}$ at the origin, and the solution never settles down to a steady state, since it goes like $t^{2/3}$. ($p = +\frac{3}{2}\sqrt{3}\ell U$ is again not a branch point of $\hat{\psi}$.)

(6) $0 < U < \beta/\ell^2$, "slow eastward". This is the only case in which a standing wave pattern is set up, but it is still not true that the current

is undisturbed upstream. The dominant branch points of $\hat{\psi}$ are once more on the imaginary p-axis and of the inverse square-root type, so that the steady state is approached as $t^{-1/2}$. The transients oscillate at one frequency, given by the right-hand side of (3.10) taking the positive sign. We now have, for $p=0$, that $m_1=0$ and $m_{2,3}=\pm i\{\beta/U-\ell^2\}^{1/2}=\pm ik_0$, say, so that the steady solution is

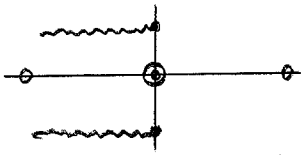

Fig. 11

$$\left.\begin{aligned}\psi_d &= -\frac{\Delta}{k_0^2}\cos k_0 x\\ \psi_u &= -\frac{\Delta}{k_0^2}\end{aligned}\right\} \qquad (3.13)$$

The stationary disturbance has penetrated <u>both</u> far upstream and far downstream. The pattern for $\ell=\pi/L$ is again shown, in Figure 12.

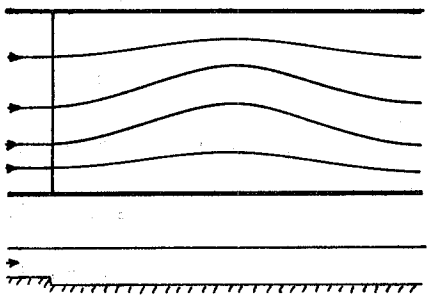

Fig. 12

(<u>Slow eastward</u>)

We shall now briefly look at these results in the light of group velocity considerations.

4. Group velocity. It is interesting to correlate the above results with the dispersion properties of free Rossby waves in the channel $0<y<L$. As well as showing why the steady solutions turn out as they do, consideration of the group velocity accounts for the different rates at which the steady solutions are approached for large time.

In a frame of reference moving with the fluid, the frequency σ of Rossby waves of the form $\sin \ell y . e^{i(kx-\sigma t)}$, where ℓ is an integral multiple of π/L, is

$$\sigma = -\beta \frac{k}{k^2+\ell^2} . \tag{4.1}$$

Hence the group velocity of this "waveguide mode" along the channel is

$$c_g = \frac{\partial \sigma}{\partial k} = \beta \frac{k^2-\ell^2}{(k^2+\ell^2)^2} . \tag{4.2}$$

The dependence of c_g upon k is sketched in Figure 13.

The connection between Figure 13 and the distinction between "fast" and "slow" currents is immediately apparent. For the given ℓ under consideration, we may say that the basic current U is "fast" if it can sweep all the free-wave energy downstream. This shows why the transients (for fixed x) ultimately decay very rapidly with time when the current is fast (cases (3) and (4)).

The current is "slow" if there are some waves whose energy can propagate upstream. There will then exist "critical" waves whose spatial distribution of energy remains centered on a given x-locality as $t \to \infty$, two waves if U is westward and one if U is eastward. For each of these

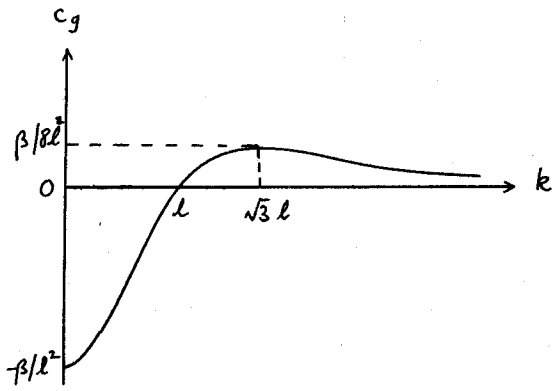

Fig. 13

waves $\partial c_g/\partial k \neq 0$, which accounts for the $t^{-1/2}$ behavior of the amplitude, in terms of the usual stationary-phase calculation: one can say that these are "critical neighborhoods" δk in k-space, shrinking as $t^{-1/2}$, which represent the only wavenumbers still contributing significantly to the amplitude of the transients at a fixed value of x. It is also obvious from Figure 13 why for large t the residual oscillations have two frequencies for the slow westward case (1), and one frequency for the slow eastward case (6).

In case (2), where $U = -\beta/8\ell^2$, we have $\partial c_g/\partial k = 0$ but $\partial^2 c_g/\partial k^2 \neq 0$. Stationary-phase considerations now show that the "critical neighborhood" δk, which surrounds $k = \sqrt{3}\,\ell$, is bigger than before in the sense that it shrinks only as $t^{-1/3}$. Correspondingly, this is the behavior of the transient amplitude at fixed x.

The standing waves with $k^2 = \beta/U - \ell^2$, that are possible only in the slow eastward case, can have a westward group velocity relative to the fluid. However, it may be verified that this is never strong enough to win against the current, and so the waves always appear downstream. The only other disturbance that can affect a steady solution far upstream and far downstream is a $k = 0$ wave. This has group velocity $-\beta/\ell^2$, which shows why the steady solutions involve penetration of an x-independent mean-flow modification far upstream in the slow eastward case and far downstream in all the other steady cases.

The critical eastward case is special in that a $k = 0$ wave is the only possible stationary disturbance; no x-dependence is allowed in a steady solution. But the presence of the step requires x-dependence, and so no steady solution is possible at all, in linearized theory. We note also that the group velocity of the $k = 0$ wave is in this case exactly $-U$.

Note that the "fast" cases illustrate the fact that the flow is in general modified a little way upstream even though free waves cannot carry energy upstream. This is mentioned in order to emphasize that Porter and Rattray's formulation for the latitude-independent problem, although correct for $U > 0$, is not to be justified by an appeal to group-velocity considerations alone.

To conclude §§ 3 and 4, we consider the general character of the whole solution as given by the Fourier series (3.5). Usually this will tend to be dominated (in a qualitative sense) by the first term. If $U < 0$ a steady flow pattern will be set up, similar to that shown in Figure 5 but with finer details superimposed both near the step and in the downstream

unidirectional flow. The same remarks apply, with reference to Figure 9, when $U > \beta L^2/\pi^2$. When $0 < U \leq \beta L^2/\pi^2$ Figure 12 is relevant except in the singular cases $U = \beta L^2/n^2\pi^2$ $(n = 1,3,5,\ldots)$, for which there are no steady solutions. Also, if U is sufficiently close to one of these critical values, the structure of the mode with that particular value of n will take over as the dominant contribution to the pattern. The flow far downstream, for $0 < U \leq \beta L^2/\pi^2$, will be modified both by the standing waves $(k \neq 0)$ and by x-independent contributions $(k = 0)$ from higher modes, for which the current is "fast".

5. The finite-amplitude solution for a westward current.

The finite-amplitude solutions found by Porter and Rattray can be considered "non-trivial", in the sense that the advection of disturbance relative vorticity by disturbance velocities does not vanish. They satisfy the potential-vorticity equation (1.1) when f is taken as a linear function of y, such as

$$f = f_0 + \beta y,$$

where f_0, β are strictly constant. The solutions have a similar linear dependence on y and, as will be seen, it is this feature that allows them to be valid for finite amplitude. The limitations of the beta-plane model should be borne in mind: although of interest in themselves the solutions are not directly applicable to a spherical earth, since they have to be considered unbounded in the y-direction as an essential part of their nature. (This artificiality is also reflected in the flow reversals obtained by Porter and Rattray for intense standing-wave patterns in eastward currents over large

downward steps (see their Figure 1b). The interpretation of these as "instabilities", incidentally, is inappropriate since the velocities are nowhere of a greater order of magnitude than in slightly weaker patterns which do have continuous streamlines.)

We now construct the finite-amplitude solution corresponding to the flow found in § 2, that is, such that there is uniform westward flow both far upstream and far downstream as in Figure 2. The uniform upstream and downstream depths are h_u and h_d, no longer supposed nearly equal. In terms of the total velocity stream function $\Psi(x,y)$, the finite-amplitude matching conditions at the step derived as before from (1.1), or from (5.3) below, are

$$\left.\begin{aligned} h_d \frac{\partial \Psi_d}{\partial y} &= h_u \frac{\partial \Psi_u}{\partial y} \\ \frac{\partial \Psi_d}{\partial x} &= \frac{\partial \Psi_u}{\partial x} \\ \frac{f_0 + \beta y + \nabla^2 \Psi_d}{h_d} &= \frac{f_0 + \beta y + \nabla^2 \Psi_u}{h_u} \end{aligned}\right\} \text{ at } x = 0. \qquad (5.2)$$

It should be noted that the second condition is not that the transport $h\partial\Psi/\partial x$ is continuous. (Porter and Rattray assume that both transport components are continuous; this does not affect their solution (11) which is correct for eastward flow, but it appears to account for an error in equation (12), which except for the first term in the square brackets (the term 1) should be multiplied by r_3/r_2 in their notation. Figures 2-5 may well contain this error also.) The correct condition, continiuty of $v = \partial\Psi/\partial x$, may also be seen as expressing conservation of y-momentum; the fluid experiences no impulsive force in the y-direction as it crosses the step (although it does in the x-direction).

The potential-vorticity equation (1.1), with f given by (5.1), will

be used in the integrated form

$$f_0 + \beta y + \nabla^2 \Psi = \text{func}(\Psi). \tag{5.3}$$

We now show that (5.3) and (5.2) can be satisfied by a suitable choice of the far upstream and downstream velocities $U_u, U_d\ (<0)$ and the constants $m_u<0, m_d>0, A, B$ in

$$\left.\begin{aligned} \Psi_d &= -U_d y + (y+B)\frac{A}{m_d}\exp(m_d x) \\ \Psi_u &= -U_u y + (y+B)\frac{A}{m_u}\exp(m_u x). \end{aligned}\right\} \tag{5.4}$$

The second of (5.2) is already satisfied. The first is satisfied if

$$h_d\left(-U_d + \frac{A}{m_d}\right) = h_u\left(-U_u + \frac{A}{m_u}\right). \tag{5.5}$$

The third is satisfied if

$$A = \beta\,\frac{h_d - h_u}{h_u m_d - h_d m_u} \tag{5.6}$$

and

$$B = f_0/\beta. \tag{5.7}$$

Finally,

$$\nabla^2 \Psi_d = m_d^2(\Psi_d + U_d y),$$

so that the left-hand side of (5.3) for $x<0$ is

$$f_0 + \beta y + \nabla^2 \Psi_d = f_0 + (\beta + m_d^2 U_d) y + m_d^2 \Psi_d.$$

If we make $\beta + m_d^2 U_d = 0$ this is a function of Ψ_d only, as required. Thus, after similarly considering (5.3) for $x>0$, we have (remembering that $m_d>0, m_u<0$ and that $U_d, U_u<0$)

$$m_d = \left(\frac{\beta}{-U_d}\right)^{1/2}, \quad m_u = -\left(\frac{\beta}{-U_u}\right)^{1/2}, \tag{5.8}$$

as the final pair of relations that must be satisfied if (5.4) is to be the required solution.

By substituting (5.6) and (5.8) into (5.5) we may simplify it to

$$h_d^2 U_d = h_u^2 U_u \,. \qquad (5.9)$$

Note that the mass transports at $x = \pm\infty$ are not equal.

U_d, U_u, m_d, m_u, A and B are connected by the five relations (5.6)-(5.9). Thus for given h_u, h_d we may specify one quantity, say U_u. If U_u is specified (5.9) gives U_d, (5.8) gives m_u and m_d, and then (5.6) determines A.

Figure 2 can be regarded as a schematic representation of the solution (5.4), in terms of lines of constant $h\Psi$. Note that the slope of each streamline is discontinuous at the step, and that the lines are closer together upstream than they are downstream, in accordance with (5.9).

Before leaving the subject of this type of solution, we should remark that Porter and Rattray's transformed equation (9) can be used to find westward-flow solutions by applying boundary conditions of no disturbance at $s = \pm i\infty$, instead of at $s = 0$. Thus a formal solution similar to their solution (11) may be written down for topography with an arbitrary dependence on x.

References

Lighthill, M. J. 1967 J.Fluid Mech. 27: 725

Longuet-Higgins, M. S. 1964 Proc.Roy.Soc.A 279: 446

Longuet-Higgins, M. S. 1965 Proc.Roy.Soc.A 284: 40

Porter, G. H. and M. Rattray 1964: Deutsche Hydrographische Z. 17: 164

Veronis, G. 1963: J.Mar.Res. 21: 110

Coupled Disc Dynamos

Richard C. J. Somerville

Introduction

Systems of coupled homopolar disc dynamos have been studied as possible analogies to the homogeneous dynamos which are thought to maintain the terrestrial and stellar magnetic fields. In spite of the comparative physical and mathematical simplicity of the disc systems, they have been shown to possess complicated modes of behavior, apparently resembling those of the earth's dynamo in important respects. In particular, the disc system's capability of reversing its fields is interesting in view of paleomagnetic evidence that the geomagnetic field has undergone reversals.

The case of two identical coupled disc dynamos was first discussed by Rikitake (1958), who found that reversals were possible, in contrast to Bullard's (1955) single dynamo, which cannot reverse. Lebovitz (1960) showed that systems of three or more dynamos are unstable in the absence of viscous damping, but he was unable to determine the stability of the undamped two-dynamo system (the single dynamo is stable). Allan (1962) then investigated the two-dynamo case in more detail, chiefly by integrating the equations numerically. The present work is the beginning of an effort to extend and supplement Allan's results, and the discussion which follows is based largely upon his.

Basic equations

We consider two electrically conducting discs, each rotating about an axle in a magnetic field parallel to the axle, so that a potential difference exists between the periphery of each disc and its axle. A circuit employing brushes connects the periphery of each disc to its own axle via a coil wound around the axle of the other disc. In each circuit the potential difference produces a current flowing through the coil to produce the very magnetic field giving rise to the potential difference at the other disc, and it is in this sense that the system is a pair of self-exciting dynamos.

The dynamos are considered to be identical in that each is subjected to the same externally-applied torque G, each disc has the same moment of inertia C, and each circuit has the same resistance R, mutual inductance M between coil and disc, and self-inductance L. Now letting subscripts 1 and 2 be used to distinguish the discs, we denote the angular velocities by Ω_1 and Ω_2 and the currents by I_1 and I_2.

The equations are then

$$L\frac{dI_1}{dt} + RI_1 = \Omega_1 M I_2$$

$$L\frac{dI_2}{dt} + RI_2 = \Omega_2 M I_1$$

$$C\frac{d\Omega_1}{dt} = C\frac{d\Omega_2}{dt} = G - M I_1 I_2 .$$

Now letting $n = (1, 2)$, we scale with

$$I_n = \left(\frac{G}{M}\right)^{1/2} x_n$$

$$\Omega_n = \left(\frac{GL}{CM}\right)^{1/2} y_n$$

$$t = \left(\frac{CL}{GM}\right)^{1/2} t'$$

Dropping the prime, we have now

$$\frac{dx_1}{dt} + \mu x_1 = y_1 x_2$$
$$\frac{dx_2}{dt} + \mu x_2 = y_2 x_1$$
$$\frac{dy_1}{dt} = \frac{dy_2}{dt} = 1 - x_1 x_2 ,$$

We denote this system of equations by S. The parameter is

$$\mu = \frac{R}{L}\left(\frac{LC}{MG}\right)^{1/2}$$

We have at once that the difference in angular velocities is constant:

$$y_1 - y_2 = a.$$

Writing the equilibrium curves in four-space parametrically, we have

$$x_1 = \pm k \qquad y_1 = \mu k^2$$
$$x_2 = \pm k^{-1} \qquad y_2 = \mu k^{-2},$$

so that

$$\mu\left(k^2 - k^{-2}\right) = a$$

or

$$k^2 = \frac{a}{2\mu} + \left[1 + \left(\frac{a}{2\mu}\right)^2\right]^{1/2}.$$

Thus we shall treat the degenerate four-dimensional system S as a three-dimensional one with parameters (μ, k) or, alternatively, (μ, a). Allan (1962) gives a discussion of the cases for which $\mu = 0$ or $a = 0$ or both. The general case, for which neither parameter is 0, seems to be accessible only numerically.

Computational Procedure

We have integrated S numerically for several sets of non-zero parameter values, using the Adams-Bashforth difference method. Writing S schematically as

$$\frac{d}{dt} Q_i = F_i \ ,$$

where the Q_i are the dependent variables and the F_i are functions of the Q_i and the parameters, and denoting the finite time increment by Δt, and letting superscript n denote a value at time $t = n\Delta t$, the Adams-Bashforth method is then

$$Q_i^{n+1} = Q_i^n + \left[\frac{3}{2} F_i^n - \frac{1}{2} F_i^{n-1}\right] \Delta t \ .$$

This method is of only second order accuracy, and a higher order Runge-Kutta scheme, for example, would surely be preferable. Although very small time steps $(\Delta t \sim 10^{-4})$ have been necessary in the present calculations, S is so simple that a typical complete integration, including peripheral operations, requires only about 15 seconds with a fast computer (Control Data 6600).

All of the solutions reported below have been verified by at least one other integration using a smaller time increment. As a further check on the computer programs, many of Allan's integrations have been recomputed. Initial conditions for these preliminary calculations have generally been taken to be fairly small departures from the equilibrium state, and the integrations typically have been continued to $t \sim 50$.

Results

Although the number of integrations completed to date is insufficient to characterize the behavior of solutions over any extensive region of the two-dimensional parameter space, several distinct types of solutions have appeared (see Table I). Perhaps the most spectacular of these is the "true reversal", in which the currents oscillate about one equilibrium value,

abruptly pass through zero, and then perform mirror-image oscillations. The number of oscillations between reversals and the times at which reversals occur do not in general seem to fit any regular pattern.

Table I. Some typical solutions in the general case $(a \neq 0, \mu \neq 0)$

μ	a	Solution type	Source	
			Allan(1962)	present work
0.1	0.1	regular reversal	X	verified
0.25	0.9375	stable oscillation		X
0.5	1.875	stable oscillation		X
1.0	3.75	true reversal	X	verified
1.0	8.67	true reversal		X
2.0	7.5	true reversal		X

In addition to three cases at relatively large μ and a which exhibited the apparently irregular true reversal, and to Allan's example (at relatively small μ and a : $\mu = a = 0.1$) of a case with apparently regular reversals, we have examined two cases at intermediate μ and a which manifest a third type of behavior (see Table I). This takes the form of a seemingly stable small oscillation about the equilibrium state. The initial conditions were somewhat closer to the equilibrium value for these cases than for the true reversal cases, and it seems likely that this circumstance, rather than the choice of μ and a , is responsible for the failure to reverse. To shed light on this conjecture, also made by Allan, a series of integrations of cases differing only in their initial conditions is planned.

Solutions in phase space

The time dependent solutions of S may of course be regarded as trajectories in phase space. Planar projections of these trajectories for a reversing case typically take the form of spirals about an equilibrium point, interrupted by excursions across an axis into spirals about the other equilibrium point. Allan (1962) has shown that the four-dimensional volume in phase space tends to zero as $t \to \infty$. That is, if the initial values are $(x_1^\circ, x_2^\circ, y_1^\circ, y_2^\circ)$, then the transformation Jacobian

$$\underline{J} = \frac{\partial(x_1, x_2, y_1, y_2)}{\partial(x_1^\circ, x_2^\circ, y_1^\circ, y_2^\circ)}$$

satisfies

$$\frac{d\underline{J}}{dt} = \underline{J}\, \mathrm{div}\, \underline{V},$$

where, from S,

$$\underline{V} = \left(-\mu x_1 + y_1 x_2, -\mu x_2 + y_2 x_1, 1 - x_1 x_2, 1 - x_1 x_2\right).$$

Therefore,

$$\mathrm{div}\, \underline{V} = -2\mu,$$

so that

$$\underline{J} = \underline{J}_0 e^{-2\mu t}.$$

This result incidentally emphasizes an additional difficulty, if this model is intended to be applicable to the geomagnetic dynamo problem. For $\mu \equiv RL^{-1}\left(LCM^{-1}G^{-1}\right)^{1/2}$ in the earth's core is likely to be small, perhaps $\sim 10^{-3}$, and numerical integrations with such a small μ are likely to consume much time before the system "forgets" its initial state.

The above analysis cannot specify the topological details of the

manner in which the phase volume shrinks to zero, and this phenomenon is yet to be studied in detail numerically. For the present, we have examined the case $\mu = 1$, $a = 3.75$, as a typical "true reversal" example. There the connected spirals occupy a bounded region when projected into the (x_1, y_1) plane, and isoplething x_2 in this region apparently indicates that it is single-valued over part of the region and double-valued over another part, so that the trajectories appear ultimately to be confined to two merging surfaces. Each surface contains one of the spirals, so that the trajectory does not intersect itself on reversing. The gross features of the phase-space structure are rather similar to those obtained by Lorenz (1963) from a rather different (but also "reversing") set of equations.

Concluding remarks

The pair of identical coupled disc dynamos may be viewed as among the simplest in a hierarchy of such systems. More complicated systems may be formed by the inclusion of, e.g., non-identical dynamos, self-induction, parallel loads, viscous torques, etc. The ordinary differential equations typical of all of these systems seem particularly well suited to numerical integration (and quite possible to analog as well as digital computation). Although the study of such systems may well ultimately be an unsatisfactory substitute for investigating the magnetohydrodynamic equations themselves, it is clear that even the simplest coupled disc dynamo systems are presently very imperfectly understood.

Acknowledgments

It is a pleasure to thank Prof. P. H. Roberts, who suggested the problem, and Drs. F. Bisshopp, A. Chorin, L. N. Howard, and C. Rooth for generous assistance.

The author gratefully acknowledges the support of a postdoctoral fellowship in the Advanced Study Program, National Center for Atmospheric Research, Boulder, Colorado.

References

Allan, D. W., 1962 Proc.Camb.Phil.Soc., 58: 671

Bullard, E. C., 1955 Proc.Camb.Phil.Soc., 51: 744

Lebovitz, N. R., 1960 Proc.Camb.Phil.Soc., 56: 154

Lorenz, E. N., 1963 J.Atmos.Sci., 20: 130

Rikitake, T., 1958 Proc.Camb.Phil.Soc., 54: 89

Dissipation of the Radial Modes of Oscillation of a Homogeneous Self-Gravitating Sphere

Wayne R. Thatcher

Abstract

The radial oscillations of a homogeneous, isotropic, perfectly elastic self-gravitating sphere are considered. Small departures from perfectly elastic behaviour in shear deformation are introduced, and an expression is derived which relates this elastic defect to parameters which are determinable from mode decay observations. Using as data the

observed attenuation of the fundamental radial mode $_0S_0$, the relaxation time for a simple viscoelastic rheological model is computed. Some general aspects of viscoelastic behaviour which pertain to dissipation of radial motion in a homogeneous sphere are briefly discussed.

Introduction

Free oscillations of the earth excited by large earthquakes decay with time in a manner which may be determined by analysis of strain gauge records made in the several days following an earthquake. Ground displacement is determined as a function of time, and this time series is Fourier analyzed to recover the "spectrum" of the free oscillations. The spectrum consists of a large number of distinct peaks to each of which corresponds a particular frequency. To date over 200 eigenfrequencies have been resolved. Normal mode frequencies computed for earth models with a radially varying density structure (determined using seismic body wave observations) agree with those observed to within a few percent.

The theoretical calculations are made for a radially homogeneous and isotropic non-rotating elastic sphere, and the spectrum thus determined consists of an infinite set of discrete lines. The assumptions which lead to significant errors are sphericity, the absence of rotation, and perfect elasticity. The effect of ellipticity is presently being studied (J. Dahlen, PhD thesis, La Jolla): frequencies appear to be shifted, and some previously toroidal modes have spheroidal components of motion. Rotation removes the $(2\ell+1)$-fold degeneracy in the eigenfrequencies for a particular azmuthal order number ℓ . Departures from perfectly elastic behaviour produce a

breadth to each line in the Fourier spectrum of the surface displacement field. The combined effects of rotation and anelasticity are often difficult to separate in actual observations: split lines may be "hidden" within a broad central peak, or the local amplitude of members of a split multiplet may produce a spurious line width in adjacent peaks ("different" values of Q, the specific attenuation factor, are reported for identical modes when data from different stations are analyzed).

The mode attenuation observations are potentially important in determining the short term rheological behaviour of the materials of the earth's deep interior. When (and if!) something unequivocal can be said concerning the exact mechanism of dissipation, it will also be possible to meaningfully investigate properties such as composition, phase, and temperature using seismic attenuation data.

1. Elastic Oscillations of a Homogeneous Sphere

Following the notation of Gilbert (GFD notes, 1967) the displacement field $\underline{s}(r,\theta,\varphi)$ (with $e^{i\omega t}$ time dependence) on a sphere may be represented as follows:

$$\underline{s}(r,\theta,\varphi) = \hat{r}\,U + \nabla_1 V - \hat{r} \times \nabla_1 W \qquad (1.1)$$

where U, V, W are scalar functions of (r,θ,φ) and

$$\nabla_1 \equiv \hat{\theta}\,\frac{\partial}{\partial\theta} + \frac{\hat{\varphi}}{\sin\theta}\,\frac{\partial}{\partial\varphi}$$

Expanding these scalar functions in spherical harmonics

$$\text{viz} \qquad U(r,\theta,\varphi) = \sum_{\ell=0}^{\infty} \sum_{m=-\ell}^{\ell} U_\ell^m(r)\, Y_\ell^m(\theta,\varphi)\,,$$

and substituting into the linearized momentum equation and Poisson's

equation for the gravitational potential, one obtains an eighth order system of coupled first order ordinary differential equations. This system decouples into a sixth order system, representing spheroidal oscillations (P-SV motion), and a second order system, the toroidal oscillations (SH motion).

A special case of the spheriodal oscillations occurs when $\ell = 0$. Here motion is purely radial, the sixth order system reduces to a coupled second order system, and becomes analytically tractable. The equations are

$$\frac{d}{dr}\begin{bmatrix} U \\ R \end{bmatrix} = \begin{bmatrix} -2\pi\sigma^{-1}r^{-1} & \sigma^{-1} \\ -\rho\omega^2 - 4\pi\rho g r^{-1} + 4\pi\gamma r^{-2} & 2(\lambda\sigma^{-1} - 1)r^{-1} \end{bmatrix} \times \begin{bmatrix} U \\ R \end{bmatrix} \qquad (1.2)$$

where

$$R = (\lambda + 2\mu)U'(r) + \lambda 2 r^{-1} U(r) \quad \text{for } \ell = 0,$$
$$\sigma = \lambda + 2\mu$$
$$\gamma = \lambda + \mu - \lambda^2\sigma^{-1}$$

and we have suppressed indices ℓ, m in U and R (which are both zero here).

U and R must be continuous and R vanishes on the surface $r = a$.

In the case of a homogeneous sphere all of the coefficients in (1.2) are constant (in particular $\frac{g}{r} = 4\pi G\rho$), and the equations are easily decoupled. The equation for $U(r)$ is

$$U'' + \frac{2}{r}U' + \left(k^2 - \frac{2}{r^2}\right)U = 0$$

where $$k^2 = \frac{\rho\omega^2 + 16\pi\rho G}{3\sigma} \qquad (1.3)$$

which has a solution regular at the origin

$$U(r) = j_1(kr) = \frac{\sin kr}{(kr)^2} - \frac{\cos kr}{kr} \qquad (1.4)$$

The system (1.2) may be used to find R in terms of U, and sub-

stituting (1.4) for U and requiring $R(a)=0$, after a moderate amount of manipulation the period equation is found:

$$\tan ka = \frac{ka}{1+\left(\frac{ka\alpha}{2\beta}\right)^2} \tag{1.5}$$

where $\alpha^2 = \frac{\nu}{\rho}$

$$\beta^2 = \frac{\mu}{\rho}$$

The values of k which satisfy (1.5) are then substituted into equation (1.3) and the eigenfrequencies ω of the radial oscillations are determined.

2. Normal Modes with Small Dissipation

From the linearized momentum equation and Poisson's equation Gilbert (GFD notes 1967) has obtained

$$\omega^2 \int_{\text{SPHERE}} dV \rho \underline{s}^2 = \int_{\text{SPHERE}} dV \left\{ \kappa K + \mu M + 4\pi G \rho^2 s^2 + \rho \Lambda \frac{\partial \phi_0}{\partial r} \right\} + \int_{\text{ALL SPACE}} dV \left\{ (4\pi G)^{-1} |\nabla \phi_1|^2 + 2\rho \underline{s} \cdot \nabla \phi_1 \right\} \tag{2.1}$$

where $\Lambda = (\underline{s}\cdot\nabla)\underline{s} - 2r^{-1}s_r^2$

$$K = (\partial_r U + F)^2$$

$$M = \frac{1}{3}(2\partial_r U - F)^2 + r^{-2}\ell(\ell+1)\left[(r\partial_r V - V + U)^2 + (r\partial_r W - W)^2\right] + r^{-2}(\ell-1)\ell(\ell+1)(\ell+2)\left[V^2 + W^2\right]$$

$$F = r^{-1}\left[2U - \ell(\ell+1)V\right]$$

ϕ_1 is the perturbation in the gravitational field.

$U = U_\ell^m(r)$ and similarly for V, W.

The integral relation (2.1) was constructed so that $\underline{s}$ and ϕ_1 are stationary with respect to variations. If we assume that K is a

constant and take the variational derivative of equation (2.1) we thus obtain

$$\delta(\omega^2)\int_V dV \rho s^2 = \int_V dV \delta\mu M \qquad (2.2)$$

Departures from perfect elasticity may be conveniently treated analytically by introducing complex elastic constants.

$$\text{i.e.} \quad \mu \rightarrow \mu_0 - i\Delta\mu$$

It may be easily shown that making the eigenfrequency complex

$$\text{i.e.} \quad \omega \rightarrow \omega_0 - i\Delta\omega$$

is equivalent to transforming the line at ω_0 in the Fourier spectrum of the displacement into a Gaussian centered at ω_0 with a full width of half maximum of $2\Delta\omega$.

Then

$$\begin{aligned}\delta(\omega^2) &= \delta\left[(\omega_0 - i\Delta\omega)\right] \\ &= \delta\left[\omega_0^2 - 2i\omega_0\Delta\omega - (\Delta\omega)^2\right] \\ &\simeq -2i\omega_0\delta(\Delta\omega) \text{ if } \Delta\omega \text{ is small}\end{aligned}$$

or $\delta(\omega^2) = -2i\omega_0\Delta\omega$ for a variation from the perfectly elastic state

Similarly $\delta\mu = -i\delta(\Delta\mu) \equiv -i\Delta\mu$

Making these substitutions in (2.2) it is found that

$$2\omega_0\Delta\omega\int_V dV \rho s^2 = \int_V dV \Delta\mu M \qquad (2.3)$$

For purely radial oscillations of a homogeneous sphere, equation (2.3) may be considerably simplified. In this case ρ and μ_1 are constants, M and $\underline{s}$ have particularly simple forms, and the result is

$$\Delta\mu = \frac{3\rho\omega_0\Delta\omega\int_0^a r^2 dr\left[U(r)\right]^2}{2\int_0^a r^2 dr\left[\frac{dU}{dr} - \frac{2U}{r}\right]^2} \tag{2.4}$$

It now remains to relate this quantity $\Delta\mu$ to the mechanical behaviour of a specific rheological model.

3. A Simple Rheological Model

For a linear viscoelastic material consider a generalized stress-strain law of the form

$$\left.\begin{aligned} s_{ij} &= \int_0^t G(t-\tau)\,\frac{de_{ij}}{d\tau}\,d\tau \equiv G(t) * \dot{e}_{ij}(t) \\ \tau_{kk} &= 3K\epsilon_{kk} \end{aligned}\right\} \tag{3.1}$$

where τ_{ij}, ϵ_{ij} are the stress and strain tensors and s_{ij}, e_{ij} are their deviators, i.e.

$$s_{ij} = \tau_{ij} - \tfrac{1}{3}\tau_{kk}\delta_{ij}$$

$$e_{ij} = \epsilon_{ij} - \tfrac{1}{3}\epsilon_{kk}\delta_{ij}$$

and $G(t)$ is called the relaxation modulus or memory function of the material.

For the purposes and scope of this analysis an extremely simplified form for $G(t)$ is considered, that for what is termed a Maxwell solid:

$$G(t) = E\,e^{-\alpha t}\,, \tag{3.2}$$

where E is Young's Modulus of elasticity.

Taking the Laplace transform of the first of equations (3.1), using the convolution theorem and $G(t)$ as in (3.2), and denoting Laplace transformed functions with a bar, s as the transform variable, one obtains, after finally putting $s = i\omega$, that

$$\frac{\bar{\sigma}_{ij}}{\bar{e}_{ij}} = \frac{E\omega^2}{\omega^2+\alpha^2} - i\,\frac{E\omega\alpha}{\omega^2+\alpha^2}$$

Identifying the ratio $\bar{\sigma}_{ij}/\bar{e}_{ij}$ with the shear modulus μ, and recalling that $\mu = \mu_0 - i\Delta\mu$, one finds that

$$\Delta\mu = \frac{E\omega\alpha}{\omega^2+\alpha^2} \tag{3.3}$$

Assuming that $\omega >> \alpha$ we then have

$$\alpha^{-1} \simeq \frac{E}{\Delta\mu\,\omega} \tag{3.4}$$

4. A Direct Derivation

The analysis of section 2 sheds little light on the general nature of the motion and the energy dissipation involved. A direct, more physically obvious approach is employed here in an attempt to clarify the analysis as well as to verify the previous results. It should be noted that the method used here becomes more difficult and cumbersome when considering non-radial oscillations.

The general procedure is to compute the change in kinetic energy over one cycle of the motion and equate this to the energy dissipated in the same time interval.

For the radial displacement field take

$$s(r,t) = e^{-\gamma t}u(r,t)$$
$$\text{where } u(r,t) = j_1(kr)\sin\omega_0 t \tag{4.1}$$

The change in kinetic energy is then

$$\Delta E = \int_0^a r^2 dr \left\{ \frac{\rho}{2}\left[\{\dot{s}(r,0)\}^2 - \{\dot{s}(r,T)\}^2 \right] \right\}$$

Assuming γT is small (small damping) it is found that

$$\Delta E = 2\pi \rho \omega_0 \gamma \int_0^a r^2 dr \left[j_1(kr) \right]^2 \tag{4.2}$$

The energy dissipation over one cycle is

$$\Delta D = \int_0^a r^2 dr \left[\int_0^T \tau_{ij} \frac{d\epsilon_{ij}}{dt} dt \right]$$

Neglecting $e^{-\gamma t}$ in equation (4.1) for this calculation leads to errors of $O(\beta^2)$ only. Also, if $u \sim \sin \omega t$ the energy dissipation may be written

$$\Delta D = \int_0^r r^2 dr \int_0^T s_{ij} \dot{e}_{ij} dt \tag{4.3}$$

where the dot $(\cdot)$ denotes differentiation with respect to time.

In spherical coordinates

$$s_r = \tau_r - \frac{1}{3}(\tau_r + 2\tau_\theta)$$

$$s_\theta = s_\varphi = \tau_\theta - \frac{1}{3}(\tau_r + 2\tau_\theta)$$

This may be written

$$s_r = \frac{2}{3} G * \frac{\partial}{\partial t} [\varepsilon_r - \varepsilon_\theta]$$

$$s_\varphi = s_\theta = -\frac{1}{3} G * \frac{\partial}{\partial t} [\varepsilon_r - \varepsilon_\theta]$$

Using $\varepsilon_r = \frac{\partial s}{\partial r}$, $\varepsilon_\theta = \frac{s}{r}$ and $G(t)$ for a Maxwell solid (equation 3.2), and assuming αT is small leads to the result

$$\Delta D = \frac{2\pi E \omega \alpha}{\omega^2 + \alpha^2} \left\{ 1 - \frac{\alpha^2}{2(\omega^2 + \alpha^2)} \right\} \cdot \frac{2}{3} \int_0^a r^2 dr \left[\frac{dj_1}{dr} - \frac{j_1}{r} \right]^2 \tag{4.4}$$

If the transient term of order α^2 in (4.4) is neglected, and ΔD from (4.4) is equated to ΔE from equation (4.2) one obtains

$$\frac{E \omega \alpha}{\omega^2 + \alpha^2} = \frac{3}{2} \rho \omega \gamma \frac{\int_0^a r^2 dr \left[j_1(kr) \right]^2}{\int_0^a r^2 dr \left[\frac{dj_1}{dr} - \frac{j_1}{r} \right]^2} \tag{4.5}$$

Referring to equation (3.4) it is easily seen that the above equation corresponds exactly to the result found for $\Delta\mu$ in section 2 (equation 2.4), provided γ is identified with $\Delta\omega$. This is clearly the case, as the exponential attenuation factor is immediately obtained when $\omega=\omega_0+i\Delta\omega$ is substituted into $e^{i\omega t}$.

5. Numerical Calculations and Results

Unfortunately data on the attenuation of the radial modes exists only for the fundamental, ${}_0S_0$, for which $\omega/2\Delta\omega(\equiv Q$, the quality factor or specific attenuation factor) has been found to be in excess of 1000. The results developed in section 2 up to equation (2.3) are relevant for the toroidal modes also, and for a homogeneous spherical earth the displacements for each mode may be determined in closed form (the radial factors are of $je(kr)$ type). Again however, data exists only for some overtones of the $\ell=5$ mode, and in this case analytic difficulties become prohibitively formidable, so no use of the toriodal mode dissipation is made here.

The radial integrals which occur in equation (2.4) (or equivalently, equation (4.5)) are relatively fierce, although (with perseverence!) quite straightforward to evaluate. The result only is quoted here.

$$\Delta\mu = \frac{3}{4}\,\frac{\rho a^2\omega_0^2}{Q}\,\frac{\left[\frac{\cos\xi}{\xi}-\frac{1}{\xi}+\frac{1}{4}(\xi+\sin\xi)\right]}{\xi^2\left[\frac{1}{4}(\xi-\sin\xi)-3\left(\frac{\cos\xi}{\xi}+\frac{1}{\xi}\right)+12\left(\frac{\cos\xi}{\xi^3}-\frac{1}{\xi^3}+\frac{\sin\xi}{\xi^2}\right)\right]} \qquad (5.1)$$

where $\xi \equiv 2ka$

The roots of the period equation (1.5) cannot be determined exactly

in closed form. For the degree of accuracy desired in this calculation it is acceptable to use Poisson's relation $\lambda = \mu$, in which case $\alpha = \sqrt{3}\beta$ and (1.5) becomes

$$\tan\eta = \frac{\eta}{1+\frac{3}{4}\eta^2}; \quad \eta = ka$$

Roughly plotting the left-hand side and the right-hand side of the above equation facilitates determination of the roots.

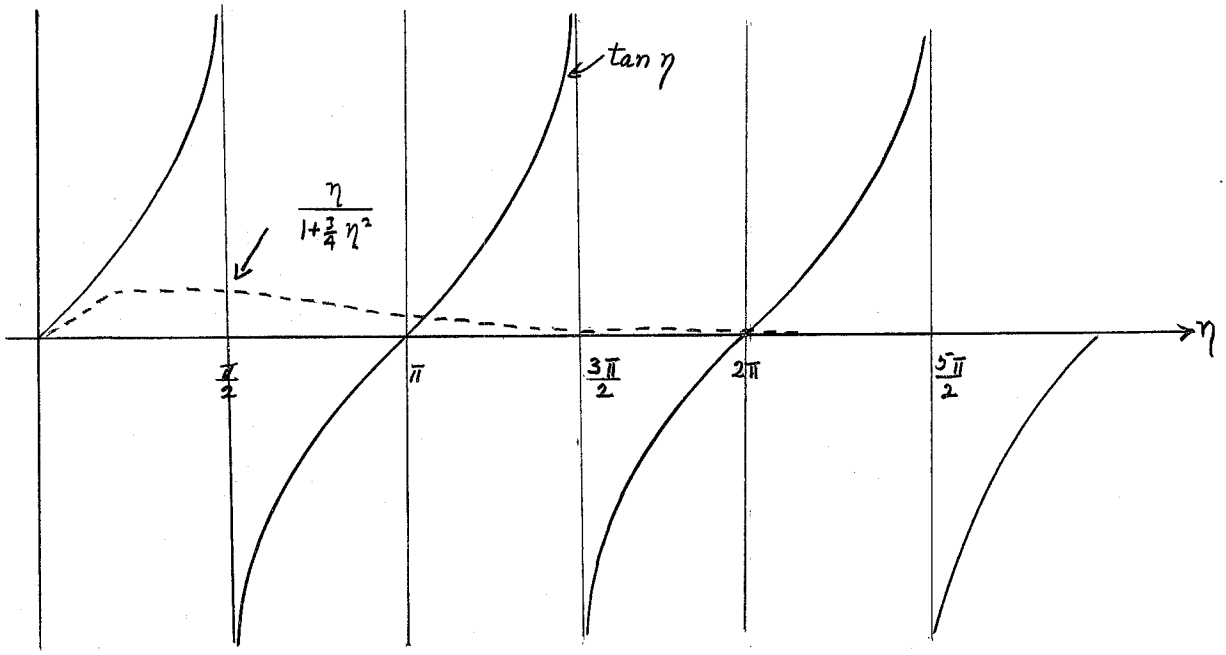

Using Newton's method of interpolation, the first root was found to occur at

$$\xi = 3.475$$

The next and higher roots occur approximately at

$$\xi \cong n\pi, \qquad n = 2,3,4,\ldots$$

The frequency and period of the fundamental spheroidal mode can then be determined using equation (1.3). This was done using the following numerical values:

$$a = 6371 \text{ km}$$

$$G = 6.67 \times 10^{-8} \text{ cgs units}$$

$$\rho = 5.52 \text{ g cm}^{-3}$$

$$\mu = 2 \times 10^{12} \text{ dynes/cm}^2$$

Then

$$\omega_0 = 2.52 \times 10^{-3} \text{ sec}^{-1}$$

$$T = 41.6 \text{ minutes (for the earth the period of } {}_0S_0 \text{ is 20.8 min.)}$$

Using this value of ω_0 in (5.1) and $Q = 5000$, it is found that

$$\Delta\mu = 1.705 \times 10^{8} \text{ dynes/cm}^2$$

And using (3.4) to find the relaxation time, with

$$E = 5.0 \times 10^{12} \text{ dynes/cm}^2$$

$$\alpha^{-1} = 1.166 \times 10^{7} \text{ sec or about 0.3 years.}$$

Only one piece of real data was employed in the preceeding calculation, and this data was for a relatively short time interval. Thus nothing can really be said concerning the long time behaviour of the model, and the only significance to be attached to the number 0.3 years is that it reflects the fact that the relaxation modulus $G(t)$ effectively decays with time, and reaches $\frac{1}{e}$ of its initial value in 0.3 years.

6. Some General Remarks

A very preliminary investigation concerning precisely satisfying the boundary condition of vanishing radial stress on the spherical surface when one employs a viscoelastic stress-strain law of the convolution integral form (see equation (3.1)) reveals some difficulties which are potentially important and significant. It appears that it is not possible to exactly satisfy the stress boundary condition with an "attenuated normal mode" solution like $e^{-\alpha t} j_l(kt) \sin \omega t$ for the radial displacement field. This point is presently being investigated, but no definite conclusions can yet be drawn.

Provided that the foregoing difficulty can be effectively dealt with, the analysis and calculations carried out here are merely the forerunner of a more difficult, but more relevant study in which realistic earth models and less simple anelastic behaviour are allowed for, and all the available mode dissipation data are utilized. The general framework of section 2 may or may not be adequate to deal with this broader problem, but in any case there will necessarily be recourse to numerical methods. Results will not be straightforward to determine, but should have consequances of definite relevance to the real earth, its internal properties and constitution.

Acknowledgements

The problem of mode dissipation, with particular reference to the radial modes, was suggested to me by Dr. Gilbert, who gave much help and encouragement. I am also indebted to Dr. Onat for numerous fruitful discussions.

References

Backus, G. E. and J. F. Gilbert 1967 Geophys. J. (to appear)

Gilbert, J. F. 1965-66 Course notes, Theoretical seismology, U.C.S.D.

Gilbert, J. F. 1967 Course notes, G.F.D., Woods Hole.

An Instability of the Flow in a Slightly Tilted Rotating Glass of Water

Rory Thompson

Abstract

Ink placed on the bottom of the glass often shows intriguing scallop shapes which sometimes grow to form turbulence. (See figures 3.) A theoretical explanation is presented which accords well with experimental results also given, to wit: The zero-order periodic motions cause a rectified mean first-order azimuthal flow which can both collect the ink into circular bands by Ekman convergence, and make the bands wiggle through a shear instability. Since the zero-order flow has resonances for certain geometries, even very slight tilts can sometimes cause remarkable commotion. Thus, geophysical fluid dynamics laboratory models should have their geometry carefully considered in view of inevitable imperfections of rotation.

Introduction

A great deal of work has gone into laboratory models of geophysical fluid phenomena, which is usually to say, rotating fluids with relatively

slow motions. Such motions are liable to be confused by extraneous influences such as slight heat conduction through the sides, wind stress, or slight imperfections of rotation. Of the latter, inconstancy of magnitude of the rotation vector $\underset{\sim}{\Omega}$ has been considered for a sphere by Aldridge (1967), and precession of $\underset{\sim}{\Omega}_{0}$, e.g., by Malkus for a sphere and by Johnson (1967) for a cylinder. Here is considered the effect of a free surface with $\underset{\sim}{\Omega}$ not quite antiparallel to gravity, though constant. Visible effects of misalignment of the axis of rotation were reported by Fultz, et al., (1959), but apparently the only studies of the effects have been by Fultz (1965), and Crow (1965), both of which dealt with the most spectacular effect: a powerful vortex which sometimes forms.

This present problem is also relevant to ocean, atmosphere, or core responses to a diurnal tidal forcing, since in the frame of the cylinder, there is a small rotating component of gravity. However, the problem was actually chosen upon asking Dr. Rooth for an amusing problem because the experiment seemed easy enough for a mathematician: essentially, to drop dye into a big glass of water on a phonograph with a magazine under one side.

Equations of Motion

In a frame rotating with the cylinder, the equations of motion are:

$$\frac{\partial u}{\partial t}+u\frac{\partial u}{\partial r}+\frac{v}{r}\frac{\partial u}{\partial \theta}+w\frac{\partial u}{\partial z}-\frac{v}{r}=-\frac{\partial p}{\partial r}+\nu\left(\frac{\partial^2 u}{\partial r^2}+\frac{1}{r}\frac{\partial u}{\partial r}+\frac{1}{r^2}\frac{\partial^2 u}{\partial \theta^2}+\frac{\partial^2 u}{\partial z^2}-\frac{u}{r^2}-\frac{2\partial v}{r^2\partial \theta}\right)+2\Omega v$$

$$\frac{\partial v}{\partial t}+u\frac{\partial v}{\partial r}+\frac{v}{r}\frac{\partial v}{\partial \theta}+w\frac{\partial v}{\partial z}+\frac{uv}{r}=-\frac{\partial p}{r\partial \theta}+\nu\left(\frac{\partial^2 v}{\partial r^2}+\frac{1}{r}\frac{\partial v}{\partial r}+\frac{1}{r^2}\frac{\partial^2 v}{\partial \theta^2}+\frac{\partial^2 v}{\partial z^2}+\frac{2}{r^2}\frac{\partial u}{\partial \theta}-\frac{v}{r^2}\right)-2\Omega u$$

$$\frac{\partial w}{\partial t}+u\frac{\partial w}{\partial r}+\frac{v}{r}\frac{\partial w}{\partial \theta}+w\frac{\partial w}{\partial z}=-\frac{\partial p}{\partial z}+\nu\left(\frac{\partial^2 w}{\partial r^2}+\frac{1}{r}\frac{\partial w}{\partial r}+\frac{1}{r^2}\frac{\partial^2 w}{\partial \theta^2}+\frac{\partial^2 w}{\partial z^2}\right) \tag{1}$$

$$\frac{\partial u}{\partial r}+\frac{u}{r}+\frac{\partial v}{r\partial\theta}+\frac{\partial w}{\partial z}=0$$

$$u=v=w=0 \quad \text{at} \quad z=0$$

$$u=v=w=0 \quad \text{at} \quad r=L$$

$$w=\frac{d(\eta^*+\eta)}{dt} \quad \text{at} \quad z=\eta^*+\eta\,,$$

where gravity (a potential force) has been absorbed in the pressure p, L is the radius of the cylinder, and η^* is the resultant equilibrium surface height, to wit:

$$\eta^*=H_0+\alpha r\cos(\theta+t), \tag{2}$$

where α is the angle of tilt. Since $\Omega>0$, (by choice) this rotates clockwise in the cylinder frame. A paraboloidal bottom to the cylinder is chosen so that the mean depth H_0 is a constant, for simplicity, the assumption $\Omega^2 L \ll g\varepsilon$ below makes the difference negligible.

Now scale these equations by

$$t\to\Omega^{-1}t,\ r\to Lr,\ z\to H_0 z,\ u\to Uu,\ v\to Uv,\ w\to Ww,\ p\to Pp,$$

and impose the physical assumptions

$$W=\alpha L\Omega,\ \frac{W}{H_0}=\frac{U}{L},\ \frac{\Omega^2 L}{g}\ll\varepsilon,$$

$$\varepsilon=\frac{U}{\Omega L}\ll 1,\ \text{and}\ E=\frac{\nu}{\Omega L^2}\ll\varepsilon.$$

Then for balance, $P=U\Omega L$. Expand the variables in the small parameter ε, so $u=u_0+\varepsilon u_1+O(\varepsilon^2)$, etc., and separate the coefficients of ε to get the zero order (linear) equations (3) and the first order equations (11).

$$\frac{\partial u_0}{\partial t} = -\frac{\partial p_0}{\partial r} + 2V_0 + E\left(\nabla^2 u_0 - \frac{u_0}{r} - \frac{2}{r^2}\frac{\partial V_0}{\partial \theta}\right)$$

$$\frac{\partial V_0}{dt} = -\frac{\partial p_0}{r\partial \theta} - 2u_0 + E\left(\nabla^2 V_0 + \frac{2}{r^2}\frac{\partial u_0}{\partial \theta} - \frac{V_0}{r^2}\right)$$

$$\frac{\partial W_0}{\partial t} = -\frac{\partial p_0}{\partial z} + E\nabla^2 W_0 \qquad (3)$$

$$\frac{\partial u_0}{\partial r} + \frac{u_0}{r} + \frac{\partial V_0}{r\partial \theta} + \frac{\partial W_0}{\partial z} = 0$$

$$W_0 = 0 \quad \text{at} \quad z = 0$$

$$u_0 = V_0 = 0 \quad \text{at} \quad z = 0$$

$$u_0 = 0 \quad \text{at} \quad r = 1$$

$$W_0 = \frac{d\eta^*}{dt} \quad \text{at} \quad z = 1$$

where $$\nabla^2 = \frac{\partial^2}{\partial r^2} + \frac{1}{r}\frac{\partial}{\partial r} + \frac{1}{r^2}\frac{\partial^2}{\partial \theta^2} + \frac{\partial^2}{\partial z^2}.$$

The above scaling also took $H_0/L = O(1)$; if $H_0/L \ll 1$, (3.3) should be replaced by $\frac{\partial p_0}{\partial z} = 0$.

Zero-order Interior Solution

The equations (3) are linear, so write $u_0 = u(r,z)e^{i(\theta+t)}$, etc., let $E \to 0$, and solve:

$$u = -\frac{i}{3}\left(\frac{\partial p}{\partial r} + \frac{2p}{r}\right),$$

$$V = \frac{1}{3}\left(2\frac{\partial p}{\partial r} + \frac{p}{r}\right), \qquad (4)$$

$$W = i\frac{\partial p}{\partial z}.$$

Substitute these into the continuity equation to get

$$\frac{\partial^2 p}{\partial r^2} + \frac{1}{r}\frac{\partial p}{\partial r} - \frac{p}{r^2} = 3\frac{\partial^2 p}{\partial z^2}, \qquad (5)$$

with boundary conditions $\frac{\partial p}{\partial r} + 2p = 0$ at $r = 1$, $\frac{\partial p}{\partial z} = 0$ at $z = 0$, and $\frac{\partial p}{\partial z} = \eta^* = \alpha r$ at $z = 1$. The other boundary conditions are dropped with

$E = 0$; they will be restored in the boundary treatment below. By the usual separation technique, one solves

$$Z''(z) + \frac{\lambda^2}{3} Z(z) = 0 \quad \text{and} \quad r^2 R''(r) + r R'(r) + (\lambda^2 r^2 - 1) R(r) = 0.$$

The solutions are $J_1(\lambda r) e^{i \frac{\lambda z}{\sqrt{3}}}$, where λ could be complex in general, except that then the u boundary condition will involve $\cos\theta$ and $\sin\theta$, i.e., will be inseparable. For λ^2 real, the $u_0 = 0$ at $r = 1$ condition becomes

$$\lambda J_1'(\lambda) + 2 J_1(\lambda) = 0. \tag{6}$$

For $\lambda^2 < 0$, there is no positive $\mu = i\lambda$ which satisfies $\mu I_1'(\mu) + 2 I_1(\mu) = 0$, since $I_1(x) = J_1(ix)$ is monotonic. From the Bessel function tables of Abramowitz and Stegun (1965) and of Jahnke and Emde (1945), the first five roots of (6) were found to be

$$\lambda_1 = 2.735, \quad \lambda_2 = 5.691, \quad \lambda_3 = 8.772, \quad \lambda_4 = 11.874, \text{ and } \quad \lambda_5 = 14.997,$$

so the solutions of (5) are linear combinations of $\left\{ J_1(\lambda_m r) \cos \frac{\lambda_n z}{\sqrt{3}} \right\}$, where the homogeneous bottom boundary condition $Z'(0) = 0$ has also been imposed. This family is complete for odd functions in r which satisfy the boundary conditions. Choose coefficients $\{a_m\}$ to satisfy the remaining (inhomogeneous) boundary condition

$$\frac{\partial p}{\partial z} = -\sum_{n=1}^{\infty} \frac{a_n \lambda_n}{\sqrt{3}} J_1(\lambda_n r) \sin \frac{\lambda_n}{\sqrt{3}} = \alpha r. \tag{7}$$

Standard Fourier-Bessel theory, e.g., equation (6.49), page 90 of Tranter (1956), gives

$$b_m \equiv -\frac{a_m \lambda_m}{\sqrt{3}} \sin \frac{\lambda_m}{\sqrt{3}} = \frac{2\lambda_m^2}{\lambda_m^2 + 3} \frac{\alpha}{J_1^2(\lambda_m)} \int_0^1 r^2 J_1(\lambda_m r)\, dr$$

as the inversion of (7) and (6). Now, it happens that

$$\frac{\partial}{\partial t}\left(t^2 J_2(t)\right) = 2tJ_2 + t^2 J_2' = t^2\left[\frac{4J_2}{2t} + \frac{2J_2'}{2}\right] = \frac{t^2}{2}\left[J_1 + J_3 + J_1 - J_3\right] = t^2 J_1(t),$$

so

$$b_m = 2\alpha \frac{\lambda_n}{\lambda_m^2 + 3} \frac{J_2(\lambda_m)}{J_1^2(\lambda_m)}.$$

This goes to zero faster than might be expected, for (6) is equivalent to $3J_0(\lambda) + J_2(\lambda) = 0$, and the zeros of J_2 approach those of J_0, hence λ_m, as $m \longrightarrow \infty$. For m = 1,2,3,4,5, b_m/α = 1.32, -.50, .30, -.18, .06, so clearly the first few eigenmodes will dominate, especially since viscosity will tend to damp the higher wave numbers more. The zero order solutions are thus:

$$p_0 = -\alpha \sum_{n=1}^{\infty} \left[\frac{\frac{2\sqrt{3}}{\lambda_m^2+3} \frac{J_2(\lambda_n)}{J_1^2(\lambda_n)}}{\sin\left(\frac{\lambda_m}{\sqrt{3}}\right)}\right] J_1(\lambda_m \pi) \cos\frac{\lambda_m z}{\sqrt{3}} \cos(\theta + t),$$

abbreviated

$$\begin{aligned}
p_0 &= \sum a_m J_1(\lambda_m \pi) \cos\left(\frac{\lambda_m z}{\sqrt{3}}\right) \cos(\theta + t), \\
u_0 &= \sum \frac{a_m \lambda_m}{6}\left(3J_0(\lambda_m \pi) + J_2(\lambda_m \pi)\right) \cos\left(\frac{\lambda_m z}{\sqrt{3}}\right) \sin(\theta + t), \\
v_0 &= \sum \frac{a_m \lambda_m}{6}\left(3J_0(\lambda_m \pi) - J_2(\lambda_m \pi)\right) \cos\left(\frac{\lambda_m z}{\sqrt{3}}\right) \cos(\theta + t), \\
w_0 &= \sum \frac{a_m \lambda_m}{\sqrt{3}} J_1(\lambda_m \pi) \sin\frac{\lambda_m z}{\sqrt{3}} \sin(\theta + t).
\end{aligned} \tag{8}$$

The above are dimensionless; dimensionalizing, one has, e.g.,

$$u_0 = -\alpha \Omega L \sum_{n=1}^{\infty} \frac{\frac{\lambda_n}{(\lambda_n^2+3)\sqrt{3}} \frac{J_2(\lambda_n)}{J_1^2(\lambda_n)}}{\sin\frac{(\lambda_n H_0)}{\sqrt{3}L}} \left(3J_0\left(\frac{\lambda_n \pi}{L}\right) + J_2\left(\frac{\lambda_n \pi}{L}\right)\right) \cos\left(\frac{\lambda_n z}{\sqrt{3}L}\right) \sin(\Omega t + \theta) \tag{8a}$$

so the magnitudes depend only on $\alpha \Omega L$ and H_0/L. The factor of $\left(\sin\left(\frac{\lambda_n H_0}{\sqrt{3}L}\right)\right)^{-1}$ implies a strong dependence on H_0/L; if $H_0/L = m\sqrt{3}\pi/\lambda_m$ for some positive integers m and n, the response is indeterminately large.

These occur at multiples of H_0/L = 1.992, .957, .625, .458, .363, etc., and are apparently inertial-elastoid responses, not gravity waves, which must have a frequency $> 2\Omega$. The width of the peaks (above any particular height) decreases rapidly with n increasing. The surface circulation patterns for the first two modes are sketched in Figure 1. Note the tendency for an anticyclonic gyre over the shallow part, cyclonic over the deep.

Zero-order Boundary Solution

While E very small allows viscosity to be ignored throughout most of the fluid, the high order terms become important in a region of relative height $E^{1/2}$ from the bottom. Letting $\zeta = E^{1/2}\zeta$ and somewhat rescaling (3) in the usual fashion for boundary layers, the boundary equations ($\zeta = O(E^{1/2})$) are:

$$\frac{\partial u_0}{\partial t} = -\frac{\partial p_0}{\partial r} + \frac{\partial^2 u_0}{\partial \zeta^2} + 2V_0$$

$$\frac{\partial v_0}{\partial t} = -\frac{\partial p_0}{r\partial\theta} + \frac{\partial^2 v_0}{\partial \zeta^2} - 2u_0$$

$$0 = -\frac{\partial p_0}{\partial \zeta} \qquad (9)$$

$$\frac{u_0}{r} + \frac{\partial u_0}{\partial r} + \frac{\partial v_0}{r\partial\theta} + \frac{\partial w_0}{\partial \zeta} = 0$$

$$u_0 = v_0 = w_0 = 0 \quad \text{at} \quad \zeta = 0$$

solution merges with interior for $\zeta >> 1$.

This problem might be called a time-dependent Ekman layer problem. In the same fashion as the steady Ekman problem, and writing $\frac{\partial}{\partial t} \to i$, one gets $u_{\zeta\zeta\zeta\zeta} - 2iu_{\zeta\zeta} + 3u = -\frac{2\delta p}{r\partial\theta} - i\frac{\partial p}{\partial r}$, which has characteristic roots $\pm(1-i)/\sqrt{2}$ and $\pm(1+i)\sqrt{3/2}$.

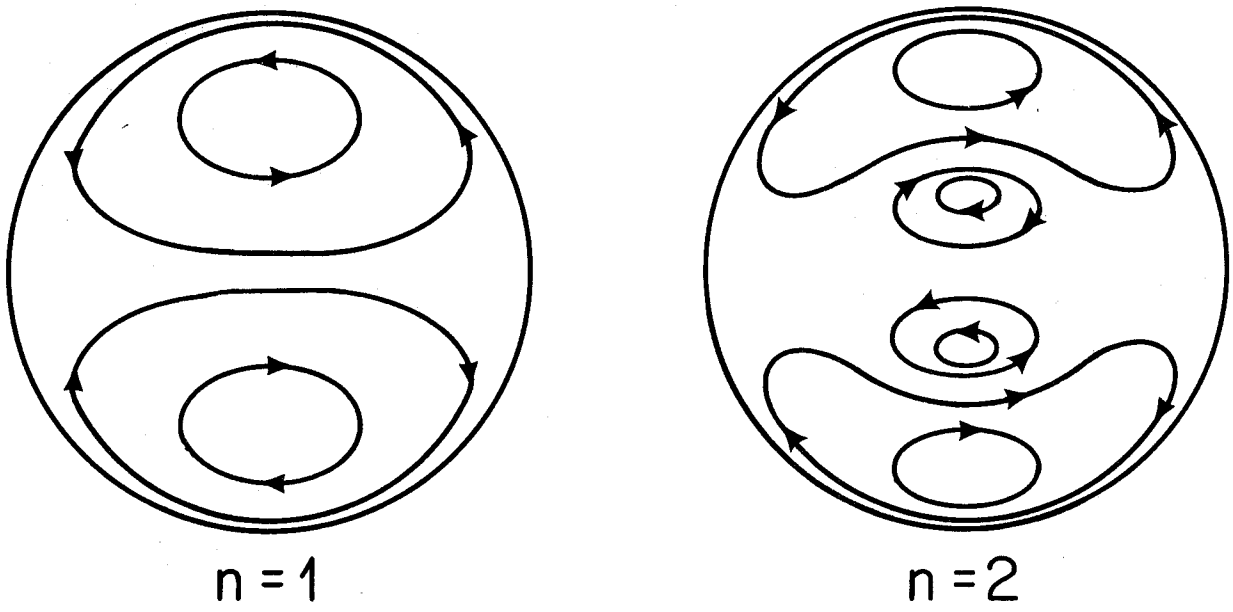

Fig. 1

Sketch of surface zero-order velocities for n = 1 and 2, with $\sin(\lambda_n H_o / \sqrt{3}\, L)$ positive.

Boundedness as $\zeta \to \infty$ excludes the roots with positive real parts, so imposing $u = v = 0$ at $\zeta = 0$ gives

$$u = -\frac{i}{3}\left(\frac{\partial p}{\partial r} + \frac{2p}{r}\right) + \frac{i}{2}\left(\frac{\partial p}{\partial r} + \frac{p}{r}\right)e^{-\frac{1+i}{\sqrt{2}}\zeta} - \frac{i}{6}\left(\frac{\partial p}{\partial r} - \frac{p}{r}\right)e^{-\sqrt{\frac{3}{2}}(1+i)\zeta}$$

$$v = \frac{1}{3}\left(2\frac{\partial p}{\partial r} + \frac{p}{r}\right) - \frac{1}{2}\left(\frac{\partial p}{\partial r} + \frac{p}{r}\right)e^{-\frac{1+i}{\sqrt{2}}\zeta} + \frac{1}{6}\left(\frac{\partial p}{\partial r} - \frac{p}{r}\right)e^{-\sqrt{\frac{3}{2}}(1+i)\zeta},$$

and imposing continuity and $w = 0$ at $\zeta = 0$ gives

$$w = \nabla_2^2 p\left[\frac{i}{3}\zeta + E^{-1/2}\left\{\frac{-1+i}{2\sqrt{2}}e^{\frac{-1+i}{\sqrt{2}}\zeta} - \frac{-1+i}{2\sqrt{2}} - \frac{1+i}{6\sqrt{6}}e^{-\sqrt{\frac{3}{2}}(1+i)\zeta} + \frac{1+i}{6\sqrt{6}}\right\}\right].$$

Note the extra term due to non-steadiness soon swamps the (modified) Ekman convergence, as one proceeds into the interior.

Restoring the factor $e^{i(\theta+t)}$ and taking real parts, one has in the bottom boundary:

$$u_0 = \sum \frac{a_m \lambda_n}{6}\left\{(3J_0 + J_2)\sin(\theta+t) - 3J_0 e^{-\frac{\zeta}{\sqrt{2}}}\sin\left(\theta+t+\frac{\zeta}{\sqrt{2}}\right) - J_2 e^{-\sqrt{\frac{3}{2}}\zeta}\sin\left(\theta+t-\sqrt{\tfrac{3}{2}}\zeta\right)\right\}$$

$$v_0 = \sum \frac{a_m \lambda_n}{6}\left\{(3J_0 - J_2)\cos(\theta+t) - 3J_0 e^{-\frac{\zeta}{\sqrt{2}}}\cos\left(\theta+t+\frac{\zeta}{\sqrt{2}}\right) + J_2 e^{-\sqrt{\frac{3}{2}}\zeta}\cos\left(\theta+t-\sqrt{\tfrac{3}{2}}\zeta\right)\right\} \qquad (10)$$

$$w_0 = \sum \frac{a_m \lambda_n}{\sqrt{3}} J_1(\lambda_n r)\left\{\zeta\sin(\theta+t) - \frac{E^{1/2}}{\sqrt{2}}e^{-\frac{\zeta}{\sqrt{2}}}\left(\cos\left(\theta+t+\frac{\zeta}{\sqrt{2}}\right) + \sin\left(\theta+t+\frac{\zeta}{\sqrt{2}}\right)\right) + \right.$$
$$\left. + \frac{E^{1/2}}{3\sqrt{6}}e^{-\sqrt{\frac{3}{2}}\zeta}\left(-\cos\left(\theta+t-\sqrt{\tfrac{3}{2}}\zeta\right) + \sin\left(\theta+t-\sqrt{\tfrac{3}{2}}\zeta\right)\right) + E^{1/2}\left(\frac{1}{\sqrt{2}} + \frac{1}{3\sqrt{6}}\right)\cos(\theta+t) + E^{1/2}\left(\frac{1}{\sqrt{2}} - \frac{1}{3\sqrt{6}}\right)\sin(\theta+t)\right\}.$$

Feeding this transient Ekman suction back into the interior had only the effect of rotating the pattern by $E^{1/2}$. Equations (11) will be used in the first-order forcing in the boundary layer.

First-order Mean Motion

The first-order equations of motion are [see the paragraph before (3)]

$$\frac{\partial u_1}{\partial t}+u_0\frac{\partial u_0}{\partial r}+\frac{v_0}{r}\frac{\partial u_0}{\partial\theta}+w_0\frac{\partial u_0}{\partial z}-\frac{v_0^2}{r}=-\frac{\partial p_1}{\partial r}+2v_1+E\left(\nabla^2u_1-\frac{u_1}{r^2}-\frac{2\partial v}{r^2\partial\theta}\right)$$

$$\frac{\partial v_1}{\partial t}+u_0\frac{\partial v_0}{\partial r}+\frac{v_0}{r}\frac{\partial v_0}{\partial\theta}+w_0\frac{\partial v_0}{\partial z}+\frac{u_0v_0}{r}=-\frac{\partial p_1}{r\partial\theta}-2u_1+E\left(\nabla^2v_1+\frac{2}{r^2}\frac{\partial u_1}{\partial\theta}-\frac{v_1}{r^2}\right) \qquad (11)$$

$$\frac{\partial w_1}{\partial t}+u_0\frac{\partial w_0}{\partial r}+\frac{v_0}{r}\frac{\partial w_0}{\partial\theta}+w_0\frac{\partial w_0}{\partial z}=-\frac{\partial p_1}{\partial z}+E\nabla^2w_1$$

$$\frac{\partial u_1}{\partial r}+\frac{u_1}{r}+\frac{\partial v_1}{r\partial\theta}+\frac{\partial w_1}{\partial z}=0$$

$$u_1=v_1=w_1=0 \quad \text{at} \quad z=0$$

$$u_1=v_1=w_1=0 \quad \text{at} \quad r=1$$

$$w_1=-\eta_0\frac{\partial w_0}{\partial z} \quad \text{at} \quad z=1.$$

The mean motion only will be considered, denoted by a super-bar. Since θ and t only occur in the combination $(\theta+t)$, a time average is also a θ-average, i.e., a steady state has been reached. Write

$$G(r,z)\equiv \overline{u_0\frac{\partial u_0}{\partial r}}+\overline{\frac{v_0}{r}\frac{\partial u_0}{\partial\theta}}+\overline{w_0\frac{\partial u_0}{\partial z}}-\overline{\frac{v_0^2}{r}},$$

$$F(r,z)=\overline{u_0\frac{\partial v_0}{\partial r}}+\overline{\frac{v_0}{r}\frac{\partial v_0}{\partial\theta}}+\overline{w_0\frac{\partial v_0}{\partial z}}+\overline{\frac{u_0v_0}{r}},$$

$$M(r,z)=\overline{u_0\frac{\partial w_0}{\partial r}}+\overline{\frac{v_0}{r}\frac{\partial w_0}{\partial\theta}}+\overline{w_0\frac{\partial w_0}{\partial z}}.$$

These are known, from (8) though cumbersome, except that $F(r,z)=0$ in the interior, from $\sin(\theta+t)\cos(\theta+t)=0$, etc.

The first-order mean equations are:

$$G(r,z)=-\frac{\partial\bar p_1}{\partial r}+2\bar v_1+E\left(\nabla^2\bar u_1-\frac{\bar u_1}{r^2}\right)$$

$$F(r,z)=-2\bar u_1+E\left(\nabla^2\bar v_1-\frac{\bar v_1}{r^2}\right) \qquad (12)$$

$$H(r,z)=-\frac{\partial p_1}{\partial z}+E\nabla^2\bar w_1$$

$$\frac{\bar{u}_1}{r} - \frac{\partial \bar{u}_1}{\partial r} - \frac{\partial \bar{w}_1}{\partial z} = 0$$

$$\bar{u}_1 = \bar{v}_1 = \bar{w}_1 = 0 \quad \text{at } z=0$$

$$\bar{u}_1 = 0 \quad \text{at } r=1 \qquad (\text{and } \bar{v}_1 = \bar{w}_1 = 0 \text{ there})$$

$$\bar{w}_1 = -\overline{\eta^* \frac{\partial w_0}{\partial z}} \quad 0 \quad \text{at } z=1$$

Standard boundary-layer theory suggests splitting the problem into two parts: interior and boundary layers. The interior equations are:

$$\begin{aligned} G(r,z) &= -\frac{\partial \bar{p}_1}{\partial r} + 2\bar{v}_1 \\ 0 &= -2\bar{u}_1 \\ H(r,z) &= -\frac{\partial \bar{p}_1}{\partial z} \\ \frac{\bar{u}_1}{r} + \frac{\partial \bar{u}_1}{\partial r} + \frac{\partial w_1}{\partial z} &= 0 \end{aligned} \tag{13}$$

$\bar{w}_1 = 0$ at $z = 1$, and other boundary conditions to match the boundary equations.

In the interior,

$$\bar{u}_1 = 0 \tag{14}$$

then implies $\frac{\partial \bar{w}_1}{\partial z} = 0$ from (13.4), which with the top boundary condition (12.7) implies

$$\bar{w}_1 = 0 \tag{15}$$

(There <u>are</u> mean vertical motions, but they are much smaller than the first order scaling εU.)

Eliminating p_1 between (13.1) and (13.3) gives

$$\frac{\partial \bar{v}_1}{\partial z} = \frac{1}{2}\frac{\partial G}{\partial z} - \frac{1}{2}\frac{\partial H}{\partial r} \tag{16}$$

but leaves $\bar{v}_1$ ambiguous by any axially symmetric geostrophic flow.

To relieve this ambiguity, let's go to the boundary, to get $\bar{V}_1(r,0+)$.

Let $\zeta = E^{1/2}\zeta$ in (12), suppress writing r, and apply a bit more scaling of the usual boundary variety to get the mean first-order flow in the boundary:

$$
\begin{aligned}
G(\zeta) &= 2\bar{V}_1 + \frac{\partial^2 \bar{u}_1}{\partial \zeta^2} - \frac{\partial \bar{p}_1}{\partial r} \\
F(\zeta) &= -2\bar{u}_1 + \frac{\partial^2 \bar{v}_1}{\partial \zeta^2} \\
0 &= -\frac{\partial \bar{p}_1}{\partial \zeta} \qquad (17) \\
\frac{\bar{u}_1}{r} &+ \frac{\partial \bar{u}_1}{\partial r} + \frac{\partial \bar{w}_1}{\partial \zeta} = 0 \\
\bar{u}_1 &= \bar{v}_1 = \bar{w}_1 = 0 \quad \text{at} \quad \zeta = 0 \\
\bar{u}_1 &\text{ and } \bar{w}_1 \to 0 \text{ as } \zeta \to \infty
\end{aligned}
$$

All that is desired from (17) is an expression for $\bar{V}_1$ for $\zeta \gg 1$, but unfortunately, everything works itself in. Substituting $\bar{u}_1$ from (17.2) in (17.1) and solving gives (with primes denoting derivatives with respect to ζ)

$$\bar{V}_1 = \frac{1}{4}\left(2G + F'' + 2\frac{\partial p_1}{\partial r}\right) + e^{-\zeta}(a\cos\zeta + b\sin\zeta), \qquad (18)$$

after boundedness as $\zeta \to \infty$ is imposed. $\bar{V}_1(0) = 0$ gives $a = -\frac{1}{4}\left(F''(0) + 2\frac{\partial p_1}{\partial r}\right)$.

Now substituting (18) in (17.2) gives

$$\bar{u}_1 = \frac{1}{8}\left(2G'' + F''''\right) + 2e^{-\zeta}(-b\cos\zeta + a\sin\zeta) - F(\zeta) \qquad (19)$$

so $\bar{u}_1(0) = 0$ gives

$$b = \frac{1}{8}\left(2G''(0) + F''''(0)\right).$$

Substituting (19) in the continuity equation (17.4), integrating, and

using $\overline{W}_1(0) = 0$ gives

$$\overline{W}_1(\zeta \to \infty) = + \frac{E^{1/2}}{2}\left(\frac{1}{\eta} + \frac{\partial}{\partial \eta}\right)\left\{\frac{1}{4}(2G'(0) + F'''(0)) + \int_0^\infty F(\zeta)\, d\zeta + b - a\right\} \tag{20}$$

which must be zero, by (15). Now b is "known", and so is a, except for $\frac{\partial p_1}{\partial \eta}$, which is therefore determined from (20); integrating (20) with respect to η, there exists a constant C such that

$$\frac{C}{\eta} = \frac{1}{4}(2G'(\eta,0) + F'''(\eta,0) + \int_{bdy} F(\eta,\zeta)\, d\zeta + \frac{1}{8}(2G''(\eta,0) + F''''(\eta,0) + \frac{1}{4}F''(\eta,0) + \frac{1}{2}\frac{\partial \bar{p}_1}{\partial \eta}(\eta,0^+). \tag{21}$$

This tacks down $\frac{\partial \bar{p}_1}{\partial \eta}(\eta,0^+)$ and hence $\bar{V}_1(\eta,0^+)$, and hence $\bar{V}_1(\eta,\zeta)$, by (16), except for an arbitrary potential vortex, which has a non-divergent Ekman layer, so is only damped by internal friction. Specifically,

$$\bar{V}_1(\eta,0^+) = \frac{C}{\eta} + \frac{G(\eta,0^+)}{2} - \frac{1}{4}\left[2G'(\eta,0) + F'''(\eta,0)\right] - \int_{bdy} F - \frac{1}{8}\left(2G''(\eta,0) + F''''(\eta,0) + 2F''(\eta,0)\right). \tag{22}$$

If one could tie down C, the problem would be formally solved, requiring but a few hundred pages of algebra to work out the various G'_2, F'_2, and their integrals. It seems tempting to conclude that since there is no net suction, there is no need for side-wall boundary layers, so $\overline{V}_1(1,0^+) = 0$. This would determine C. Alternatively, one could choose C so there is no pole at $\eta = 0$. [G contains a singularity there]; this would be more attractive if one did not often observe a vortex there.

Perhaps it should be pointed out that Rosenblat (1959) showed that small $\overline{W}_1 < 0$ cancels the sort of centrifugally forced $\overline{V}_1$ considered here in a wider boundary layer, of width $\sqrt{\frac{\nu}{\Omega R_0}}$. Actually, it would be nice to therefore take $\overline{V}_1 = 0$ at the bottom, but here $\overline{W}_1 = 0$, and a $\overline{V}_1$ is observed just above a bottom layer anyway.

Possible Shear Instability

The G's etcetera have proven too cumbersome to handle in detail. Near a resonance, the expression can be simplified by retaining only the leading terms, so in the interior

$$G(n,z) \approx \frac{a_m^2 \lambda_n}{6}\left\{\frac{3J_0}{\lambda_m n}(3J_0-J_2)-\frac{3}{4}(3J_0+J_2)(3J_1+J_3)-\frac{1}{2}J_1J_2-\sin^2\left(\frac{\lambda_n z}{\sqrt{3}}\right)\left[\frac{3J_0}{\lambda_m n}(3J_0-J_2)-\right.\right.$$

$$\left.\left.-\frac{3}{4}(3J_0+J_2)\left(\frac{17}{3}J_1+J_3\right)-\frac{1}{2}J_1J_2\right]\right\}-\frac{a_m^2}{12}\frac{(3J_0-J_2)^2}{n}\left(1+\cos\frac{2\lambda_n z}{\sqrt{3}}\right),$$

where all the J's are functions of $\lambda_m n$. Unfortunately, it cannot be simplified this much in the boundary layer. For instance, even taking shallow water to simplify the sums over J's to polynomials gave

$$\overline{u_0\cdot\nabla u_0}=\left(\frac{\alpha}{16}\right)^2\left\{\frac{50}{n}\left[1-2e^{-\frac{\zeta}{\sqrt{2}}}\cos\frac{\zeta}{\sqrt{2}}+e^{-\frac{2\zeta}{\sqrt{2}}}\right]+n\left[-220+e^{-\frac{\zeta}{\sqrt{2}}}\left[\left(460+\frac{40}{\sqrt{3}}+\frac{805}{\sqrt{2}}\right)\cos\frac{\zeta}{\sqrt{2}}+\right.\right.\right.$$

$$\left.+120\sin\frac{\zeta}{\sqrt{2}}\right]+e^{-\sqrt{\frac{3}{2}}\zeta}\left[-20\cos\sqrt{\frac{3}{2}}\zeta\right]-240e^{-\frac{2\zeta}{\sqrt{2}}}+\left(20-\frac{40}{\sqrt{3}}\right)e^{-\left(\frac{\sqrt{3}+1}{\sqrt{2}}\right)\zeta}\cos\left(\frac{\sqrt{3}+1}{\sqrt{2}}\zeta\right)\Big\}+$$

$$+n^3\left\{170+e^{-\frac{\zeta}{\sqrt{2}}}\left[\left(-384-16\sqrt{\tfrac{3}{2}}-\frac{96}{\sqrt{2}}\zeta\right)\cos\frac{\zeta}{\sqrt{2}}-\left(144+\frac{96}{\sqrt{2}}\zeta\right)\sin\frac{\zeta}{\sqrt{2}}\right]+e^{-\sqrt{\frac{3}{2}}\zeta}\left[\left(44-\right.\right.\right.$$

$$\left.-24\sqrt{3}+8\sqrt{6}\zeta\right)\cos\sqrt{\tfrac{3}{2}}\zeta+\left(8+8\sqrt{6}\zeta\right)\sin\sqrt{\tfrac{3}{2}}\zeta\Big]+216^{-2\frac{\zeta}{\sqrt{2}}}+2e^{-2\sqrt{\frac{3}{2}}\zeta}+$$

$$\left.\left.+\left(40\sqrt{3}-48\right)e^{-\left(\frac{\sqrt{3}+1}{\sqrt{2}}\right)\zeta}\cos\left(\frac{\sqrt{3}+1}{\sqrt{2}}\right)\zeta\right\}\right\}$$

While the above expressions are long, they do seem to be fairly well-behaved in n, except for the pole at $n=0$. $J_0(\lambda_m n)$, $J_1(\lambda_m n)$ and $J_2(\lambda_m n)$ tend to have about m bumps between 0 and 1 and otherwise be well-behaved. Thus, it is not unreasonable to expect all of the G's, F's, and derivatives to be fairly well-behaved, and to wiggle about m times.

Thus, all of this algebra makes it very plausible that $\bar{V}_1$ may have a vortex at the center, then wiggle through a few maxima and minima. But then the mean vorticity $\frac{1}{r}\frac{\partial}{\partial r}(r\bar{v})$ goes through extrema, which has two consequences. First, there will be a (higher-order) Ekman convergence under positive vorticity, leading to any ink in the boundary layer being collected into rings. (And in fact, the rings were the clue to this whole study.) Second, if $|\bar{V}_1|$ is large enough so the Reynold's number based on it and on the jet width exceeds about 10, there will be a barotropic shear instability, causing waves on the ring of wavelength about 6 times the jet width to grow exponentially, form vortices at finite size, and break down to turbulence, if there is enough energy. For a width of about 3 cm, the requisite velocity is about 3 cm/minute. Anyway, since $\underset{\sim}{u}_o$ is proportional to the tilt $\propto \Omega L$, $|\bar{V}_1|$ is proportional to $(\propto \Omega L)^2$. Near a resonance, $|\bar{V}_1|$ will also be proportional to $\left(\sin\left(\frac{\lambda_m H_o}{\sqrt{3}L}\right)\right)^{-2}$, so near a resonance, lines of constant $|\bar{V}_1|$ in the $\left(\frac{H_o}{L}, \propto \Omega L\right)$ plane will be on lines of constant $\propto \Omega L \left|\sin\left(\frac{\lambda_n H_o}{\sqrt{3}L}\right)\right|^{-1}$, or lines (24) $\propto \Omega L = K_m \left|\frac{H_o}{L} - \frac{m\pi\sqrt{3}}{\lambda_m}\right|$, where K will be constant near a particular resonance.

Thus, the unstable region of the plane will include vees touching the no-tilt $(\propto = 0)$ line, and presumably including all of the region with large enough tilt.

Observations

It should be obvious by now that most of the previous was dreamed up to explain what now follows, though the theory guided the selection of test parameters. E.g., the vees were searched for, and found, right

at the predicted depths! See Figure for the results of the experiments. The experiments were done in a plastic cylinder with radius 14.5 cm, so the predicted first-mode resonance would be at a depth of 28.85 cm, the second at 13.88 and 27.75 cm, and the third at 9.06, 18.13, and 27.19 cm. Unfortunately, the tank was not quite deep enough to reach the first mode, but there are nice deep vees observed at 13.9, 27.5 and 18.0 cm, at all of which edge waves (a particular kind of shear instability) were observed with no measurable tilt imposed.

The circled dots indicate that nothing much was observed. The $\textcircled{R_n}$ means n rings of ink on the bottom were observed, indicating fair forced mean zonal velocities, but not enough to go unstable. Note that for shallow water the rings tended to have spacings comparable to the depth, so the number of rings times the depth is nearly constant. In shallow water, the increased importance of the bottom viscous layer was able to prevent the instabilities, even with the compound inviscid resonance at $H_0/L = 0$.

The $\textcircled{I_n}$ denotes that an instability developed on a ring, as pictured in figure. These instabilities look remarkably like barotropic shear instabilities. They obey the Taylor-Proudman law of independence of z remarkable, even if the mean shear is not independent of z. The wavelengths of the instabilities are often about 6 cm, which suggests a jet width of about 1 cm from shear instability theory. This accords well with the observed bottom ink-band widths, (though is much smaller than the ring spacing) but then requires a $|\bar{V}_1|$ of 10 cm/min, whereas the observed $|\bar{V}_1|$ just above the bottom is only 1 or 2 cm/min. However, the expression for

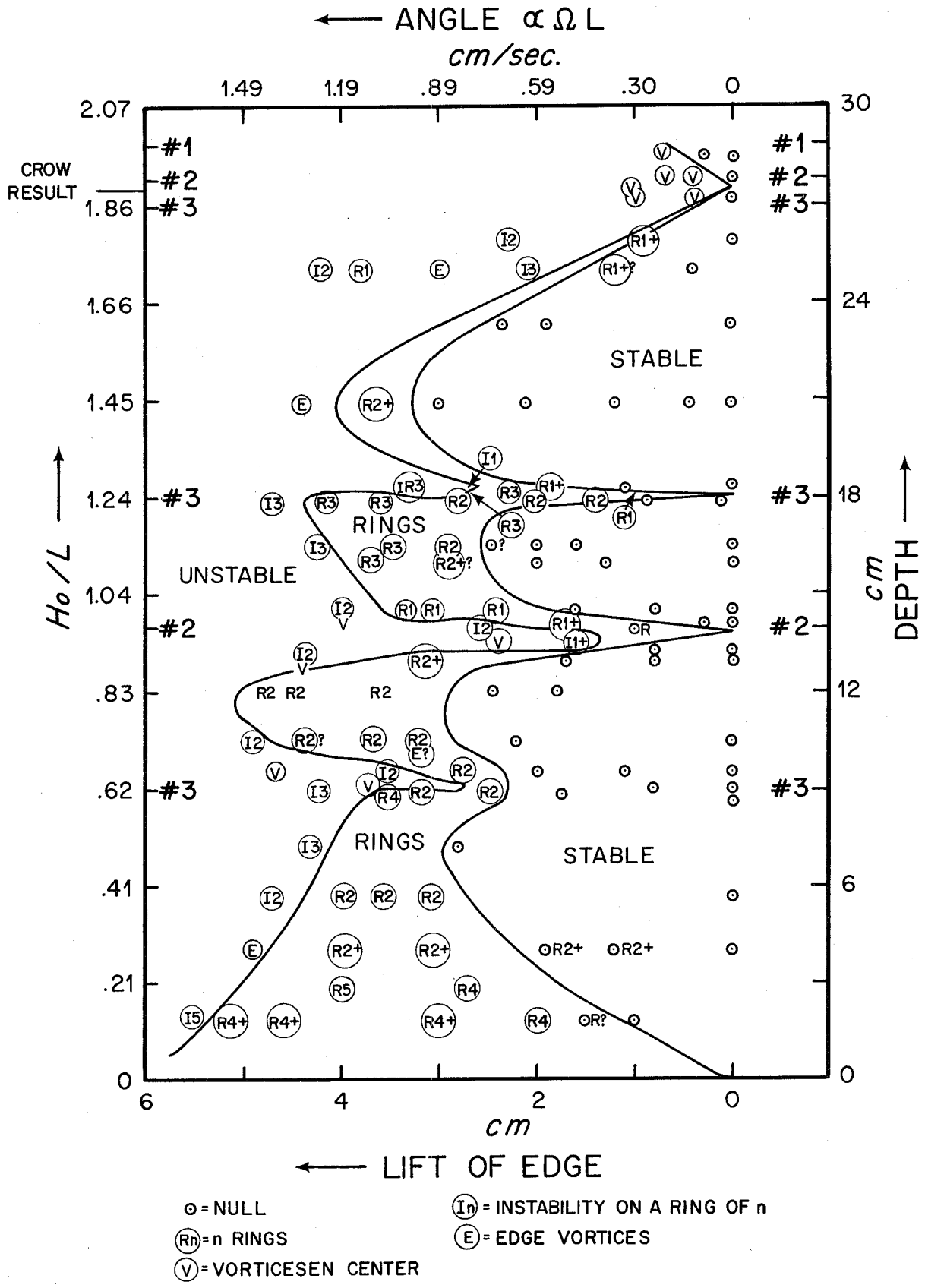
← ANGLE ∝ Ω L
cm/sec.
1.49
1.19
.89
.59
.30
0
2.07
1.86
1.66
1.45
1.24
1.04
.83
.62
.41
.21
0
#1
#2
#3
CROW RESULT
Ho/L
30
24
18
12
6
0
cm
DEPTH
STABLE
RINGS
UNSTABLE
RINGS
STABLE
6
4
2
0
cm
← LIFT OF EDGE
⊙ = NULL
(Rn) = n RINGS
(V) = VORTICESEN CENTER
(In) = INSTABILITY ON A RING OF n
(E) = EDGE VORTICES

Fig. 2

A

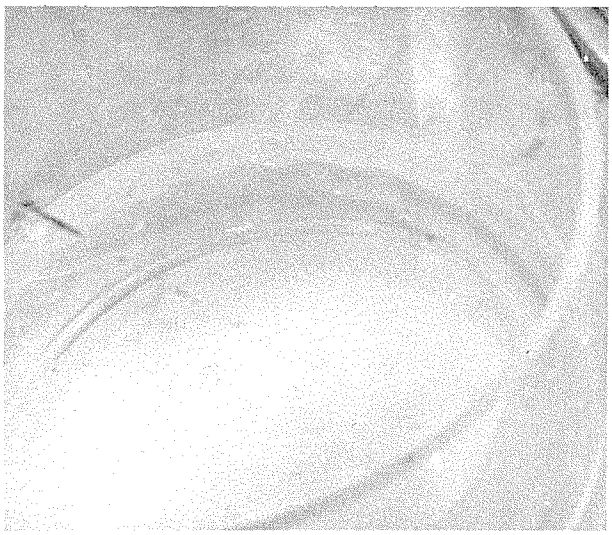

D

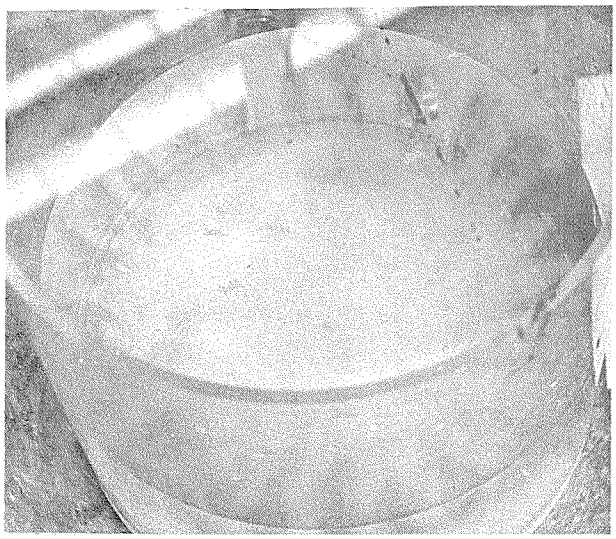

B

E

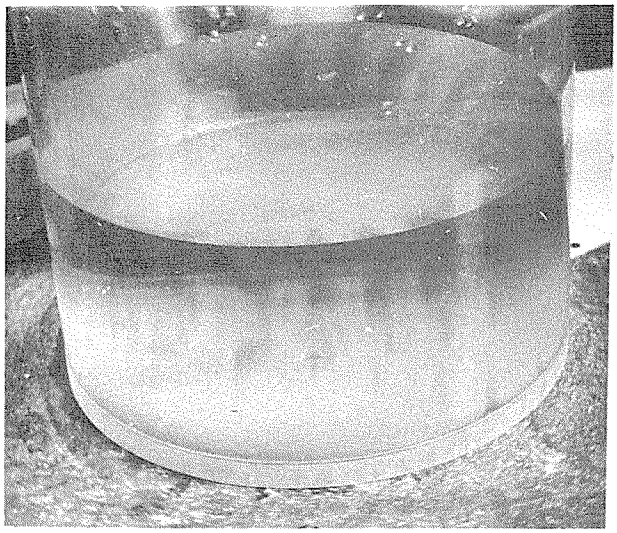

C

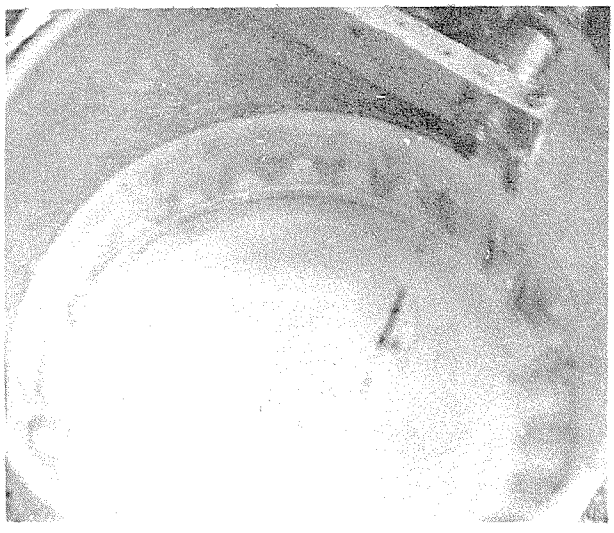

Growth and
Decay of an Instability

figure 3

$|\overline{V_1}|$ depends on z, so perhaps the vertically averaged $|\overline{V_1}|$ is as high as 10. Otherwise, there may be a bit of a squeeze to get a Reynold's number of 10 out.

Future Studies

At one time, it had seemed possible that the corner vortices (at $r = L$) were due to a centrifugal instability of the (oscillating) concave flow past the corner, in the style of Görtler (1940), except that here the radius of curvature is not necessarily small compared to the boundary layer thickness. The Taylor number here seems to be too small for this explanation, but it does suggest an interesting experiment I intend to study this fall. Taylor's rotating cylinder experiments will be repeated, but with the inner cylinder oscillating torsionally. This should be a theoretically tractable study of an instability on an unsteady basic flow.

Along the lines of the current work, further laboratory work is necessary, especially for observations near the first resonance. For instance, the vee which is centered at 1.90 looks suspiciously like the first mode displaced downward a trifle (so overlapping the second mode vee), perhaps due to neglecting the deviation of the surface from η^* in the W boundary condition, (i.e., the Froude number was not as small in the experiment as the theory).

References

Abramowitz, Milton and Irene Stegan, editors 1965 Handbook of Mathematical Functions, Dover, New York

Aldridge, K. D. 1967 Scientific Report HRF/SR-7, Hydrodynamics of Rotating Fluids Project, Dept. of Geology & Geophysics, M.I.T.

Crow, Steven C. 1965 Geophysical Fluid Dynamics Notes, Vol. II, W.H.O.I.

Fultz, David et al. 1959 Meteorological Monographs 4 (21), Amer.Meteor. Soc., Boston, Mass.

Fultz, David 1965 in a symposium review by Kücheman, J.Fl.Mech., 21: 1

Jahnke, E. and F. Emde 1945 Tables of Functions, Dover, New York.

Johnson, Leonard 1967 Geophysical Fluid Dynamics Notes, Vol. II, W.H.O.I.

Rosenblat, S. 1959 J. Fluid Mech. 6: 206-220.

Tranter, C. J. 1957 Integral Transforms in Mathematical Physics, London: Methuen & Co., Ltd.

Seminars

and

Abstracts of Lectures

The Axisymmetric Convective Regime for a Rigidly-bounded Rotating Annulus

Michael E. McIntyre

ABSTRACT

A boundary-layer theory was presented describing the axisymmetric convective flow of liquid in a rigidly-bounded annulus rotating about its (vertical) axis with angular velocity Ω , due to the imposition of a horizontal temperature difference ΔT between the cylindrical side walls. The theory is based on a self-consistent set of approximations valid when $\Delta T/\Omega^2$ is large enough for the heat transfer across the annulus to be convection-dominated, but not large enough to prevent rotation from being a strong controlling influence on most of the flow. These conditions are characteristic of the experimentally-observed upper symmetric regime near the transition to the wave regime. The Prandtl number ν/κ is assumed large, and there is a restriction on the tallness of the annulus (aspect ratio H/L less than about 2).

The side-wall boundary layer equations turn out to be only weakly non-linear under the conditions of the problem, and the lid boundary layers may be taken as Ekman layers. Matching the boundary-layer solutions to certain horizontal averages of the interior fields results in a closed problem, the 'primary problem', which expresses the most important physical interactions governing the flow. The determination of the interior flow details becomes a subsequent 'secondary problem' in which viscosity and conductivity are important throughout the interior. The interior streamlines are not necessarily parallel to the isotherms. The secondary problem

was discussed qualitatively but not solved explicitly.

A preliminary comparison with an available numerical experiment is satisfactory when the more obvious effects of finite boundary-layer thickness are allowed for; comparison with suitable laboratory experiments has not yet been carried out.

Linear Theory of Wind-driven Circulation in One- and Two-layer Oceans with Non-uniform Depth

Pierre Welander

ABSTRACT

An extension is given of the linear theory of wind-driven circulation for an ocean of uniform depth (by Stommel, 1948). Firstly, the bottom is made non-uniform. It is shown that the position of the frictional boundary current balancing an interior "Sverdrup-topographic" regime depends on the field of $\frac{f}{H}$ (f is the Coriolis parameter, H the depth). When $\frac{f}{H}$ increases polewards or equatorwards the boundary current is found on the western or eastern side, respectively. If both of these regimes occur, the boundary currents on each side are joined by a free jet along a contour for which $\frac{f}{H}$ is extremum. If the $\frac{f}{H}$-contours are closed in the interior a strong interior gyre is added. (Such a closed-contour region of large scale is found in the North Atlantic near the Azores.)

This homogeneous model has been discussed earlier in the literature. An interpretation in terms of a thermal model seems, however, to be new.

The transport stream-function is modelled by a temperature, and the $\frac{f}{H}$-field by the stream-function of a two-dimensional incompressible flow, $curl\ \frac{\tau^w}{H}$ represents a heat source and $\frac{Df}{H^2}$, a thermal conductivity (D is the Ekman depth). In the special case of H = constant, the model has been suggested earlier by Stommel.

Secondly, a stratification is introduced, in a two-layer approximation. The lower layer is assumed deep compared to the upper layer. One can then show that the velocities in the lower layer are small. Therefore the upper-layer solution can be derived as if no lower-layer motion occurs. The upper circulation is qualitatively the same as in the uniform depth model by Stommel. The shape of the interface and the interface stresses (by law of Ekman friction) are then computed. The lower-layer problem is then solved as a second step. It formally looks like a one-layer problem, with known total depth and known driving surface stresses, that are found to be essential only along a narrow western strip. The lower circulation has a directly-forced boundary current at the western side. If $\frac{f}{H}$ increases polewards this current recirculates completely within the western boundary, but if $\frac{f}{H}$ decreases polewards it feeds an eastern frictional boundary current through an interior geostrophic flow. In the "mixed case" free jets occur again. An important change is that interior regions of closed $\frac{f}{H}$-contours now only produce a weak associated gyre, because the interior interface stresses are small.

The theory will be presented in detail in the November issue of Tellus (1967).

Linearized Flow in Rotating Systems

Frederic E. Bisshopp

ABSTRACT

The linearized equations governing incompressible, viscous flow which deviates slightly from rapid uniform rotation are treated in a boundary layer approximation. For a number of problems in which the flow is confined to the region between horizontal plates, representations of the solutions, valid everywhere but in vanishingly small 'corners', are given. Cases where a rigid side wall moves at a velocity which differs from one or both of the plate velocities are treated by means of an integral transform which has many features in common with a Fourier sine-transform. A heuristic derivation of the inversion theorem is given.

Simplification by Stratification

Pierre Welander

ABSTRACT

It is suggested that a simple theory of turbulent transfer can be developed more simply for the case of a stably-stratified fluid than for a neutral or unstably-stratified fluid. The argument is that the stratification limits the size of eddies that can contribute to the transport. If the eddy-scale L_e and eddy-lifetime T_e are small compared to the scale L and characteristic time-scale T of the mean fields, one may use the

same assumption of "local statistical equilibrium", as is utilized in kinetic theory derivations. A specific example is given, that may apply to the oceanic thermocline problem: Consider a turbulent Boussinesq fluid, statistically homogeneous horizontally, in which a horizontal stress (momentum transport) τ^{o}_{xz} and vertical heat transport q^{o}_{z} are applied. These transports are constant vertically (neglecting the heat flux Δq_z from dissipation). The equations for the time-dependent (turbulent) motion can be written in terms of $\bar{v}$, $\rho^* = g\left(\frac{\rho}{\rho_0} - 1\right)$, and $\left(p^* = \frac{p}{\rho_0} + gz\right)$, the only parameters are $\tau^* = \frac{\tau^{o}_{xz}}{\rho_0}$ and $q^* = \frac{g \alpha q^{o}_{z}}{C \rho_0}$, where α is the thermal expansion, C the specific heat per unit mass, if we assume that the contribution from viscous-conductive eddies is negligible. The gradients $\frac{d\bar{u}}{dz}$ and $\frac{d\bar{\rho}^*}{dz}$, well away from boundaries (many eddy sizes away) are then, by dimensional arguments $\frac{d\bar{u}}{dz} = k_1 \frac{q^*}{\tau^*}$, $\frac{d\bar{\rho}^*}{dz} = k_2 \cdot \left(\frac{q^*}{\tau^*}\right)^2$. Hence,

$$R_i = \frac{d\bar{\rho}^*}{dz} \Big/ \frac{d\bar{u}}{dz} = \text{constant}.$$

Observations suggest a value around $0,1$.

Next, consider a time-dependent situation where as described before $L_e << L$, $T_e << T$. Then one may believe that the above flux-gradient relations hold <u>locally</u>. However, τ^* and q^* are no longer constant, but determined from the "divergence equations" $\frac{\partial \bar{u}}{\partial t} = \frac{\partial \tau^*}{\partial z}$, $\frac{\partial \bar{\rho}^*}{\partial t} = \frac{\partial q^*}{\partial z}$. From these one derives two equations in q^* and τ^* only:

$$\frac{\partial}{\partial t}\left(\frac{q^*}{\tau^*}\right) = \frac{1}{k_1} \frac{\partial^2 \tau^*}{\partial z^2}, \quad \frac{1}{g} \frac{\partial^2 q^*}{\partial z^2} = \frac{2k_2}{k_1} \frac{1}{\tau^*} \frac{\partial \tau^*}{\partial z}.$$

These can be integrated in time from given initial fields $\tau^*(z)$, $q^*(z)$, (in special cases analytically). Small deviations from the steady state τ', q' are shown to be governed by a diffusion type equation

$\frac{\partial \tau'}{\partial t} = K \frac{\partial^2 \tau'}{\partial z^2}$, $\frac{\partial q'}{\partial t} = K \frac{\partial^2 q'}{\partial z^2}$, where K is a constant. If $\frac{k_1}{k_2} < 2$ one finds $K > 0$ and stability, if $\frac{k_1}{k_2} > 2$ small deviations grow to "fronts". The value of the constants k_1, k_2 cannot be found from the present theory. One should try to get estimates from a more mechanical theory of the turbulence, or from experiments.

Introduction to Turbulence Theory

Steven A. Orszag

ABSTRACT

A description of the basic physical processes occurring in turbulence is given. Turbulence is characterized by enhancement of the various transfer processes - for example, enhanced transfer of momentum leads to an effective eddy viscosity. The ratio of this eddy viscosity to the ordinary kinematic viscosity is the Reynolds number which can be thought of as the strength of the turbulence.

The theory of the inertial range due to Kolmogorov is described. This theory uses simple dimensional analysis to derive the form of the energy spectrum for small scales.

The nature of analytic approaches to the theory of turbulence is explained. In particular, the "quasi-normal" theory of Proudman and Reid, and Tatsumi is explained in some detail. It is explained why this theory is unsatisfactory in that it leads to negative energy densities after a finite time. This deficiency is traced to memory integrals that give too

large a weight to instants when the system is far from a quasi-stationary equilibrium. This difficulty with the memory effects is resolved by making the quasi-normal equations markoffian in the energy density. The resulting markoffian quasi-normal equations preserve energy density positivity and all the other consistency requirements usually imposed on a turbulence theory. These latter include conservation of energy by nonlinear interaction, inviscid equipartition solutions, etc. The markoffian quasi-normal equations have been integrated numerically and at moderate Reynolds numbers ($R_L \sim 50$) are in good agreement with Kraichnan's direct-interaction equations. The markoffian quasi-normal equations are vastly simpler to compute than the direct-interaction equations. In fact, one justification of these markoffian equations is that they appear to be the simplest turbulence equations that do not violate any of the physically-required consistency conditions.

Turbulent Distortion of Very Small Ink Blobs

Robert H. Kraichnan

ABSTRACT

This talk started with a review of the treatment by Batchelor (1959) of the distortion, by turbulence in an incompressible fluid, of weakly diffusive blobs of ink which initially have spatial dimensions very small compared to any length scale of the turbulence. Batchelor supposed that a typical blob experienced constant rates of strain in coordinates which

moved and rotated with the blob. This led, by simple analysis, to the prediction that the wavenumber spectrum of the fluctuations in intensity of ink concentration took the form $(gk)^{-1}\exp(-ak^2/g)$ at high wavenumbers k, where g is the magnitude of the most negative rate of strain in principal axes and a is the molecular diffusivity.

Two modifications of Batchelor's treatment were proposed. First, the strain experienced by a typical blob can be expected to fluctuate in time rather than stay constant; second, the instantaneous strain rate can be expected to fluctuate from place to place according to the local character of the turbulence. Both modifications can be crudely explored by assuming slow variations of the strain rate and averaging Batchelor's final spectrum formula over a statistical distribution of strain rates. For reasonable choices of statistics, the $(gk)^{-1}$ spectrum below diffusive cut-off survives, where g now is taken as a root-mean-square value of strain rate. However, the $\exp(-ak^2/g)$ cut-off is modified into a much gentler cut-off, approximately like $\exp\left[-(ak^2/g)^{2/3}\right]$ if the strain statistics are Gaussian and even more gentle if the strain statistics exhibit large flatness factors. Most of the contribution to the spectrum at very high k arises from the exceptional regions of the fluid where the most negative strain rate is unusually large. That is, the very high k excitation is highly intermittent in physical space.

In the second part of the talk, the treatment of this problem by the Lagrangian-history-direct-interaction approximation was outlined. This is a closure approximation which involves tracing the history of correlations back along particla trajectories. It was found to yield results very much

like those of the modified Batchelor theory: a $(gk)^{-1}$ spectrum below cut-off, and a cut-off which is faster than algebraic but much slower than Gaussian. Specifically, the final expression goes like $\exp\left[-(ak^2/g)^{3/4}\right]$.

REFERENCES

Batchelor, G. K. 1959 J.Fluid Mech., 5: 113

Kraichnan, R. H. 1965 Phys.Fluids, 8:575

Kraichnan, R. H. 1966 Phys.Fluids, 9: 1728, 1884, 1937

Estimates for Turbulence

Louis N. Howard

ABSTRACT

The purpose of this talk is to present the basic ideas of my 1963 paper "Heat transport by turbulent convection" (J.Fluid Mech. 17: 405-432) as an indication of the kind of information accessible by the approach used there and as background to the discussions of Malkus and Busse. More recent work on other turbulence problems following this same general method will be presented by them.

The problem attacked in that paper was turbulent convection between parallel, horizontal, rigid, perfectly heat-conducting plates, the lower one hotter than the upper. The mathematical model for the fluid between the plates is the Boussinesq equations. The central idea is to obtain some information of physical interest about the turbulent flow without detailed consideration of the motion by using some properties common to

all statistically steady solutions of the equations and boundary conditions as constraints on a variational problem for some functional of the flow - in the present case the heat transport. The solution to this variational problem will then provide a bound on the value which this functional can have for the actual turbulent flow. How reliable this upper bound will be as an estimate of the actual heat flux is not clear from the start, but one may take the viewpoint that any (finite) upper bound is better than no information at all. There is also however the hope that investigation of enough problems of this nature will give some suggestions of quantities which turbulent flows do tend to maximize.

The constraints utilized in the convection problem are the two simplest integral consequences of the Boussinesq equations, the so-called "power integrals".

$$R\langle wT\rangle = \langle |\nabla \vec{u}|^2 \rangle \tag{1}$$

and

$$\langle w\cdot T\rangle + \langle wT\rangle^2 - \langle \overline{wT}^2\rangle = \langle |\nabla T|^2\rangle \,. \tag{2}$$

Here $\vec{u}$ is the (dimensionless) velocity, T the deviation of the temperature from its horizontal average, w the vertical component of $\vec{u}$ and R the Rayleigh number. $\langle\ \rangle$ indicates the average over the whole layer, $\overline{\ }$ the horizontal average. The heat flux is measured in dimensionless form by the Nusselt number,

$$N = 1 + \langle wT\rangle. \tag{3}$$

The 1963 paper contains the solution to the problem of maximizing N subject to (1), (2) and the boundary conditions that $\vec{u}$ and T vanish on $z = 0,1$. It also gives an investigation of the same problem when in addition the continuity equation $\nabla\cdot\vec{u} = 0$ is added as a constraint, under

the assumption that only a single horizontal wave number is present in the fields $\vec{u}$ and T, a hypothesis consistent with the Euler equations, but not implied by them.

Here we indicate briefly how the constraints (1) and (2) do in fact lead to results of interest.

a) The simplest bit of information about turbulent convection comes from (1) alone - it shows that $\langle wT \rangle \geq 0$, and equals 0 only if there is no motion. Thus $N > 1$ for any statistically steady convection.

b) Another fact of some interest comes from writing (2) in the form

$$\langle wT \rangle = \langle |\nabla T|^2 \rangle + \langle (wT - \langle wT \rangle)^2 \rangle \tag{4}$$

and thus $\langle wT \rangle \geq \langle |\nabla T|^2 \rangle$; multiplying this by (1) shows that whenever $\langle wT \rangle \neq 0$,

$$R \geq \frac{\langle |\nabla T|^2 \rangle \langle |\nabla \vec{u}|^2 \rangle}{\langle wT \rangle^2} \tag{5}$$

The right-hand side of (5) is bounded from below, for instance by $\frac{\langle T_z^2 \rangle \langle w_z^2 \rangle}{\langle T^2 \rangle \langle w^2 \rangle} \geq \pi^4$; thus if R is <u>small</u> enough, $\langle wT \rangle$ must be zero and hence $N = 1$. The minimum of the right-hand side of (5) among all fields $\vec{u}$ and T satisfying the boundary conditions and $\nabla \cdot \vec{u} = 0$ can be shown to be the minimum critical Rayleigh number R_c of the linear stability problem, here about 1708. Thus if $R < R_c$ these simple estimates actually suffice to determine N completely, of course we are really interested in large R.

c) That (1) and (2) do in fact imply an upper bound on N can be seen as follows:

We have: $T^2 = \left(\int_0^z T_z \, dz\right)^2 \leq \int_0^z T_z^2 \, dz \int_0^z 1 \, dz \leq z \langle |\nabla T|^2 \rangle$.

Likewise, $\overline{T^2} \leq (1-z)\langle |\nabla T|^2 \rangle$, by starting at $z = 1$, hence $\overline{T^2} \leq \langle |\nabla T|^2 \rangle \min(z, 1-z)$.

Similarly,

$$\overline{w^2} \le \langle |\nabla w|^2 \rangle \mathrm{Min}(z, 1-z) \le \langle |\nabla \vec{u}|^2 \rangle \mathrm{Min}(z, 1-z).$$

Thus $\overline{wT} \le \overline{w^2}^{1/2}\,\overline{T^2}^{1/2} \le \langle |\nabla \vec{w}|^2 \rangle^{1/2} \langle |\nabla T|^2 \rangle^{1/2} \mathrm{Min}(z, 1-z) = A \langle wT \rangle \mathrm{Min}(z, 1-z)$,

where

$$A = \langle |\nabla T|^2 \rangle^{1/2} \langle |\nabla u|^2 \rangle^{1/2} / \langle wT \rangle \ge R_c^{1/2}$$

Consequently,

$$\int_0^1 \left(\overline{wT} - \langle wT \rangle\right)^2 dz \le 2 \int_0^{A^{-1}} \langle wT \rangle^2 (1 - Az)^2 dz = \frac{2}{3A} \langle wT \rangle^2$$

It then follows from (4) that

$$\langle wT \rangle \ge \langle |\nabla T|^2 \rangle + \frac{2}{3A} \langle wT \rangle^2 = A^2 \frac{\langle wT \rangle^2}{\langle |\nabla \vec{u}|^2 \rangle} + \frac{2}{3A} \langle wT \rangle^2 = \frac{A^2}{R} \langle wT \rangle + \frac{2}{3A} \langle wT \rangle^2$$

Thus $\langle wT \rangle \le \frac{3A}{2}\left(1 - \frac{A^2}{R}\right)$; the maximum of this for positive A occurs at $A^2 = R/3$, and so $\langle wT \rangle \le \frac{3}{2}\left(\frac{R}{3}\right)^{1/2}\left(1 - \frac{1}{3}\right) = \left(\frac{R}{3}\right)^{1/2}$. We thus obtain the upper bound

$$N \le 1 + \left(\frac{R}{3}\right)^{1/2}.$$

The 1963 paper solves the Euler equations for maximizing $\langle wT \rangle$ subject to (1) and (2) and so obtains a slightly better upper bound, which for large R is asymptotic to $\frac{3}{8}\left(\frac{R}{3}\right)^{1/2}$.

Consideration of the continuity equation as an additional constraint, with the single horizontal wave number hypothesis, leads to an upper bound which for large R is approximately $\left(\frac{R}{248}\right)^{3/8}$. (Recent work by Busse indicates however that the single wave number fields cease to give maximum N if R is large enough, and in fact he finds that the $R^{1/2}$ estimate is nearly achieved asymptotically for very large R). The details of this calculation are however to lengthy to present here.

Precessional Torques and Geomagnetism

Willem V.R. Malkus

If left to itself, the core would precess more slowly than the mantle, because of the difference in densities. But coupling between the mantle and the core creates torques which give rise to motions in the core, and these may be a cause of geomagnetism.

We consider the following system:

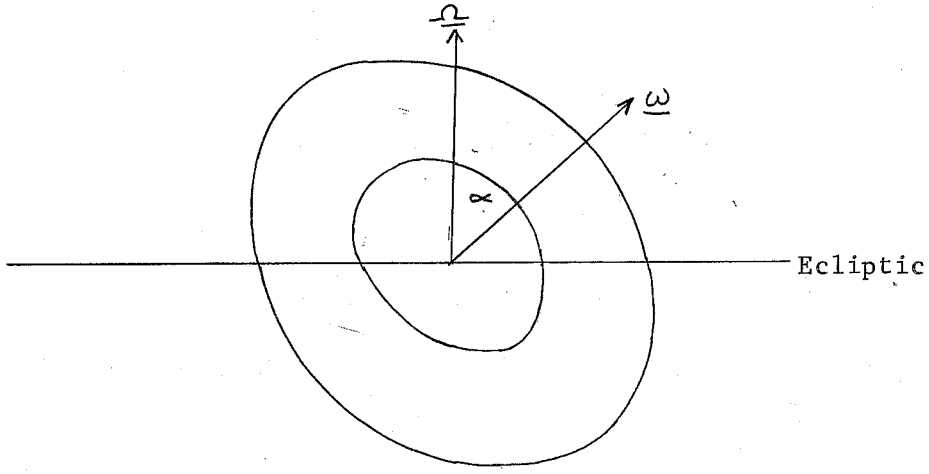

Here $\underline{\omega}$ is the rotation vector and $\underline{\Omega}$ is the precession vector, and

$$\underline{V} = \underline{\omega} \times \underline{r} + \underline{u}$$

is the fluid velocity in a spheroidal container, relative to coordinates rotating with $\underline{\Omega}$. $\underline{u}$ is the departure from a solid rotation $\underline{\omega} \times \underline{r}$, and the absolute velocity is

$$\underline{V}_{abs} = \underline{\Omega} \times \underline{r} + \underline{V} .$$

The equations are then

$$\frac{\partial \underline{u}}{\partial t} + 2(\underline{\Omega}+\underline{\omega}) \times \underline{u} - (\underline{u} + \underline{\omega} \times \underline{r}) \times (\nabla \times \underline{u}) = -\nabla p + \nu \nabla^2 \underline{u} + \underline{r} \times (\underline{\Omega} \times \underline{\omega}).$$

Poincaré (1910) took $\nabla \times \underline{u} = \text{const}$. Then, taking S to be the

surface of the spheroidal container on which

$$\frac{x^2+y^2}{a^2} + \frac{z^2}{b^2} = 1$$

(the eccentricity e is defined by

$$b^2 = a^2(1-e^2),$$

we apply the boundary condition

$$u \cdot n = 0 \,, \quad n \text{ normal},$$

but do not satisfy the boundary condition

$$u \times n = 0 \,.$$

We then have

$$u = \beta\left(0, \frac{z}{b^2}, -\frac{y}{a^2}\right),$$

with

$$\beta = \frac{2\omega\Omega a^2 b^2 \sin\alpha}{\omega(a^2-b^2) - 2\Omega a^2 \cos\alpha} \,.$$

This is an inertial circulation that does no work and is composed of flow in ellipses around the x-axis.

There is also a Stokes solution, given by Roberts and Stewartson (1965), for the very viscous case with

$$\frac{\nu}{a^2} >> \omega > \Omega$$

and

$\underline{u} \cdot \nabla \underline{u}$ negligible:

$$\underline{u} = -\frac{a^4 b^4 \omega \Omega \sin\alpha}{\nu(3a^4+3a^2b^2+4b^4)} \left[1 - \frac{x^2+y^2}{a^2} - \frac{z^2}{b^2}\right]\left(\frac{z}{b^2}, 0, -\frac{x}{a^2}\right).$$

This does work and is a uniform flow around the y-axis.

Now if a fluid is essentially in solid rotation around an axis only slightly different from the axis of rotation of its container, we may expect that a boundary layer of the Ekman type will form. Busse has recently

performed a boundary layer analysis to second order in amplitude, revealing internal circulations such as are shown on the following graph:

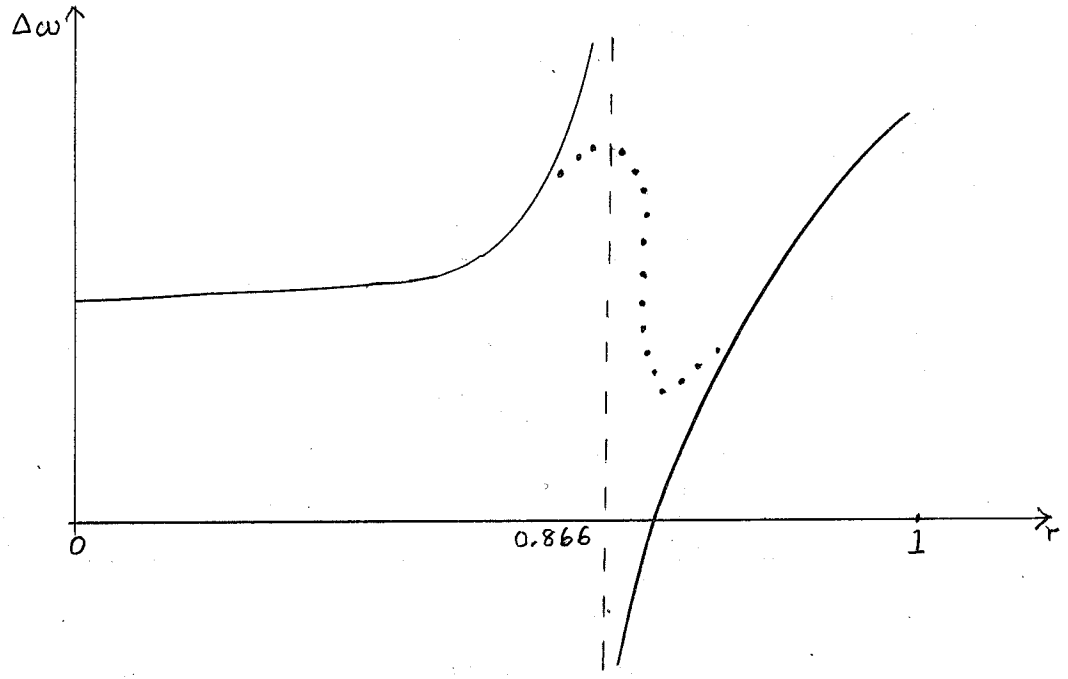

Here r is the dimensionless radius of the container, and $\Delta\omega$ the departure from solid rotation. The solid lines, tending to infinity near $r = 0.866$, are the theoretical curves for an inviscid fluid, and the dotted line represents results obtained from experiments, generally substantiating the theory but revealing departures due to viscous effects other than in the boundary layer.

Experimentally, Rossby wave-like instabilities are observable, and the relevant dimensionless parameter appears to be

$$R_E \equiv \frac{V_0 \delta}{\nu} = \frac{V_0}{\sqrt{\nu\omega}} = \frac{\varepsilon^2}{E^{1/2}} ,$$

the instability occurring at $R_E \doteq 13$. Here,

$$V_0 = \varepsilon^2 \omega a$$

where ε is the non-dimensional boundary layer amplitude; and E is an Ekman number approximately of order 10^{-6}.

An interesting set of additional data from these experiments is shown on the following graph.

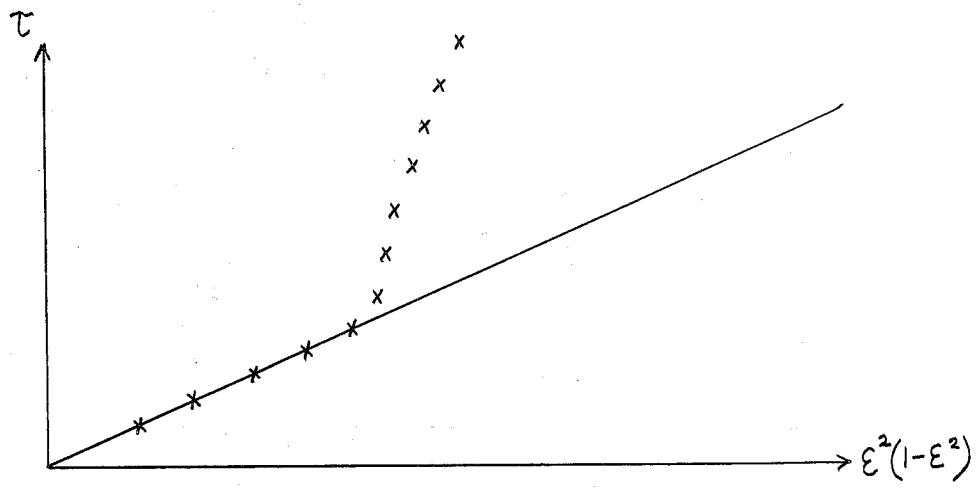

Here τ is the torque on the motor used to drive the experiment. The crosses represent the experimental points, which depart from the theoretical solid line at the point at which the wave instabilities appear.

Another type of experiment, in which the angle between ω and Ω is exaggerated to $\frac{\pi}{2}$, is schematically diagrammed below.

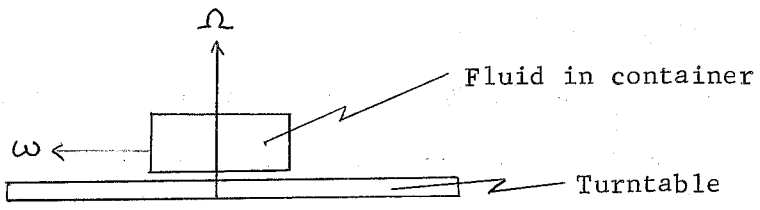

Here the container is itself rotating at rate ω, while being

supported on a turntable rotating at rate Ω . Typically, ω is 600 or 1800 r.p.m., while Ω is 1 to 50 r.p.m. The graph shows the result:

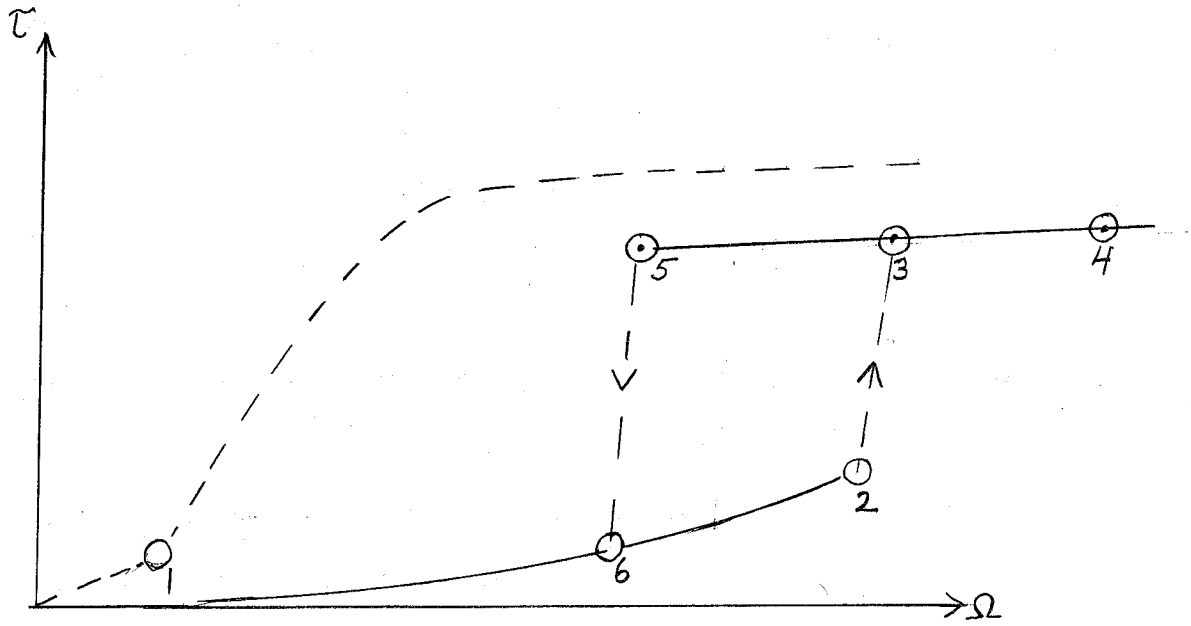

Here, point 1 is the instability point for a sphere, and the dashed curve is for the sphere. The solid curve is for a 10% spheroid. As Ω is increased, the spheroid experiment follows the lower solid curve to its instability at 2, then jumps to 3 and continues toward 4. With decreasing Ω , however, the sequence is 4, 3, 5, and then a jump to 6 on the lower curve. Thus there is a kind of hysteresis loop. The depth of the turbulent Ekman layer at the transition at 5 is approximately equal to the eccentricity. What can we say theoretically about this depth?

Ekman's laminar theory in 1905 of the manner in which a frictional layer near a boundary merges into a geostrophic flow far from the boundary has been extended to the turbulent case by Ellison (in Surveys in Mechanics, pp. 400-430, Cambridge University Press, London, 1956). The basic equation is familiar:

$$\frac{\partial \underline{V}}{\partial t} + 2\underline{\omega} \times \underline{V} + \underline{V} \cdot \nabla \underline{V} + \nabla p - \nu \nabla^2 \underline{V} = 0$$

An approach familiar in meteorology, and due essentially to Prandtl, represents the stress τ as

$$\tau = c \frac{\partial V}{\partial z}$$

with

$$c = k u^* z$$

and

$$u^* = \sqrt{\frac{\tau}{\rho}} \quad .$$

The symbols have their usual meanings, and the thickness δ is given by

$$\delta = \frac{u^*}{\omega}$$

This method, giving a complete but speculative and empirical theory, can perhaps be improved upon via the extremal problem approach discussed in an earlier lecture. We also note here that there is a need for effort on the experimental side as well, for the laboratory results are presently very incomplete.

We now explore an analagous treatment for the hydromagnetic case. The equations are

$$\left(\frac{\partial}{\partial t} - \nu \nabla^2\right) \underline{V} = -\frac{1}{\rho} \nabla p' - (\underline{V} \cdot \nabla) \underline{V} + (\underline{H} \cdot \nabla) \underline{H} - 2\underline{\omega} \times \underline{V}$$

$$\nabla \cdot \underline{V} = \nabla \cdot \underline{H} = 0$$

$$\left(\frac{\partial}{\partial t} - \eta \nabla^2\right) \underline{H} = \nabla \times (\underline{V} \times \underline{H})$$

$$= (\underline{H} \cdot \nabla) \underline{V} - (\underline{V} \cdot \nabla) \underline{H}$$

Here

$$p' = p_0 + \frac{1}{2} \rho \underline{H} \cdot \underline{H}$$

and

$$\underline{H} = \pm \sqrt{\frac{\mu}{4\pi\rho}}\, \underline{H}$$

where

ν = kinematic viscosity

$\underline{V}$ = velocity

ρ = (constant) density

μ = (constant) permittivity

p_o = pressure

$\underline{H}$ = magnetic field

$\eta = (4\pi\mu\sigma)^{-1}$ = magnetic diffusivity

σ = electrical conductivity

H = "magnetic velocity" .

An important identity is then

$$-(\underline{V}\cdot\nabla)\underline{V}+(\underline{H}\cdot\nabla)\underline{H}=\left[(\underline{H}+\underline{V})\cdot\nabla\right](\underline{H}-\underline{V})+\left(\frac{\partial}{\partial t}-\eta\nabla^2\right)\underline{H}.$$

Thus we may write

$$\left(\frac{\partial}{\partial t}-\eta\nabla^2\right)\underline{\delta}-(\eta-\nu)\nabla^2\underline{V}=-\frac{1}{\rho}\nabla P-(\underline{\delta}\cdot\nabla)\underline{\delta}+2\underline{V}\cdot\nabla\underline{\delta}-2\underline{\omega}+\underline{V},$$

where

$$\underline{\delta}=\underline{H}-\underline{V}$$

and

$$P=-p'$$

Then, taking $\eta=\nu$ to simplify the argument, and scaling with

$$H^2\sim(\omega R)V_o$$

$$R_o=\frac{V_o}{\omega R}$$

$$d\longrightarrow\frac{d}{R}\equiv\delta$$

and defining the magnetic Reynolds number as

$$R_M=\frac{V_o d}{\eta},$$

we obtain

$$R_M^{-1}R_o^{1/2}\left(\frac{\partial}{\partial t}-\eta\nabla^2\right)\underline{\delta}=-\frac{1}{\rho}\nabla P-(\underline{\delta}\cdot\nabla)\underline{\delta}+R_o^{1/2}2\underline{V}\cdot\nabla\underline{\delta}-\delta 2\underline{\omega}\times\underline{V}).$$

Now the third term on the right-hand side is negligible, and if we replace $\underline{V}$ by $\underline{\delta}$ in the final term ($\underline{V}$ and $\underline{\delta}$ are of the same order), the equation takes the form of the momentum equation. Now this suggests that δ , the scale of the boundary layer, is

$$\delta \sim \frac{u^*}{R_o^{1/2}\omega}$$

so that the magnetic boundary layer is thicker than the non-magnetic one. Thus since the boundary layer depth is large in comparison to the eccentricity, the case of a hydromagnetic turbulent earth would seem to belong in the upper branch of the instability curve.

We may expect further and more precise results in the future, as the experimental program is continued and the hydrodynamic-hydromagnetic analogy is improved and extended.

REFERENCES

Malkus, W.V.R. 1963 J.Geophys.Res. 68: 2871

Roberts, P. H. and K. Stewartson 1965 Proc.Camb.Phil.Soc. 61: 279

Stewartson, K. and P. H. Roberts 1963 J.Fluid Mech., 17: 1-20

These notes submitted by

Alexandre Chorin and
Richard Somerville

Geomagnetic Secular Variation (GSV)

Raymond Hide

Geomagnetical observations can be carried out for the earth only at its surface, and have been carried out only during the last few centuries. Moreover, they have been carried out only at widely scattered and badly distributed stations. Many crucial quantities are therefore unknown: e.g., the strength of the toroidal field and the conductivity of the mantle.

Today the central problem of explaining geomagnetic phenomena has been narrowed down to the study of the magnetohydrodynamics of the core. Other explanations (such as permanent magnetism) fail quantitatively by many orders of magnitude.

What other celestial bodies have magnetism? The sun is one. Sunspots are magnetic anomalies, and high resolution magnetograms (magnetic maps) of the sun are presently available. The magnetic field of the sun can be studied through the Zeeman effect.

As to the planets, probes to Moon, Mars and Venus found no magnetic field. Jupiter is known to have a magnetic field (of approximately 50 gauss), as can be inferred for example, from the study of its radio emission, which can be explained on the basis of an interaction between a magnetic field and an analogue of the Van Allen belt. It is reasonable to believe that Jupiter's field originates in its "atmosphere and oceans." This is possible because the magnetic Reynolds number of Jupiter's "oceans" is conceivably much larger than that of the earth's oceans, because Jupiter

is bigger and its motions are swifter. Saturn may also have a magnetic field, but this is not certain.

The idea of a dynamo as a source of a magnetic field was first applied to the sun's field. In general, for a celestial body to have a magnetic field, it must have a fluid region (not necessarily a core), motions swift enough, and conductivity large enough for the magnetic Reynolds number R_M to be large enough.

The earth's field is measured as $B(t,\theta,\lambda,r)$ where t is the time, θ the longitude, λ the latitude, and r the radius (some measurements of the variations of B with r can be made by going into mines).

The table shows the spectrum of geomagnetic phenomena.
There is evidence to the effect that:

the rotation of the earth plays a role in the dynamics of the geomagnetic field;

the amplitude of the main dipole slowly decreases;

the earth's field drifts westward (secular variation) at the rate of approximately 0.2 degrees latitude/year ($\sim$ 0.2 mm/sec).

Paleomagnetic evidence shows that the earth's field reverses itself. There is also some paleomagnetic evidence to the effect that it changes its amplitude. There is also observational evidence of the existence of strong toroidal fields in the core.

The analysis of measurements of the field in spherical harmonics dates to Gauss (c. 1835). The best reference is the book by Chapman and Bartels. The field is mainly a dipole, and decreasing in time (at the present rate of decrease, the field will disappear in about 2000 years). The posi-

tion of the pole is nearly constant.

Spectrum of Geomagnetic Phenomena

PERIOD		ORIGIN	COMMENTS
Seconds	Years		
10^{17}	3.10^{9}	?	?
10^{16}			
10^{15}	3.10^{7}	INTERNAL AND DIPOLAR	DIPOLE REVERSALS
10^{14}			
10^{13}			
10^{12}			
10^{11}			
10^{10}	300	INTERNAL, NON=DIPOLAR	SECULAR VARIATION
10^{9}	30		
10^{8}			
10^{7}			
10^{6}	3.10^{-2}	EXTERNAL	MAGNETIC STORMS
10^{5}	3.10^{-3}	EXTERNAL	DIURNAL VARIATION
10^{4}			
10^{3}			
10^{2}			
10^{1}		EXTERNAL	MICROPULSATIONS
10^{0}			
10^{-1}		EXTERNAL	SUB-ACOUSTIC

The change in the earth's rotation rate is an unexplained

phenomenon. One approach is to seek a mechanism for momentum transfer between core and mantle. There are many other interesting geomagnetic phenomena; for example, a correlation between the longitude of the moon and the horizontal magnetic field at Capetown. There is much uncertainty in all observations, and many assertions have to be taken with a grain of salt.

The existence of the core was discovered by seismologists, through the fact that the core, which is fluid, can transmit only compression waves. The source of core motions is uncertain. Two possibilities are thermal convection and precessional torques.

The equations describing the magnetohydrodynamics of the core are

$$\frac{\partial \underline{B}}{\partial t} = \eta \nabla^2 \underline{B} + \nabla \times (\underline{u} \times \underline{B}), \quad \eta \sim 1 \ m^2/sec$$

$$\nabla \cdot \underline{u} = 0$$

$$\nabla \cdot \underline{B} = 0$$

$$\frac{\partial \underline{u}}{\partial t} = -(\underline{u} \cdot \nabla)\underline{u} + 2\underline{\Omega} \times \underline{u} = -\frac{1}{\rho}\nabla p + \nu \Delta \underline{u} + (\nabla \times B) \times B + g\rho'/\rho$$

and the appropriate boundary conditions.

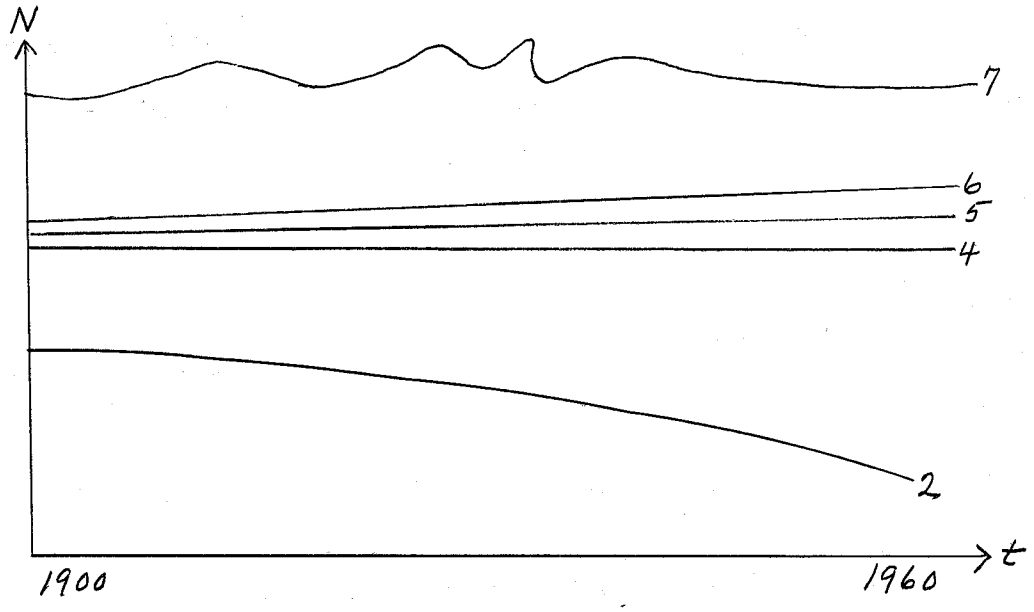

It is important to be able to extrapolate the field at the surface of the earth to the core boundary. The preceding graph is due to Cain and Hide.

Here N is the total number of lines of force emerging from the core, without regard to sign. The curves are labeled with the order of the highest-order spherical harmonic retained in the analysis, and the schematic graph is interpreted as follows:

The lowest curve (2) shows the decreasing dipole field, and the highest (7) shows the unreliable nature of the high-harmonic data. But for the intermediate curves (4, 5, 6), Cain and Hide were able to obtain N's which were approximately constant in time.

Other phenomena have yet to be explained. The westward drift may be a consequence of dynamo action, or it may be a manifestation of magnetohydrodynamic waves. The speed of Alfvén waves in the core, $V_A = \frac{B_T}{\sqrt{\mu\rho}}$ is about 10 cm/sec; however, the effects of rotation, while speeding half these waves, slow the other half to approximately the speed of the secular variation (see Hide, 1966).

References

General:

Bullard, E. C., 1964 Proc.Roy.Soc.London (Bakerian lecture on reversals)

Hide, R., 1967 Planetary and Space Sciences, 14: 579

Hide, R., 1967 Science, 157: 55

Hide, R. and P. H. Roberts, 1961 Phys.Chem.Earth, 4: 25

Irving, E. 1964 "Paleomagnetism", Publ: Wiley

Hindmarsh, Lowes, Roberts, Runcord (Editors), 1967. "Magnetism and the Cosmos", Publ: Oliver and Boyd

Jacobs, J. A., 1963 "Earth's Core and Geomagnetism", Publ: Pergamon

Munk, W. H. and G. McDonald 1960 "Rotation of the Earth", Publ: Cambridge Univ. Press

Rikitake, T., 1966 Electromagnetism and Earth's Interior, Report of Pittsburgh Conference in J.Geomag.Ceoelect.

Marsdent and Cameron, 1966 The Earth Moon System, Plenum, New York

Analysis of GSV (Recent references)

Vestine and Collaborators (Rand). See also

Vestine and Kahle, 1966 J.Geophys.Res. 71: 527

Roberts and Scott, 1966 J.Geomag.Ceoelect., 17: 137

Cain, J. C. and R. Hide, 1967 (to appear)

Theory of GSV

Allan and Bullard, 1967 Proc.Camb.Phil.Soc., 62: 783

Hide, R. 1966 Phil.Trans.Roy.Soc., A, 259: 615

Hide, R. and P. H. Roberts, 1962 Adv.Appl.Mech., 7: 215

Malkus, W. V.R. 1967 J.Fluid Mech. 28: July

Roberts, P. H., 1967 Introduction to Magnetohydrodynamics (Longman)

Stewartson, K., 1967 Proc.Roy.Soc. A (just out)

These notes submitted by

Alexandre Chorin and
Richard Somerville

Bounds on the Transport of Mass and Momentum in Turbulent Shear Flow

Friedrich Busse

ABSTRACT

In all cases, where fluid flow of a stationary turbulent nature occurs, it can be considered as the mechanism by which physical quantities are transported due to a given force. A basic question is the relation between the transported quantity and the applied force. Since it cannot be expected that an analytical theory can give this relation, it is of importance to obtain exact upper and lower bounds on this relation. Such bounds can be obtained by variational methods in analogy to those developed by L. N. Howard (1963, J.Fluid Mech., 17: 405) in the case of turbulent convective heat transport in a layer heated from below.

For the discussion of the problem we assume the geometry of a fluid contained between two rigid parallel plates with distance d. We base the mathematical description on the dimensionless Navier-Stokes equations of motion using d as length scale and $\frac{d^2}{\nu}$ as scale for the time. Making the assumption that the turbulent flow is statistically stationary we obtain time independent quantities by averaging over planes parallel to the plates, which will be indicated by a bar. The average velocity V is determined by the equation

$$\partial_z \underset{\sim}{V} = \overline{\underset{\sim}{u}w} - \langle \underset{\sim}{u}\omega \rangle - PF(z)\underset{\sim}{i} \qquad (1)$$

We have introduced a cartesian system of coordinates with the z-direction perpendicular to the plates. $\underset{\sim}{u}$ is the component parallel to plates of the fluctuating part $\underset{\sim}{v}$ of the velocity field and w is the z-component. The average over the entire fluid layer is indicated by the angular brackets.

In the case when the plates are resting and a pressure gradient P in the direction of the unit vector $\underset{\sim}{i}$ parallel to the plates is given, $F(z)$ is equal to z. Since plane Poiseulle flow is the laminar solution of this problem, we call it the Poiseulle case. Correspondingly we define the Couette case, in which the plates are moving with the velocities $\mp P\underset{\sim}{i}$ and $F(z)$ is equal to one.

Using (1) an integral relation including only the fluctuating part $\underset{\sim}{v}$ of the velocity field can be obtained.

$$\langle |\nabla \underset{\sim}{v}|^2 \rangle + \langle |\overline{w}\underset{\sim}{u} - \langle \underset{\sim}{u} w \rangle|^2 \rangle - P\langle F(z)\underset{\sim}{i}\cdot\underset{\sim}{u}\, w\rangle = 0 \qquad (2)$$

From (1) and (2) the energy balance can be derived,

$$\langle |\nabla \underset{\sim}{v}|^2 \rangle + \langle |\partial_z \underset{\sim}{v}|^2 \rangle = P^2\langle F(z)\rangle \pm \langle F(z)\underset{\sim}{i}\cdot\underset{\sim}{u}\, w\rangle P, \qquad (3)$$

where the + sign refers to the Couette case, the - sign to the Poiseulle case. Using the equation for the mass flux in the Poiseulle case

$$\langle \underset{\sim}{v}\cdot\underset{\sim}{i}\rangle = -\langle \partial_z \underset{\sim}{v}\cdot\underset{\sim}{i}\cdot F(z)\rangle = P\langle F^2(z)\rangle - \langle F(z)\underset{\sim}{i}\cdot\underset{\sim}{u}\, w\rangle$$

we conclude that for given P the massflux has its maximum for the laminar solution $\underset{\sim}{v}\equiv 0$. The minimum of the massflux is determined by the maximum of $\langle F(z)\underset{\sim}{i}\cdot\underset{\sim}{u}\, w\rangle$ since this is a positive definite quantity according to (2). In the Couette case the same quantity determines the maximum momentum transport at a given rate P of shear, while the laminar solution provides the lower limit.

In order to obtain an upper bound for $\langle F(z)\underset{\sim}{i}\cdot\underset{\sim}{u}\, w\rangle$ at a given P we ask for the maximum μ of this quantity among all vector fields $\underset{\sim}{v}$ that satisfy condition (2). This extremum problem is equivalent to the following problem without side condition.

Given $\mu > 0$, find the minimum value $P(\mu)$ of the functional

$$R(\mu, \underset{\sim}{v}) = \frac{\langle |\nabla \underset{\sim}{v}|^2 \rangle}{\langle F(z)\, \underset{\sim}{u} \cdot \underset{\sim}{i}\, w \rangle} + \mu \frac{\langle |\overline{\underset{\sim}{u} w} - \langle \underset{\sim}{u} w \rangle|^2 \rangle}{\langle F(z)\, \underset{\sim}{u} \cdot \underset{\sim}{i}\, w \rangle^2} \qquad (4)$$

among all fields $\underset{\sim}{v}$, that vanish at $z = \pm \frac{1}{2}$ and have $\langle \underset{\sim}{u} w \cdot \underset{\sim}{i}\, F(z) \rangle > 0$.

An absolute minimum for $P(\mu)$ is given by the minimum P_0 of the first term on the right side of (4). No fluctuating fields $\underset{\sim}{v}$ are possible for values of P less than P_0 . This corresponds to results obtained by Orr (1907, Proc.Roy.Irish Acad. (A) 27: 69) and more recently by Serrin (1959, Arch.Rat.Mech.Anal. 3: 1), who were interested in lower bands for the Reynolds number, below of which the laminar solution is stable.

The extremum $P(\mu)$ of the functional (4) is of particular interest in the limit $\mu \to \infty$. In this limit the analysis yields

$$P(\mu) = \frac{4}{3}(8\mu)^{1/2} \quad \text{in the Couette case,}$$
$$P(\mu) = 12\mu + 8(8\mu)^{1/2} \quad \text{in the Poiseulle case.} \qquad (5)$$

Since μ provides an upper bound for $\langle F(z)\, \underset{\sim}{i} \cdot \underset{\sim}{u}\, w \rangle$ the physical interpretation of these results is on hand. In the literature of turbulent shear flow a drag coefficient λ has been introduced to describe the relation between the dimensionless pressure gradient and the Reynolds number. According to (5) λ is upper bounded by a constant in both cases. The numerical value of this constant is higher than the experimental data by one order of magnitude.

In his paper on turbulent convective heat transport, Howard has improved the upper bound by imposing the continuity equation as additional constraint. In this case the extremum problem leads to Euler-Lagrange

equations, which admit solutions with wavelike dependence in the directions parallel to the plates. Howard uses in his analysis solutions with a single wavenumber. It can be shown, however, that for large values of μ, the upper bound is described by solutions with more than one wavenumber. As a result of his analysis Howard is able to show that the experimentally observed heat transport comes relatively close to the upper bound. In addition the solution of the Euler-Lagrange equation resembles many properties of the observed flow. This leads to the expectation that by improving the techniques for obtaining upper bounds a detailed picture of the physical processes in turbulent flow can be approached. A realization of this expectation would suggest that turbulent flow is the optimal mechanism allowed by the Navier-Stokes equations for any transport process involving fluid flow at high Reynolds numbers.

Large-amplitude Bénard Convection in a Rotating Fluid

George Veronis

ABSTRACT

Linear stability theory of Bénard convection in a rotating fluid (Chandrasekhar, 1961) has shown that fluids with large $(>>1)$ Prandtl number, σ, exhibit behavior markedly different from that of fluids with $\sigma << 1$. This difference in behavior extends also into the finite amplitude range (Veronis, 1959, 1966). Here I will report on a numerical study of two-dimensional Bénard convection in a rotating fluid confined between free

boundaries, with σ = 6.8 and σ = .2 for the range of Taylor number $0 \leq T^2 \leq 10^5$ and for Rayleigh numbers, R , extending an order of magnitude from the critical value of linear stability theory. The behavior of water (σ = 6.8) is dominated by the rotational constraint even for relatively moderate values ($\sim 10^3$) of T^2 . A study of the resultant velocity and temperature fields shows how rotation controls the system, with the principal behavior reflected by the thermal wind balance, i.e., the horizontal temperature gradient is largely balanced by the vertical shear of the velocity component normal to the temperature gradient. A fluid with a small Prandtl number (σ = .2) becomes unstable to finite amplitude disturbances at values of the Rayleigh number significantly below the critical value of linear stability theory. The subsequent steady velocity and temperature fields exhibit a structure which is quite different from that of fluids with large σ . The rotational constraint is balanced primarily by non-linear processes in a limited range of Taylor number ($T^2 \leq 10^{3.6}$). For larger values of T^2 the system first becomes unstable to infinitesimal oscillatory disturbances but a steady, finite amplitude flow is established at supercritical values of R which are nonetheless smaller than the values that one would expect from linear theory. The ranges of Taylor number in which the above phenomena occur are different from those which were estimated on the basis of an earlier study (Veronis, 1966) which made use of a minimal representation of the finite amplitude velocity and temperature fields. No subcritical, finite-amplitude oscillatory motions were found in the present study. Comparison with some of the experimental features observed and reported by Rossby (1966) is also

discussed and it is pointed out that some of the differences between theory and experiment may be traced to the restrictive conditions (two-dimensionality and free boundaries) of the present study.

References

Chandrasekhar, S. 1961 Hydrodynamic and Hydromagnetic Stability, Oxford: Clarendon Press

Rossby, H. T. 1966 An experimental study of Benard convection with and without rotation. Ph.D. Thesis, M.I.T.

Veronis, G. 1959 J.Fluid Mech. 5: 401

Veronis, G. 1966 I J.Fluid Mech. 24: 545

Veronis, G. 1966 II J.Fluid Mech. 26: 49

Marginal Convection in a Uniform Rotating Fluid Sphere Containing Heat Sources

Paul H. Roberts

ABSTRACT

The problem of marginal convection in a stationary fluid sphere containing heat sources has been considered by Chandrasekhar (1956a, b), Bisshopp (1958), Roberts (1965a), and Bisshopp and Niiler (1965). Some of this material is conveniently drawn together in Chandrasekhar's treatise on stability (1961). Other relevant studies have been made by Namikawa (1957), Roberts (1960), and Chamalaun and Roberts (1962). The precise definition of the problem, and the derivation of the governing equations and boundary conditions, are given by Chandrasekhar, and we give here only a brief summary.

Consider a homogeneous fluid sphere of radius r_0 rotating with uniform angular velocity $\Omega \underline{1}_z$ about the z-axis. ($\underline{1}_s$ is used to denote a unit vector in the s-direction.) Neglect all external forces on the sphere and ignore any flattening which the rotation engenders*. Assume that there is a uniform distribution of heat sources in the fluid which, in the absence of conduction, would cause the temperature of every element to rise at the rate ϵ. Imagine, however, that conduction carries the heat away to the surface, which is maintained at a constant temperature, T_0. We wish to examine the stability of this steady state with respect to convective perturbations, buoyancy forces being provided by the force of self-gravitation of the whole mass of fluid.

In the absence of convection, the temperature distribution in the sphere is

$$\Theta_0(\underline{r}) = T_0 + \frac{1}{2r_0}\beta(r_0^2 - r^2), \quad \beta = \frac{r_0 \epsilon}{3\kappa}, \tag{1}$$

where κ is the thermal diffuxivity, $\underline{r}$ is the radius vector drawn from the centre of the sphere, $r = |\underline{r}|$, and β is the temperature gradient at the surface of the sphere. We measure length in units of r_0, time in units of r_0^2/ν, and temperature fluctuations Θ in units of $\beta \nu r_0/\kappa$, where ν is the kinematic viscosity of the fluid. The perturbation equations governing, $\underline{u}$, the fluid velocity, ϖ, the perturbation of pressure (scaled), and Θ depends then on three dimensionless parameters: the Prandtl number, p; the Taylor number, T, and the Rayleigh number, R:

---

*We will presently adopt the Boussinesq approximation $g \to \infty$, $\alpha \to 0$, $g\alpha \to$ finite limit. In the same limit, $\Omega^2 r_0/g \to 0$, so that centrifugal will not distort the spherical shape of the body.

$$p = \frac{\nu}{\kappa}, \quad T = \left(\frac{2\Omega r_o^2}{\nu}\right)^2 \equiv \lambda^2, \quad R = \frac{g\alpha\beta}{\nu\kappa} r_o^4 , \tag{2}$$

where α is the coefficient of volume expansion, and $-g\underline{r}/r_o$ is the acceleration due to gravity at $\underline{r}$. The perturbation equations are, in the Boussinesq approximation,

$$\frac{\partial \underline{u}}{\partial t} + \lambda \underline{1}_z \times \underline{u} = -\underline{\nabla}\varpi + R\Theta\underline{r} + \nabla^2\underline{u}, \tag{3}$$

$$p\frac{\partial \Theta}{\partial t} = \underline{r}\cdot\underline{u} + \nabla^2\Theta , \tag{4}$$

$$\underline{\nabla}\cdot\underline{u} = 0. \tag{5}$$

It is easily shown that the solutions to (3-5) separate in ϕ, where (r,ϕ,z) are cylindrical polar coordinates; i.e., we can seek normal mode solutions of the form

$$\underline{u}(r,\phi,z,t) = \underline{u}(r,z)e^{st+im\phi} , \tag{6}$$

where m (= integer) and s are constants. (The tilde is henceforward omitted.) We shall be particularly interested in the asymmetric $(m \neq 0)$ modes, since one can give some rather general reasons why they may be expected to occur before (i.e., at lower R) than the symmetric $(m = 0)$ modes, provided T is sufficiently great:

One of the most striking features of convection in a self-gravitating sphere is that, depending on position, $\underline{\Omega}$ and $\underline{g}$ may lie at any angle to one another. In some respects then, the convection that occurs will be a compromise between convection in a Bénard layer rotated about a vertical axis, and Bénard convection in a layer rotated about a horizontal axis. Let us consider these two extremes separately.

Convection in a Bénard layer in which $\underline{g}$ and $\underline{\Omega}$ are parallel is governed by (4-5) and by

$$\frac{\partial \underline{u}}{\partial t} + \lambda \underline{1}_z \times \underline{u} = -\underline{\nabla}\varpi + R\Theta\underline{1}_z + \nabla^2\underline{u} . \tag{3.//}$$

The definitions of R and T are appropriately modified, and $z = 0, 1$ mark the horizontal boundaries of the fluid. As Chandrasekhar (1961) has shown, steady convection is governed, according to (3-5.//) by

$$\left(\nabla^6 + T\frac{\partial^2}{\partial z^2}\right) u_z = R\left(\frac{\partial^2}{\partial x^2} + \frac{\partial^2}{\partial y}\right) u_z . \qquad (7.//)$$

The problem is separable in x and y, and if we seek Fourier harmonic solutions of the form

$$u_z = W(z)\exp\left[i(\ell x + my)\right], \quad (\ell^2 + m^2 = a^2), \qquad (6.//)$$

we obtain

$$\left(\frac{\partial^2}{\partial z^2} - a^2\right)^3 W + T\frac{d^2W}{dz^2} = -Ra^2 W. \qquad (8.//)$$

Suppose

$$a = AT^{\alpha}, \text{ as } T \longrightarrow \infty , \qquad (9.//)$$

where A and α are constants. There are three main possibilities:

(a) $\alpha < 1/6$. In the interior flow $[d/dz = O(1)]$ far from the containing walls, (8.//) becomes

$$D^2 W + \frac{Ra^2}{T} W = 0. \qquad (10a)$$

The solution satisfying $W = 0$ on $z = 0, 1$ and having the smallest Rayleigh number is

$$W \propto \sin \pi z , \qquad (11)$$

giving $Ra^2/T = \pi^2$, i.e.

$$R = \frac{\pi^2 T}{a^2} \qquad (12a)$$

Minimization of R over a gives $a \to \infty$, showing that the value of a assumed is "too small". Suppose instead, then, that (b) $\alpha > 1/6$. Now (8.//) simply gives

$$-a^6 W = -Ra^2 W, \qquad (10b)$$

giving

$$R = a^4. \qquad (12b)$$

This shows that, for these very small-scale motions, rotation has no effect. Minimization of R gives $a \to 0$, showing that the a assumed was "too large". We are left with an a that is "just right":

(c) $\alpha = 1/6$. Now (8.//) gives

$$D^2 W + \frac{a^2}{T}\left(R - a^4\right) W = 0. \tag{10c}$$

Again (11) gives the smallest Rayleigh number, and (12a,b) are replaced by their sum

$$R = a^4 + \frac{\pi^2 T}{a^2} \tag{12a}$$

This does have a minimum, viz. $a = a_c, R = R_c$, where

$$a_c = \left(\frac{1}{2}\pi^2 T\right)^{1/6}, \qquad R_c = 3\left(\frac{1}{2}\pi^2 T\right)^{2/3}. \tag{13}$$

We may note, in passing, that the first correction term to R in (13) for rigid boundaries is only a factor of $T^{-1/12}$ smaller. [For free boundaries, it is $O\left(T^{-1/3}\right)$]. Thus $T = 10^6$ should not be thought of as a large Taylor number! The present derivation of the celebrated "two-thirds law" (13) illustrates a technique useful for the sphere problem, since we may expect that convection cells in the sphere in which $\underline{g}$ and $\underline{\Omega}$ are approximately parallel will be governed by a similar law.

Consider next the second extreme: a Bénard layer in which $g = g\underline{1}_z$ and $\Omega = \Omega \underline{1}_x$ are perpendicular. It is easily shown that the governing equations are (4-5) and

$$\frac{\partial \underline{u}}{\partial t} + \lambda \underline{1}_x \times \underline{u} = -\underline{\nabla} \varpi + R\Theta \underline{1}_z + \nabla^2 \underline{u}. \tag{3.⊥}$$

In place of (7.//), this gives

$$\left(\nabla^6 + T\frac{\partial^2}{\partial x^2}\right) u_z = R\left(\frac{\partial^2}{\partial x^2} + \frac{\partial^2}{\partial y^2}\right) u_z. \tag{7.⊥}$$

Again the problem is separable in x and y, and seeking solutions of the form

$$w_z = W(z)\exp[i(\ell x + my)], \tag{6.⊥}$$

we obtain

$$\left(\frac{d^2}{dz^2} - \ell^2 - m^2\right)^3 W - T\ell^2 W = -R(\ell^2 + m^2)W. \tag{8.⊥}$$

We now see that, if $\ell = 0$, i.e. if convection occurs in rolls parallel to $\underline{\Omega}$, (8.⊥) reduces to $(a = m)$

$$\left(\frac{d^2}{dz^2} - a^2\right)^3 W = -Ra^2 W, \tag{14.⊥}$$

which is <u>exactly</u> the equation which governs convection in the absence of rotation. Taking this fact over to the spherical case, we might surmise that modes of convection might exist in which m is large, and in which variations in z are comparatively small or absent, and in which R is about the same as in the non-rotating case for the same value of m. It is true that, $R \sim m^4$ for large m [see (22i and ii) below], so that the motions will certainly have a higher critical Rayleigh number than (13) unless $m \leq O(T^{1/6})$, but one might feel that, provided this inequality is obeyed, these motions will yield the smallest critical Rayleigh numbers. One must be cautious, however, since curvature effects will prevent the formation of infinitely long rolls parallel to $\underline{\Omega}$, and once they are "cut-off to fit into the sphere" $(\ell \neq 0)$, the critical R may be increased drastically.

Armed with these qualitative arguments, we may now tackle the spherical problem supposing (6), where

$$m = MT^{\alpha}, \quad \text{as } T \longrightarrow \infty, \tag{9}$$

and M and α are constants. There are six main cases:

(i) $\alpha > 1/4$, (ii) $\alpha = 1/4$, (iii) $1/4 > \alpha > 1/6$, (iv) $\alpha = 1/6$, (v) $1/6 > \alpha \geq 0$, and (vi) $\alpha = M = 0$. We consider these successively:

(i) Here rotation is a small perturbation on conductive and viscous effects. The governing equations become that for a non-rotating sphere (c.f. e.g. Roberts, 1965b). If $S = r u_r$ we can seek solutions $S \propto P_\ell^m(\cos\theta) e^{im\phi}$, giving

$$\left[\frac{d^2}{dr^2} + \frac{2}{r}\frac{d}{dr} - \frac{\ell(\ell+1)}{r^2}\right] S = -\ell(\ell+1) R S. \tag{14i}$$

Here P_ℓ^m denotes the associated Legendre polynomial for which $\ell \geq m$; in fact, let us take $\ell = m$. The solution to (14i) vanishes except in a boundary layer near the surface. Write

$$r = 1 - \epsilon \zeta, \tag{15i}$$

where ϵ, the boundary layer thickness, vanishes as $m \to \infty$, and $d/d\zeta = O(1)$. We obtain from (14i)

$$\frac{3m^4}{\epsilon^2}\frac{d^2 S}{d\zeta^2} - m^6(1 + 6\epsilon\zeta) S = -m^2 R S, \tag{16i}$$

i.e.

$$\frac{d^2 S}{d\zeta^2} = 2\epsilon^3 m^2 (\zeta - \zeta_s) S, \tag{17i}$$

where

$$\zeta_s = \frac{1}{6\epsilon m^4}\left(R - m^4\right). \tag{18i}$$

Equation (17i) shows that

$$\epsilon = \frac{1}{(2m^2)^{1/3}}. \tag{19}$$

The solution to (17i) vanishing with distance into the sphere $(\zeta \to +\infty)$ is

$$S \propto Ai(\zeta - \zeta_s). \tag{20i}$$

where Ai denotes the Airy function. Since $S = 0$ on $\zeta = 0$, we must have

$$Ai(-\zeta_s) = 0. \tag{21i}$$

The smallest root ($J_s = 2.338$) of this equation gives the smallest R in the range (i), viz:

$$R_c = m^4 + 11.1345\, m^{1\frac{2}{3}} \qquad (22i)$$

(ii) This case is a compromise between (i) and (ii) and is not very easy or very interesting!

(iii) In this case, the governing equation for S turns out to be remarkably similar to (7.1)

$$\left(\nabla^6 + T\frac{\partial^2}{\partial z^2}\right) S = -R L^2 S, \qquad (14iii)$$

where

$$L^2 = x_i \frac{\partial}{\partial x_i} + \left(x_i \frac{\partial}{\partial x_i}\right)^2 - \nabla_1^2$$

The change of variable

$$\rho' = 1 - \rho\left(1 + \tfrac{1}{2} z^2\right), \qquad \rho = \sqrt{(x^2 + y^2)},$$

turns the neighbourhood of the equator into $\rho' = 0$. Also (14iii) becomes

$$\left[-m^6\left(1 + 3z^2 + 6\rho' - \frac{3}{m^2}\frac{\partial^2}{\partial \rho'^2}\right) + T\frac{\partial^2}{\partial z^2} + R m^2 (1 + z^2)\right] S = 0. \qquad (16iii)$$

The solutions separate in the form

$$S = Y(\zeta) Z(\tau) \qquad (20iii)$$

where ζ and τ are scaled variables

$$\zeta = \rho'(2m^2)^{1/3}, \qquad \tau = \left(\frac{8m^6}{T}\right)^{1/4} z,$$

and we obtain

$$\frac{d^2 Z}{d\tau^2} + \left(\gamma + \tfrac{1}{2} - \tfrac{1}{4}\tau^2\right) Z = 0. \qquad (17iii)$$

This is Weber's equation. The separation constant, γ, must be a positive integer, n, or zero. Also Y obeys (17i), (20i) and (21i), provided (18i) is replaced by

$$\mathcal{Z}_s = \frac{1}{6\epsilon m^6}\left[R - m^4 - \frac{(2n+1)}{(2m^2)^{1/2}}T^{1/2}\right]. \qquad (18ii)$$

The smallest root of (21i), and $n=0$, gives the smallest R for this range:

$$R_c = m^4 + 11.1345\, m^{4/3} + 1.4142\, m T^{1/2} \qquad (22ii)$$

The solution (20iii) is in the form of a necklace round the equator.

(vi) In this case, studied independently by Roberts (1965a) and Bisshopp and Niiler (1965), convection occurs in an axial cell of thickness $T^{1/6}$, in which

$$w_z = F(z) J_0(\xi\rho), \qquad (23vi)$$

and F obeys

$$\frac{d^2F}{dz^2} = \left(\frac{\xi^6}{T} - \frac{R\xi^2}{T} z^2\right)F. \qquad (24)$$

The critical value of ξ is $1.108T^{1/6}$, giving

$$R_c = 20.7126\, T^{2/3}, \qquad (22vi)$$

(cf. 13). It is seen, from (23vi), that the thickness of the cell in the ρ-direction is $O(T^{-1/6})$. This case, like cases (iii) to (v), is rotation dominated. There is also the possibility of overstability (cf. Roberts, 1965a).

(v) This case is a small perturbation of case (vi). It may be shown that (22vi) is replaced by

$$R_c = 20.7126\, T^{2/3} - \Lambda m^2 T^{1/3}, \qquad (22v)$$

where $\Lambda = \Lambda(p)$ is always positive.

(iv) This is the crucial case, as (22v and vi) already indicate.

For minimization of R_c over m gives $m = 0$ in case (22vi), and $m = \infty$ in case (22v), clearly indicating that the required minimum lies between them, i.e. in case (iv). Such indeed is the case. It may be shown that

$$u_z = F(z) Ai\left(\frac{\rho \rho_c}{(2m^2)^{1/3}}\right), \qquad (22iv)$$

where F satisfies an equation of the same general structure as (24) but with different (complex) coefficients. For given p and M (cf. 9), we minimize over all ρ_c to obtain $R_c(M)$. We may then minimize over M for fixed p. The following results are obtained:

p	$M = \frac{m}{T^{1/6}}$	θ	$\frac{R}{T^{2/3}}$
0.025	0.202	34.5	0.2018
0.1	0.318	33.8	1.22
0.3	0.374	33.6	2.88
1.0	0.531	32.3	14.13
3.0	0.664	33.1	18.31
10	0.716	34.2	18.88
40	0.729	34.4	19.01

The solution (21iv) vanishes outside a cylinder of radius ρ_c, and $\theta = \sin^{-1}\rho_c$, in the table above, gives the colatitude in degrees of the intersection of the cylinder with the surface of the sphere. It may be observed that θ is almost independent of p. It is interesting to observe that the critical Rayleigh numbers, shown above, seem to be always (for $p < 1$) less than the corresponding critical Rayleigh numbers for overstable solutions for which (Roberts, 1965a), we have

p	$R/T^{2/3}$
0.025	0.3766903
0.1	2.242779
0.2	5.267309
0.4	11.90700
0.5	15.34496
0.65	20.56526

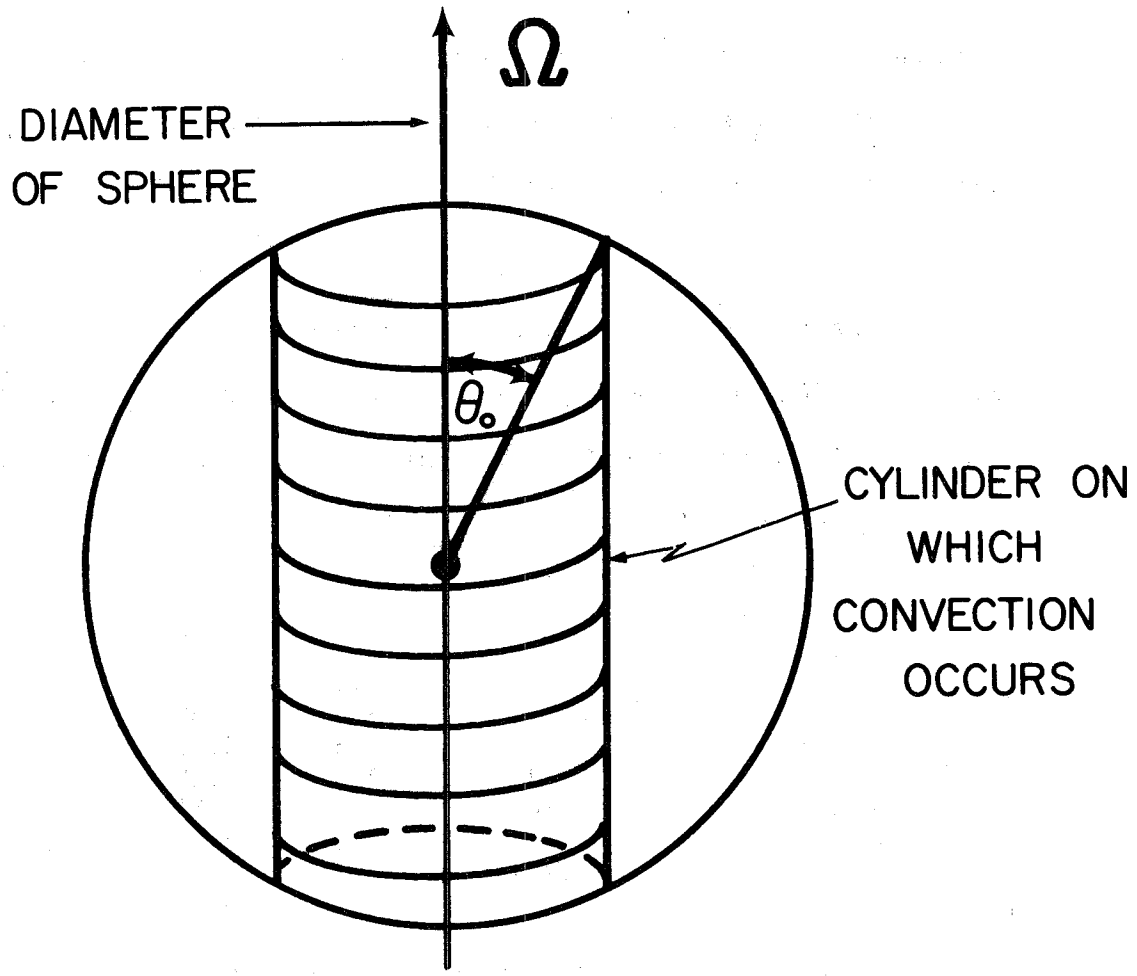

Marginal convection in a rotating sphere.

We have attempted to confirm the validity of the general features described above in two ways both stemming from a series expansion of the solution of (3-5) about $T = 0$:

(A) We have demonstrated, fairly conclusively, that the theory, in the axisymmetric case (vi) above, is approached by the series expansion solution as T increases.

(B) We have verified for particular values of p the general proposition that, apart from small T, the smallest critical Rayleigh

number belongs to an asymmetric mode.

The general feature that is exhibited by the solution we have obtained is that, at moderate and large rotation rates, the most easily excited convective modes are asymmetric with respect to the axis of rotation. This may be of some relevance to the theory of the geodynamo. It is known that homogeneous dynamos cannot be axisymmetric (see lecture 2A in the dynamo series in these volumes). Moreover, it is interesting to note that the types of flow predicted by the present theory do not have a zero regenerative term Γ on the Braginskiĭ theory (see lecture 4 of the dynamo series).

REFERENCES

Bisshopp, F. E. 1958 Phil.Mag., 3(3): 1342

Bisshopp, F. E. and P. P. Niiler 1964 J.Fluid Mech. 23: 459

Chamalaun, T. and P. H. Roberts 1962 Continental Drift. chap.vii (New York: Academic Press)

Chandrasekhar, S. 1957 Phil.Mag., 2: 845 and 1282

Chandrasekhar, S. 1961 Hydrodynamic and Hydromagnetic Stability. (Oxford: Clarendon Press)

Namikawa, T. 1957 J.Geomag. and Geoelec., 9: 182

Roberts, P. H. 1965a Astrophys.J. 141: 240

Roberts, P. H. 1965b Mathematika, 12: 128

Motions of the Earth's Core and Mantle, and Variations of the Main Geomagnetic Field

Raymond Hide

ABSTRACT

A recent theoretical study (1) of free hydromagnetic oscillations of a thick rotating spherical shell of an incompressible fluid pervaded by a strong toroidal and weak poloidal magnetic field suggests that if the average strength of the toroidal magnetic field in the Earth's liquid core is 10^{-2} weber/m^2 (10^2 oersted) then the hypothesis that the geomagnetic secular variation (G.S.V.) is mainly a manifestation of the interaction of free hydromagnetic oscillations of the core with the Earth's poloidal magnetic field is consistent with present knowledge of the G.S.V. and of the physical conditions prevailing in the Earth's deep interior.

The "free-oscillations" theory of the G.S.V. (in contradistinction to other theories) embodies the assumption that the total number of lines of magnetic force emerging from the surface of the core does not change significantly on the time-scale of the G.S.V. This assumption gains support from a recent analysis of the field at the core surface (2).

Associated with the magnetic modes of free hydromagnetic oscillations of the Earth's core, periods of the order of decades to centuries, are very rapid inertial modes, periods of the order of days (1). Concomitant variations in the poloidal magnetic field due to these inertial modes would fail to penetrate the weakly conducting mantle, but the eddy currents induced in the lower mantle by these modes might increase the mechanical coupling between core and mantle.

Theory also indicates (a) that horizontal variations in the properties of the core-mantle interface that would escape detection by modern seismological methods might nevertheless produce measurable geomagnetic effects; (b) that the rate of drift, relative to the Earth's surface, of nonaxisymmetric features of the main geomagnetic field might be much faster than the average zonal speed of hydrodynamic motion of core material relative to the surrounding mantle; and (c) why magnetic astronomical bodies usually rotate. Among the consequences of (a) and (b) are the possibilities that (i) the shortest interval of time that can be resolved in paleomagnetic studies of the geocentric axial dipole component of the Earth's magnetic field might be very much longer than the value often assumed by many paleomagnetic workers, (ii) reversals in sign of the geomagnetic dipole might be expected to show some degree of correlation with processes due to motions in the mantle (for example, tectonic activity, polar wandering), and (iii) variations in the length of the day that have hitherto been tentatively attributed to core motions may be due to some other cause.

References

(1) Hide, R., 1966 Phil.Trans.Roy.Soc. A 259: 615

(2) Cain, J. C. and R. Hide, 1967 (in preparation)

(3) Hide, R., 1967 Science, 157: 55

Internal Constitution of the Earth

Sydney Clark

ABSTRACT

The lectures were intended as general background type. The first, on the constitution of the earth presented the evidence that the mantle is inhomogeneous, the location of the inhomogeneity, and the chemical and mineralogical constitution of the mantle and core. The second lecture dealt with the rheological properties of the interior. On the assumption that a Newtonian viscosity leads to an appropriate description of processes of deformation, means of deducing its numerical values at various depths were presented. In the final lecture the results of observations of the earth's external potential field and of terrestrial heat flow were given, and the difficulty in reconciling them with a static model of the earth was described.

Seismic Data and Internal Structure of the Earth

M. Nafi Toksöz

ABSTRACT

A review of seismological data utilized for the study of the velocity structure of the earth's interior is covered. Travel times of body waves, dt/d measurements utilizing large arrays, phase and group velocities of Rayleigh and Love waves and earth's free oscillations are discussed. Structures of the earth's mantle and core obtained from the above data are discussed

with particular emphasis on transition zones and boundaries.

Lateral variations of the upper and lower mantle structures are obtained from interpretation of regional data. Presence of significant lateral inhomogeneities both in the upper and lower mantle are indicated. Seismic results are correlated with geoid heights, heat flow data, and surface topography. Correlation coefficients between seismic and geoid height spherical harmonic coefficients is greater than all others. This indicates some dependence between seismic velocity and density dependence in the upper mantle.

Convection in Horizontal Layers with Internal Heat Generation

Paul H. Roberts

ABSTRACT

Recently Tritton and Zarraga have made a largely qualitative study of cellular convection produced by the instability of a layer of fluid heated uniformly throughout its body, cooled from above, and thermally insulated below. The fluid was acqueous zinc sulphate solution, and the heating was produced by electrolytic current. The flow was vizualized and photographed using polystyrene beads which, because of a differential expansion, came out of suspension in regions where the fluid was hotter or colder than average.

The development of the cellular pattern as the Rayleigh number, R, (see below) was varied and was in many respects similar to that for

Bénard convection. There were, however, two striking differences. First, the fluid descended in the centre of the cells and ascended at the peripheries. Second, and perhaps more surprisingly, the horizontal scale of the convection increased systematically with increasing Rayleigh numbers. (This last observation may be relevant to theories of convection within the Earth's mantle, to mesoscale convection in the atmosphere, and to patterns formed in ice.)

Adopting the Boussinesq approximation, the character of the convection depends on two dimensionless parameters, p, the Prandtl number, and the Rayleigh number R:

$$p = \frac{\nu}{\kappa} , \qquad R = \frac{g\alpha\gamma d^5}{\nu\kappa^2}$$

Here g is the acceleration due to gravity, α is the coefficient of volume expansion, ν is the kinematic viscosity, κ is the thermal diffusivity, d is the depth of the layer and γ is the rate at which the heat sources would cause the temperature of each element of fluid to rise in the absence of convection and conduction. It was shown that the critical Rayleigh number, R_c, at which thermal convection can first occur with zero amplitude, is 2772, the semi-wavelength of the corresponding instability pattern being 1.195d. A crude theory of the subsequent finite-amplitude convection was presented, the basic simplification being that, to an adequate approximation, Fourier decompositions of the convective motions in the horizontal (x,y) directions can be represented by their dominant (planform) term above. A discussion of this hypothesis was given, with illustrations drawn from the (better studied) Bénard situation. It

was also pointed out that the hypothesis, when applied to Bénard convection, first predicted successfully that immediately above R_c the preferred mode of convection would be in rolls and not in hexagons (Roberts, 1965). When applied to the present situation, in the range $7000 < R_c < 20,000$ it was found that convection in rolls is always marginally stable to convective perturbations of other wave-numbers, that convection in hexagons with motion, up at their centres is always unstable, and that convection in hexagons with motions down at their centres is unstable for $R < R_h(p)$ where $R_h(p)$ for water ($p = 6.8$) is about 8750. For $R > R_h$, they are stable provided their wave-number, a, lies in a band $a_1 < a < a_2$, where $1/a_1$ and a_2 increase as R increases. Thus the observed pattern of motions is accounted for (the Tritton-Zarraga experiments do not reliably indicate the pattern below R = 11,000). Unfortunately, however, the wave-numbers they observe appear to be less than a_1. Bearing in mind the subtlety of questions of preferred mode, it was concluded that either the experiments do not realize the conditions of the theory with sufficient accuracy (the temperature variation of electrical conductivity undoubtedly resulted in some 10% variations in heating rate), or, more likely, the present crude theory is not sufficiently accurate.

REFERENCES

Roberts, P. H. 1965 Proc.Conf.Non-Equilib.Thermodynam. Var.Tech. & Stab. Chicago, (Publ.U.of Chicago Press, 1966)

Roberts, P. H. 1968 J.Fl.Mech. (to appear)

Tritton, D. J. and M. N. Zarraga, 1968 J.Fl.Mech. (to appear)

Steady Fluid Flow in a Precessing Spheroidal Shell

Friedrich Busse

ABSTRACT

The inviscid equations of motion for the steady flow in a rotating container in general do not have a uniquely determined solution. Poincaré (1910, Bull.Astr. 27: 321) solved the problem of the fluid motion in a precessing spheroidal shell by assuming that the vorticity of the motion is constant. Using a linear boundary layer analysis Roberts and Stewartson (1963, J.Fluid Mech. 17: 1; 1965, Proc.Camb.Phil.Soc. 61: 279) have shown that the motion indeed has constant vorticity in the limit of vanishing viscosity. In the case, however, of a finite angle between the vorticity vector of motion and the axis of rotation of the shell the nonlinear term in the boundary layer equation become important. It is shown that they cause a differential rotation of the interior fluid. In the limit of vanishing viscosity the vorticity has a constant direction but its magnitude depends on the distance from the axis. It is interesting to note that the same motion caused by the precession of shell can be produced by a "tidal" bulge of shell rotating with a constant angular velocity. The amplitude of both effects is very small in the case of the liquid core of the earth. It seems likely, however, that the inhomogeneous vorticity of the steady motion leads to shear flow instabilities. Hence a turbulent state of motion may be caused by the action of the precession and the tides in the liquid core of the earth.

Shear Flow Instabilities in Rotating Systems

Friedrich Busse

ABSTRACT

Shear flow occurring in the form of a differential rotation is a frequent phenomenon in the dynamics of rotating fluid systems. An example is the cylindrical shear layers formed at the transition of two fluid bodies rotating about the same axis but with different rates. The case of the fluid flow between two infinite parallel rotating plates with a circular part of one or both plates rotating at a slightly different rate has been studied in detail by Stewartson (1957, J.Fluid Mech. 3: 17). Often steady shear flow is induced by forced oscillations. The flow in a spheriodal shell is an example of this type of shear flow (see for instance, the lecture by Malkus and the abstract by Busse in this volume).

For the description of the instability of axisymmetric shear flow in a rotating system we use boundary layer theory assuming that the Ekman number E and the Rossby number ε - which represents the amplitude of the shear flow - are both small parameters. The dissipation in Ekman boundary layer leads to a critical value of the order $E^{1/2}$ in which the shear flow becomes unstable. The governing equation is closely related to the Rayleigh stability equation in the theory of hydrodynamic stability of parallel flow in a non-rotating system. In fact, both equations become formally identical in the limit when the circular flow can be approximated by parallel flow.

Measurements of the critical Rossby number have been made by Hide

in the case which has been studied theoretically by Stewartson as mentioned above. The stability analysis applied to this case shows reasonable agreement with the experimental observations. The fact that a linear stability theory is adequate indicates that in many cases subcritical instabilities of finite amplitude do not occur in a rotating system in contrast to the corresponding instabilities of parallel shear flow in an inertial system. A physical explanation for this fact is that the dimensional motions are suppressed due to the Taylor-Proudman theorem. Hence the extended theory of inviscid hydrodynamic instabilities seems to have a more direct application to the shear flow in rotating systems than for the case without rotation, for which it was developed originally.

Bounds on the Turbulent Transport of Heat and Momentum

Willem V.R. Malkus

ABSTRACT

L. N. Howard's paper (1963) on heat transport contains the first quantitative consequences of the equations of motion concerning turbulent convection. The significance of this work and its applicability to other problems of turbulence was not immediately apparent, perhaps because the bounds placed on heat flux were considerably larger than those found in laboratory observations. Howard had found the extreme value of heat flux between horizontal surfaces for an arbitrarily prescribed Rayleigh number under the constraints that the fluid motions satisfy; the boundary condi-

tions, the dissipation rate integral, the entropy production integral and the horizontal integral requiring conservation of the vertical flux. A second, lower, maximum heat flux was found under the above constraints plus the continuity condition, but was restricted to those solutions of the extremizing Euler-Lagrange equations which had only a single horizontal wave number. Even this latter solution gave a heat flux much larger than is observed.

Since laboratory measurements of convection have been made at rather low Reynolds number, it seemed desirable to further restrict Howard's extreme flows. In the summer of 1964 R. Halpern and the author reformulated the extreme problem for the case of infinite Prandtl number. This removes the non-linear momentum advection terms as possible contributors to the heat flux, substituting a fourth-order linear relation between vertical velocity and fluctuation temperature for the dissipation-rate integral constraint. The qualitative results of this study were in keeping with laboratory measurement, encouraging one to pursue the external studies further.

A survey of allied problems was made the topic of a course on turbulent flow given at U.C.L.A. in the spring of this year. The author, with the invaluable assistance of F. Busse, explored various paths opened by Howard's paper. The first path led to Couette shear flow, for it was clear that Reynolds number would play the role of the square of the Rayleigh number in this analogous problem. This meant that the analogy to Howard's second extreme for a single horizontal wavenumber would correspond to the "Blausius $\frac{1}{4}$-power" regime of the shear flow. F. Busse has

formulated this shear flow study to include Couette, Pouseille and "thermal" shear flows, executing the work in a masterful way reported upon in a following abstract.

Other paths outlined in the course were followed, for a short distance at least, by various students. Two classes of questions were asked. The first of these was, "What other integrals deduced from the equations of motion are significant constraints on the extreme values of turbulent fluxes?" The infinite set of moment integrals called virial equations seemed hopeful, but the first steps in this direction are still being taken by a somewhat stumbling student. The infinite set of integrals constructed from the product of derivatives of the velocity times derivatives of the Navier-Stokes equations contain, as a first member, the dissipation rate integral. The second members seem to be only symmetry constraints on vorticity, while the third members include the vorticity integral. This latter is an important constraint on two-dimensional flows, but its contribution as a three-dimensional constraint seems slight. Its properties are still being explored.

The second class of questions concerned turbulent flows in the same simple parallel plane geometry as the Howard problem and with only the same dissipation rate type integrals as constraints. However each was closen to exhibit some unexplored effect or to question the merit of one extreme versus another. For example, in the heat flux plus salt flux problem one can compare maximum dissipation rate to maximum heat flux, and determine which extreme more nearly approaches the observations. The author's bias assures him that the dissipation rate extreme will prove to

be the useful one. Thermal convection with shear flow and convection with rotation will introduce stabilizing parameters and Prandtl number dependence into the extremal problem. However work on these was barely started. The extremal problem for Taylor and Couette flow between rotating cylinders is being studied by E. Nickerson with some success. He has found a "drag coefficient" which upper bounds known data, and is now exploring the "Taylor-stable, Couette-unstable" region of this flow.

As an example of this survey of Howard-like problems, the work on magnetic-Ekman-Couette flow undertaken by the author and R. Gans is outlined here. The extreme dissipation rate is sought for flows in plane parallel geometry satisfying: the total dissipation rate integral, the first "cross integral" linking magnetic and velocity fields, the divergence conditions on both fields, and the horizontal mean momentum transfer conservation integral. The latter contains the imposed constraint of rotation as a Coriolis term in the mean horizontal velocity. Ten Euler-Lagrange equations of the mean-field boundary-layering type result from the extremization. As an example, the three produced by variation of the fluctuating magnetic field are

$$0 = 2(1-\lambda_1)\mathcal{R}_M^{-1}\partial_j\partial_j h_i + \lambda_2(\mathcal{R}^{-1}+\mathcal{R}_M^{-1})\partial_j\partial_j v_i - \partial_i\varphi -$$

$$-2\lambda_2\mathcal{R}_0\,\varepsilon_{ijk}\,\zeta_j v_k - \frac{d}{dz}\left[(S_i h_z + S_j h_j \zeta_i) - (T_i v_z - T_j v_j \zeta_i)\right],$$

where $\mathcal{R}$ is the Reynolds number, $\mathcal{R}_M$ is the magnetic Reynolds number, $\mathcal{R}_0$ the Rossby number, λ_1, λ_2, S_i and T_i are functions of the mean fields only, φ is a scalar Lagrangian potential, v_i is the fluctuating velocity field, h_i is the fluctuating magnetic field, and ζ_i is the unit vector

in the z-direction. The equations are quasi-linear in the fluctuating variables and separable in the horizontal coordinates. One is confident that boundary layer solutions will soon emerge, with machine help if necessary. However, despite the vast simplification from the primitive equations, the task ahead is considerable. Justifications for this task are bounds on turbulent Ekman flows, bounds on magnetic fields induced by turbulent shear flow, and bounds on the role of rotation in strengthening magnetic fields.

With several of the "simplest" extreme flows as guides, the future holds many exciting problems ranging from extreme values for the rate of collapse of stars to the extreme effects of "self-roughening" boundaries. Each problem can be formally "correct" in providing upper bounds. A generous fate can make their solutions quantitatively close to the unaccessible turbulent reality.

Reference

Howard, L. N. 1963 J.Fluid Mech. 17: 405